Pharmacometrics to characterize pharmacokinetics and optimize treatment in understudied populations

by

MANNA SEMERE GEBREYESUS

A Thesis Presented for the Degree of

DOCTOR OF PHILOSOPHY

In the Division of Clinical Pharmacology

Department of Medicine

UNIVERSITY OF CAPE TOWN

June 2025

Primary supervisor: Professor Paolo Denti

Co-supervisor: Doctor Roeland E. Wasmann

Copyright

Contributions to the field

This thesis includes some of the following contributions to the field of pharmacometrics and clinical pharmacology.

Full-length original articles

- **Gebreyesus MS**, Dresner A, Wiesner L, Coetzee E, Verschuuren T, Wasmann R, Denti P. Dose optimization of cefazolin in South African children undergoing cardiac surgery with cardiopulmonary bypass. CPT: Pharmacometrics & Systems Pharmacology. 2024 Sep;13(9):1595-605. https://doi.org/10.1002/psp4.13196.

- **Semere Gebreyesus M**, Wasmann RE, McIlleron H, Oladokun R, Okonkwo P, Wiesner L, Denti P, Rawizza HE.2024.Population pharmacokinetics of rifabutin among HIV/TB co-infected children on lopinavir/ritonavir-based antiretroviral therapy. Antimicrob Agents Chemother68:e00354-24. https://doi.org/10.1128/aac.00354-24.

- **Manna Semere Gebreyesus**, Andre Joubert, Phumla Sinxadi, Karen Sliwa, Gary Maartens, Lubbe Wiesner, Paolo Denti, Roeland E. Wasmann. Application of a population pharmacokinetic model as a tool for monitoring adherence in heart failure patients. (yet to be published)

- **Gebreyesus MS**, Decloedt EH, Cluver CA, Hunfeld NG, Helgadóttir H, Björnsson ES, Wasmann RE, Denti P. Population pharmacokinetics of esomeprazole in patients with preterm preeclampsia. British Journal of Clinical Pharmacology. 2022 Oct;88(10):4639-45. https://doi.org/10.1111/bcp.15416

The author has also contributed to the following article:

- Mwita JC, Joubert A, Saidu H, Sani MU, Damasceno A, Mocumbi AO, Sinxadi P, Viljoen CA, Hoevelmann J, **Gebreyesus MS**, Denti P. Objectively measured medication adherence using assays for carvedilol and enalaprilat in patients with heart failure in Mozambique and Nigeria. International Journal of Cardiology Cardiovascular Risk and Prevention. 2023 Dec 1;19:200213. https://doi.org/10.1016/j.ijcrp.2023.200213

Scientific conference abstracts

- **Gebreyesus MS**, Decloedt EH, Cluver CA, Hunfeld NG, Helgadóttir H, Björnsson ES, Wasmann RE, Denti P. Population pharmacokinetics of esomeprazole in patients with preterm preeclampsia.
  - Poster virtual presentation: 29th Annual Meeting Population Approach Group Europe (PAGE), 2021. Abstract 9780.

- **Gebreyesus MS**, Dresner A, Wiesner L, Coetzee E, Verschuuren T, Wasmann R, Denti P. Dose optimization of cefazolin in South African children undergoing cardiac surgery with cardiopulmonary bypass.

- Poster presentation: Third World Conference of Pharmacometrics (WCoP), 2022, Cape Town, South Africa. Abstract 199.
- Oral virtual presentation: 55th Annual South African Society for Basic and Clinical Pharmacology (SASBCP), October 12th, 2022, Virtual Conference.
- Oral presentation: 19th world congress of basic and clinical pharmacology, 05 July 2023, Glasgow, Scotland (as part of a group of speakers within a workshop theme titled "what can modeling do for you? Rational design and interpretation of clinical studies")

❖ **Semere Gebreyesus M**, Wasmann RE, McIlleron H, Oladokun R, Okonkwo P, Wiesner L, Denti P, Rawizza HE. Population pharmacokinetics of rifabutin among HIV/TB co-infected children on lopinavir/ritonavir-based antiretroviral therapy.

- Oral presentation: 48th annual department of medicine research symposium, 12 October 2023, University of Cape Town, South Africa.
- Oral virtual presentation: 14th International workshop on clinical pharmacology of tuberculosis drugs, 26 September 2023.
- Poster presentation: 31st Annual Meeting Population Approach Group Europe (PAGE), 2023, A Coruña, Spain. Abstract 10362.
- Poster presentation: 19th world congress of basic and clinical pharmacology, 2023, Glasgow, Scotland. Abstract 754.

Declaration of work

I, **Manna Semere Gebreyesus**, hereby declare that the work on which this dissertation/thesis is based is my original work, both in concept and execution, (except where acknowledgements indicate otherwise) and that neither the whole work nor any part of it has been, is being, or is to be submitted for another degree in this or any other university. **Chapters 4, 5,** and **7** of the thesis have been published or are under review in an international journal and contents remain unchanged from the printed versions except where formatting was required to maintain consistency in the thesis. All co-authors gave their written consent to include the publications as part of a PhD.

I hereby declare that this thesis/dissertation has been submitted to the Turnitin module (similarity and originality checking software). Plagiarism is to use another's work and pretend that it is one's own and I know that plagiarism is wrong. I confirm that I have discussed and resolved any concerns emanating from the Turnitin report with my supervisor.

I empower the university to reproduce for research either the whole or any portion of the contents in any manner whatsoever.

Declaration on the Inclusion of Publications in a PhD Thesis

"I confirm that I have been granted permission by the University of Cape Town's Doctoral Degrees Board to include the following publication(s) in my PhD thesis, and where co-authorships are involved, my co-authors have agreed that I may include the publication(s):"

- Gebreyesus MS, Dresner A, Wiesner L, Coetzee E, Verschuuren T, Wasmann R, Denti P. Dose optimization of cefazolin in South African children undergoing cardiac surgery with cardiopulmonary bypass. CPT: Pharmacometrics & Systems Pharmacology. 2024 Sep;13(9):1595-605. https://doi.org/10.1002/psp4.13196.

- Semere Gebreyesus M, Wasmann RE, McIlleron H, Oladokun R, Okonkwo P, Wiesner L, Denti P, Rawizza HE.2024.Population pharmacokinetics of rifabutin among HIV/TB co-infected children on lopinavir/ritonavir-based antiretroviral therapy. Antimicrob Agents Chemother68:e00354-24. **https://doi.org/10.1128/aac.00354-24.**

- Manna Semere Gebreyesus, Andre Joubert, Phumla Sinxadi, Karen Sliwa, Gary Maartens, Lubbe Wiesner, Paolo Denti, Roeland E. Wasmann. Application of a population pharmacokinetic model as a tool for monitoring adherence in heart failure patients. (yet to be published).

- Gebreyesus MS, Decloedt EH, Cluver CA, Hunfeld NG, Helgadóttir H, Björnsson ES, Wasmann RE, Denti P. Population pharmacokinetics of esomeprazole in patients with preterm preeclampsia. British Journal of Clinical Pharmacology. 2022 Oct;88(10):4639-45. **https://doi.org/10.1111/bcp.15416**.

Date: 27th June 2025

Student Name: Manna Semere Gebreyesus

Student Number: SMRMAN003

Acknowledgements

I would like to extend my heartfelt gratitude to:

- The Lord God, who gave me courage throughout this PhD journey.
- My supervisor Professor Paolo Denti and co-supervisor Dr Roeland Wasmann, for their guidance and expertise throughout every stage of this degree, from proposal development to data analysis and paper publication. I am grateful for their enthusiasm, invaluable advice, and timely feedback. They have gone beyond the call of duty in their encouragement and support, and completing this PhD would have been difficult otherwise.
- All colleagues at the pharmacometrics unit of the University of Cape Town. Their willingness to lend a listening ear and exchange ideas was instrumental in helping me navigate through challenging analyses.
- My family, who instilled in me the value of education.
- My husband, whose love and support made this possible. For his patience, encouragement, and for sharing this journey with me.
- The Division of Clinical Pharmacology, Prof Lubbe Wiesner, and The University of Cape Town's ICTS High-Performance Computing team.
- The patients and participants of the clinical trials, whose data formed the foundation of the analysis presented in this thesis.

Abstract

Pharmacometrics to characterize pharmacokinetics and optimize treatment in understudied populations

Clinical trials frequently exhibit a lack of participant diversity, with underrepresentation of certain demographics, including pregnant women, individuals at the extremes of age (such as children or the elderly), and specific racial or ethnic groups (such as people of African ancestry). Consequently, suitable dose labelling is lacking at the time of drug approval for these groups, leaving healthcare practitioners with a dilemma: either exclude these groups from treatment or make dosing recommendations based on data from a potentially non-representative population, posing a risk of suboptimal or toxic treatment outcomes. Post-marketing pharmacokinetic studies in these populations are challenging due to low consent rates, difficulties with frequent blood sampling, unbalanced study designs resulting from the opportunistic nature of such studies, or resource constraints in developing countries, all contributing to sparse data. Pharmaceutical companies may also lack the incentive to invest in these studies when the medication's market performance is already stable and there is no immediate return on investment.

In this thesis, I apply pharmacometrics for understudied populations with limited data across various therapeutic areas, including: optimizing dose of cefazolin, an antibiotic used for surgical site infection prophylaxis, in children undergoing cardiac surgery with cardiopulmonary bypass; optimizing dose of rifabutin, an antibiotic used for TB, during lopinavir/ritonavir (LPV/r)-co-treatment in children with TB-HIV co-infection; showcasing a model-based adherence monitoring tool using enalapril, an angiotensin-converting enzyme inhibitor for hypertension and heart failure, in a small cohort of African heart failure patients, and characterizing pharmacokinetics of esomeprazole, a proton pump inhibitor for hyperacidity and being investigated for preeclampsia, in patients with preterm preeclampsia.

Using data contributed by 22 children on cefazolin, I suggested a continuous infusion regimen for bypass surgeries, which improves the probability of target attainment compared with the intermittent weight-based regimen used in clinical settings. Using data from 28 children on rifabutin, I developed a parent-metabolite model to assess the weight-based dosing used in the studies, proposing a weight-band based regimen for rifabutin without and with LPV/r for controlled exposures across age groups. For enalapril, I devised a model-based adherence assessment method based on data from 30 adults, including 6 African heart failure patients, which improves adherence monitoring since it considers variations in pharmacokinetics and dosing schedules. Finally, I used modeling to identify pharmacokinetic changes in esomeprazole during pregnancy using data from 59 adults (including 10 pregnant) on esomeprazole.

In summary, using pharmacometrics, I could interpret limited data from understudied populations to characterize pharmacokinetics, evaluate existing practices and guide the consideration of alternative dosing scenarios.

Table of contents

List of Figures

Supplementary Figures

List of Tables

Supplementary Tables

Abbreviations and acronyms

AIC	Akaike Information Criterion
ART	Antiretroviral therapy
AUC0–24	The 24-hour area under the concentration-time curve
BLQ	Below the limit of quantification
BOV	Between-occasion variability
BSV	Between-subject variability
CI	Confidence Interval
CL	Clearance
C_{max}	Maximum plasma concentration
C_{min}	Minimum plasma concentration
CYP	Cytochrome
F	Oral bioavailability
FDA	Food and Drug Administration Unbound
F_u	fraction
FFM	Fat-free mass
FOCE-I	First-order conditional estimation with eta-epsilon interaction
GOF	Goodness-of-fit
HIV	Human immunodeficiency virus
K_a	Absorption rate constant
LLOQ	Lower limit of quantification
MAC	Mycobacterium Avium Complex
MTT	Mean transit time
NCA	Noncompartmental analysis
NN	Number of absorption transit compartments
NONMEM	Non-linear mixed-effects modeling
NNRTI	Non-nucleoside reverse transcriptase inhibitors
NRTI	Nucleoside reverse transcriptase inhibitors
OFV	Objective function value
PD	Pharmacodynamics
P-gp	P-glycoprotein
PI	Protease inhibitors
PsN	Perl-speaks-NONMEM
PTA	Probability of target attainment
Q	Intercompartmental clearance
SIR	Sampling importance resampling
TB	Tuberculosis
TBW	Total body weight
T_{max}	Time to maximum plasma concentration
V	Volume of distribution

Vc	Volume of distribution of the central compartment
V_p	Volume of distribution of the peripheral compartment
VPC	Visual predictive check
WHO	World Health Organization

Chapter 1 Introduction and literature review

1.1 Drug development and understudied populations

Clinical trials often lack participant diversity (Food & Drug Administration, 2020; Sharma and Palaniappan, 2021). Historically, adherence to standard inclusion/exclusion criteria in Phase I-III trials, driven by ethical and safety considerations, has led to the exclusion of specific populations without robust justifications. Underrepresented populations in clinical trials often include women in general, especially those who are pregnant or lactating, individuals at the extremes of age (such as children and the elderly), the obese, specific racial or ethnic groups (such as black or Middle Eastern populations), people with disabilities, individuals with comorbid diseases, or those with orphan diseases. For example, the Drug Trials Snapshots summary report released by the Food and Drug Administration (FDA) in 2020 revealed that merely 7% of global clinical trial participants from 2015 to 2019 were black. With regards to geographical distribution, a mere 2% of non-U.S. participants identified as black. In considering specific therapeutic areas with heightened morbidity and mortality rates among the black population and in advanced age, such as cardiovascular diseases (Carnethon *et al.*, 2017), only 3% of clinical trial participants were black, and 2% were above the age of 65. Moreover, there are disparities in global clinical trial participation, with most participants from developed countries, despite higher impact of morbidity and mortality in low resource settings of developing countries, and where environmental factors, healthcare practices, and genetic factors might be different (Food & Drug Administration, 2020).

These limitations impede the applicability of drug efficacy and safety outcomes to diverse populations likely to use the product. Consequently, dose labelling at the time of drug approval may not encompass these excluded groups, leaving healthcare practitioners to either exclude specific populations from treatment or make dosing recommendations based on data

extrapolated from a potentially non-representative population (Colbers *et al.*, 2019; Food and Drug Administration, 2020). Furthermore, the inclusion of dosing information for underrepresented populations in drug labels may take several years post-approval as specific pharmacokinetic and safety data become available (Colbers *et al.*, 2019). For example, safety and pharmacokinetic data of cobicistat during pregnancy became available over 6 years after Cobicistat-boosted antiretrovirals were in market, and its use was discouraged during pregnancy due to reduced exposure (Eke *et al.*, 2023). Therefore, it is essential to address the data scarcity and lack of dose optimization in specific populations at the time of drug approval to avoid inadequate and potentially adverse treatment outcomes.

The central theme of this thesis is the utilization of pharmacometrics to optimize dosing in understudied populations with scarce data, with a focus on pregnant women, children, and individuals of the black African racial demographic.

1.2 Dose optimization in understudied populations

Variability in treatment response across diverse populations may be attributed to differences in pharmacokinetics (PK) (variations in exposure) or pharmacodynamics (PD) (variations in the response at the target level). Exposure-response analysis is essential for dose optimization, which aims to minimize toxicity while maximizing efficacy for the majority, if not all, of the patient populations. The analysis of exposure-response, typically conducted in Phase I-III clinical trials, may not encompass data from diverse populations. Therefore, post-approval, certain populations may exhibit insufficient efficacy or adverse effects that were not identified during pre-marketing studies. In cases where disease progression, and treatment response are similar, it is reasonable to assume similar exposure-response relationship among different populations, and efficacy can be extrapolated from previous studies (in another population). In this case, it is sufficient to perform pharmacokinetic studies, along with safety studies, in

specific populations to observe exposure with the aim of finding the dose which achieves similar exposures linked with efficacy in previous studies. Population pharmacokinetic modeling and simulation can be utilized for this purpose, to understand the mechanisms that underlie differences in PK within sub-populations and simulate doses that achieve the desirable exposures in the majority of patients. In cases where there is uncertainty about similarities in disease progression or treatment response, in addition to safety studies, it is essential to conduct efficacy studies in specific populations alongside pharmacokinetic studies. Alternatively, if reliable efficacy metrics are available, pharmacokinetic/ pharmacodynamic (PK/PD) studies can be conducted to establish the exposure-response relationship, as well as pharmacokinetic studies to optimize the dose which achieves exposure reported to be beneficial in the PK/PD studies (FDA, 2003; Sun *et al.*, 2018).

1.3 Pharmacokinetics in understudied populations

Differences in body size, body composition, and activity of metabolizing enzymes due to factors like sex, age, and genetic polymorphisms associated with ethnicity may result in variations in drug exposure. Additionally, specific factors unique to certain populations, such as diet, socioeconomic conditions, and lifestyle, could impact medication adherence and treatment outcomes. The interplay between these diverse factors could further complicate treatment.

1.3.1 Pharmacokinetics during pregnancy

Physiological changes occur throughout pregnancy as a continuous process linked to gestational age, typically returning to baseline around three months postpartum, though individual variations may exist. Many alterations in a normal pregnancy are ascribed to elevated levels of various hormones, including oestradiol and progesterone. Concurrently, complications such as gestational diabetes, anaemia, gestational hypertension, or preeclampsia

can impact PK. The presence of supplements or co-medications, such as vitamins or anti-nausea drugs, may induce drug interactions (Costantine, 2014).

Pregnancy-related changes in rate of drug absorption can occur through delayed gastric emptying and reduced intestinal motility, influenced by progesterone's effect on gastric smooth muscles. Bioavailability may be affected by increased gastric pH due to higher mucus production, potentially reducing the absorption of weakly acidic drugs through ionization, while weakly basic drugs might experience enhanced absorption. Nevertheless, the increased cardiac output and intestinal perfusion during pregnancy may counterintuitively boost drug absorption. Antacids taken for gastroesophageal reflux or iron-containing supplements may bind with concurrently administered medications, leading to a decrease in their bioavailability. Bioavailability alterations may also stem from higher or lower pre-systemic clearance (CL), contingent on the metabolic route. Increased activities of metabolic enzymes have been reported during pregnancy, for e.g., CYP3A4 activity increases, with 72% higher CL of its probe drug, midazolam, reported during the third trimester compared to postpartum. Similarly, CYP2D6 activity increases from 26% during the second trimester to 48% by the third trimester compared to postpartum. Other enzymes such as CYP1A2 have decreased activity during pregnancy, decreasing from 67% to 35% compared to postpartum levels from the second to the third trimester, respectively (Thummel and Lin, 2014; Feghali et al., 2018).

Changes in drug distribution during pregnancy are influenced by factors such as higher tissue perfusion and modified plasma protein or tissue binding. Near term, there is a 33% rise in cardiac output, a 50% increase in plasma volume, and a 32% augmentation in total fat mass, leading to expanded drug distribution for both hydrophilic and lipophilic drugs. Concentrations of plasma

proteins like albumin and alpha-1 acid glycoprotein (AAG) decrease by 31% and 19%, respectively, potentially amplifying the distribution of highly bound drugs when CL is restricted (Ke *et al.*, 2014; Feghali et al., 2018).

Alterations in drug CL during pregnancy result from changes in the expression of metabolizing enzymes and an increased fraction of unbound drug. Renal CL elevates due to a rise in glomerular filtration rate (GFR) by up to 40%, alongside enhanced tubular secretion involving increased activity of transporters such as P-glycoprotein (P-gp) and organic cation transporter OCT2, as observed by increased CLs of digoxin and metformin, respectively (Ke *et al.*, 2014; Thummel and Lin, 2014). Consequently, dose adjustments are advisable for certain drugs during pregnancy due to heightened CL, exemplified by antihypertensives like nifedipine (CYP3A4 induction) and metoprolol (CYP2D6 induction), as well as antibiotics like amoxicillin and cefazolin (increased renal CL) (Eke *et al.*, 2023).

1.3.2 Pharmacokinetics during childhood

Physiological and developmental variations within the paediatric population such as body size and composition, physiological and anatomical differences, and maturation of organ function result in different PK from adults. Gastric pH is higher in neonates and infants, becoming similar to that of adults by age two, which can improve the absorption of acid sensitive drugs, such as the beta lactam antibiotics, while reducing absorption of weakly acidic drugs, such as acetaminophen. Generally, rate of absorption is slower in neonates and infants compared to older children due to lower gastric emptying time (Kearns *et al.*, 2003).

Drug disposition is influenced by plasma protein binding, body composition, blood flow, and organ function, in addition to a drug's properties. Body composition changes throughout childhood, with decrease in total body water (from 85% in preterm neonates to 75% in term neonates, and reaching 60% at 5 months) and changes in fat as age increases (from ~12% in

term neonates to ~30% at 6 months to ~ 20% at 2 years), which could affect volume of distribution (Vd) of drugs (becoming lower for hydrophilic and higher for lipophilic drugs as age increases) (Anderson and Holford, 2009; Gallagher *et al.*, 2020). Neonates and young infants have lower amount of drug binding proteins, albumin, and AAG , and in neonates, higher levels of free fatty acids and bilirubin could displace drugs from binding sites to albumin. This leads to higher unbound fraction of drug, increasing Vd and for drugs with low Vd, increasing CL (O'Hara *et al.*, 2015).

Most metabolic enzymes are not fully mature at birth (i.e., have lower expression compared to adults), meaning that CL for substrate drugs would be lower than what would be expected based on a child's weight. Overall, most hepatic enzymes are expected to mature to adult levels by 2-3 years, however, the timeline for enzyme maturation differs. For example, reports indicate that CYP2C19 and CYP2D6 mature within the first year, Uridine glucuronosyltransferase (UGT) within 3 months, N-acetyltransferase 2 (NAT2) within 1 to 4 years, and CYP1A2 within 3 years (Thummel and Lin, 2014). Factors such as foetal exposure to tobacco and infant diet (formula rather than breast feeding) might accelerate the rate of enzyme maturation (O'Hara *et al.*, 2015). Moreover, young children have a larger organ size (e.g., liver mass is higher) and higher blood flow per kg of body weight compared to adults (Thummel and Lin, 2014). Once maturation is reached, children would have higher CL per kg of body weight compared to adults, and allometry (where Vd scales linearly with body size, whereas CL scales less than linearly, with an exponent of 0.75) can be used to predict CL by scaling from the mature CL value reported in adults (Anderson and Holford, 2008; Holford, Heo and Anderson, 2013). Further, maturation-independent organ function needs to be considered, such as in critically ill paediatric patients, where hepatic function could be reduced while renal CL could be augmented (Dhont *et al.*, 2020).

1.3.3 Race and ethnicity associated alterations in pharmacokinetics

Race and ethnicity could contribute to interindividual variability in PK, which could be related to genetic variations, physiology, diet, and environmental factors such as exposure to pollutants. A primary cause is attributed to interracial variations in frequencies of genetic polymorphisms in metabolic enzymes, transporters, or binding proteins. For example, CYP2B6 poor metabolizers are more frequent among blacks (~47%) compared to Asians (~17%), resulting in higher potential of increased efavirenz exposures and higher risk of neurologic adverse effects at standard doses (Wang, Neiner and Kharasch, 2019; Olafuyi *et al.*, 2021). Lower levels of AAG have been reported among Chinese compared to Caucasians, which increases unbound fraction of drugs such as propranolol, due to genetic polymorphisms affecting AAG expression. Weight-for-age and fat mass is reported to be higher in healthy Caucasians compared to Asians, which could lead to higher Vd of lipophilic drugs in the former (Olafuyi *et al.*, 2021). Diet may also play a role – compared to the high levels of fat in European diets, African and Mediterranean diets tend to be low fat and spicy with vegetables and herbs. High fat diets increase bile secretion and lipophilic drug absorption, while vegetarian diets reduce gastric emptying time and could reduce rate of absorption. Further, herbs used in traditional medicines can affect PK – for e.g., in Africa, it is reported that ~90% of the population uses some form of traditional medicine, which is usually underreported to health care providers, although it can potentially lead to drug interactions (Calitz *et al.*, 2014).

Cultural and socioeconomic factors could also affect outcomes by influencing adherence to

treatment. Reports have indicated higher nonadherence to anti-hypertensive medications in Africa, at ~62%, compared to other regions such as Europe (~37%) and Asia (~44%). Nonadherence has been associated with health literacy, unemployment, education level, medication-associated side effects, discontinuing medication prematurely with cessation of

symptoms, polypharmacy or complex treatment regimens, and a preference to take traditional medicines (Abegaz *et al.*, 2017).

1.4 Pharmacometrics in understudied populations

Traditional analysis of pharmacokinetic data using non-compartmental analysis (NCA) requires rich blood sampling with relatively smaller participant size, with strict adherence to predetermined sampling schedules, to accurately determine pharmacokinetic parameters. However, frequent blood sampling, even with efforts for more sensitive analytical methods to reduce blood volumes, could raise concerns in participants or guardians over blood loss, particularly in children, during pregnancy or the elderly, reducing consent rates. Strict adherence to sampling schedules could interfere with patient care and might not always be feasible. To overcome these challenges, pharmacometrics (model-based analysis of pharmacokinetic data) can be utilized, where studies are designed so that more participants are included, but sparse sampling is performed (e.g., 2-3 samples per individual at different time points). In this way, data from all the participants inform the parameters, while minimizing the sampling burden on each individual participant. Moreover, with pharmacometrics, sampling times are more flexible as long as accurately documented, since rather than relying on specific samples taken at particular time points to determine parameters, modeling is used to predict the full pharmacokinetic curve. In some cases, there is data sparsity due to limited participant size, which could occur due to resource constraints, low consent rates, or because data is collected opportunistically. Using pharmacometrics, limited participant data can be pooled with data from other populations, such as healthy participants, or prior information from literature can be integrated in pharmacometric models as strong or weak evidence so that individual parameter estimations can be informed not just with the observed sparse data but also from the prior information about the parameter's distribution (Thomson and Elliott, 2011).

Non-compartmental methods of analysis are less time consuming and computationally intensive, which makes them attractive, but have other limitations as well. In such methods, the physiological mechanisms underlying PK are not integrated. However, accurate characterization of PK often requires considering physiological mechanisms to make accurate predictions, which necessitates pharmacometrics. For example, mechanisms of renal and non-renal CL, pre-systemic metabolism (at intestinal and hepatic sites), or saturable CL, can be differentially determined with semi-mechanistic compartmental models. Fully mechanistic physiologically based pharmacokinetic (PBPK) models can be used to extrapolate *in vitro* information as well as information from other populations on specific mechanisms, such as changes in enzyme expression, to make accurate predictions.

Moreover, in non-compartmental methods, individual pharmacokinetic parameters are directly calculated from observed concentrations, and a comparison of summary metrics of the individual parameters can be made between populations or treatment groups, indicating whether they are higher or lower. This can be problematic in cases of unbalanced studies, where only data from one treatment group or one visit are available, which might be the case in opportunistic studies. Higher variability is then introduced during these comparisons with NCA, which might skew the results. With pharmacometrics, parameter variability can be effectively captured and quantified, and the influence of specific intrinsic or extrinsic patient-related characteristics can be quantified and accurately attributed to the affected parameter. Pooling data from all individuals enables to inform predictions in case of unbalanced studies where data on some occasions for some groups might not be available.
Additionally, with pharmacometrics, new scenarios can be simulated, enabling the assessment of the appropriateness of innovative dosing regimens.

1.5 Therapeutic applications of pharmacometrics in this thesis

This thesis explores varied populations and therapeutic areas where pharmacometrics was used to characterize PK and optimize dose.

1.5.1 Dose optimization of cefazolin in South African children undergoing cardiac surgery with cardiopulmonary bypass

1.5.1.1 Cardiopulmonary bypass

Paediatric cardiopulmonary bypass (CPB) surgeries are conducted to repair congenital heart defects or acquired heart conditions that require an operation to be performed on the heart or its vessels. In such procedures, the CPB device temporarily takes over cardiac and respiratory functions. The heart is rendered ischemic by clamping the aorta and its activity arrested by a cardioplegia solution to decrease oxygen consumption. The patient is connected to the CPB device by means of cannula – venous cannula collect the venous blood and via gravity deposit it in a reservoir, then a systemic pump pumps the blood into a heat and a gas exchanger, and the oxygenated blood is returned back to the arterial circulation via arterial cannula. Some part of the oxygenated blood is mixed with cardioplegia solution, to arrest the heart, then is returned back to the heart via a separate pump. Priming solutions are added to the CPB circuit prior to connecting to the patient to deair the circuit so that there is no risk of gas embolism. Priming solutions may consist of electrolytes, glucose, colloidal solutions such as albumin, and depending on the patient's pre-bypass haemoglobin levels, whole blood (Sarkar and Prabhu, 2019).

PK could be altered during CPB due to various factors. Hemodilution due to the priming solutions of the CPB circuit could lead to reduction in concentration of drug and other blood components, including plasma proteins, at initiation of the CPB. Lower protein binding might be observed due to the reduced concentration of plasma proteins as well as due to the use of the anticoagulant, heparin, which could increase free fatty acids by activating lipase, leading to competition with albumin binding drugs since free fatty acids bind to albumin. An

inflammatory response is induced during CPB because blood is flowing through non-endothelial tubes and inflammatory mediators can affect drug metabolism or distribution. Hypothermia, often induced during such surgeries to protect organs, could reduce rates of metabolic enzymatic reactions (Paruk *et al.*, 2017; van Saet and Tibboel, 2023). Furthermore, there could be drug loss in the CPB circuit due to adsorption of drug onto the tubes of the circuit. The extent of adsorption could depend on the type and length of the tubing used (Zeilmaker-Roest *et al.*, 2020).

1.5.1.2 Surgical site infections

Patients who develop surgical site infections (SSIs) post-surgery face an elevated risk of mortality, where the mortality risk is 2-11 times higher, emphasizing the importance of effective surgical antibiotic prophylaxis. Reports indicate a higher incidence of SSIs in developing countries, with cumulative incidence per 100 surgical procedures of up to 23.6, compared to 2.9 in European countries and 2.6 in the USA (Morad Asaad and Ahmad Badr, 2016). In paediatric cardiac surgeries, SSI rates range from 1.7 to 8% with risk factors including prematurity, younger age, longer surgery, suboptimal antibiotic prophylactic dosing, and surgeries with CPB (Izquierdo-Blasco *et al.*, 2015). SSIs commonly manifest within 30 days post-surgery and can be superficial or deep tissue infections (Borchardt and Tzizik, 2018). Methicillin-Sensitive *Staphylococcus aureus* (MSSA) is the most common pathogen isolated in both superficial and deep SSIs. Ensuring effective infection prophylaxis is essential to prevent surgical site infections. Cefazolin is an antibiotic used for surgical prophylaxis since it provides adequate coverage against pathogens that cause SSIs, including MSSA (Bratzler *et al.*, 2013). However, cefazolin PK could be altered during surgeries with CPB, resulting in lower plasma concentrations, which could be a risk factor for prophylactic under coverage (Paruk *et al.*, 2017).

1.5.1.3 Cefazolin Pharmacology

Cefazolin is a first-generation cephalosporin, used for prevention and treatment of bacterial

infections. It has broad spectrum activity against gram positive bacteria and has some activity against gram negative bacteria. It is a first line antibiotic of choice in MSSA infections. Moreover, it is often used for prophylaxis of SSIs in various types of surgeries. MSSA is claimed to be the causative agent in more than 50% of SSIs occurring in cardiac surgeries (Engelman *et al.*, 2007). Cefazolin is available as intravenous or intramuscular injection. It is ~80% albumin bound and has a small Vd (~ 10 L/70 kg). It is a hydrophilic drug, with 80-100% excreted unchanged renally by glomerular filtration within 24 hours. To a small extent, it is also excreted via tubular secretion and biliary excretion. Its half-life is short, ~1.8 h (Reller *et al.*, 1973).

Cefazolin is a time-dependent antibiotic, where the time above the minimum inhibitory concentration (MIC) is the efficacy metric. For surgical prophylaxis, free cefazolin concentrations above four times the minimum inhibitory concentration (MIC) of common pathogens for 100% of the dosing interval ($100\%\ fT_{>4\times MIC}$) throughout the surgical duration until a few hours post-skin closure are recommended since intraoperative contamination can occur at any point during surgery. Current guidelines suggest cefazolin dosing for surgical prophylaxis in children at 25-50 mg/kg, within 1 hour of skin incision, with redosing after 4 hours if surgery exceeds two half-lives or in cases of excessive blood loss (Bratzler *et al.*, 2013). Dosing guidelines for surgeries with CPB are lacking. There have been reports in adults that there is association of prolonged high cerebrospinal fluid concentrations of cefazolin with seizures. These case reports have been after multiple doses of cefazolin, with the drug discontinued after occurrence of seizures 2-12 days post initiation of therapy, and serum levels measured post discontinuation of treatment 8-28 hours after the last dose. The lowest serum concentration reported was 360 mg/L (T. P. Bechtel, Slaughter and Moore, 1980).

1.5.2 Population pharmacokinetics of rifabutin among children with HIV and TB on lopinavir/ritonavir-based antiretroviral therapy

1.5.2.1 HIV/TB co-infection

Co-infection with both tuberculosis (TB) and HIV is a prevalent and deadly combination, with each disease accelerating the progression of the other. People with HIV face a higher likelihood, approximately 16 times more, of developing TB compared to those without HIV, and it is the primary cause of mortality among people with HIV (World Health Organization, 2023). Low-and-middle-income countries (LMICs) are disproportionately affected, with 82% of TB deaths among HIV-negative and HIV-positive people occurring in African and Southeast Asian countries in 2021. Of the 187 000 TB-related deaths globally among HIV-positive people in 2021, 11% were children (World Health Organization, 2022). TB/HIV co-treatment is challenging in both adults and children due to potential drug interactions.

Guidelines for paediatric HIV treatment have included dolutegravir-based antiretroviral treatment (ART) as the first line treatment regimen. Lopinavir/ritonavir (LPV/r)-based HIV regimen is an alternative first line (ABC+3TC+LPV/r) and a preferred second line (AZT+3TC+LPV/r (ATV/r)) regimen for children who are above 4 weeks and below 10 years old and a preferred second line regimen for adolescents above 10 years old and above 30 kg (AZT+3TC+ATV/r (LPV/r)) (World Health Organization, 2021). Rifampicin, a mainstay of standard TB treatment, is a common perpetrator of drug interactions with HIV drugs, through potent induction of cytochrome P450 enzymes (such as CYP3A4, CYP2C9, CYP1A2), UDP-glucuronosyltransferase (UGT) enzymes, and transporter proteins such as P-gp. For example, it leads to significant reductions in dolutegravir concentrations, necessitating a change in dosing frequency to 50 mg BID rather than 50 mg OD (Cattaneo and Gervasoni, 2023), and significantly reduces concentrations of ritonavir-boosted protease inhibitors (PI/r) such as LPV/r. To overcome the interaction, dose adjustment of LPV/r (either doubling the dose or super-boosting with ritonavir) can be done but could lead to hepatotoxicity. In children, the unavailability and poor palatability of standalone ritonavir makes this option difficult. Another

option is to substitute rifampicin with rifabutin, a less potent inducer within the rifamycin class, which does not reduce LPV/r concentrations to sub-therapeutic levels and can be used concomitantly (Boulanger, Hollender, Farrell, Stambaugh, Maasen, Ashkin, Symes, Luis A. Espinoza, *et al.*, 2009; Lan *et al.*, 2014; Naiker *et al.*, 2014; Moultrie *et al.*, 2015). Another perpetrator during TB/HIV co-treatment is ritonavir, a potent inhibitor of CYP3A4 and P-gp, while inducing other enzymes and drug transporters. Ritonavir can increase exposure to rifabutin and its metabolite, 25-desacetyl rifabutin (des-rifabutin), which are substrates of CYP3A4, and in adults, the dose of rifabutin is reduced from 300 mg OD when it is used for TB alone to 150 mg OD during co-treatment with LPV/r. In children, a rifabutin dose of 10-20 mg/kg/day is used for treating TB and Mycobacterium Avium Complex (MAC) (Department of Health and Human Services, 2023), but there is lack of adequate data regarding optimal dosing during co-treatment with LPV/r (Moultrie *et al.*, 2015).

1.5.2.2 Rifabutin Pharmacology

Rifabutin is a rifamycin antibiotic which has been used to treat MAC infections and TB infections. Compared to the other rifamycins, rifabutin is highly lipophilic, which improves its tissue penetration and is responsible for its different PK. It has a high steady state Vd (V_{ss}/F) of 9 L/kg and a long terminal half-life of 45 h, in adults. Oral bioavailability after a single dose is 20%, attributed to high biliary excretion and pre-systemic metabolism. Rifabutin is up to 95% eliminated by metabolism, mainly through hydroxylation by CYP3A4 and through deacetylation by arylacetamide deacetylase (AADAC) enzymes. 25-O-desacetyl rifabutin (des-rifabutin) is a major active metabolite from the AADAC pathway and is further metabolized by CYP3A4. Rifabutin can induce hepatic enzymes, such as CYP3A4, and efflux transporters, such as P-gp. It can reduce its own exposure with chronic administration or that of concomitantly administered substrates of the enzyme. Up to 42% reduction in rifabutin exposure was reported from day 1 to day 28 at rifabutin doses ranging from 300 – 1200 mg in adults with HIV, and the extent of

exposure reduction was dose independent. This induction is less potent than that reported for rifampicin, which makes rifabutin a better option to reduce drug-drug interactions during co-treatment with CYP3A4 substrates. The PK profile of rifabutin is similar in children to that of adults, albeit with a shorter half-life (Blaschke *et al.*, 2006).

Although the clinical relevance of des-rifabutin has mainly been related to its activity, since it contributes to the therapeutic effects of rifabutin, high rifabutin and des-rifabutin exposures can potentially cause haematologic abnormalities, such as neutropenia. The exact mechanism of these adverse effects is unclear but may involve direct toxicity to blood cells or indirectly through immune mediated processes (Moultrie *et al.*, 2015; Crabol *et al.*, 2016; Peloquin, 2023). Concomitant administration of drugs that might increase rifabutin exposure through inhibition of its metabolism, thus require dose adjustment or monitoring of adverse effects.

1.5.3 Application of a population pharmacokinetic model as a tool for monitoring adherence in heart failure patients

1.5.3.1 Heart failure

A universal definition of heart failure was proposed in 2021 as, "a clinical syndrome with symptoms and/or signs caused by a structural and/or functional cardiac abnormality and corroborated by elevated natriuretic peptide levels and/or objective evidence of pulmonary or systemic congestion" (Bozkurt *et al.*, 2021). The global prevalence of heart failure was documented at 56.2 million in 2019 (Yan *et al.*, 2023). The prevalence of heart failure has increased in African countries due to lifestyle changes that amplify risk factors for cardiovascular diseases, including obesity, smoking, diet, hypertension, and diabetes, as well as coronary artery disease. In sub-Saharan Africa, approximately 30% of admissions to cardiac units are attributed to heart failure (Gtif *et al.*, 2021).

There is dearth of data regarding heart failure outcomes in LMICs , with most of the data coming

from North America and Europe. The International Congestive Heart Failure (INTER-CHF) study, collecting data from 5823 patients across 6 geographic regions including Africa, Asia, South America, and the Middle East, reported that the highest mortality rate was in Africa, at 34% 1-year post follow-up, even after adjusting for cardiac and non-cardiac variables, including demographics. They concluded that the variations in regional mortality rates in heart failure could be due to quality of health care access, or environmental and genetic factors (Dokainish *et al.*, 2017).

Noncompliance with medication has been identified as the most reliable predictor of hospitalization among heart failure patients in the United States (Riegel and Knafl, 2013). Medication nonadherence is when a patient does not follow their prescribed medication regimen, either by not filling the prescription, not taking it at the recommended dose or dosing interval or discontinuing treatment prematurely. This lack of adherence can lead to serious consequences, potentially causing negative clinical outcomes that might be erroneously attributed to treatment failure rather than nonadherence. Reports on adherence to cardiovascular medications vary, from 10% to 99% adherence, with limited data available from African countries (van der Wal and Jaarsma, 2008; Verena *et al.*, 2010; Oosterom-Calo *et al.*, 2013; Shah *et al.*, 2015). Understanding the impact of adherence is crucial to address poor treatment outcomes in these regions, where there is a high mortality rate without a clear explanation (Dokainish *et al.*, 2017).

1.5.3.2 Traditional versus model-based methods of monitoring adherence

Traditional methods of evaluating patient adherence have included both indirect and direct methods. Indirect methods involve patient self-reporting, pill count, or assessing prescription refill rates, while direct methods include directly observed therapy and biochemical screening (measuring drug concentration in a biological sample). Indirect methods, being subjective, are susceptible to bias and necessitate accurate documentation, such as refill dates or dispensed

amounts. They may also overestimate adherence due to patient influence or inaccurate documentation. On the other hand, direct methods are more precise and objective but may pose challenges in implementation and incur higher costs (Hawkshead and Krousel-Wood, 2007).

Observing patients directly while taking their medication is feasible only when patients can visit the clinic and could be impractical for chronic treatment. Traditional biochemical screening determines whether the drug can be detected in a biological sample at a concentration equal to its lower limit of quantification (LLOQ) or limit of detection (LOD). This method is qualitative and presents several drawbacks: (i) It relies on the sensitivity of the assay, meaning a patient classified as nonadherent might be considered adherent with a more sensitive assay. (ii) Using the LLOQ or LOD for all patients identifies extreme cases of nonadherence, neglecting interindividual pharmacokinetic differences. (iii) Adherence is evaluated at a single point in time, making it unable to detect irregular adherence, leading to potential bias from the "white coat effect," where patient adherence increases around the time of clinic visits (Hawkshead and Krousel-Wood, 2007; Groenland *et al.*, 2021).

Model-based quantitative methods can be used to improve adherence assessment. Measured plasma concentrations can be compared with model predictions, accounting for covariates such as weight, renal function, and dose. If the patient is adherent, the measured concentration would be expected to be equal to or higher than the predicted concentration (Groenland *et al.*, 2021).

1.5.3.3 Enalaprilat pharmacology

Enalapril belongs to the class of drugs known as angiotensin-converting enzyme inhibitors (ACEIs), commonly used to treat conditions such as hypertension, heart failure, and kidney diseases. ACEIs function by promoting vasodilation and lessening the heart's workload, through the prevention of sodium and fluid retention. They do this by binding to angiotensin-converting enzyme, found in plasma and in tissues, to prevent activation of Angiotensin I, which is a potent

vasoconstrictor and also mediator of the release of aldosterone, which plays a role in sodium and fluid retention (Zaman, Oparil and Calhoun, 2002; Yancy *et al.*, 2017).

Enalapril exhibits favourable absorption, approximately ranging from 53% to 74%. The maximum concentration (C_{max}) is reached around 1 hour, and by 4 hours, it becomes undetectable due to rapid CL. Enalapril is a prodrug and undergoes conversion into its active metabolite, enalaprilat, through de-esterification in the liver by carboxylesterase 1 (CES1). This enzyme displays variability in expression and activity among individuals due to genetic variation. Carriers of the loss-of-function variant have been noted to have reduced exposure to the active metabolite enalaprilat, with approximately 31% lower C_{max} and around 28% lower $AUC_{0-\infty}$ (Wang *et al.*, 2016; Her *et al.*, 2021). Approximately 36-44% of the administered enalapril dose is bioavailable as enalaprilat, with C_{max} observed 3-4 hours after enalapril administration. Enalaprilat demonstrates biphasic CL, featuring a rapid initial phase with a half-life of 2-6 hours and a prolonged terminal phase with a half-life of ≥ 36 hours. The fast initial phase reflects renal CL of enalaprilat, primarily through glomerular filtration. In contrast, the extended terminal phase is believed to lack contribution to drug accumulation but holds pharmacodynamic significance, indicating a slower equilibration with tissues. Achieving steady-state concentrations of enalaprilat takes approximately 30-60 hours, and it remains detectable in serum around 96 hours post-dose. In cases of renal impairment, enalaprilat plasma concentrations may increase due to reduced renal CL, as well as heightened bioconversion, as observed by increased and delayed C_{max} of enalaprilat. Significant correlation of enalaprilat exposure and glomerular filtration rate (GFR) has been reported for GFR < 60 ml/min (Lowenthal *et al.*, 1985; Kelly *et al.*, 1986).

1.5.4 Population pharmacokinetics of esomeprazole in patients with preterm preeclampsia

1.5.4.1 Preeclampsia

According to WHO reports, 14% of maternal deaths globally are attributed to hypertensive

disorders, of which preeclampsia and eclampsia are leading causes (World Health Organization, 2018). The incidence of preeclampsia is seven times higher in developing countries, possibly due to the risk factors including race and ethnicity (more prevalent in black demographic), diet, obesity, environmental conditions, very young or very old pregnancies, a previous or family history of preeclampsia, and a history of cardiovascular or metabolic disorders such as diabetes. Further, developing countries have more severe outcomes, possibly associated with poor or delayed access to health care resources (Khan *et al.*, 2022).

Preeclampsia is associated with maternal systemic vascular dysfunction and inflammation, leading to hypertension, due to inadequate placental implantation. It is diagnosed by new-onset hypertension and one or more signs of end-organ injury presenting after 20 weeks of gestation. Multiple end organs could be injured, including the kidneys leading to albuminuria; the brain, which can cause visual disturbances and seizures (eclampsia), and the haematological system, causing hemolysis and coagulopathy. It also affects the foetus, restricting growth, and could cause low-birth weight or still birth. Although expected to resolve postpartum, there could be long term consequences on maternal health, predisposing to a higher risk of cardiovascular and cerebrovascular diseases. When preeclampsia occurs before 34 weeks of gestation, it is called ‘early-onset’ or ‘preterm’, which is more severe in terms of disease progression compared to the late-onset type. To date, the only treatment for preeclampsia is delivery, which could increase the likelihood of neonatal complications in preterm cases (Overton, Tobes and Lee, 2022).

Preeclampsia is initiated by a hypoxic condition in the placenta. In the initial stages of placental development, placental cells are anticipated to migrate to the uterine arteries and modify the endothelial lining as well as the smooth muscles. This re-modeling aims to decrease resistance in the uterine arteries, facilitating increased blood supply to the placenta. However, in cases of preeclampsia, there is insufficient modification of the uterine arteries, due to inadequate invasion

by placental cells to the uterine smooth muscles. Consequently, the placenta becomes hypoxic, triggering the release of free radicals, pro-inflammatory biomarkers and disrupting the regulation of circulating angiogenic factors it releases. The concentrations of antiangiogenic soluble substances, such as soluble fms-like tyrosine kinase-1 (sFlt-1) and soluble endoglin (sEng), rise, with a more pronounced increase observed in severe preeclampsia. Concurrently, proangiogenic factors like vascular endothelial growth factor (VEGF) and placental growth factor (PlGF) decrease. sFlt-1 binds to circulating vascular endothelial growth factor, restricting its ability to promote vascular homeostasis. Moreover, sFlt-1 increases sensitivity to angiotensin II and impairs endothelial nitric oxide synthase (eNOS) phosphorylation, leading to sustained vasoconstriction. sEng binds to the endothelial cell receptor endoglin, disrupting signalling and homeostasis. This, in turn, results in maternal systemic endothelial dysfunction and organ damage, in addition to systemic inflammation (Tjoa *et al.*, 2011; Marín *et al.*, 2020).

1.5.4.2 Proton pump inhibitors for preeclampsia

Proton pump inhibitors (PPIs) are used to manage hyperacidity conditions and are prescribed during pregnancy. Their potential application in preeclampsia was hypothesized to involve the upregulation of heme-oxygenase-1 (HO-1), leading to a reduction in the secretion of soluble fms-like tyrosine kinase-1 (sFlt-1) and soluble endoglin (sEng). This effect was believed to occur through the decreased expression of hypoxia-inducible factor-1α, coupled with their antioxidant and anti-inflammatory properties. Preclinical studies testing this hypothesis demonstrated that proton pump inhibitors diminished the secretion of sFlt-1 and sEng, while enhancing the expression of vascular endothelial growth factor (VEGF) in primary placental cells and explants in a concentration-dependent manner. Additionally, PPIs induced vasodilation in blood vessels obtained at caesarean from preeclamptic pregnancies and reduced blood pressure in mouse models of preeclampsia, likely mediated by the observed decrease in endothelin-1, a vasoconstrictor elevated in preeclampsia, and increasing the

expression of eNOS. Furthermore, they decreased the secretion of pro-inflammatory cytokines from placental explants and endothelial cells, upregulated antioxidant proteins, and mitigated leukocyte adhesion to umbilical endothelial cells. Esomeprazole exhibited the highest potency in eliciting these effects among the PPIs (Onda *et al.*, 2017).

A Phase II randomized, double-blind, placebo-controlled clinical trial was conducted in South Africa, involving pregnant women diagnosed with preterm preeclampsia. Participants received either esomeprazole 40 mg once daily or a placebo. No significant differences were observed in biomarker levels, time to delivery, or neonatal/maternal outcomes between the treatment and placebo groups. The study hypothesized that the lack of significant outcomes could be attributed to potential underdosing (Cluver *et al.*, 2018). Of note, the PK of esomeprazole in pregnant women has not been reported, despite the possibility of pharmacokinetic alterations during pregnancy.

1.5.4.3 Esomeprazole pharmacology

Esomeprazole is a weakly basic drug and is available as intravenous or oral formulation. The oral formulations are enteric coated, either as capsules or as multi-unit pellet system (MUPS) tablet formulations, to protect from the acidic gastric environment. Its absorption is fast, with peak concentration achieved around 1.5 hours, and bioavailability of 64% after a single dose. It is 97% bound to albumin, and this is constant over a concentration range of 2 to 20 μM (0.691 to 6.91 mg/L). It is mainly excreted via metabolism (80%), with only 1% excreted renally unchanged, and has a short half-life of ~ 1 to 1.5 h. It is metabolized by two enzymes, approximately two-thirds by CYP2C19 to 5-hydroxy esomeprazole and 5-O-desmethyl esomeprazole and the remain third by CYP3A4 to esomeprazole sulphone, which is further metabolized by CYP2C19 (Hassan-Alin *et al.*, 2000; Andersson, Hassan-Alin, *et al.*, 2001).

Esomeprazole autoinhibits its own metabolism by CYP2C19, which leads to its increased

exposure with repeated dosing, likely due to increased bioavailability and decreased CL. Further, dose non-proportionality becomes evident at higher doses, with an exposure increase exceeding 2 times (~2.64) when the dose is escalated from 20 to 40 mg after single dose (Hassan-Alin *et al.*, 2000; Andersson, Röhss, *et al.*, 2001). CYP2C19 is a polymorphic enzyme, with up to 25-35% of Caucasians and blacks carrying one copy of a loss-of-function allele, and 2-5% of Caucasians and blacks carrying two copies of a loss-of-function allele. Around 30% of blacks and Caucasians carry one copy of the extensive metabolizer genotype (El Rouby, Lima and Johnson, 2018).

Esomeprazole PK could be altered during pregnancy, associated with increased expression of CYP3A4 and reduced expression of CYP2C19, which could alter its bioavailability as well as its CL (Thummel and Lin, 2014; Feghali et al., 2018). Considering esomeprazole's increased exposure with repeated dosing and dose non-linearity at higher doses in non-pregnant individuals, its PK in these scenarios during pregnancy is unclear. Moreover, reduced albumin levels in pregnancy and in preeclampsia might reduce binding, which could increase its Vd and its CL, although this might not change its half-life (Costantine, 2014).

1.6 Thesis Justification

Identifying factors that influence treatment outcomes in varied populations is essential to guarantee that every patient receives appropriate care. Pregnancy induces various physiological changes influencing PK , while children exhibit distinctive developmental and physiological variances from adults. Variations in treatment outcomes among different racial and ethnic groups could be due to genetic, dietary, and environmental factors which could alter PK , as well as socioeconomic factors and healthcare-seeking behaviour affecting medication adherence. Ethical and safety concerns, sometimes lacking ample justification, have resulted in pregnant women and children being an understudied population in clinical trials, along with challenges in conducting clinical trials within these groups. Apprehensions about potential risks linked to treatment in clinical trials also diminish consent rates from both

participants and guardians. The fact that over 80% of clinical trials take place in developed countries means that the information on treatment outcomes may not sufficiently address the unique challenges encountered by individuals in LMICs.

As a result, there is a lack of adequate data in these populations to inform dosing decisions or improve treatment, primarily due to small sample sizes or sparse data. Dosing is often extrapolated from a non-representative population, potentially resulting in unfavourable outcomes. Pharmacometrics can be used not only during drug development to identify the safe dose for maximum efficacy, but also post-marketing in clinical settings to optimize dosing among sub-populations. It can be used to determine whether lack of efficacy or associated adverse effects may be solved by adjusting the dose or improving adherence to treatment rather than changing the drug. Pharmacometrics is a useful tool to address the challenges of limited data in understudied populations since it enables pooling data from different studies, integrating prior knowledge, incorporating physiological mechanisms behind pharmacokinetic processes, and simulating new scenarios to predict the probability of successful treatment outcomes within a population. The aim of this thesis is to employ pharmacometrics to analyse data from understudied populations, aiming to characterize PK and optimize treatment strategies.

1.7 Objectives

❖ To characterize cefazolin PK and optimize its dose for children weighing under 25 kg undergoing cardiac surgery with cardiopulmonary bypass.

❖ To analyse the PK and optimize treatment of rifabutin and its metabolite 25-O-desacetyl rifabutin during co-treatment with lopinavir/ritonavir (LPV/r) in children with tuberculosis and HIV co-infection.

❖ Utilize population PK modeling to develop a model-based method for adherence monitoring by deriving individualized reference concentrations, using sparse data from African heart failure patients and data from healthy participants taking enalapril.

❖ To investigate the PK of esomeprazole in pregnant patients with preterm preeclampsia, strengthening the data with that from healthy participants.

Chapter 2 Studies and data description

In this thesis, I analysed data from 4 studies, which are the subject of the following chapters. The analyses and results have been formatted as scientific manuscripts and, for this reason, some details on the study and data had to be omitted. In this chapter, I provide a more detailed description of these studies and the data included.

2.1 Dose optimization of cefazolin in South African children undergoing cardiac surgery with cardiopulmonary bypass

This study was a prospective observational study conducted at Red Cross War Memorial Children's Hospital (RCWMCH) in Cape Town, South Africa. The aim of the study was to evaluate paediatric prophylactic cefazolin dosing practices at RCWMCH during cardiac surgeries with cardiopulmonary bypass (CPB). Inclusion criteria were children below 25 kg, requiring cardiac surgery with CPB, informed consent obtained from guardians for study participation and sample storage. The University of Cape Town's Faculty of Health Sciences Human Research Ethics Committee approved the study (HREC/REF: 536/2011). Exclusion criteria were expected CPB time of less than 30 minutes, history of allergy to penicillins or cephalosporins, renal or hepatic dysfunction, history of recent pre-existing infection, and exposure to antibiotics in the week prior to the surgery. The standard dosing practice at RCWMCH was 50 mg/kg intravenous bolus cefazolin, given via a peripheral intravenous line at induction of anaesthesia, with a second dose given 4 hours after the first dose. For long surgeries, the second dose was intra-operative, and a third dose was given while patients were in ICU post-surgery. Moreover, some anaesthetists added a further 50 mg/kg dose of cefazolin to the CPB circuit prior to going on bypass while others did not. Participants in the study received the standard dosing, with a subset of participants receiving further cefazolin dose into the CPB circuit. Specifically, the study aimed to evaluate whether, with the standard paediatric dosing used at RCWMCH, cefazolin plasma concentrations remain above four times the minimum inhibitory concentration for common

pathogens during the intraoperative period and up to a few hours post-surgery during cardiac surgeries with CPB, and whether further cefazolin dosing into the CPB circuit should become standard practice.

Figure 2.1 shows the study schematic. Blood samples were taken prior to the first dose (baseline), 3 minutes after the initial dose (peak level), at the time of sternal incision, immediately prior to the start of CPB, once full flow CPB is established, every 30 minutes while on CPB, immediately before and after the end of CPB, at skin closure, and immediately before the next dose of cefazolin (trough level). Blood samples were stored in ice for up to 6 h after collection, then centrifuged and plasma samples stored at -70°C. Samples were analysed by validated LC-MS/MS assay at the University of Cape Town's pharmacology department. Concentrations were quantified by validated LC-MS/MS assay, with a concentration range of 0.586 to 110 mg/L. The within-day and between-day precision (coefficients of variation) was below 9% for all quality control levels during the validation, and below 8% during patient sample analysis.

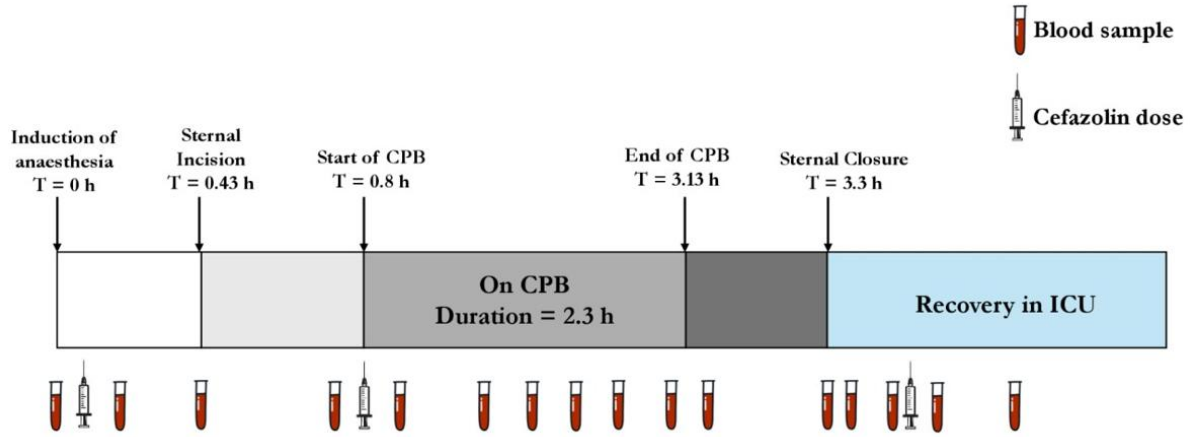

Figure 2.1. Schematic of the cefazolin study, with surgery time of 2.3 h as example

2.2 Population pharmacokinetics of rifabutin among children with HIV and TB on lopinavir/ritonavir-based antiretroviral therapy

Data for this work was obtained from prospective Phase I/II open-label PK and safety

studies conducted in three paediatric age cohorts (<1 year, 1-3 years, and 3-15 years old) enrolled from the paediatric HIV clinic at the university college hospital in Nigeria as part of the APIN PEPFAR program (Rawizza et al., 2019). The aim of these studies was to evaluate rifabutin PK and safety during co-treatment with lopinavir/ritonavir. Ethical approval was obtained from research ethics committees at the University of Ibadan/University College Hospital Nigeria, at the University of Cape Town, and Mass General Brigham, Boston. Written informed consent was obtained from the legal guardians of the study participants, and direct assent was obtained from children aged 7 years and older. Inclusion criteria for the younger cohorts (<1-year old and 1-3 years old) included antiretroviral therapy (ART)-naïve HIV infected children 2 weeks to <1-year old and 1-3 years old, for whom LPV/r-based ART is the first line regimen recommended; active TB diagnosis; and weight of at least 3 kg. The 3-15 years old cohort, on the other hand, were those who were ART-experienced with TB co-infection and required LPV/r-based ART given as second-line due to first line ART failure. Exclusion criteria for all age cohorts included baseline labs with grade 2 or higher abnormalities for ALT, AST, creatinine, platelets, hemoglobin, and ANC, suspected TB meningitis; acute respiratory distress; and taking medication that could interact with rifabutin or LPV/r.

Cohorts <1-years old and 1-3 years old initially started on TB-treatment with 20 mg/kg/day rifabutin (along with daily isoniazid 10 mg/kg, pyrazinamide 35 mg/kg, and ethambutol 20 mg/kg). After 2 weeks, they initiated LPV/r treatment according to WHO weight bands along with two nucleoside reverse transcriptase inhibitors (NRTIs), abacavir and lamivudine, during which the rifabutin dose was reduced to 5 mg/kg/day for the <1-year-old cohort and to 2.5 mg/kg/day for the 1-3 years old cohort. For both cohorts, intensive blood sampling (pre-dose, 2, 4, 8, 12, and 24 h after observed rifabutin dose) was conducted at week 2 (rifabutin steady state after TB-only treatment) as well as week 4 (rifabutin steady state after TB/HIV co-

treatment). Further intensive sampling was conducted at week 6 for the <1-year old cohort while sparse sampling was conducted at weeks 6 and 12 (pre-dose and 3 or 5 h) for the 1-3 years old cohort. For the 3-15 years old cohort, intensive sampling was conducted at weeks 2, 4, and 8 (rifabutin steady state after TB/HIV co-treatment). **Figure 2.2** shows the study schematic.

Blood samples were centrifuged within 30-60 minutes of collection, and plasma samples were stored at -80°C, after which they were analysed at the university of cape town pharmacology unit to determine rifabutin and des-rifabutin levels concurrently using validated LC-MS/MS assay. Assay accuracy was between 99.1% and 109% while precision (%CV) was less than 9.2% at all quality control standards. The calibration range in the assay was 3.91 to 1000 µg/L for rifabutin and 0.780 to 200 µg/L for des-rifabutin.

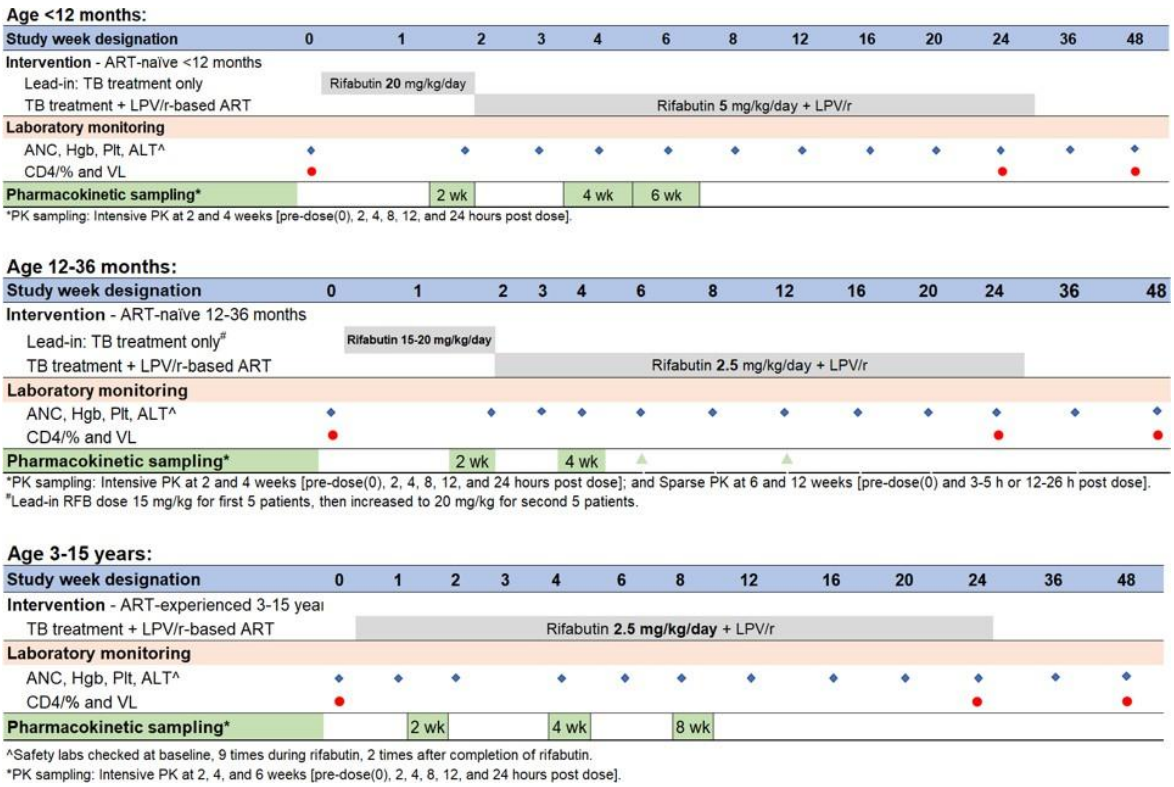

Figure 2.2. Schematic of the rifabutin-LPV/r interaction study in three paediatric age cohorts.

2.3 Application of a population pharmacokinetic model as a tool for monitoring adherence to enalapril in heart failure patients

Data for this work was obtained from a study in heart failure patients conducted at Groote Schuur Hospital in Cape Town, South Africa. The aims of the study were to develop assay of enalaprilat, the active metabolite of enalapril, in plasma and dried blood spot (DBS) using LC-MS/MS and to predict adherence in heart failure patients using a model-based adherence assessment tool. Ethical approval was obtained from the University of Cape Town Faculty of Health Science Research Ethics Committee (HREC/REF:480/2018). Inclusion criteria were patients ≥ 18-years old diagnosed with clinically stable heart failure (New York Heart Association Functional Class II-III) at steady state on the current dose of enalapril for at least 28 days. Exclusion criteria include pregnancy/3 months post-partum, anaemia, renal or hepatic failure, and hemodynamic instability. The heart failure patients included in the study had been taking 5 or 10 mg enalapril given twice daily and blood sampling was conducted at pre-dose, 1.5, 3, 5, 8, and 12 h post-dose. Enalaprilat concentrations were quantified by validated LC-MS/MS assay, validated at a concentration range of 0.200 to 200 ng/mL (Joubert et al., 2022). The accuracy was between 96.2% and 102.4% and intra-day/inter-day precision was below 10% for all quality control levels during the validation.

Due to the limited patient enrollment in the heart failure study and the consequent shortage of data, additional data was sourced from an enalapril bioequivalence study conducted by Cipla in healthy participants in India to compare two formulations of 20 mg enalapril maleate tablets, with a washout period of 7 days between the formulations. Ethics approval was obtained by an independent ethics committee (protocol number: 02-080, v: 02) and informed consent obtained from participants. The study was open label, single dose, and balanced two-arm crossover bioavailability study randomized to avoid bias in sequence allocation. Included were healthy male participants (18−45 years old and 45−90 kg), with acceptable ECG/lab

results, and abstaining from alcohol/cigarettes for at least 24 h prior to dosing and throughout blood sampling. Exclusion criteria included history of allergic responses to angiotensin converting enzymes; history of cardiovascular, renal, hepatic, pulmonary, hematological, gastrointestinal, and psychiatric disorders; clinically significant illness or hospitalization within a week to 3 months preceding study commencement; having taken prescription medications within 14 days prior to study, and chronic alcohol consumption, heavy smoking or drug addiction. Blood samples were collected at 0, 0.5, 1, 1.5, 2, 2.33, 2.66, 3, 3.33, 3.66, 4, 5, 6, 8, 12, 16, 24, 36, 48, and 72 h post-dose after both formulations. Plasma samples were analysed by validated LC-MS/MS at Medlar Laboratories, India, with a concentration range of 1.0 to 200 ng/mL.

2.4 Population pharmacokinetics of esomeprazole in patients with preterm preeclampsia

Data for this analysis were obtained from a study of pregnant women with preeclampsia and two studies in healthy, non-pregnant participants. The study in preeclamptic patients, also called the Preeclampsia Intervention with Esomeprazole (PIE) study, was conducted at Tygerberg Hospital in Cape Town, South Africa (Cluver et al., 2018). PIE was a phase II, placebo-controlled, double-blind, and randomized trial which aimed to assess the safety and efficacy of 40 mg daily esomeprazole (Nexium capsules) to prolong gestation by 5 days, improve maternal/neonatal outcomes, and reduce circulating biomarkers associated with preeclampsia. Study approval was obtained from the South African Medicines Control Council. Inclusion criteria were pregnant women with single pregnancies with diagnosis of preterm preeclampsia (between 26- and 32-weeks gestation) for whom expectant management (i.e., hospital admission with close maternal/foetal surveillance ending at 34 weeks of gestation with delivery) had been recommended. Exclusion criteria were maternal or fetal compromise necessitating immediate delivery (such as eclampsia, severe

hypertension, cerebrovascular event, severe renal impairment, pulmonary edema, HELLP syndrome, disseminated intravascular coagulation), possibility of foetal malformation, and current use or contraindication to proton pump inhibitors. A subgroup of patients in the esomeprazole treatment arm underwent pharmacokinetic sampling after the first dose at 0.25, 0.5, 0.75, 1, 1.5, 2, 4, 8, 10, and 24 h. A validated LC-MS/MS analysis was used to quantify esomeprazole concentrations. Intra-and inter-day accuracies and precision were >85% and <15%, respectively. The LLOQ was 1 ng/mL.

Further data, sourced from two studies in healthy, non-pregnant participants, was included to strengthen the modeling work. One study, conducted at the University Hospital of Iceland, aimed to describe the PK of esomeprazole after single and multiple dosing (day 5) in males and females as well as gastrin levels in response to treatment in males and females (Helgadóttir et al., 2021). Study ethical approval was obtained from the National Bioethics Committee of Iceland (VSN-15-080). Included were adult participants (20-50 years old) without a history of gastrointestinal disorders or use of treatment for acid suppression. Exclusion criteria were obesity (BMI>30 kg/m2), chronic infectious diseases, pregnancy, and participants taking CYP450 enzyme inducers or inhibitors. This was an unblinded and single arm trial where participants received 40 mg esomeprazole (Actavis) tablet under fasting conditions for five days. Blood sampling was performed after day one and day five of treatment at pre-dose, 0.5, 1, 1.5, 2, 2.5, 3, 3.5, 4, 5, 6, 7, and 8h post-dose. Sample analysis was performed by LC-MS at a verified laboratory at an Iceland pharmaceutical company and the calibration range was 5.03−4028 ng/mL.

The second study was conducted at the Haga teaching hospital in the Netherlands and aimed to compare the PK of 40 mg esomeprazole (Nexium MUPS) and 40 mg pantoprazole relative to their acid-inhibitory effects and CYP2C19 phenotype (Hunfeld et al., 2010). Ethical

approval was obtained from the institutional review board of the hospital. Inclusion criteria were adults (18–35 years old), with normal lab results as well as Helicobacter pylori negative, normal gastric pH (pH < 4 for more than 70% of the time in a 24h period), and known CYP2C19 genotype. Excluded were pregnant women, those with gastrointestinal disorders, with BMI which deviates more than 15% of normal BMI (18.5–25 kg/m2), and with history of drug/alcohol abuse. The trial was two-way, randomized, crossover, and investigator blinded. Participants were randomized to five-day treatment with 40 mg esomeprazole or 40 mg pantoprazole once daily, and after a 14-day washout period, were switched to the other treatment. Unlike the PIE study and the Icelandic study were meals were given 2 h post-dose, in this study, meals were 5 min post-dose. Pharmacokinetic sampling was performed on day one and day five at pre-dose, 0.083, 1, 2, 3, 4, 5, 6, 7, and 8 h post-dose. Sample analysis to quantify esomeprazole and pantoprazole levels using HPLC at the Central Hospital Pharmacy laboratory. For our analysis, we only used the esomeprazole concentrations, and the calibration range was 0.025–2.5 mg/L. Inter-day precision of the assay was below 11.1% while accuracy was -4.0% to +2.0%.

Chapter 3 Methodology

In this thesis, pharmacometrics was used to analyse pharmacokinetic data obtained from understudied populations. This chapter provides an overview of pharmacometrics.

3.1 Pharmacometrics

Pharmacometrics applies mathematical and statistical models to quantify disease, trial, or drug information to guide decisions in drug development and clinical use. Disease models characterize the time course (progression) of disease and can quantify factors that affect the time course, such as treatment. Trial models are used to predict the impact of different study designs on the outcomes of clinical trials. The most common models in pharmacometrics, drug models, are used to determine pharmacokinetic (PK) and pharmacodynamic (PD) parameters, using data from clinical trials, observational studies, or preclinical investigations. PK examines the time course of drug exposure within the body, focusing on the rate and extent of absorption from the site of administration, distribution to tissues, and elimination through metabolism and/or excretion. On the other hand, PD establishes a correlation between drug exposure and the rate and extent of therapeutic or adverse response.

Population PK models incorporate data from all individuals in a study simultaneously to determine population parameters (parameters that describe the PK curve for the population) and variability parameters (parameters that describe how the PK curve differs among and within individuals in the population). Additionally, covariates that influence variability are identified, such as age, weight, sex, genotype, organ function, drug-drug interactions, and food. Beyond their descriptive capabilities, these models can be used to simulate exposures in novel scenarios, such as new populations or alternative dosing regimens, without the need for initiating a new clinical trial. The exposures derived from PK models can also be linked to response, to quantify the typical rate and extent of response, along with response variability

and potential covariates (PK-PD models). The models employed in pharmacometrics are referred to as nonlinear mixed-effects models.

3.2 Nonlinear mixed-effects models to describe pharmacokinetics

The term ‘nonlinear’ describes the underlying nonlinearity in the relationship between the dependent and independent variables in the model, while the term ‘mixed-effects’ refers to the nature of the parameters used to describe the data: fixed effects parameters and stochastic or random effects parameters . Fixed effects parameters are population parameters which are the same among individuals in the population, and any variation can be explained by covariate effects. Random effects parameters capture the variability in PK parameters that are unexplained by covariates, accounting for interindividual and interoccasion parameter variability as well as residual unexplained variability, which accounts for measurement or data collection errors or model misspecification.

Nonlinear mixed-effects models have three components:

3.2.1 Structural model

PK structural models can be empirical, semi-mechanistic, or fully mechanistic. In empirical PK models, compartments are used as mathematical depictions of the extent and rate of drug absorption and disposition (distribution, and elimination) from the body. Semi-mechanistic models integrate physiologic parameters to some compartments within the empirical model, e.g., including a liver compartment with parameters derived from physiologic liver blood flow rate and extraction. In fully mechanistic, or PBPK models, all parameters (e.g., compartment volumes, flow rates, rate of enzyme expression) are based on physiologic processes.

Empirical structural models are described in this thesis.

a. Absorption models

Absorption models describe the rate at which a drug appears in plasma (Ka) after extravascular administration. Bioavailability measures the proportion of the dose reaching the plasma unchanged. Intravenous (IV) administration serves as the reference standard for 100% bioavailability. In the absence of IV data, when only extravascular data are available, it is not possible to separately identify bioavailability and disposition parameters such as CL and Vd. Consequently, by convention, bioavailability (F) is fixed to 1, and only relative parameters—apparent CL (CL/F) and apparent Vd (Vd/F)—can be estimated, rather than the true parameters. Attempting to estimate both CL and F under these conditions would result in a non-identifiable model, e.g., multiple combinations of CL and F can yield the same CL/F value. Absolute bioavailability can be estimated when both IV and extravascular data are available, while relative bioavailability can be determined when data from multiple extravascular formulations are included. In this thesis, bioavailability was fixed to 1 while its variability was estimated to account for differences in drug exposure that are unrelated to CL or Vd (Mould and Upton, 2013).

There are various ways to model absorption, and the most common methods include:

- First-order absorption with or without a lag time parameter to characterize delay in absorption
- Transit compartment model followed by first order absorption, where the drug must pass through a series of absorption compartments before reaching the plasma (Savic et al., 2007). This is a better depiction of delay in absorption as it mimics the gradual drug appearance in plasma rather than the sudden appearance in plasma after a certain delay (i.e., with a lag time parameter), and is flexible to account for individuals who may have significant absorption delays compared to others.
- Zero-order absorption where absorption is modelled as an infusion (zero order with constant rate) where the time or rate of infusion can be estimated.

- ❖ Mixed-order absorption (sequential zero-order and first-order absorption), where the dose is modelled as an infusion into the absorption compartment, and then absorbed into the central compartment by a first order process.

b. Disposition models

Disposition models describe the rate at which the drug disappears from plasma, which could be through distribution initially and a combination of distribution and elimination in the latter phase of the PK profile. Plasma concentration declines over time exponentially (**Equation 1**), and this decline can be described using one or more differential equations. Semilog plots of concentration versus time of the observed data indicate the number of differential equations that need to be used, or the number of compartments within the disposition model. For example, a straight line on a semilog concentration–time plot typically suggests a one-compartment model, whereas a curve or biphasic decline—characterized by a steep initial slope followed by a shallower terminal slope—indicates a two-compartment model. However, when data are sparse in both the early (absorption/distribution) and terminal phases, semilog plots may fail to reveal the underlying model structure due to insufficient resolution of multi-exponential kinetics. The distribution phase in a two-compartment model occurs shortly after absorption and may overlap with it, particularly when absorption is slow. If early data are lacking, this distribution phase may be missed entirely, leading to incorrect model classification as a one-compartment system. In such cases, the model can become structurally non-identifiable, meaning that different compartmental models may fit the data equally well, but with unreliable or unstable parameter estimates. Therefore, model structure must often be justified using external evidence when the dataset alone is uninformative. Reviewing literature from prior studies involving the same or similar drugs with rich sampling can guide model selection and reveal whether distribution delays (e.g., deep tissue distribution) are expected. Bayesian methods can also be valuable in these situations,

allowing prior parameter distributions from previous studies to be formally incorporated into the model. By evaluating how well these priors align with the current data, a posterior distribution of parameters is generated—effectively combining historical and new information to improve parameter stability and inference (Mould and Upton, 2012).

$$C(t) = \left(\frac{Dose}{V_d}\right) \times e^{-\left(\left(\frac{CL}{V_d}\right)\times t\right)}$$

Equation 1

Where C(t) is the concentration at time t, Vd is volume of distribution and CL is clearance.

c. The Population PK (PopPK) structural model

The PopPK structural model aims to predict the observed concentration-time profiles from all individuals in a population simultaneously. **Equation 2** shows how model predictions are linked to parameters while accounting for covariates and prediction error.

$$Y_{ijk} = f\left(\phi_{ijk}; X_{ijk}\right) + \varepsilon_{ijk}$$

Equation 2

Where i denotes the i^{th} individual, j denotes the j^{th} occasion within each individual, and k denotes the k^{th} observation within each occasion of each individual.

The function $f(\Phi_{ij} ; X_{ijk})$ describes the individual predictions which depend on the model-estimated vector of parameters, i.e., Φ_{ij}, as well as the independent variables, X_{ijk}, which include the dose, dosing, and sampling times, as well as covariates. Y_{ijk} are the model predicted values for each individual on each occasion and time point. ε_{ijk} describes the remaining deviation between individual predicted values and observed values.

3.2.2 Statistical model

The statistical model denotes the unexplained variability of parameters within the population PK model using probability distributions. For PK parameters, lognormal distributions are usually used since this constrains them to be positive in accordance with expected plausible physiological values, but other distributions maybe selected depending on the expected range

of values. Random variability occurs across two levels: at the parameter level (Level one random effects (L1) which describe between-subject or between-occasion variability) and at the observation level (Level two random effects (L2) which describe residual unexplained variability).

- **Level one random effects (L1)**

In PK studies, concentration data is collected longitudinally at various time points across the individuals in the study. The repeated concentration measures within each individual collected over time are correlated and grouped together by the individual identifier (ID) and occasion data items.

The L1 random effects account for this correlation.

a. Between-subject variability (BSV):

BSV describes variability between the population prediction and individual predictions.

$$\theta_1 = \theta \times e^{\eta_i}$$

Equation 3

Where θ_i is the individual parameter (for the ith individual within the population) and θ is a population parameter.

Part of the deviation between the predictions of individual parameters and the population parameter could be explained by covariates associated with the ith individual, with the remaining unexplained variability described with η_i, the random effect at the individual level. η_i is a random variable assumed to be normally distributed with a mean of 0 (mean around the 'true' population value) and variance of ω^2. Thus, for a population, each parameter follows a lognormal distribution with the estimated parameters being a typical value of θ and a variance of ω^2. Since the variance is included into the model with a log-normal distribution and is not in the same space as the typical value, the variance is reported as a coefficient of variation (CV%) in the original scale using the equation below:

$$CV\ (\%) = \sqrt{exp(\omega^2) - 1} \times 100\%$$

Equation 4

b. Between-occasion variability (BOV):

BOV describes parameter variability within an individual overtime, e.g., absorption parameters are highly variable even within an individual on different occasions due to variabilities in gastric pH, gastric and intestinal motility, activity of digestive enzymes, and liver metabolism. For instance, PK sampling consists of obtaining blood samples after a dose at various pre-defined time points throughout a PK Day, but a baseline sample is also taken prior to the PK Day dose, which is a trough sample from a dose which is often unobserved and is a different occasion. This makes it essential to add BOV on absorption parameters (Karlsson and Sheiner, 1993). For other parameters, such as CL, it might be necessary to add

BOV if the PK sampling is performed at different visits which might be widely apart (e.g., days or weeks apart) and it is expected that the PK might change due to autoinduction or autoinhibition or due to patient health improvement with treatment. BOV is estimated assuming each occasion has its own random effect, but all occasions follow the same distribution (same variance).

$$\theta_{ij} = \theta_i \times e^{\eta_{ij}}$$

Equation 5

Where θ_{ij} is the individual parameter at the jth occasion, θ_i is the individual parameter for the i^{th} individual , and η_{ij} is the random effect for that individual at the jth occasion.

The incorporation of BOV in NONMEM necessitates adjustments to the dataset depending on the chosen NONMEM subroutine (ADVAN). ADVANs utilizing approximations or user-defined differential equations (ADVAN 6, 8, 9, 13, 14, 15) differ from lower ADVANs by estimating changes for incremental time points between records while looking one record ahead. Unlike lower ADVANs that perform estimation at each observed record (time point) and carry the prediction forward, these ADVANs estimate the profile backward. In cases of consecutive occasions with different times (e.g., occasion 1 at time -0.0833 and occasion 2 at time 0), parameter values from occasion 2 are carried backward. Therefore, to prevent the loss of information and safeguard the previous record with different occasions or time-varying covariates, it is crucial to include a dummy record between the two records. This dummy record should have the same occasion as the previous record, but other values, including time, should be the same as the next record, with an event identifier (EVID = 2) indicating that it is a dummy (non-observation) record. This is demonstrated using an example dataset below.

For lower ADVANs (1,2,3,4,5,7,10,11,12), which use a closed form solution, the **"Last Observation Carried Forward (LOCF)"** method is used for predictions in NONMEM. As

shown below, between -0.0833 h and 0 h, the PK parameter applied for predictions will be taken from occasion (OCC) 1 until 0 h when the PK parameter from occasion 2 will be applied.

ID	EVID	MDV	TIME	AMT	OCC	WHAT
1	1	1	-24	100	1	Yesterday dose
1	0	0	-0.0833	0	1	Pre-dose sample
1	1	1	0	100	2	PK day dose
1	0	0	2	0	2	2 h sample
1	0	0	4	0	2	4 h sample

For ADVANs which use differential equations (6,8,9,13,14,15), NONMEM uses the **"Next Observation Carried Backward (NOCB)"** for predictions. As shown below, between -0.0833 h and 0 h, the PK parameter applied for predictions will be taken from occasion 2 until 0 h, which will also be taken from occasion 2.

ID	EVID	MDV	TIME	AMT	OCC	WHAT
1	1	1	-24	100	1	Yesterday dose
1	0	0	-0.0833	0	1	Pre-dose sample
1	1	1	0	100	2	PK day dose
1	0	0	2	0	2	2 h sample
1	0	0	4	0	2	4 h sample

To protect switching occasion within the same individual, dummy records are inserted just before the change in occasion. These will have EVID=2 with TIME and DATE of the next occasion (proceeding row), but the value of occasion will be that of the previous record. In this way, NONMEM is tricked to use LOCF rather than NOCB, and each occasion keeps its own information (Denti, 2024). This is shown below.

ID	EVID	MDV	TIME	AMT	OCC	WHAT
1	1	1	-24	100	1	Yesterday dose
1	0	0	-0.0833	0	1	Pre-dose sample
1	**2**	**2**	**0**	**0**	**1**	**Dummy**
1	1	1	0	100	2	PK day dose
1	0	0	2	0	2	2 h sample
1	0	0	4	0	2	4 h sample

c. Covariance of L1 random effects

The default assumption during structural model development is that there is no correlation among the random effects parameters. However, it is essential to assess the validity of this assumption by examining correlation diagnostic plots of the random effects parameters, typically before moving on to covariate modeling At the population level, it's possible for two parameters to demonstrate a substantial correlation ($r^2 \geq 0.9$), implying that a change in one parameter corresponds closely to a change in another parameter with an equal fit to the data (Owen and Fiedler-kelly, 2014). This correlation may be inherent, such as an increase in the rate of absorption (Ka) being correlated with a decrease in mean transit time (MTT). Including a full variance-covariance relationship for all random effects parameters could result in model overparameterization and hinder convergence of the estimation. Thus, the choice of inclusion of correlation would depend on – identification of a potential covariate that can explain the correlation in which case the covariate can be included, improved model fit, as well as non-worsening of estimation precision. Neglecting to account for high correlations between L1 random effects may lead to simulations generating implausible combinations of individual parameters and needs consideration (Mould and Upton, 2012).

- **Level two random effects (L2):**

The Residual Unexplained Variability (RUV) or residual error is the L2 and accounts for the

deviation of the individual predictions from the observed values. This discrepancy could be due to model misspecification, data collection errors (e.g., errors in dosing or sampling times), or analytical assay errors.

$$DV = IRES + IPRED$$

Equation 6

Where DV refers to individual predicted values accounting for residual error, IRES refers to the individual residuals, and IPRED the individual model predicted values.

The RUV is described by the term ε_{ijk} in **Equation 2** and is a random effect which is normally distributed with mean 0 and an estimated variance of σ^2. RUV is generally explained by additive and proportional error models. Additive error is constant regardless of the magnitude of the prediction and is more important for low predictions. Proportional error is proportional to the magnitude of the prediction and is more important for high predictions. Thus, a combined additive and proportional error model generally best describes the RUV for PK models.

$$Additive\colon\ Y = f(\theta, Time) + \varepsilon$$
$$Proportional\colon\ Y = f(\theta, Time) \times (1 + \varepsilon)$$
$$Combined\ additive\ and\ proportional\colon\ Y = f(\theta, Time) \times (1 + \varepsilon_1) + \varepsilon_2$$

Equation 7

Where Y refers to the observed drug concentration at a given time point, f(θ, Time) refers to the individual predicted concentrations at a given time, and ε refers to the residual unexplained variability (ε_1 is the proportional error component and ε_2 is the additive error component).

Throughout this thesis, the combined error model was applied.

Correlation of RUVs needs to be considered during simultaneous modeling of two types of observations quantified from the same analytical sample, e.g., parent drug with its metabolite, two biomarkers, or two drugs. In this case, the same factors have contributed to the deviation between the model-predicted concentration and the observed concentration for the two observation types. Thus, the RUVs for the two observations need to be correlated by

including the L2 data item in the dataset and assigning the two types of observations obtained at the same time point the same value within the L2 column (Beal and Sheiner, 2008).

3.2.3 Covariate model

Covariates are intrinsic or extrinsic patient or study design factors (independent variables provided in a dataset) that can explain part of the parameter variability in the population in a predictable manner. Stepwise covariate modeling allows for the inclusion of covariates as independent variables that influence fixed effects parameters, with relationships defined using specific functional forms (e.g., linear, power, or allometric). Covariate selection is guided by the likelihood ratio test, based on changes in the objective function value (OFV). In the forward inclusion step, covariates are added if $\Delta OFV > 3.84$ ($P < 0.05$), while in backward elimination, they are retained if $\Delta OFV > 6.63$ ($P < 0.01$). This approach helps reduce unexplained random variability, improves model predictability, and facilitates direct interpretation of covariate effects on pharmacokinetic parameters. Alternative approaches include Full Covariate Modeling (FCM), in which all plausible covariates are included in the model simultaneously from the outset, without a selection process. Another method is Full Random Effects Modeling (FREM), where covariates are treated as dependent variables and jointly modelled with pharmacokinetic parameters within the random effects structure. FREM estimates the correlation between covariates and parameters directly from the data, without requiring a predefined functional relationship. While these methods can offer advantages in handling correlated or missing data, they are generally more computationally intensive and less straightforward to interpret. (Sanghavi *et al.*, 2024).

In this thesis, stepwise covariate modeling was used. Covariates were included *a priori* during early model development in cases where there was theoretical evidence of their impact on parameters, such as body size on disposition parameters. Selection of other covariates for

testing depended on the study question or trends identified in diagnostic plots (parameter versus covariate plots). Included covariates were either categorical (e.g., phenotype, sex, concomitant medication, study, or site) or continuous (e.g., age, body size, creatinine clearance, malnutrition, neutrophil count), and were included on parameters using functional relationships as described below. There are different ways of including parameter-covariate relationships, and only a summary is provided below:

i. Categorical covariates

The model parameters can be estimated separately for different categories of covariates or the proportional change in a parameter can be estimated, as below:

$$\mathrm{IF(COTREATMENT.EQ.0)TVCL} = \theta_1$$
$$\mathrm{IF(COTREATMENT.EQ.1)TVCL} = \theta_1 \times (1 + \theta_2)$$

Equation 8

Where θ_1 is typical value of CL (TVCL) when there is no drug-interaction, while θ_2 describes the proportional change in TVCL during drug-interaction.

ii. Continuous covariates

Continuous covariates can be incorporated into the model using various mathematical functions, with the appropriate function to use determined based on prior knowledge of the mechanisms involved or observed trends in parameter versus covariate plots. Continuous covariates are centred or normalized to the average value in the population or to a reference value (e.g., 70 kg) so that the typical parameter value is estimated for the average covariate value in the data, rather than for an implausible covariate value (e.g., estimating CL for a weight of 70 kg rather than a weight of 0). Centering or normalizing enables the estimation of parameters within the observed range of data and improves estimation precision (Owen and Fiedler-kelly, 2014).

a. Linear relationship

$$TVCL = \theta_1 \times (1 + \theta_2 \times (eGFR - 100))$$

Equation 9

Where TVCL = typical value of clearance, θ1 = typical value of clearance for an individual with average eGFR (estimated glomerular filtration rate) of 100 mL/min, θ_2 = fractional change in eGFR from 100 mL/min.

To avoid estimating a negative value for TVCL, the outer limits of the initial estimates for θ_2 are constrained using the below calculations:

$$Lower\ limit = \frac{1}{Median_{covariate\ value} - Maximum_{covariate\ value}}$$

$$Upper\ limit = \frac{1}{Median_{covariate\ value} - Minimum_{covariate\ value}}$$

Equation 10

b. Power relationship

$$TVCL = \theta_1 \times \left(\frac{covariate}{covariate_{average}}\right)^{\theta_2}$$

Equation 11

The lower bound of the exponent, θ_2, can be constrained depending on the expected relationship, to be positive or negative.

c. Piecewise linear or broken stick relationship

$$IF(COVARIATE \leq BREAK) COVCL = \theta_2 \times (COVARIATE - BREAK)$$
$$IF(COVARIATE > BREAK) COV_{CL} = \theta_3 \times (COVARIATE - BREAK)$$
$$TVCL = \theta_1 \times (1 + COV_{CL})$$

Equation 12

In this case, there are two slopes for the lower and upper part of the covariate range (θ_2 and θ_3, respectively), joined or centered by a breakpoint (BREAK). θ_1 is the typical value of CL at

the breakpoint. The breakpoint can be estimated, with the initial estimates informed by parameter- covariate diagnostic plots, or it can be fixed based on prior information.

Allometry

Dose calculations are made by using disposition parameters: Vd for loading dose and CL for maintenance doses. One of the fundamental covariates that can predict these disposition parameters is body size. Children are smaller than adults, but linear scaling underpredicts CL with a decrease in size, and results in underdosing. Thus, children require a higher mg/kg maintenance dose than adults, and rather than linear scaling, allometric scaling is used to account for this.

Allometry refers to the scaling relationships between physiologic characteristics (e.g., organ size, metabolic rates) and body size, where the relationship is expressed as a power relationship with the scaling exponent indicating how the physiological mechanism changes with body size.

$$\mathrm{TV} = \theta_1 \times \left(\frac{\mathrm{weight}}{\mathrm{averageweight}}\right)^{\theta_2}$$

Equation 13

Where TV is the typical value for a disposition parameter, θ_1 is the typical CL estimate for the average weight in the population (or a standard weight of 70 kg), and θ_2 is the scaling exponent.

Disposition PK parameters scale with body size in a predictable manner, which enables to predict drug disposition across the wide ranges of body sizes from children to adults as well as across different species. Disposition parameters relating to body structure, i.e., volumes of distribution, scales linearly with body size, while parameters that relate to function such as metabolic processes, i.e., intercompartmental and elimination CLs, scale less than linearly

with size (with a scaling exponent, i.e. θ_2, of 0.75). These relationships are based on studies across a range of drugs and species (Anderson and Holford, 2009).

Based on this theory, allometric scaling is often included *a priori* early during model development, in line with accounting for the most obvious and important things first.In addition to weight, body composition could affect drug distribution characteristics, with lipophilic drugs preferring fat sequestration. And although fat does not have metabolic activity, changes in distribution can indirectly affect drug CL. To reflect this, another size descriptor that can be used is normal fat mass (NFM), which enables evaluation of the contributions of fat free mass (FFM) and fat mass to the prediction of disposition parameters (Holford and Anderson, 2017). NFM is calculated using the equation below:

$$\mathrm{NFM} = \mathrm{FFM} + \mathrm{Ffat} \times (\mathrm{Weight} - \mathrm{FFM})$$

Equation 14

Where Ffat is the fraction of fat mass which is appropriate for the parameter being estimated. FFM can be calculated using the equation below:

$$\mathrm{FFM} = \mathrm{WHSmax} \times \mathrm{Height}^2 \times \left(\frac{\mathrm{Weight}}{\mathrm{WHS}_{50}} \times \mathrm{Height}^2 + \mathrm{Weight}\right)$$

Equation 15

Where WHSmax = 42.92 kg/m2 and 37.99 kg/m2 in males and females, respectively, and WHS50 = 30.93 kg/m2 and 35.98 kg/m2 in males and females, respectively.

When Ffat is estimated to be zero, FFM can be used as the body size descriptor. For example, sex differences can often be accounted for by using FFM, since females have higher fat mass than males.

In this thesis, allometric scaling was incorporated from the early stages of model development; however, its impact on model fit was consistently evaluated by examining the objective function value.

Organ maturation in children

Despite accounting for changes in body size or composition, CL mechanisms are not fully mature at birth, and not accounting for maturation effects would result in overprediction of CL in neonates and infants. Maturation of CL is included in the model using the Hill model, which results in a maturation curve that approaches mature, adult CL values over time (i.e., 100% maturation). From the curve, the age at which full maturation is reached can be determined. Since CL pathways start developing before birth, rather than postnatal age, postmenstrual age (PMA) is commonly used in the Hill model (Anderson and Holford, 2009).

$$\mathrm{TVCL} = \theta_1 \times \frac{\mathrm{PMA}^{\mathrm{HILL}}}{\mathrm{PMA}_{50}^{\mathrm{HILL}} + \mathrm{PMA}^{\mathrm{HILL}}}$$

Equation 16

Where PMA_{50} is an estimate of the age at which CL is 50% mature (50% to being explained by allometry alone), and the HILL coefficient describes the steepness of the maturation curve (how fast full maturation is attained).

PMA_{50} and the Hill exponent are estimated in the model, with initial estimates informed by literature as well as exploratory plots of individual CL versus PMA.

In this thesis, allometric scaling with fixed exponents was applied as abovementioned and maturation function was additionally evaluated on CL for paediatric data. However, some question this approach. One alternative perspective suggests that allometric exponents should be estimated from the data rather than fixed, as fixing them presumes universally applicable physiological principles. Estimating these exponents allows for potential identification of drug- or population-specific PK but requires rich data—ideally spanning a well-distributed weight range—especially when estimating separate exponents for multiple disposition parameters in multicompartment models. By contrast, using fixed exponents is grounded in physiological theory, adds no additional parameters, and tends to yield more stable models. Another widely discussed method is PBPK modeling. PBPK incorporates physiological

attributes (e.g., organ size, blood flow), drug-specific characteristics (e.g., enzyme kinetics, lipophilicity), and developmental biology (e.g., enzyme maturation) to simulate age-specific PK without relying on empirical scaling assumptions. This approach is considered particularly valuable in children under two years of age, where developmental changes in metabolism are most pronounced. However, its application is often limited by the availability of biological data and, in practice, may not outperform simpler empirical approaches when only sparse clinical data are available (Johnson and Ke, 2021).

3.3 Overview of model development and application

3.3.1 Software

In this thesis, the following software were used (Keizer, Karlsson and Hooker, 2013):

- R v3.6.1 to R v4.3.0 (https://cran.r-project.org/)

For initial data exploration and formatting (tidyverse package), and for post-processing of model outputs, including generation of model diagnostics (xpose and xpose4 packages).

- NONMEM v7.4.3 to v7.5.(https://www.iconplc.com/solutions/technologies/nonmem)

For model development with First Order Conditional Estimation with Interaction (FOCE-I) algorithm.

- PsN (http://uupharmacometrics.github.io/PsN/install.html)

To implement various commands to support the model development, such as obtaining visual predictive check (VPC) and bootstraps.

- Pirana

Graphical user interface for easier management of the modeling workflow, model execution, and interpretation of results.

- Notepad++

To edit NONMEM model scripts.

Computations were preformed using facilities provided by the University of Cape Town's ICTS High Performance Computing team: hpc.uct.ac.za.

3.3.2 Raw data exploration

Before developing the PK model, an initial graphical examination of raw data is conducted, including concentration-time profiles, covariate distributions, and covariate co-linearity. The goal is to identify any unexpected PK profiles, such as below the lower limit of quantification (BLQ) concentrations at unexpected time points or individual profiles deviating significantly from others. Additionally, the exploration aims to identify general trends, like whether mono or bi-exponential disposition is prevalent, and to spot correlated covariates. In cases of covariate correlation, the one with more physiological significance or a composite covariate is chosen. If outlier data points or individuals are observed, decisions to exclude them are made in collaboration with the clinical team to avoid disrupting the model development process and a sensitivity analysis is conducted in the later stages of model development to assess the impact of exclusion. Following data exploration, the dataset is prepared in a format compatible with the modeling software used, which was NONMEM in this thesis.

3.3.3 Handling concentrations below the lower limit of quantification (BLQ)

There are various methods (M1-M7) of handling BLQ concentrations (Beal, 2001). In this thesis, the M6 method was used, where BLQ concentrations were handled depending on their position in the plasma concentration-time profile. For points shortly after the dose, PK BLQs contain important information that the observed drug concentration has not yet exceeded the quantification limit and enables delay in absorption to be reasonably estimated. To retain this information, the last BLQ in absorption and the first BLQ in elimination were censored (CENS = 1) and imputed with a value equal to half of the quantification limit in the dataset and were included in the model fit. The additive error was increased by half of the LLOQ for

these CENS = 1 values since they were imputed and thus less reliable. Trailing BLQ values (CENS = 2) were excluded from the model fit (as shown in **Equation 17** by assigning large additive error without proportional error), but were retained for the model diagnostics since otherwise the data would be shown selectively.

$$IF(CENS = 1)\ THEN\ ADD = ADD + \left(\frac{LLOQ}{2}\right)$$
$$IF(CENS = 2)\ THEN$$
$$PROP = 0$$
$$ADD = 1000000000000$$
$$ENDIF$$

Equation 17

3.3.4 Steps of model development

The general modeling steps used in this thesis are outlined as follows. To inform the structural model development, literature search was performed to understand the drug's PK properties. If an established PK model existed in literature, it served as a starting model, with fit to the new data evaluated with a visual predictive check (VPC) and improving fit thereafter. Initial estimates for population parameters were derived from literature as a best guess starting point since using initial estimates that are quite far from final parameter values could result in extended model run times and potential convergence to local minima, where the model outputs a set of parameter estimates different from the true values.

The structural model development started with a simple one-compartment model with first-order absorption and elimination. Following this, alternative absorption models (with lag time or transit) and disposition models (two or three-compartment) were explored. Depending on the PK properties, more complex models were tested, such as incorporating pre-hepatic extraction from the gut, first-pass extraction from the liver and saturable CL. The stochastic model was attributed to the correct parameters chosen for the study design to avoid interfering with structural model identification. For instance, if concentrations were collected

on multiple occasions, between-occasion variability (BOV) was included on all absorption parameters, and between-subject variability (BSV) on Vd was estimated parsimoniously - typically, BSV on Vd is estimated better with first-dose data rather than steady-state data. Residual measurement error was included with additive and proportional components from the first stage of model development.

While covariate modeling was typically performed after identifying an appropriate structural model, covariates with a large influence were included during early structural model development, such as allometric scaling, maturation, and drug-drug interactions, since it could be difficult to obtain convergence without including the effect (Owen and Fiedler-kelly, 2014). Allometric scaling, with fixed exponents as previously mentioned (Equation 12), was included *a priori* on all disposition compartments so as not to create discrepancy between the compartments, with the preferred body size descriptor (weight, FFM, NFM) tested. Other covariates were tested univariately, then stepwise, with forward inclusion and backward elimination. Covariates were generally included on absorption and central disposition parameters. Mixture models were used in case of pooled datasets where covariates were only available for part of the data (**Chapter 7**). In case where external device parameter was missing (**Chapter 4**), the parameter was prudently fixed to a literature value after conducting sensitivity analysis amongst different literature values and calculations based on existing data.

Model development proceeded by making one change at a time in order to compare the goodness-of-fit statistic, which is the OFV in NONMEM, between a parent and daughter model in order to identify the specific change that improved or worsened the model. The algorithm in NONMEM aims to search for the parameter values that maximize the likelihood of the estimated model parameters given the observed data, and does so by minimizing the

OFV, which is proportional to -2 log likelihood of the model, given the data. If two models are nested, meaning the daughter model can collapse into the parent model when the additional parameter is removed, the likelihood ratio test (LRT) can be used to assess significance of the OFV. The difference in OFV between two nested models follows a χ^2-distribution and the critical ΔOFV at a significance level of 5% is 3.84 for one extra parameter added ($p<0.05$, 1df) during forward inclusion, while for backward elimination, the critical ΔOFV at a significance level of 1% is used, which is 6.635 for one parameter removed ($p<0.01$, 1df). For non-nested models, the Akaike Information Criterion (AIC) was used to compare models, where AIC was calculated as below from the OFV:

$$AIC = 2(number\ of\ parameters) + OFV$$

Equation 18

Other than the ΔOFV, model fit during each step was also guided by various diagnostics, as mentioned in Section 3.3.8. High η-shrinkage was evaluated to identify parameters that may be less reliably estimated, as sparse individual-level data can cause estimates to shrink toward the population mean and reduce power to detect significant covariate effects. High ε-shrinkage, reflecting the extent to which individual residuals are pulled toward zero, was also assessed as an indicator of potential model overparameterization or poor fit due to limited data (Mould and Upton, 2013).

3.3.5 Simultaneous modeling of data from multiple sources

In situations where data is limited, either due to small sample size or infrequent pharmacokinetic sampling, estimating all pharmacokinetic parameters may be challenging. One approach is to fix some parameters or use Bayesian priors to inform the estimation of parameters based on an established PK model from literature. However, differences in study conditions (such as in participant demographics or aspects of study design) may make these options less suitable. When feasible, a more effective strategy involves simultaneously

modeling data from various sources or studies to strengthen the data and enhance power to detect covariates. In such cases, developing a model requires a nuanced approach that goes beyond simply pooling the data, considering the likely heterogeneity present in the data, such as variations in dosing, sampling, and differences between healthy and patient populations (Svensson et al., 2012).

When data from multiple studies was pooled in this thesis, data from the various studies were visually examined separately to identify study-specific variations in demographics, covariates, and trends in PK profiles. The initial phase of model building focused on the study with rich data, allowing for the identification of a robust structural model and significant covariate effects. Subsequently, data from additional studies were incorporated, prioritizing richness of data. For each dataset integration, the existing model's fit to the new dataset was evaluated using a VPC. Study-specific covariates were assessed to enhance model fit, such as variations in absorption models due to fed versus fasted status between studies. Moreover, enhancements in both the structural and stochastic models were re-evaluated, such as the body size descriptor for allometric scaling and addressing extra variability in unobserved concentrations. Sparse data were incorporated last and the full model fit evaluated (Svensson et al., 2012).

3.3.6 Estimation precision of parameters

Precision or uncertainty of estimation were obtained as confidence intervals through bootstrap, sampling importance resampling (SIR), or using the model-reported standard errors. In NONMEM, standard errors are computed from the variance-covariance matrix, assuming normal distribution as the sample size increases.

In cases of complex models where obtaining standard errors is computationally demanding or when dealing with small sample sizes where the normality assumption may not be

appropriate, the non-parametric bootstrap is favoured. Bootstrap involves creating multiple datasets by resampling with replacement from the original dataset. Each dataset is then used as input for the model, generating new sets of parameter estimates, and enabling the determination of confidence intervals (Lindbom, Pihlgren and Jonsson, 2005). However, for small datasets, SIR is more appropriate due to the limited degree of reshuffling that can be done on a small dataset. SIR involves simulating sets of parameters from the model's variance-covariance matrix. Subsequently, X parameter sets are randomly sampled from the simulation, and the model fit for each set is evaluated on the study data. Resampling of parameter sets is performed based on the likelihood of the data given the parameter set and the likelihood of the parameters in the distribution. This process is repeated for a user-defined number of iterations (Dosne *et al.*, 2016; Dosne, Bergstrand and Karlsson, 2017).
Although there are no standard cutoff values for acceptable precision, wide confidence intervals can indicate inadequacy of the data to support estimation of a parameter or potential overparameterization of the model.

3.3.7 FOCE-I for parameter estimation in NONMEM

There are various estimation methods in NONMEM (Bauer, 2019). In this thesis, the first order conditional estimation with interaction (FOCE-I) method was used for all model runs. The search for optimal sets of parameters is a stepwise progression from the initial parameter estimates, updating parameter estimates at each iteration, until a point is reached where change in any of the parameters does not improve fit further (i.e., convergence or global minima). With the earlier FO method, individual parameters were obtained as an extra step (post hoc) after final population parameter estimates (fixed effects with their variances and RUV) were determined. The individual parameters are also called empirical bayes estimates (EBEs) since they were determined assuming the prior population parameters as true, also considering the data. With FOCE, EBEs are estimated at each iteration by integration overall

all possible individual random effects (etas) for each individual's joint density of observed data and etas and linearizing around the current conditional estimate of the etas (in other words, typical values are centred at the mode of the distribution of individual etas, where the distribution is conditional upon the observed data). FOCE-I further accounts for interaction between the L1 and L2 random effects, and the prediction corresponds to the individual rather than the population prediction. Thus, FOCE-I allows for more precise parameter estimates.

3.3.8 Model evaluation

The objective throughout this thesis was to develop fit-for-purpose models that captured key features of the data while avoiding unnecessary complexity to avoid overfitting — particularly given the limited richness of the datasets. Model evaluation was conducted using a range of diagnostics. Goodness-of-fit (GOF) plots—such as observed versus population and individual predictions, and conditional weighted residuals versus time or predictions — were used to assess systematic bias or model misspecification. VPCs were employed to assess the model's predictive performance by comparing observed percentiles (e.g., median, 10th, and 90th) with prediction intervals generated through simulation. Numerically, changes in the OFV were used to assess model improvement, while parameter precision was evaluated through bootstrap or sampling importance resampling (SIR), focusing on the width of confidence intervals. Shrinkage of random effects was also assessed to identify potential model misspecification or insufficient data to support reliable individual parameter estimation. In addition, biological plausibility of parameter estimates and consistency with known trends were considered. Where possible, external validation was used to confirm that external observations fell within the model's predictive range (Keizer, Karlsson and Hooker, 2013).

3.3.9 Model application – Simulations

Once a suitable 'fit-for-purpose' model is established, it can be utilized in simulations to generate dosing recommendations, guide future study designs (such as optimizing sampling times) or assess the study's power to identify covariates. Simulations for dosing recommendations involve creating pharmacokinetic profiles for a hypothetical population under various dosing regimens or administration routes, utilizing a range of pharmacokinetic parameters derived from the study population. Stochastic or Monte Carlo simulations are conducted with the final PopPK model, involving the random sampling of parameters from a probability distribution (where random effects are used for sampling). This process predicts the probability of the outcome measures or, in other words, estimates the range of outcome measures (such as exposures, trough concentrations, time above minimum inhibitory concentration (T>MIC)) (Trang, Dudley and Bhavnani, 2017). In cases where the model incorporates multiple random effects parameters, potential correlations among these parameters must be considered to prevent the simulation of implausible parameter combinations in individuals (Mould and Upton, 2012).

The population used in the simulations can be the study population, where the simulations are iterated a number of times. This allows for the sampling of a range of variable parameters from the model for each individual, generating a distribution of the simulated output measures per individual. Alternatively, the simulation can be performed with a large representative virtual population with a normal distribution of covariates, with the same consideration as above when reporting simulated output categorically (e.g., 1000 simulations per each weight or age category) (Mould and Upton, 2012).

3.4 Methods to handle some challenges during model development

3.4.1 Initialization to baseline values

In compartmental PK modeling, differential equations are used to show the rate of change in drug amount or concentration within each compartment. To facilitate the computation by the differential solver (decrease run times), initial conditions are set for each compartment with values close to 0. Parameters are also assigned plausible initial values (based on the expected PK), initiating the search for optimal parameters based on the observed data. Initialization serves another purpose in scenarios of high variability in baseline or trough concentrations.

In PK studies, besides samples collected post-dose on the PK Day, trough samples (pre-dose) are obtained just before administering the PK Day dose. These are often sourced from an unobserved dose or baseline, where the PK Day dose might be the sole exposure to the drug. Trough samples offer insights into PK aspects, such as CL and the absence of absorption initiation. If all baseline samples are below quantifiable limits, they can be discarded, assuming individuals were not exposed to the drug before the PK Day dose. In the case of repeated administration at steady-state, pre-dose trough concentrations are expected to align with post-dose trough concentrations, since the drug is cleared at the same rate as it is administered at steady-state.

Issues like errors in drug administration or non-adherence can introduce high variability in baseline samples, complicating the acquisition of precise parameter estimates. This variability may inflate the additive error and the variability parameters. Improper handling of baseline samples can interfere with structural model development (e.g., identifying two versus one-compartment model). One approach to address this challenge is to introduce an additional parameter quantifying the extra-variability on between-occasion variability specifically for the baseline samples, since they are considered as a distinct occasion from the PK Day

occasion. Another option involves employing the 'initialization' method, as described by Dansirikul et al. (Dansirikul, Silber and Karlsson, 2008).

There are different methods of initialization. In the B1 method, typical and between-subject variability parameters are estimated for the baseline values, with an underlying assumption about the distribution of baseline values for the population. In the B2 method, observed baseline values and residual error are used to inform the model baseline predictions, with no assumption made about the distribution of baseline values. The B3 method is a mix of the B1 and B2 methods. The B2 method is advantageous since it carries no assumptions regarding the population distribution of baseline values and is described below. In this approach, the dataset is adjusted to create a variable so that doses before the baseline concentration are discarded, and disposition compartments are initialized to pre-dose trough concentrations. For those individuals with pre-dose trough concentrations that are quite different from the rest of the population, this informs the model to start computations for the compartments from the observed values. If this is not done, since the PopPK model borrows information from all individuals for its predictions of typical values and variability, it would result in inflated variability that is not necessarily inherent in the population but is rather due to error in observations, and the model predicted individual baseline values would also be higher or lower than those observed, resulting in model misfit. Moreover, similar to the rest of the observations, residual unexplained variability is included in the individual baseline concentrations which are used to inform the model.

3.4.2 Mixture models

Mixture models enable us to account for missing categorical covariate data and assume that the population consists of two or more subpopulations (or subcategories of covariates). Individuals in the population are partitioned into one of these sub-populations according to a

probability model, with each sub-population having its own parameter. For instance, if a drug is metabolized by a polymorphic enzyme with poor and extensive metabolizers, CL obtained from the PK model, without the covariate included, might show bimodal distribution, indicating two distinct sub- populations. In a case where the phenotype is missing in some or all of the individuals, a mixture model can be used, which models the mixture of probability distributions of the covariate in the sub-populations (Ette and Williams, 2007). The output of the model will then be each individual's assignment into a particular sub-group, the parameter estimates for each sub-group, as well as the probability of assignment into each sub-group (unless it is fixed based on prior information). The proportion of individuals in the population belonging to each sub-category of covariates can be fixed to the proportion observed in the individuals within the dataset that don't have missing covariates (or based on literature reports of distribution of the covariates in subpopulations) or it can be estimated based on the likelihood of the PK concentration data alone or also based on the observed categories for individuals that don't have missing covariates (Keizer et al., 2012).

Chapter 4 Dose optimization of cefazolin in South African children undergoing cardiac surgery with cardiopulmonary bypass

4.1 Abstract

Cefazolin is an antibiotic used to prevent surgical site infections. During cardiac surgery with cardiopulmonary bypass (CPB), its efficacy target could be underachieved. We aimed to develop a population pharmacokinetic model for cefazolin in children and optimize the prophylactic dosing regimen.

Children under 25 kg undergoing cardiac surgery with CPB and receiving cefazolin at standard doses (50 mg/kg IV every 4-6 hours) were included in this analysis. A population pharmacokinetic model and Monte Carlo simulations were used to evaluate probability of target attainment (PTA) for efficacy and toxicity with the standard regimen and an alternative regimen of continuous infusion, where loading and maintenance doses were calculated from model-derived individual parameters.

Twenty-two patients were included, with median (range) age, body weight, and eGFR of 19.5 (1-94) months, 8.7 (2-21) kg, and 116 (48 – 159) mL/min, respectively. Six patients received an additional dose in the CPB circuit. A two-compartment disposition model with an additional compartment for the CPB was developed, including weight-based allometric scaling and eGFR. For a 10 kg patient with eGFR of 120 mL/min/1.73m^2, clearance was estimated as 0.856 L/h. Simulations indicated that the standard dosing regimen fell short of achieving the efficacy target >40% of time within a dosing duration and in patients with good renal function, PTA ranged from <20% to 70% for the smallest to the largest patients, respectively, at high MICs. In contrast, the alternative regimen consistently maintained target concentrations throughout the procedure for all patients while using a lower overall dose.

4.2 Introduction

Postoperative mortality, defined as death within 30 days after surgery, is the third greatest cause of mortality, accounting for 7.7% of all deaths (Nepogodiev et al., 2019). Postoperative patients with surgical site infections (SSIs) face 2-11 times higher mortality risk (Ban et al., 2017). SSIs, the most common healthcare-associated infections post-surgery, could occur at incision sites (superficial) and/or deep soft tissues or organs within 30 days (Borchardt and Tzizik, 2018). In paediatric cardiac surgeries, SSI rates range from 1.7 to 8% (Milad A. Alshaya, Nouf S. Almutairi and A. Shaath, Rahmah A. Aldosari, Sadeem K. Alnami, Alaa Althubaiti, 2021), with risk factors including prematurity, younger age, longer surgery, cardiopulmonary bypass (CPB), and suboptimal antibiotic prophylactic dosing (Izquierdo-Blasco et al., 2015). Due to lack of standardized guidelines for optimal antibiotic prophylactic regimens in paediatric cardiac surgery, recommendations are largely based on expert opinion, with dosing relying on extrapolations from adult data, and variations in regimens used in practice have been reported (Rangel et al., 2011; Bratzler et al., 2013; Bath et al., 2016; Jaworski et al., 2019).

Cefazolin, an FDA-approved surgical prophylactic antibiotic, provides adequate coverage against pathogens that cause SSIs, including methicillin-Sensitive Staphylococcus aureus (MSSA), the most common pathogen isolated in both superficial and deep SSIs (Bratzler et al., 2013; Milad A. Alshaya, Nouf S. Almutairi and A. Shaath, Rahmah A. Aldosari, Sadeem K. Alnami, Alaa Althubaiti, 2021). Cefazolin is up to 80% plasma protein bound, and 80-100% is excreted unchanged renally within 24 hours (Reller et al., 1973; Tortoriello et al., 2003). The goal for surgical prophylaxis is to maintain free cefazolin concentrations above four times the minimum inhibitory concentration (MIC) of common pathogens for 100% of the dosing interval (100% $fT > 4 \times MIC$) throughout the surgical duration until a few hours post-skin closure, since intraoperative contamination can occur at any point during surgery

(Bratzler et al., 2013). High cerebrospinal fluid concentrations of cefazolin have been associated with seizures in adults, where the lowest seizure-associated plasma concentration was 360 mg/L (Thomas P. Bechtel, Slaughter and Moore, 1980).

Cefazolin pharmacokinetics could be altered during cardiac surgery with CPB due to factors such as systemic inflammation and hemodilution (increasing volume of distribution), altered protein binding (raising clearance), and factors like hypothermia and organ dysfunction (reducing clearance) (Paruk et al., 2017). Current guidelines suggest cefazolin dosing for surgical prophylaxis in children at 25-50 mg/kg, with redosing after 4 hours if surgery exceeds two half-lives (~1.2-2.2 h with normal renal function) or in cases of excessive blood loss (Bratzler et al., 2013). However, specific dosing guidelines for paediatric cardiac surgery with CPB are lacking. Past reports have indicated that standard intermittent intravenous dosing may not meet cefazolin efficacy targets and there are differing practices in terms of adding a further dose into the CPB device (De Cock et al., 2017; Calic et al., 2018; Jeffrey J Cies et al., 2019). Therefore, evaluating adequacy of local regimens during CPB surgery is essential.

We performed a population pharmacokinetic analysis for intravenous cefazolin in a cohort of paediatric patients undergoing cardiac surgery with CPB. Our objectives were to characterize the pharmacokinetics of cefazolin in paediatric patients during cardiac surgery with CPB, assess adequacy of the standard regimen, and identify alternative dosing strategies.

4.3 Methods

Study design

An observational study was conducted at Red Cross War Memorial Children's Hospital (henceforth referred to as RCWMCH) in Cape Town, South Africa. Paediatric patients undergoing cardiac surgery who required CPB, were below 25 kg, and were administered cefazolin were eligible for inclusion. Exclusion criteria included expected CPB time of less than 30 minutes, history of allergy to beta-lactam antibiotics, and pre-existing hepatic or renal dysfunction.

The standard regimen at RCWMCH was 50 mg/kg IV cefazolin infused over 45 sec where the first dose was given following induction of general anaesthesia and the second dose 4-6 hours later, either intraoperatively or postoperatively in ICU depending on the surgical duration. A maximum of three doses were given, where the third dose was in ICU for long surgeries. Some physicians added a dose into the priming fluid of the CPB circuit at the start of surgery (hereby called CPBdose).

Blood samples were collected at baseline, 3 minutes post-dose for each dose, at sternal incision, pre-CPB at cannulation of the aorta, at initiation of full-flow CPB, every 30 minutes during CPB (or every 60 minutes during CPB lasting longer than 120 minutes), prior to termination of CPB, 10-15 minutes after termination of CPB, at sternal closure, 1-2 and 3-4 hours after the second dose in ICU. A schematic of the procedure is given in **Figure S. 4.1.**

Research ethics and patient consent

This study was approved by the University of Cape Town Faculty of Health Sciences Human Research Ethics Committee (536/2011), which complies with the ethical standards of the South African Medical Research Council, International Convention on Harmonization Good Clinical Practice (ICH GCP), and the Declaration of Helsinki. Informed written consent was

obtained from parents or legal guardians of the children to participate in the study and to store specimens for immediate and future analysis.

Details of the population pharmacokinetic modeling are included in the **supplementary material.**

Monte Carlo simulations

We performed Monte Carlo simulations of cefazolin concentrations to evaluate target attainment using different dosing strategies. We simulated a surgical period of 5.5 hours, the longest surgery time observed in the original study patients, since long surgical time (> 2 hours) is expected to affect plasma cefazolin concentrations (Caffarelli et al., 2006). Target cefazolin concentrations need to be maintained during surgery and a few hours post-surgery to mitigate the risk of SSI. Thus, target attainment was evaluated for a dosing duration of 12 hours starting from induction of anaesthesia, which also accounts for the post-surgical period that patients are in ICU.

MSSA is the most common pathogen in SSIs and its epidemiological cut-off value according to EUCAST is an MIC of 2 mg/L ("The European Committee on Antimicrobial Susceptibility Testing. Breakpoint tables for interpretation of MICs and zone diameters, version 12.0, 2022."). Given that the goal for cefazolin is to achieve a free concentration exceeding 4 times the Minimum Inhibitory Concentration (MIC) for 100% of the time (100% fT > 4×MIC) against susceptible pathogens, attainment of 8 mg/L free concentration (i.e., 40 mg/L total concentration, assuming free fraction of 0.2) was the evaluated target. The lowest total cefazolin plasma concentration at which seizures have been reported in adults is 360 mg/L (Thomas P. Bechtel, Slaughter and Moore, 1980), and this total concentration was used as a toxicity target.

Probability of target attainment (PTA) simulations were performed as follows. The first simulation consisted of 1000 Monte Carlo simulations for each of the 22 study patients, performed to evaluate the time in which free cefazolin concentrations are below the efficacy target, within target (i.e., above the efficacy target and below the toxicity target), and above the toxicity target. The priming fluid volumes for the CPB pump were the same as those given in the original study. The second simulation was using a virtual paediatric population of 5000 patients (Wasmann *et al.*, 2021), uniformly divided into five weight groups (< 5 kg, 5-10 kg, 10-15 kg, 15-20 kg, and 20-25 kg) , each group associated with three renal function profiles: 50, 80, and 130 mL/min/1.73 m^2. A range of MIC values corresponding to the distribution of MSSA (0.125 to 2 mg/L) were evaluated ("The European Committee on Antimicrobial Susceptibility Testing. Breakpoint tables for interpretation of MICs and zone diameters, version 12.0, 2022"). A dosing strategy was deemed efficacious if ≥90% (a conventional threshold in antimicrobial PK/PD modeling (Mouton *et al.*, 2012)) of evaluated participants per weight and renal function group met the target of 100% fT>4×MIC. Priming fluid volumes were based on the standard practice at RCWMCH: for infants <10 kg 400 mL, for children 10-20 kg 600 mL, and for children 20-30 kg 800 mL. Four dosing regimens were evaluated, where "CPBdose" refers to an additional dose into the CPB priming solution, as below:

a. The standard regimen of 50 mg/kg IV bolus dose every 4 hours:

i. Without CPBdose

ii. With CPBdose (in the study patients, the CPBdose was the same as the bolus doses given, i.e., 50 mg/kg, and this was used for our standard regimen simulations)

b. An alternative regimen of continuous infusion where a loading dose was administered at induction of anaesthesia and an infusion was administered throughout the dosing duration, starting from 20 minutes after induction of anaesthesia:

iii. Without CPBdose

iv. With CPBdose (0.5 × Loading dose) (half the loading dose was used since this is more pragmatic for concentrations achieved)

The loading and maintenance doses for the continuous infusion regimen were calculated from the model's population predicted parameter values and individualized by patient weight and renal function. A prudent target plasma concentration (Ctarget) of 100 mg/L was used, which is approximately equivalent to the median plasma cefazolin concentration observed in the study patients. Dose calculations are shown in **Table 4.1**, and can be calculated for a paediatric patient using a dose calculator app where the user can input patient characteristics to derive the dose for a continuous infusion regimen using the developed model: https://drugdosecalculator.shinyapps.io/cefazolin/

Table 4.1. Dose calculations for continuous infusion regimen.

Individual parameters based on population predictions and allometric scaling	
V_{ss} for patient	CL for patient
$V_{ss} = (TVV_c + TVV_p) \times \left(\frac{Weight}{10kg}\right)$ (2) TVV_{ss}	$CL = TVCL \times \left(\frac{Weight}{10kg}\right)^{0.75} \times (\frac{CRCL}{120mLmin})$ (3)
PK formulas for calculating continuous infusion regimen	
Loading dose	Maintenance dose/hour
$V_{ss} \times C_{target}$ (4)	$CL \times C_{target}$ (5)
CPBdose	
0.5 × Loading dose (6)	
V_{ss} = steady state volume (L) , TVV_{SS} = typical steady state volume (L) TVV_C = typical central volume(L), TVV_P = typical peripheral volume (L) CL = clearance (L/h), TVCL = typical clearance (L/h) C_{target} = Target concentration (mg/L) Weight = weight of patient (in kg), 10 kg = Typical weight in our study population CRCL = creatinine clearance of patient (in mL/min) 120 mL/min = typical creatinine clearance	

4.4 Results

Patient and study characteristics

Included were twenty-two children (41% female) who required cardiac surgery with CPB due to conditions such as atrioventricular septal defect, pulmonary atresia, and tetralogy of fallot. Six of the children received an additional CPBdose of 50 mg/kg. Two of the children died by two-week follow-up, one due to methicillin-Resistant S. aureus (MRSA)-induced sternal sepsis, and another one due to cardiac failure. Three other children developed infections (mediastinitis, sternal infection, sepsis), and three developed post-operative pneumonia, but survived.

The median (range) age, weight, and eGFR of the included patients were 19.5 (1-94) months, 8.7 (2.0-21) kg, and 116 (48.0-159) mL/min, respectively. None of the post-dose plasma concentrations were below the lower limit of quantification or removed as outliers, resulting in a total of 249 concentrations in the analysis. Baseline study and patient characteristics are given in **Table 4.2**.

Table 4.2. Patient demographic and study characteristics, as median (range) where applicable.

Patient/study characteristics (n=22)	Median (range), where applicable
Surgical duration (hours)	2.38 (0.567 – 5.63)
Priming fluid volume (L)	0.40 (0.25 – 0.55)
Number of concentrations analysed	249
Male/female, n (%)	13/9 (59%/41%)
Age (months)	17 (1 – 94)
Weight (kg)	8.5 (2.0 – 22)
Height (cm)	77 (45 – 117)
Fat free mass (kg)[1]	8.0 (2.0 – 15)
Serum creatinine (mg/dL)	0.294 (0.215 – 0.407)
Creatinine clearance (mL/min)[2]	116 (48.0 – 159)
Fat-free mass calculated by Janmahasatian et al. (Janmahasatian *et al.*, 2005) Calculated by modified Schwartz formula (Schwartz and Work, 2009): $0.413 \times (\frac{height(cm)}{serum\ creatinine(mg/dL)})$	

Population pharmacokinetic model

Cefazolin pharmacokinetics was described by a two-compartment disposition model (compared to one compartment, ΔOFV = -75.1, $p < 0.001$) with first order elimination, plus the additional compartment for the CPB system. Disposition parameters were allometrically scaled by body weight (ΔOFV = -82.9) and were normalized to 10 kg. eGFR was added as covariate on clearance rather than maturation or age since cefazolin is renally cleared and serum creatinine values were available. This was significant (ΔOFV = -6.49) and reduced between-subject variability in clearance from 27.8% to 23.2%. The typical (95% CI) clearance was estimated 0.856 (0.769 – 0.934) L/h for a 10 kg patient and eGFR of 120 mL/min (**Table 4.3**).

QCPB was fixed to a typical adult cardiac output of 336 L/h, then allometrically scaled by weight and normalized by a typical adult weight of 70 kg. Estimating a scaling factor for VCPB and QCPB improved the model fit (ΔOFV = -10.4, $p < 0.001$), with an estimate (95% CI) of 0.679 (0.521 - 0.810), which is close to the expected plasma proportion of whole blood.

The additive error estimate was close to zero, likely due to lack of low concentrations in the dataset within the same range as the LLOQ. Since it is implausible for concentration data to not have additive error, it was fixed to 20% of the LLOQ (the assay accuracy of the LLOQ) (FDA, 2018). This had little effect on parameter estimation and is useful for simulations to avoid simulating low concentrations with implausible precision.

Parameter estimates, and estimation precisions are given in **Table 4.3**.

Table 4.3. Parameter estimates for cefazolin model.

Parameter	Population estimates (RSE %)	95% Confidence interval[1]	Parameter variability, % CV[2] (RSE %) [Shrinkage]	95% Confidence interval[1]
Clearance (L/h)[3,4]	0.856 (10%)	0.769 – 0.934	BSV: 23.2 (35%) [6.2%]	17.9 – 32.2
Central volume of distribution (L)[3]	1.07 (9%)	1.00 – 1.20	BSV: 18.3 (41%) [16.5%]	13.0 – 25.9
Intercompartmental clearance (L/h)[3]	1.41 (13%)	1.22 – 1.65		
Peripheral volume of distribution (L)[3]	1.61 (18%)	1.35 – 2.05	BSV: 28.5 (22%) [35.3%]	20.8 – 39.0
Volume of CPB compartment[3]	Fixed to priming volume			
Intercompartmental clearance for CPB compartment (L/h)[5]	Fixed to adult cardiac output of 336 L/h			
Scaling factor for the CPB compartment	0.679 (15%)	0.521 – 0.810		
Residual unexplained variability				
Proportional error (%)	15.5 (7%)	14.3 – 16.9	[10.4%]	
Additive error (mg/L)	Fixed to 20% of LLOQ[6]			

Condition number = 27.52

[1]95% confidence intervals were obtained by non-parametric booststrap (n=500).

[2]Between-subject (BSV) was obtained using the formula $\mathrm{sqrt}(\exp(\Omega M^2) - 1)$ and reported as approximate %CV.

[3]Allometric scaling with total body weight, values are reported for median weight of 10 kg.

[4]Renal function was added as covariate on clearance (creatinine clearance calculated by modified Schwartz formula (Schwartz *et al.*, 2009), and clearance value is reported for typical adult creatinine clearance of 120 mL/min)

[5]Scaled to a typical adult body weight of 70 kg

[6]The additive error was not statistically significant from the lower bound (20% of the lower limit of quantification (LLOQ)) and was fixed to that value (LLOQ = 0.586 mg/L)

Clearance (CL) and Volume of distribution (V_d) were modelled with below equations:

$$CL = TVCL \times \left(\frac{weight\ (kg)}{10kg}\right)^{0.75} \times \left(\frac{eGFR(mL/min)}{120\ mL/min}\right)$$

$$V_d = TVV_d \times \left(\frac{weight(kg)}{10\ kg}\right)$$

The VPC shows that the 5th, 50th, and 95th percentiles of the data are within 95% confidence intervals of the model predictions for these percentiles showing adequacy of model fit (**Figure 4.1**).

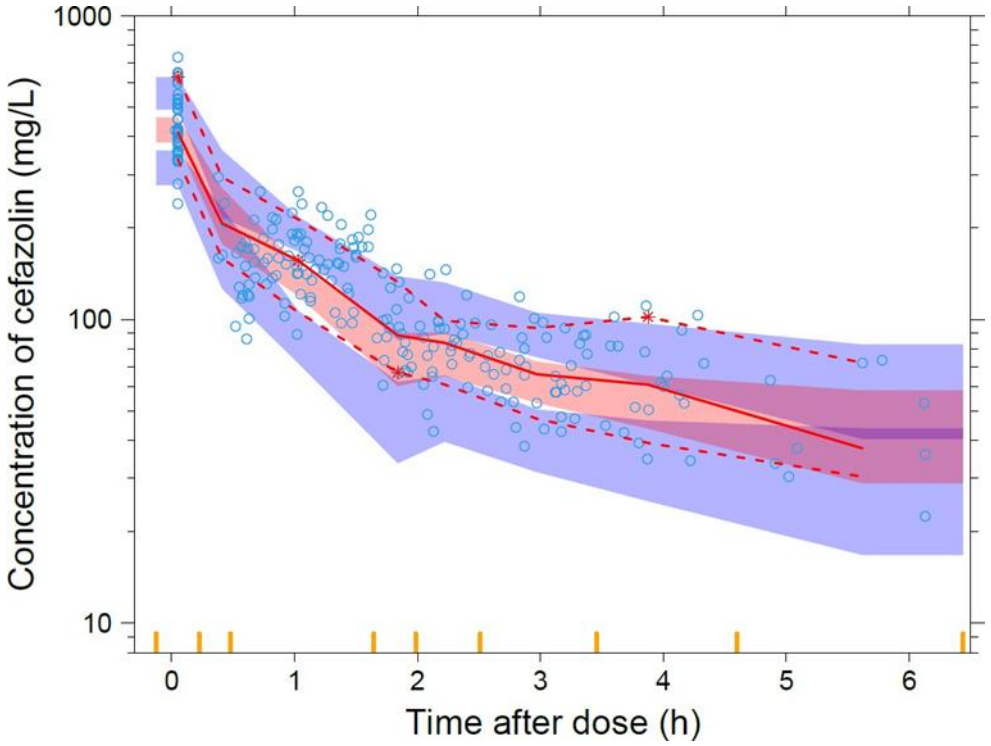

Figure 4.1. Visual predictive check (prediction corrected) of the final cefazolin model. Blue circles represent observed plasma concentrations. The solid line in the middle represents the median observed concentration, while the dashed lines below and above represent the 10th and 90th percentiles of the observed concentrations, respectively. The shaded area around each line represents the 95% model-predicted confidence intervals for the same percentiles. The yellow ticks at the base of the plot show the bins.

Simulations

Full pharmacokinetic profiles were simulated from the final model for the smallest patient, a 2 kg patient with eGFR of 50 mL/min, with the different dosing regimens. **Figure S. 4.2** **Figure** S. 4.2shows simulations with the standard regimen (50 mg/kg IV bolus dose every 4 hours) with and without a CPBdose. At the onset of CPB, serum concentrations decline sharply, followed by a slight increase in the plasma levels, as the drug redistributes. Adding a

CPBdose prevents this decline in plasma concentration, however, higher plasma concentrations are attained with longer time above the toxicity target (> 360 mg/L).

Figure S. 4.3. shows simulations for the alternative continuous infusion regimen for the same patient and dose calculation for this regimen in the patient demonstrated in **Table S. 4.1.** Cefazolin concentrations are within target (> 40 mg/L and < 360 mg/L) for 100% of the time for the evaluated duration.

Results of Monte Carlo simulations with the study patients (arranged in increasing order of renal function) are shown in **Figure 4.2**. For each patient, 1000 Monte Carlo simulations were performed, showing variability within those simulations in percentage of time within the target (> 40 mg/L and < 360 mg/L), below the efficacy target (< 40 mg/L), and above the toxicity target (> 360 mg/L). Comparing the four dosing regimens based on these simulations, the following observations can be made:

- With the standard regimen, there is variability in percentage of time that cefazolin concentrations are within target, ranging from a median of 100% to less than 50% of the evaluated time while percentage of time below the efficacy target varies ranging from 0 to more than 40% of the evaluated time. A trend of a lower percentage of time within the target and higher percentage of time below the efficacy target is observed for patients with high renal function.
- On adding a CPBdose to the standard regimen, there is reduced variability and improvement in percentage of time within the target as well as below the efficacy target, with the maximum percentage of time that cefazolin concentrations are below target lower than 40%. With this regimen, variability in percentage of time above the toxicity target is higher compared to the standard dosing regimen without CPBdose, indicating a higher probability for some of the simulated patients within each weight

and renal function group to attain cefazolin plasma concentrations above the toxicity target for longer durations.

- ❖ With the continuous infusion regimen (with or without CPBdose), concentrations are within target for all patients 100% of the time, and therefore there are no shaded areas in the plot.

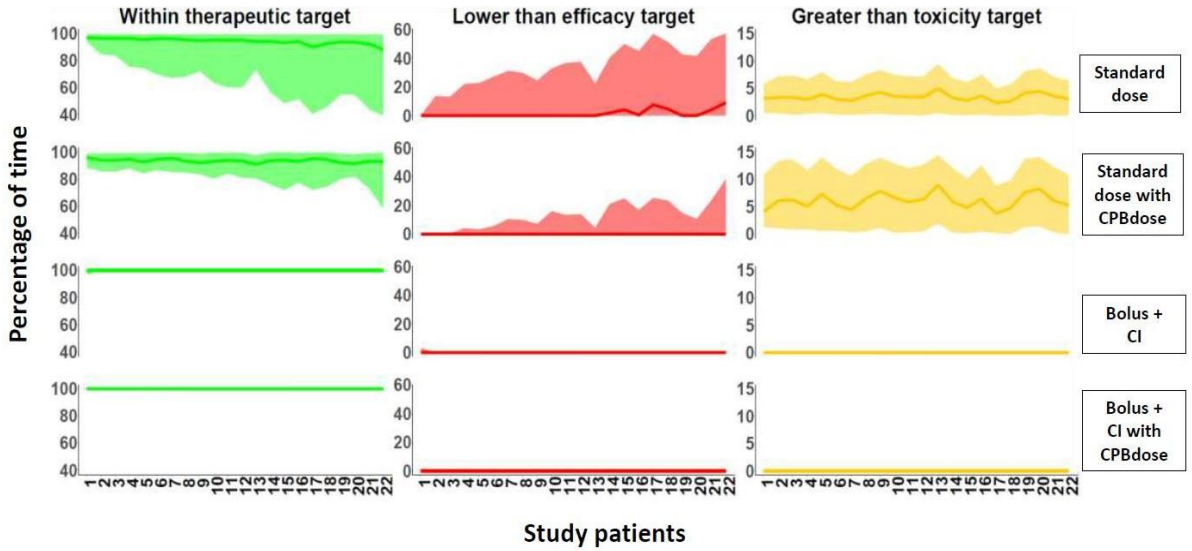

Figure 4.2. Probability distribution plot showing percent of time cefazolin concentration is within target, below the PK target, and above the toxicity target for each of the evaluated dosing regimens throughout a dosing interval of 12 hours.
Green shaded areas: within target (between 8 mg/L and 72 mg/L); Red shaded areas: below the pharmacokinetic target (8 mg/L); Yellow shaded areas: above the toxicity target (72 mg/L). Results are after 1000 Monte Carlo simulations for each of the 22 study patients (x-axis). The line within each shaded area shows the median result for the simulations. The study patients are arranged in increasing order of eGFRs from 48 to 159 mL/min/1.73m^2, as shown in Table S2. CI = continuous infusion, CPBdose = additional dose into the bypass priming solution.

Monte Carlo simulations with a virtual paediatric population showed that with the standard regimen, all weight groups with high eGFR (130 mL/min) failed to achieve the target, with the smallest weight groups performing the worst, resulting in PTA < 90% at MIC of 2 mg/L. When a CPBdose was added to the standard regimen, weights >15 kg attained PTA > 90%. With the continuous infusion regimen, all subgroups of weight and renal function attained a PTA of 100% (**Figure 4.3**).

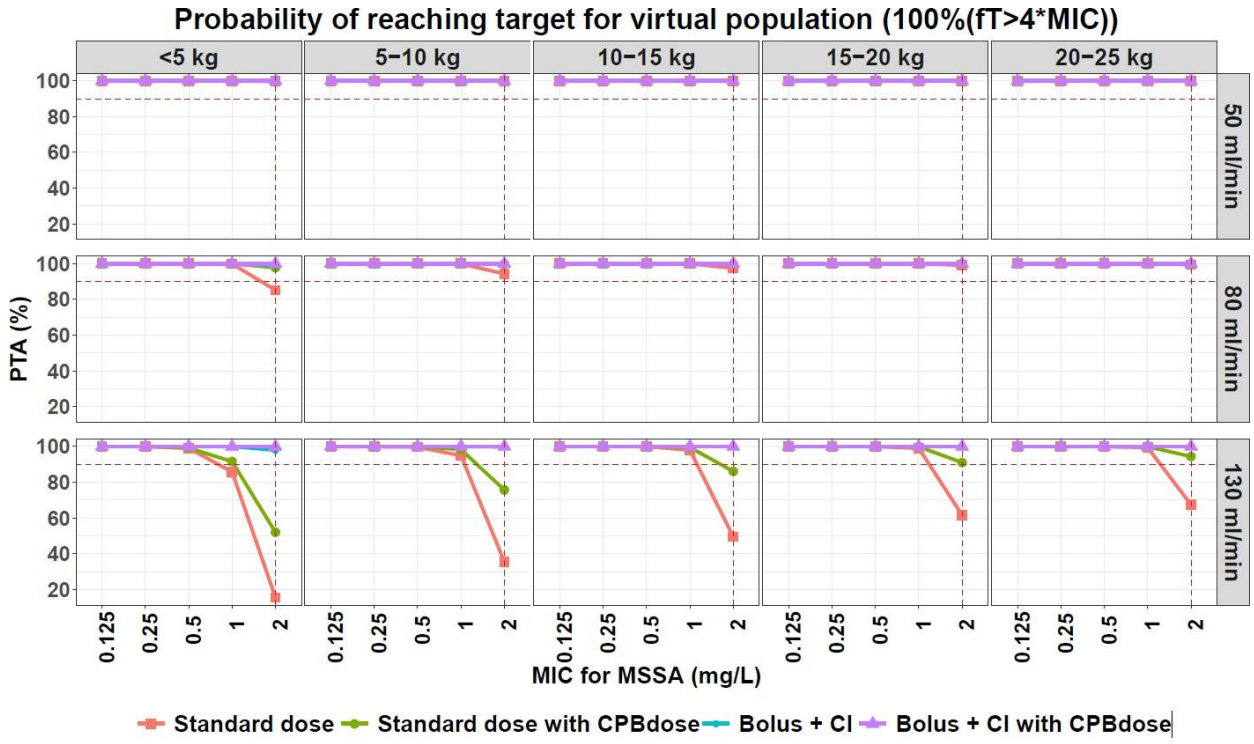

Figure 4.3. Probability of target attainment (PTA) dosing evaluations based on simulations for a virtual paediatric population.

1000 patients were simulated per weight and renal function group). Four dosing regimens were evaluated in each group. PTA target was proportion of patients that achieved a 100% fT > 4 × MIC throughout the dosing duration, performed for a range of minimum inhibitory concentrations for methicillin sensitive staphylococcus aureus. The vertical dashed line shows the susceptibility breakpoint for MSSA of 2 mg/L ("The European Committee on Antimicrobial Susceptibility Testing. Breakpoint tables for interpretation of MICs and zone diameters, version 12.0, 2022"). The horizontal dashed line shows 90% PTA. CPBdose: dose into the cardiopulmonary bypass priming solution, CI: continuous infusion.

Simulations performed with the virtual paediatric population to assess the percentage of time total cefazolin concentrations exceed the toxicity threshold showed that the standard regimen with CPBdose leads to the greatest percent of time above the toxicity target, particularly in patients with lower renal function, reaching up to 15% of the time over a 12-hour period in 50% of the patients **(Figure S. 4.5.** . In contrast, both continuous infusion regimens, with or without CPBdose, demonstrated a 0% likelihood of exceeding the toxicity target across all weight and renal function categories. **Table S. 4.2.** and **Figure S. 4.6.** (plot of average concentrations for the different dosing regimens) show total drug administered in patients

with the standard regimen of intermittent bolus dosing is higher compared with the continuous infusion regimen when compared for the same duration: total median (range) dose of 1305 (300 – 3240) mg without CPBdose and 1740 (400 – 4320) mg with CPBdose for the standard regimen versus 1130 (174 – 2651) mg without CPBdose and 1236 (201 – 2940) mg with CPBdose for the continuous infusion regimen. **Figure S. 4.6.** additionally demonstrates that the continuous infusion regimen yields consistently lower trough concentrations (C_{12}) overall, with the exception of paediatric patients exhibiting augmented eGFR, as depicted in **Figure 4.3**, who might experience inadequate exposure to higher MICs with the standard regimen. Consequently, the continuous regimen ensures controlled drug administration without the potential hazard of reaching toxic levels, as shown in **Figure S. 4.6.**

4.5 Discussion

We developed a population pharmacokinetic model of cefazolin in children undergoing cardiac surgery with cardiopulmonary bypass (CPB). Allometric scaling by body weight was included *a priori* and eGFR was a significant predictor of cefazolin clearance. We performed Monte Carlo simulations with the characteristics of the study patients and a larger in silico paediatric population to evaluate probability of target attainment (PTA) for two dosing regimens: the current weight-based intermittent bolus dosing (50 mg/kg every 4 hours) and an alternative continuous infusion regimen with individual doses calculated from model-derived fixed-effects parameters based on weight and renal function. We also evaluated the impact of adding a CPB device dose (CPBdose) for both regimens. With the standard regimen, the efficacy target is unmet >40% of the dosing interval and, although adding a CPBdose improves the percentage of time within target, it risks pushing cefazolin concentrations above toxicity levels for up to 15% of the dosing interval. In patients with high renal function, especially smaller patients, PTA falls <90% for the highest MIC tested, even with a CPBdose. In contrast, the continuous infusion regimen offers controlled cefazolin

exposure with lower total dose and ensures free cefazolin concentrations remain within target levels for 100% of the evaluated time. We recommend adding a CPBdose to the continuous infusion regimen to offset potential drug loss through the CPB circuit.

The CPB device was integrated into our model as an additional compartment. Following a sensitivity analysis, the CPB device flow rate (QCPB) was fixed to a standard adult cardiac output of 336 L/h, allometrically scaled by weight and normalized by a typical adult weight of 70 kg. There was no significant difference in terms of objective function value or parameter estimates compared to the other options considered, and it was more robust than option (ii), which is based on healthy children's physiology, which might not be applicable to our study cohort, and option (iii), which is based on a protocol from a different hospital and population with potentially distinct demographics from our study group.

Our model parameter estimates (total clearance, CL, of 0.856 L/h and total steady state volume of distribution, Vss, of 2.68 L) are reported for a typical weight of 10 kg and eGFR of 120 mL/min. After adjusting for these, as well as for unbound fraction of 0.2, our estimates of unbound CL of 0.171 L/h and unbound Vss of 0.536 L are lower than those reported by De Cock et al. in children (two-compartment model), unbound CL and Vss of 2.74 L/h and 6.35 L, respectively (De Cock et al., 2017). In this analysis, we only had total plasma concentrations, lacking measurements of unbound drug concentrations or albumin levels, and could not account for variations in albumin levels among patients or changes in protein binding with hemodilution. Further, our estimates of total CL and central volume of distribution (Vd) (1.07 L) are similar to those reported by Salvador et al. in children (one-compartment model), total CL (95%CI) of 0.589 (0.508 – 0.670) L/h and total Vd (95%CI) of 1.57 (0.862 – 2.28) L, respectively (Salvador et al., 2021). The addition of a CPB compartment in the model accounts for changes in volume of distribution due to the priming

fluids of the CPB, while there are mixed reports for CPB effect on clearance, with some reporting increased clearance during CPB and others, similar to ours, not finding an effect (De Cock et al., 2017; Asada et al., 2018; Ingrande et al., 2019). This disparity could arise from multifactorial effects on clearance; organ dysfunction and hypothermia might reduce clearance, while altered protein binding could increase clearance (Lanckohr et al., 2016). eGFR was included as a covariate on clearance (Schwartz et al., 2009), rather than maturation or age. This was based on clinical considerations that maturation function on renal clearance would be more appropriate in stable patients, while eGFR would directly capture alterations in renal function for critically ill patients undergoing surgery, in agreement with previous studies (Illamola et al., 2016; De Cock et al., 2017; Salvador et al., 2021). Temperature, median (range) 30.5 (20.0 – 35.7) °C for our study participants, was not a significant covariate on clearance, and this has also been reported in other studies (Wesley et al., 2015; De Cock et al., 2017; Ricci et al., 2020).

Previous target attainment evaluations also used an efficacy target of 40 mg/L (Jeffrey J. Cies et al., 2019), and a toxicity target of 360 mg/L (Lanoiselée et al., 2021). With the standard regimen, PTA ranged from <20 to 70% for patients with good renal function at the highest MIC evaluated, with the lowest PTA observed for the smallest patients. This is because a dose of 50 mg/kg is not consistent with the allometry of clearance, whereby smaller children have a relatively higher clearance for their size, and hence would benefit from weight-banded dosing with a larger mg/kg dose (Denti et al., 2022). To determine doses for the continuous infusion regimen, we considered it prudent to use a target concentration of 100 mg/L, the average concentration observed in the study patients, to avoid attaining concentrations higher than those reached in the standard practice. In a study to identify clinically relevant targets for effective surgical prophylaxis, Zelenitsky et al. have highlighted that cefazolin concentrations below 104 mg/L at wound closure are linked to an elevated risk of SSIs (Zelenitsky et al.,

2018). There is a heightened susceptibility to infections in this critically ill patient population, amplified by immunosuppression and proinflammatory response triggered during cardiac surgery with CPB (Rodríguez-López et al., 2022). With the continuous infusion regimen, one can opt to dose up to 1.5 times higher than the dose calculated with our algorithm to reach concentrations above 100 mg/L without reaching the toxicity threshold in at least 95% of the patients **(Figure S. 4.6.**

Cies et al. recommended CPBdose to counteract the acute decrease in cefazolin concentrations during CPB and re-dosing at the time of CPB detachment to overcome the loss of cefazolin in the CPB circuit (Jeffrey J. Cies et al., 2019). An in vitro study mimicking the CPB circuit in paediatrics has reported that in CPB systems used for >20 kg patients, recovery of cefazolin decreased by 50%, while those for <20 kg was > 80% five hours after drug administration into the system. They attributed that this could possibly be due to the type and length of tubing used in larger CPB systems with a larger contact surface area which could lead to greater drug absorption (Zeilmaker- Roest et al., 2020). In our simulations, adding a CPBdose to the standard regimen increased the risk of toxicity, while with the continuous infusion regimen, it exhibited no toxicity cost, results in a more stable profile **(Figure S. 4.3.** Figure S. *4.3.* and could counteract potential drug loss through the CPB circuit. Studies in adults have explored the use of prophylactic cefazolin through continuous infusion versus intermittent dosing in cardiac surgeries, while corresponding studies in paediatrics are lacking, with descriptions limited to intermittent dosing with or without CPB dose (De Cock et al., 2017; Ingrande et al., 2019; Jeffrey J Cies et al., 2019). Findings in adults indicate that continuous infusion regimens lead to improved pharmacokinetic and pharmacodynamic outcomes. Given cefazolin's short half-life and reduced plasma levels caused by CPB, it is necessary to administer higher intermittent dosing (higher dose and/or dosing frequency) than that recommended during off-pump (non-CPB) cardiac surgeries, as

shown by Alli et al (Alli et al., 2023). Additionally, intermittent dosing exhibits more significant interindividual variations and concentration fluctuations, as demonstrated by Adembri et al (Adembri et al., 2010). Their study also revealed that when an equivalent total dose was administered through continuous infusion, concentrations remained stable, accompanied by better penetration into myocardial tissue, along with better target attainment. Better cefazolin penetration into subcutaneous fat tissue from sternal wound with continuous infusion has also been shown by Waltrip et al.(Waltrip, 2006). Magruder et al. have shown that in two groups of matched patients receiving coronary artery bypass grafting surgery, continuous infusion regimen was associated with significant decrease in SSIs (0.5% versus 2.3% with intermittent dosing), with the difference observed in SSIs occurring at extremity or conduit harvest sites (Trent Magruder et al., 2015). The primary consideration when delivering antibiotics by continuous infusion is stability, but cefazolin remains stable and can be administered by infusion over 24 hours (Stiles, Tu and Allen, 1989).

Our continuous infusion regimen individually tailors the dose to body weight and renal function and achieves concentrations within the target range for 100% of the dosing duration, while enabling lower drug exposure. In agreement with our study, optimizing cefazolin dose based on renal function and weight has previously been suggested (Chung et al., 2023). The highest renal function level we simulated was 130 mL/min/1.73 m^2, but critically ill paediatric patients could have augmented renal clearance, and CPB initiation is associated with increase in systemic inflammatory response, which could predispose to this (Dhont et al., 2020). Thus, weight and renal function-based cefazolin dosing strategy needs to be used during such surgeries.

There are some limitations in our study. Our dataset comprised 22 participants, and due to the diverse nature of the data in terms of age, body size, renal function, surgical duration, number

of doses, and differences in the practice of administering CPBdose, having a larger participant size with a broader range of covariates would have been advantageous for covariate testing. Moreover, creatinine measurements post-surgery were unavailable, and the PK data did not allow for an assessment of changes in clearance over time. Thus, with the available data, we limited our selection to the most pertinent covariates that both improved the model and were biologically plausible. Pharmacokinetic targets for antibiotic prophylaxis are not well defined, and the targets used are to ensure eradication of an existing micro-organism through maximal time- dependent killing and prevent the development of resistance, which might be higher than what is required for prophylaxis. Asada et al. have reported a twofold rise in free cefazolin fraction during CPB and suggested free cefazolin concentrations need to be directly measured (Asada et al., 2018). With the target concentration we used to calculate dose for the continuous infusion regimen, concentrations would need to be 3.6 times higher to reach seizure-associated concentrations. Thus, even considering higher unbound cefazolin - ~50% for neonates in the ICU (Jongmans et al., 2022) – the toxicity threshold would not be reached. While cefazolin is predominantly eliminated through glomerular filtration, there is a minor contribution from tubular secretion and biliary secretion. In our model, the inclusion of a non-renal clearance parameter alongside renal clearance was not significant, and the model could not distinguish between renal and the probably very limited non-renal clearance. Consequently, our recommended dosage is tailored for patients with normal or enhanced renal function, based on our observed data where creatinine range was 0.2 to 0.4 mg/dL. For severe renal failure where renal clearance is close to zero, it is essential to validate dosing with further data. Additionally, we were unable to explore potential drug loss through the CPB device via adsorption since we did not have concentrations from the CPB device.

Our results show that with the standard weight-based regimen, the smallest patients are at greatest risk of poor prophylactic coverage and the regimen could potentially be improved in patients with high renal function, in centers with a high prevalence of micro-organisms with high MICs. Our dosing algorithm offers a personalized and standardized approach to cefazolin prophylaxis, in contrast to current literature where doses range from 25-50 mg/kg and CPB priming methods vary (Rangel et al., 2011; Bath et al., 2016; Jaworski et al., 2019). We have included a spreadsheet with patient characteristics which illustrates dose calculations (Supplementary material) and a shiny app for easy dose calculation by inputting patient characteristics provided by the user. Further clinical evaluation of this regimen is necessary to assess its performance and implementation feasibility by perfusionists.

4.6 Conclusions

Appropriate and prudent antibiotic prophylaxis is critical for adequate coverage of susceptible pathogens, reduce the risk of antibiotic resistance, and that of adverse drug reactions (NICE Clinical Guidelines, No. 74. 5, 2008; Roberts et al., 2008). We propose an algorithm for a continuous infusion regimen for cefazolin to increase the probability of achieving optimal concentrations.

4.7 Study Highlights

- *What is the current knowledge on the topic?*

Consensus on dosing practices for cefazolin as a prophylactic antibiotic in paediatric cardiac surgery with cardiopulmonary bypass (CPB) is currently absent. Variations exist within current prophylactic regimens, with dose as well as with regards to whether a CPBdose is added.

- *What question did this study address?*

What dosing strategy should be used in this patient group as evaluated by population pharmacokinetic modeling and subsequent model simulations to assess target attainment?

- *What does this study add to our knowledge?*

The frequently used intravenous regimen of 50 mg/kg q4h results in a reduced probability of target attainment in smaller patients with high renal function at higher MICs. Adding further dose to the CPB device in this regimen may increase the risk of reaching seizure-inducing concentrations. A continuous infusion regimen with loading dose calculated based on weight and renal function, enables target attainment throughout the duration of treatment.

- *How might this change drug discovery, development, and/or therapeutics?*

The continuous infusion regimen ensures adequate prophylactic coverage of among various weight and renal function subgroups and improves convenience of administering doses, especially for long surgeries whose duration is unpredictable.

4.8 Supplementary Materials

Methods

Drug assay

Plasma samples were stored on ice for a maximum of six hours, then were centrifuged and stored at -70°C. Concentrations were quantified by validated LC-MS/MS assay, with a concentration range of 0.586 to 110 mg/L. The within-day and between-day precision (coefficients of variation) was below 9% for all quality control levels during the validation, and below 8% during patient sample analysis.

Population pharmacokinetic modeling

Pharmacokinetic modeling was performed with NONMEM v7.5.0 using FOCE-I for all model runs, while Pirana v2.9.8, Perl-speaks-NONMEM v5.2.6 and R v3.6.1 were used for

computation and visualization of output (Keizer, Karlsson and Hooker, 2013). One-, two- and three- compartment disposition models were tested with first-order elimination and zero-order infusion. An additional compartment which represents the CPB pump was included. This compartment was switched on at the start of surgery and switched off at the end of surgery to mimic routine surgical practice. Volume of the CPB compartment (VCPB) was fixed to the CPB priming volume for each patient. The CPB pump flow rate (QCPB) was not available for the study patients, and we performed a sensitivity analysis with different QCPB values where:

i. QCPB was fixed to a typical adult cardiac output of 336 L/h, then allometrically scaled by weight and normalized by a typical adult weight of 70 kg.

ii. Cardiac output was calculated for each study patient based on the expected heart rate and stroke volume by age group, then QCPB fixed to the median cardiac output and allometrically scaled by weight and normalized by 10 kg.

iii. QCPB was calculated for each study patient based on weight-specific blood flow rates adapted from a hospital protocol (C. S. Mott Children's Hospital University of Michigan Medical Center, 1998), then QCPB was fixed to the median value, allometrically scaled by weight and normalized by 10 kg.

Moreover, we estimated a scaling factor for both VCPB and QCPB since cefazolin concentrations are observed in plasma while the CPB compartment contains whole blood in addition to priming fluids.

Between-subject and between-occasion random effects were assumed to follow a log-normal distribution. All pre-dose samples were expected to be below the lower limit of quantification (BLQ) and, after confirming this, they were excluded from the model fit. Combined additive and proportional error models were used to describe the unexplained residual variability.

Model selection was based on changes in the objective function value (OFV) – according to the likelihood ratio test, the OFV is assumed to be $\chi 2$ distributed and for two nested models, the model with one more parameter is chosen if ΔOFV is at least 3.84.

Allometric scaling was applied *a priori* to all disposition parameters to account for the effect of body size. Body size descriptors such as total body weight (TBW) and fat-free mass (FFM) were tested with allometric exponents fixed to 0.75 and 1 for clearances and volumes of distribution, respectively (Janmahasatian et al., 2005; Anderson and Holford, 2009). After the inclusion of allometry, other covariates, namely age, estimated glomerular filtration rate (eGFR) , and switching on of the CPB were tested as covariates on clearance of cefazolin. eGFR was calculated from height and serum creatinine using the modified Schwartz equation (Schwartz et al., 2009).

$$eGFR(mL/min/1.73m^2) = 0.413 \times \left(\frac{height(cm)}{serumcreatinine(mg/dL)}\right) \quad (1)$$

Standard covariate testing was followed: covariates were tested one at the time and then stepwise. Covariates were included based on statistical significance and physiological plausibility. Statistical significance was determined based on hypothesis testing with a generally accepted significance level of 0.05 for forward addition and 0.01 for backward elimination. The likelihood ratio test was used, where ΔOFV between two hierarchical models is assumed to be $\chi 2$ distributed and, for 1 degree of freedom, if ΔOFV is larger than the critical $\chi 2$ value of at least 3.84 during forward addition, the model with one extra parameter is accepted as significant. For backward elimination, if the difference in OFV is at least 6.635 for one extra parameter, the covariate is retained.

Convergence success of the runs, precision of parameter estimates, inspection of diagnostic plots such as standard goodness-of-fit plots and visual predictive checks (VPCs) were also

considered. A non-parametric bootstrap (500 replicates) was run on the final model to obtain 95% confidence intervals (CIs) for the parameter estimates.

Table S. 4.1. Dose calculations for continuous infusion regimen for a 2 kg patient with estimated glomerular filtration rate (eGFR) of 50 mL/min/1.73 m^2.

Continuous infusion dosing regimen for 2 kg patient with eGFR of 50 mL/min	
V_{ss} *for patient*	CL for patient
$V_{ss} \times C_{target}$	$CL \times C_{target}$
$(\mathbf{1.07\ L + 1.61\ L}) \times \left(\frac{\mathbf{2kg}}{\mathbf{10kg}}\right) = \mathbf{0.536\ L}$ $(V_c + V_p) \times \left(\frac{Weight\ in\ kg}{10\ kg}\right)$ V_{ss}	$\mathbf{0.856\ L/h} \times \left(\frac{\mathbf{2kg}}{\mathbf{10kg}}\right)^{\mathbf{0.75}} \times \left(\frac{\mathbf{50mL/min}}{\mathbf{120mL/min}}\right) = \mathbf{0.107L/h}$ $CL \times \left(\frac{Weight}{10}\right)^{0.75} \times \left(\frac{CRCL\ in\ ml/min}{120\ mL/min}\right)$
Loading dose	Maintenance dose/hour
0.536 L × 100 mg/L = 53.6 mg	0.107 L/h × 100 mg/L = 10.7 mg/h
CPBdose	
0.5 × 53.6 mg = 26.8 mg	

V_{ss} = steady state volume (L) , TVV_{SS} = typical steady state volume (L)
TVV_C = typical central volume(L), TVV_p = typical peripheral volume (L)
CL = clearance (L/h), TVCL = typical clearance (L/h)
C_{target} = Target concentration (mg/L)
Weight = weight of patient (in Kg), 10 kg = Typical weight in our study population
eGFR = estimated glomerular filtration rate of patient (in mL/min/1.73 m^2)
120 mL/min = typical eGFR

Table S. 4.2. Comparison of simulated doses for each of the study patients with the standard and alternative regimens (without additional CPBdose).

Patient characteristics				**Observed dose**[‡]	**Simulated regimens without CPBdose**[‡]	
Patient ID	Weight (kg)	CPB duration (h)	eGFR (mL/min/1.73 m^2)	Study dose (mg)	Standard regimen (mg)	Alternative regimen[#] (mg)
1	2	5.60	48	300	300	174
2	5.5	3.53	81	1275	825	580
3	5.9	1.28	85	600	885	635
4	5.4	2.30	91	600	810	623
5	8.4	2.72	97	1260	1260	933
6	6	2.08	97	600	900	713
7	5.3	2.75	99	795	795	655
8	8.9	5.17	108	1260	1335	1063
9	11.8	4.50	108	1800	1770	1337
10	10	1.32	114	1000	1500	1213
11	8.5	4.58	116	850	1275	1080
12	9.4	1.15	117	1425	1410	1177
13	18.7	1.58	119	1870	2805	2080
14	10	1.75	128	1000	1500	1331
15	7.8	1.20	129	800	1170	1103
16	12.5	1.45	131	1250	1875	1620
17	6.3	1.35	131	315	945	938
18	8.1	1.32	132	400	1215	1156
19	17	4.03	135	2550	2550	2125
20	21.6	0.583	140	2000	3240	2651
21	14	0.95	145	1400	2100	1924
22	12.6	4.55	159	1800	1890	1915
Median	8.7	2.08	117	1125	1305	1130
Range	2 – 21.6	0.583 -5.60	48 - 159	300 - 2550	300 - 3240	174 - 2651

[‡] Regimen over a dosing duration of 12 hours
Standard regimen: 50 mg/kg q 4 h
eGFR = estimated glomerular filtration rate
[#]Alternative regimen: $C_{target} = 100$ mg/L
Loading dose: Steady state volume × C_{target}
Maintenance dose: Clearance × C_{target}

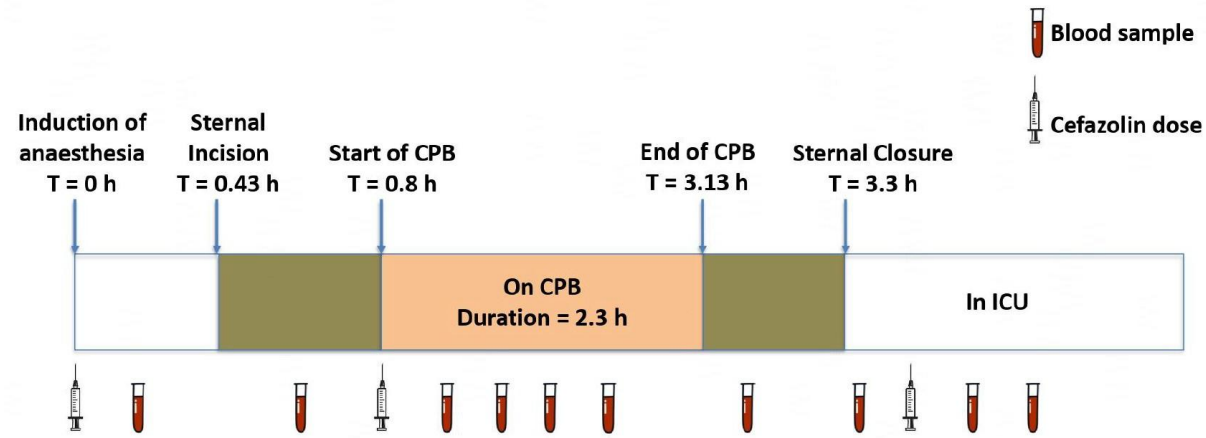

Figure S. 4.1. Timeline of surgery, cefazolin dosing and blood sampling for a patient with median surgical time of 2.3 hours.

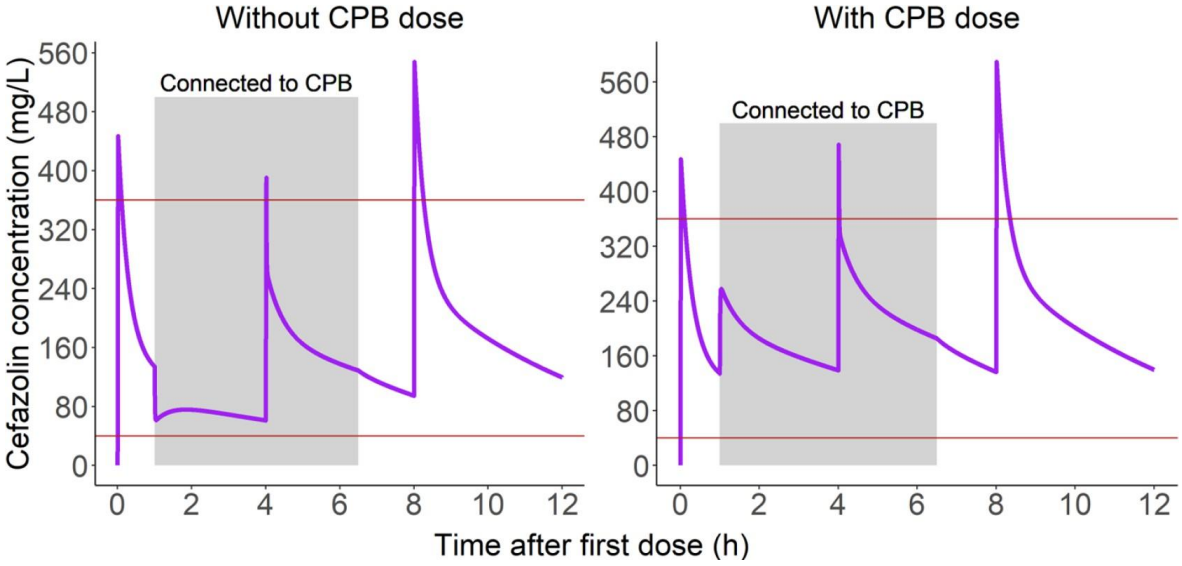

Figure S. 4.2. Cefazolin pharmacokinetic profile simulated using the final model (standard intermittent dosing regimen).

The profile was simulated for a standard dose of 50 mg/kg administered every 4 hours over a 12-hour period for a child with weight of 2 kg and eGFR of 50 mL/min/1.73 m^2. The grey shaded area shows time of surgery (patient connected to the cardiopulmonary bypass (CPB) system). Left, no CPBdose was added; right, a CPBdose of 50 mg/kg was added. Horizontal lines – pharmacokinetic target (40 mg/L) and toxicity target (360 mg/L).

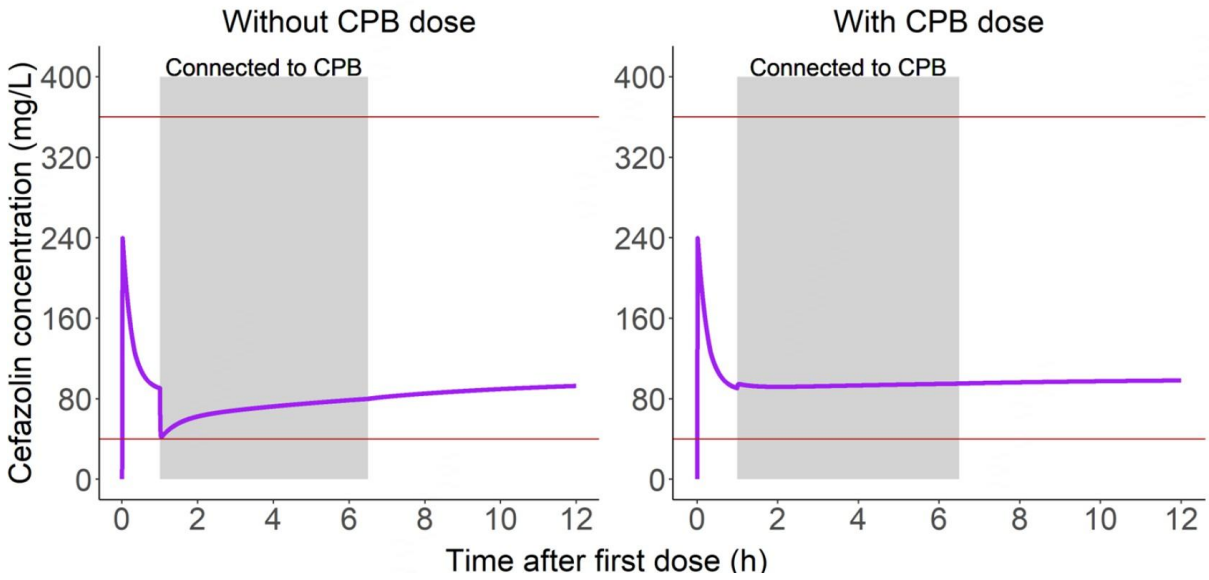

Figure S. 4.3. Cefazolin pharmacokinetic profile simulated using the final model (alternative continuous infusion regimen).

The profile was simulated for the alternative regimen continuous infusion, administered over a dosing period of 12-hours, for a child with weight of 2 kg and eGFR of 50 mL/min. Loading and maintenance doses for the continuous infusion were calculated from model-derived individual parameters. The grey shaded area shows time of surgery (patient connected to the cardiopulmonary bypass (CPB) system). Left, no CPBdose was added; right, CPBdose of 50 mg/kg was added. Horizontal lines – pharmacokinetic and toxicity targets (total cefazolin concentrations of 40 mg/L and 360 mg/L).

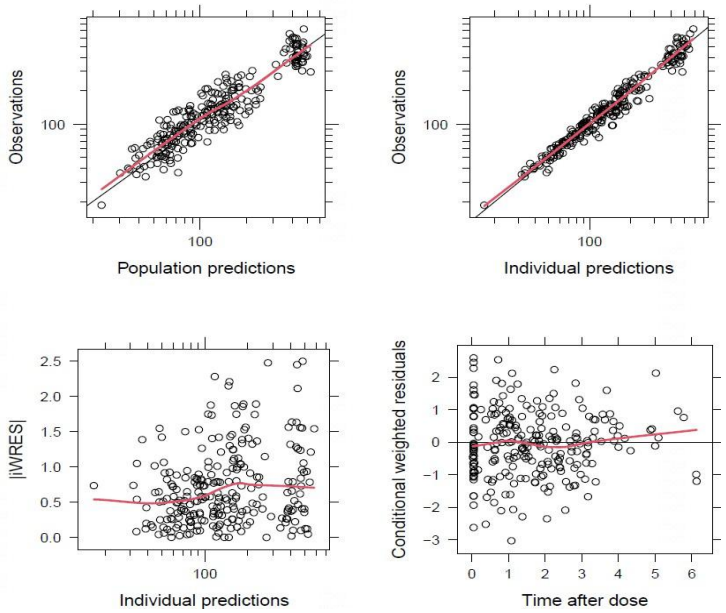

Figure S. 4.4. Goodness-of-fit (GOF) plots for the final cefazolin model.

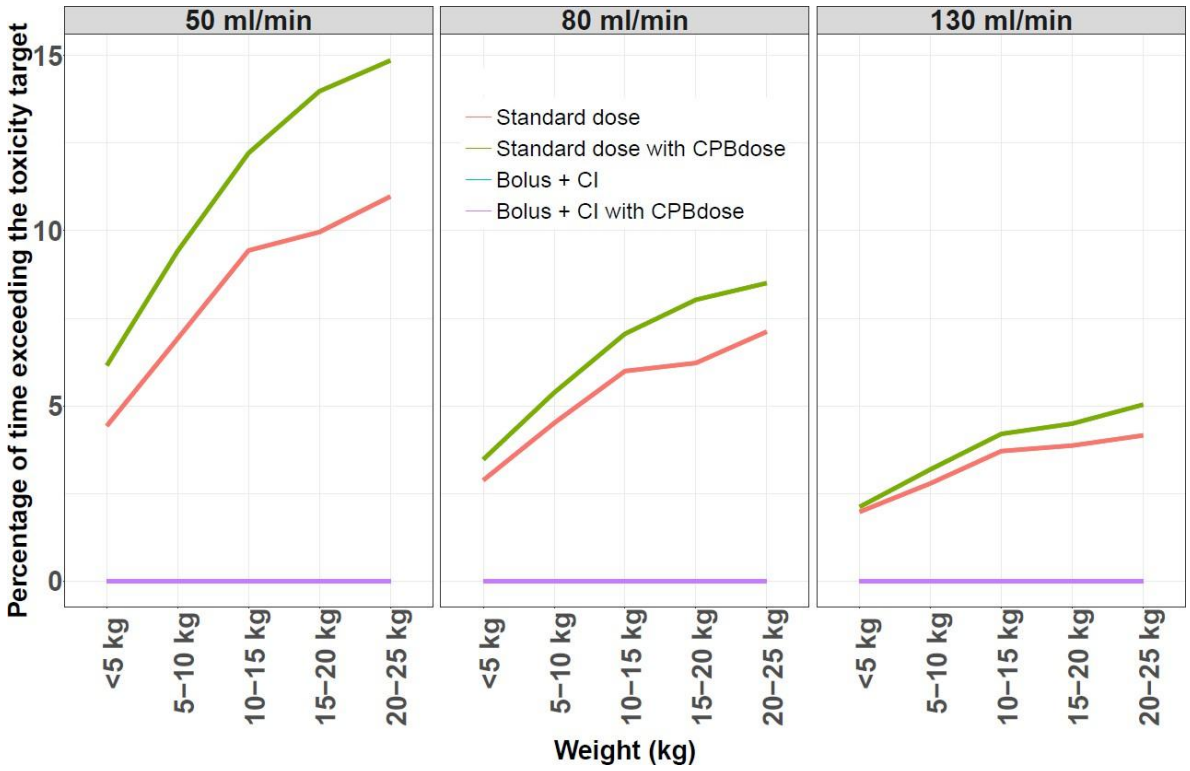

Figure S. 4.5. Probability distribution plot showing percent of time total cefazolin concentrations are above the toxicity target for each of the evaluated dosing regimens.
Toxicity target = 360 mg/L. Each of the dosing regimens were evaluated throughout a dosing period of 12 hours. Results are for simulations using a virtual paediatric population (1000 patients simulated per weight and renal function group). The lines show the median result for the simulations. CPBdose = additional dose into the bypass priming solution, CI = continuous infusion.

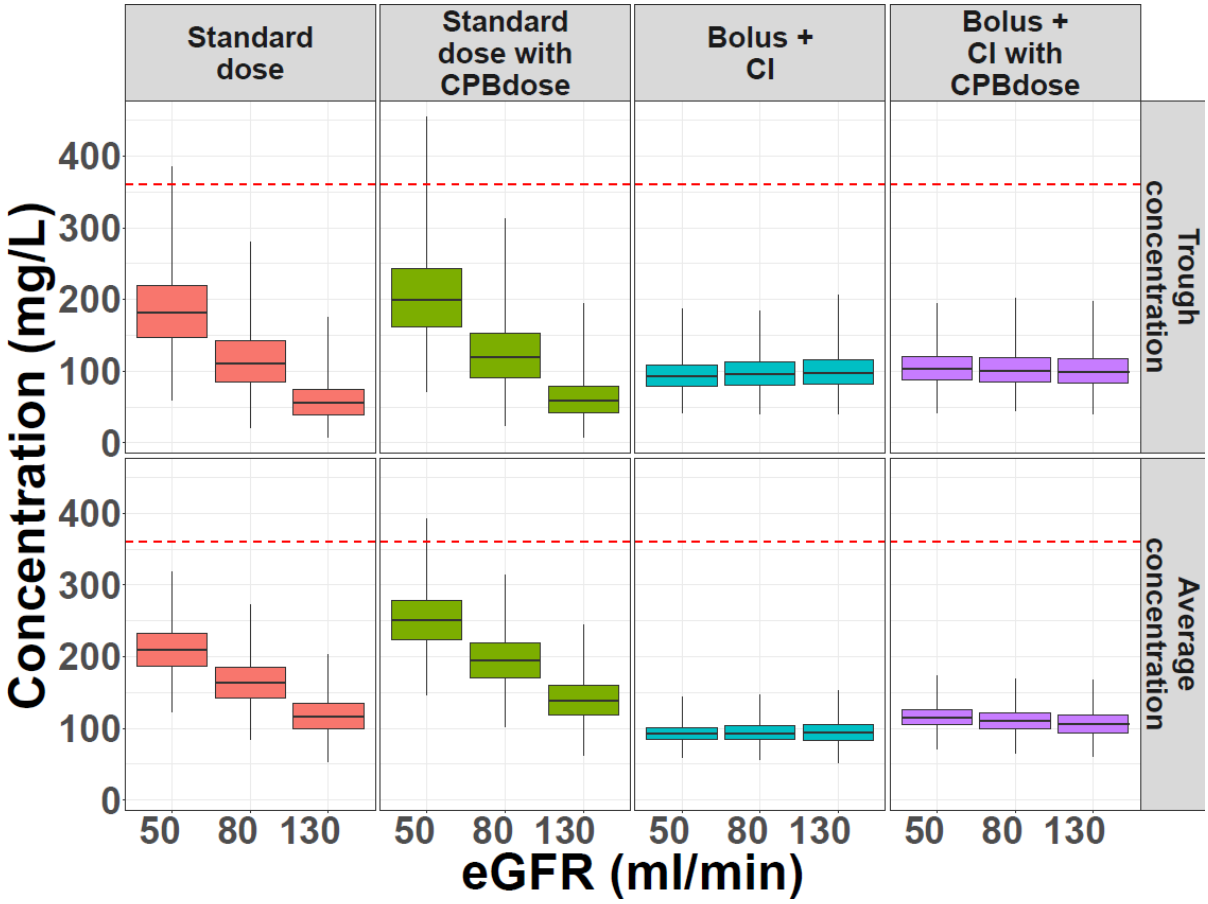

Figure S. 4.6. Total trough (C_{12}) and average concentrations for each of the evaluated dosing regimens.

Results are based on simulations for a virtual paediatric population (1000 patients simulated per weight and renal function group). Results shown here are for all weights, grouped by renal function and dosing regimen. The horizontal dashed line shows the toxicity threshold assessed, 360 mg/L.

Chapter 5 Population pharmacokinetics of rifabutin among HIV/TB co-infected children on lopinavir/ritonavir-based antiretroviral therapy

5.1 Abstract

In adults requiring protease inhibitor (PI)-based antiretroviral therapy (ART) replacing rifampicin with rifabutin is a preferred option, but there is lack of evidence to guide rifabutin dosing in children, especially with PIs. We aimed to characterize the population pharmacokinetics of rifabutin and 25-O-desacetyl rifabutin (des-rifabutin) in children and optimize its dose.

We included children from three age cohorts: (i) <1-year-old and (ii) 1-to-3-year-old, who were ART-naïve and received 15-20 mg/kg/day rifabutin for 2 weeks followed by LPV/r-based ART with 5 or 2.5 mg/kg/day rifabutin, respectively, while (iii) >3-year-old were ART-experienced and received 2.5 mg/kg/day rifabutin with LPV/r-based ART. Nonlinear mixed-effects modeling was used to interpret the data. Monte Carlo simulations were performed to evaluate the study doses and optimize dosing using harmonized weight-bands.

Twenty-eight children were included, with median (range) age 10 (0.67, 15) years, weight of 11 (4.5, 45) kg, and weight-for-age-z-scores (ZWFA) of -3.33 (-5.15, -1.32). A two-compartment disposition model, scaled allometrically by weight, was developed for rifabutin and des-rifabutin. LPV/r increased rifabutin bioavailability by 158% (95% confidence interval: 93.2%, 246%) and reduced des-rifabutin clearance by 76.6% (74.4%, 78.3%). Severely underweight children showed 26% (17.9%, 33.7%) lower bioavailability. Compared to adult exposures, simulations resulted in higher median steady-state rifabutin and des-rifabutin exposures in 6-20 kg during TB-only treatment with 20 mg/kg/day. During LPV/r co-treatment, the 2.5 mg/kg/day dose achieved similar exposures to adults, while the 5

mg/kg/day dose resulted in higher exposures in children >7 kg. All study doses maintained median Cmax <900 µg/L. The suggested weight-band dosing matches adult exposures consistently across weights and simplifies dosing.

5.2 Introduction

In 2021, it was estimated that 185,000 tuberculosis (TB)-related deaths occurred among people with Human Immunodeficiency Virus (HIV), of which 11% were children (World Health Organization., 2022). The ratio of TB-related mortality to incidence was 0.35 in children under the age of 15 with HIV, higher than 0.19 in children without HIV (Vonasek et al., 2022). According to CHAI reports, in 2022, 24% of children with HIV were on lopinavir/ritonavir (LPV/r)-based antiretroviral (ART) regimen (Clinton Health Acess Initiative (CHAI), 2023). WHO guidelines indicate that LPV/r-based ART is recommended as an alternative first-line regimen for children >3 kg aged from 4 weeks to 10 years and a preferred second-line regimen for all children and adolescents who have failed dolutegravir-based first-line ART (World Health Organization, 2021). Among adults receiving LPV/r-based ART, use of rifabutin is recommended instead of rifampicin, since rifampicin decreases the concentration of lopinavir by more than 75%, while rifabutin has no significant effect on LPV/r exposure (Boulanger, Hollender, Farrell, Stambaugh, Maasen, Ashkin, Symes, Luis A Espinoza, et al., 2009; Khachi et al., 2009; Decloedt et al., 2011; Matteelli et al., 2012; Lan et al., 2014; Naiker et al., 2014). On the other hand, CYP3A4 contributes to the elimination of rifabutin and 25-O-desacetyl rifabutin (des-rifabutin), its metabolite from arylacetamide deacetylase (AADAC) (Nakajima et al., 2011). Thus, when co-administered with inhibitors of CYP3A4 such as LPV/r, exposures of both rifabutin and des-rifabutin are increased (Department of Health and Human Services., 2022). This may result in adverse effects such as neutropenia, thrombocytopenia, arthralgias, skin discoloration, and anterior uveitis

(Moultrie et al., 2015; Crabol et al., 2016; Peloquin, 2023), and necessitates dose adjustment of rifabutin during co-treatment as well as monitoring of adverse effects.

During LPV/r therapy in adults, it is recommended that rifabutin dose be reduced to 50-75% of the standard dose (WHO, 2023). Accordingly, the adult rifabutin dose is decreased from 300 mg/day to 150 mg/day when co-administered with LPV/r, as studies have demonstrated comparable exposure levels without impairing exposures of LPV/r (Matteelli et al., 2012; Lan et al., 2014). In children, rifabutin is recommended at 5 mg/kg/day for prophylaxis of Mycobacterium Avium Complex (MAC) and at 10-20 mg/kg/day for MAC and TB treatment (Department of Health and Human Services, 2023). However, there is lack of data in children regarding the optimal dose during LPV/r-based antiretroviral therapy. A study in children administered rifabutin alongside LPV/r by Moultrie et al. involved six children and was halted due to the occurrence of grade 4 neutropenia in two of the children (Moultrie et al., 2015).

In this work, a population pharmacokinetic analysis was performed using data from three age cohorts of children with HIV/TB co-infection who received rifabutin-based TB treatment along with LPV/r-based antiretroviral therapy. The objectives were to characterize the pharmacokinetics of rifabutin and des-rifabutin and perform simulations to assess adequacy of dosing in the studies and devise a weight band-based dosing regimen to align paediatric exposure levels with those achieved in adults undergoing standard TB treatment.

5.3 Materials and methods

Study Participants. Data for this study were obtained from three prospective studies carried out in Nigeria in children who were part of the AIDS Prevention Initiative in Nigeria through the US President's Emergency Plan for AIDS Relief (APIN PEPFAR) paediatric ART

program and required protease inhibitor-based ART. The studies included three distinct age groups: <1- year-old, 1–3-year-old, and 3-15-year-old.

Drug administration and sampling. A <1 year cohort initially underwent TB treatment that included rifabutin at a dose of 20 mg/kg/day, following the US guidelines for treating opportunistic infections in children with and exposed to HIV (Department of Health and Human Services, 2023). After two weeks, they began LPV/r-based ART, at which point the rifabutin dose was adjusted to 5 mg/kg/day. Similarly, a 1–3-year-old cohort received a two-week TB regimen with rifabutin at a dose of 15-20 mg/kg/day, followed by initiation of LPV/r- based ART, with the rifabutin dose adjusted to 2.5 mg/kg/day. A 3-to-15 years old cohort were already experienced with ART and were failing on their first-line regimen, necessitating a switch to LPV/r-based ART. On the same day as the switch, they were included in the study and began TB treatment with a rifabutin dose of 2.5 mg/kg/day (Rawizza HE et al., 2021).

The rifabutin dose during LPV/r-based ART for all age cohorts in the study was decided based on extrapolation from adults with adjustments based on allometry for children, and knowledge gained from the study by Moultrie et al., where adequate concentrations were reported after a 5 mg/kg/day thrice weekly dose during LPV/r co-treatment (Anderson and Holford, 2009; Holford, Heo and Anderson, 2013; Moultrie et al., 2015; Rawizza HE et al., 2021). Rifabutin was administered as an oral suspension prepared from Mycobutin® capsules by Lupin Pharmaceuticals, as previously detailed (Haslam et al., 1999).

Blood samples were collected intensively at 0, 2-, 4-, 8-, 12-, and 24-hours post-dose during weeks 2 and 4 for all age groups. Additionally, in the cohort of children under 1 year old, samples were taken at week 6, and in the 3-15-year-old cohort, samples were collected at week 8. Sparse samples were obtained at weeks 6 and 12 (at 0 and either 3-5- or 24-26-hours

post-dose) in the 1-3-year-old cohort. The intensive samples at week 2 were obtained following rifabutin- containing TB only treatment in the <1-year and 1-3-year groups, while the week 2 intensive samples for the 3-15-year group, who had experience with ART, and samples from all other visits were taken after rifabutin with LPV/r co-treatment. Specifically, data on rifabutin only was available for the two younger cohorts, while data on rifabutin with LPV/r was available across all age groups. A schematic of the study design is included in supplementary materials **Figure S. 5.1**.

Data from the Moultrie et al. study was used for external model validation (Moultrie et al., 2015). This study was conducted in South African children with HIV ≤5-years-old, receiving LPV/r- based ART with rifabutin dosed at 5 mg/kg/day thrice weekly. Blood samples were collected after the sixth dose at 0, 2, 4, 9, 24, and 48 h. After validation, this data was incorporated into the analysis, and the parameters were re-estimated.

Drug quantification. All samples were centrifuged at 2600 rpm for 10 min to extract plasma within 1 hour after collection and were then stored at -80°C until analysis. Rifabutin and des-rifabutin concentrations were concurrently quantified at the University of Cape Town with a validated LC/MS/MS assay with a calibration range of 3.91 to 1000 µg/L for rifabutin and 0.780 to 200 µg/L for des-rifabutin (Moultrie et al., 2015).

Population pharmacokinetic analysis. A joint population pharmacokinetic model for both rifabutin and des-rifabutin was developed using nonlinear mixed-effects modeling in NONMEM (v.7.5.0). First-order conditional estimation with eta-epsilon interaction (FOCE-I) was used for all model runs. Model management was done with Pirana (v2.9.8), and post-processing of results and visualization of output were carried out with Perl-speaks-NONMEM (v5.2.6) and R (v4.3.0) (Keizer, Karlsson and Hooker, 2013). The modeling process was sequential, starting with the development of the parent (rifabutin) model,

followed by development of the metabolite (des-rifabutin) model while maintaining fixed population parameter estimates for the parent, then proceeding with the joint parent-metabolite model. Various disposition models were tested for both the parent and metabolite, including one-, two-, and three-compartment models, incorporating first-order absorption and elimination, along with the effect of LPV/r co-treatment. To describe absorption delay, lag time and transit compartments were evaluated. Allometric scaling using total body weight was applied to all disposition parameters with allometric exponents fixed to 0.75 and 1 for clearances and volumes of distribution, respectively (Anderson and Holford, 2009).

Molar conversion of the rifabutin dose and the concentrations of rifabutin and des-rifabutin was utilized to adjust for the difference in molecular weight between rifabutin (847.02 g/mol) and des-rifabutin (805 g/mol). Since in joint parent metabolite models it is in general not possible to estimate both the fraction metabolized (FM) and metabolite disposition parameters concurrently, three approaches were tested to address the challenge of model identifiability (Lavielle and Aarons, 2016):

i. Assuming full conversion of the parent to the metabolite (FM fixed to 1).

ii. Assuming volumes of distribution for the parent and metabolite are equivalent and estimate the volumes as well as FM.

iii. Estimating metabolite volumes and clearance conversion to the metabolite with a covariate on the clearance of the parent via an alternative pathway.

In certain pharmacokinetic profiles, it was observed that both the rifabutin and des-rifabutin concentrations just prior to the observed dose were dramatically lower than typically expected at steady state for a drug with a long terminal half-life like rifabutin, when the pre-dose and 24-hour concentrations should remain fairly similar. To address this issue, whenever a pre-dose concentrations fell below one-third of the concentrations 24 hours after the

observed dose, the prior dosing history was disregarded and the baseline method B2 was used (Dansirikul, Silber and Karlsson, 2008). This approach initialises all disposition compartments using the observed concentration values and the residual unexplained variability (more details in the Supplementary Material).

Between-subject and between-occasion random effects were estimated, assuming to follow a log- normal distribution. Combined error model (i.e., additive and proportional error) was used to describe the unexplained residual variability. Additionally, considering that both rifabutin and its metabolite were quantified simultaneously and from the same sample, a correlation coefficient between their residual unexplained variability terms was incorporated using the L2 method (Beal and Sheiner, 2008). Samples below LLOQ (BLQ) were received as censored and handled using a variant of the M6 method by Beal (Beal, 2001), i.e. 50% of the LLOQ was imputed for the last BLQ during absorption and the first BLQ during elimination and their additive error was increased by LLOQ/2. All other BLQs in a series were excluded from the model fit but retained for model diagnostics. Model development and selection was based on inspection of diagnostic plots and statistical significance. This latter aspect was evaluated with changes in the objective function value (OFV), whereby for two nested models, an additional degree of freedom (i.e. one extra estimated parameter) is deemed statistically significant at $p<0.05$ if the improvement in OFV is at least 3.84 points. For non-nested models, the Akaike information criterion (AIC) was used to assess goodness of fit.

Screening for covariates was performed by inspecting plots of individual empirical Bayes estimates vs. covariates and scrutinized based on physiological plausibility. Covariates tested in the model included LPV/r co-treatment, maturation (Anderson and Larsson, 2011), weight-for- age z-score (ZWFA, calculated using WHO growth charts for ≤10 years old and Centres

for Disease Control and Prevention growth charts for >10 years old), CD4 count, age group, and creatinine clearance (calculated by the modified Schwartz equation) (Schwartz et al., 2009). These were tested individually in the model and selected using a stepwise approach with $p<0.05$ on forward addition and $p<0.01$ on backward elimination. $(AUC)_{0\text{-}24h}$ and C_{max} were derived from the final model, using the individual post hoc pharmacokinetic parameters, during the intensive sampling periods with and without LPV/r co-treatment.

Model performance was assessed throughout model development using a prediction-corrected visual predictive check (pcVPC) since there were several doses and a wide weight range in the overall data (Bergstrand et al., 2011). Parameter precision of the final model was obtained using sampling importance resampling (SIR) procedure (Dosne, Bergstrand and Karlsson, 2017).

Simulations. Monte Carlo simulations were performed with the final model, including random effects parameters, to evaluate the doses used in the study and suggest weight-banded rifabutin paediatric dosing during LPV/r co-treatment using harmonized weight bands (Waalewijn, Almett, 2024). For these simulations, we used a representative in-silico population of 22,500 African children (Wasmann et al., 2021a), with uniformly distributed weight. A sample size of 500 children per unit kg was used for the simulations. Steady-state $AUC_{0\text{-}24h}$ and C_{max} were obtained for two dosing scenarios:

1. Milligrams per kilogram (mg/kg) dosing (replicating the doses used in the studies)

a. Without LPV/r co-treatment: for a scenario of TB only treatment, rifabutin dose of 20 mg/kg/day was simulated. In the study, the 3-15-year-old cohort did not receive TB only treatment, but this scenario was simulated for all the virtual paediatric population with the rifabutin dose capped to 300 mg/day, which is the adult dose.

b. With LPV/r co-treatment: during TB-HIV co-treatment, rifabutin dose of 5 mg/kg/day was simulated for <1-year-old and 2.5 mg/kg/day was simulated for ≥1- year-old, similar to the study.

2. Harmonized weight band–based dosing

Rifabutin doses optimized for scenarios without and with LPV/r co-treatment were simulated for the following harmonized weight-bands (Waalewijn, Almett, 2024): ≥6 to 10 kg, ≥10 to 15 kg, ≥15 to 20 kg, ≥20 to 25 kg, ≥25 to 30 kg, ≥30 to 35 kg, and ≥35 kg.

Targets for simulations. Rifabutin lacks clear reports defining its therapeutic range, but a relationship between the area under the concentration-time curve (AUC) and the efficacy of antituberculosis drugs has been suggested (Pasipanodya and Gumbo, 2011; Gumbo et al., 2015). Other sources propose that C_{max} exceeding 900 µg/L could elevate the risk of adverse reactions (Hafner et al., 1998; Alsultan and Peloquin, 2014; Hennig et al., 2016). In line with this, we compared the medians of our simulated exposures ($AUC_{0\text{-}24h}$) with a range of reported median $AUC_{0\text{-}24h}$ values in adults and evaluated attainment of C_{max} < 900 µg/L. For standard TB treatment (300 mg once daily (OD) rifabutin dose in adults), our comparator adult median $AUC_{0\text{-}24h}$ values varied from 5640 µg·h/L (Lan et al.) to 2790 µg·h/L (Tanuma et al.) for rifabutin and from 700 µg·h/L (Lan et al.) to 273 µg·h/L (Naiker et al.) for des-rifabutin (Tanuma et al., 2013; Lan et al., 2014; Naiker et al., 2014). During co-treatment with LPV/r (150 mg OD rifabutin dose in adults), the median $AUC_{0\text{-}24h}$ for rifabutin ranged from 7290 µg·h/L (Lan et al.) to 4770 µg·h/L (Naiker et al.), and from 4130 µg·h/L (Lan et al.) to 4120 µg·h/L (Naiker et al.) for des-rifabutin (Lan et al., 2014; Naiker et al., 2014). Furthermore, for dose optimization with weight band-based dosing, the aim was to achieve median steady-state $AUC_{0\text{-}24h}$ of at least 4500 µg·h/L, an exposure limit reported to be associated with acquired rifamycin resistance (Weiner, Benator, Burman, et al., 2005; Weiner, Benator, Peloquin, et al., 2005; Hennig et al., 2016).

5.4 Results

Participant characteristics. The study included 28 children living with HIV and TB co-infection who were enrolled in the APIN PEPFAR program in Nigeria. Baseline characteristics of the participants are presented in **Table 5.1**. Three children were less than one year old, ten were aged 1 to 3 years, and fifteen were aged 3 to 15 years. The overall median (range) age was 10 (0.67, 15) years and weight 11 (4.5, 45) kg. Severe malnutrition (weight-for-age-z-score [ZWFA] < -3) was observed in ~60% of the children, with overall ZWFA of -3.33 (-5.15, -1.32). In the oldest cohort (3-15 years old), the children had been on ART for a median of 3.8 (1.5, 8.9) years, with 4 out of 15 classified as WHO HIV stage 4, while the remaining were at stage 3. Overall, neutropenia was observed in 12 children on 26 occasions (ten occasions: grade 1; six occasions: grade 2; eight occasions: grade 3; two occasions: grade 4). A total of 462 samples were available for quantification of rifabutin and des-rifabutin, and only 16 samples (1.7%) were below the limit of quantification (BLQ). Fifteen profiles had pre-dose concentrations lower than one- third of 24-hour concentrations across different visits (**Figure S. 5.3**Figure S. *5.3*and were handled by the method of initialization, detailed in the supplementary material.

The validation dataset included six children aged 2 (0.83-3) years, weight 11 (9, 12) kg, and ZWFA -1.06 (-1.85, 0.950). Three out of the 6 children were classified as WHO HIV stage 4, while the rest were at stage 3. Neutropenia was observed in four of the children (one: grade 1, one: grade 2, and two: grade 4) (Moultrie et al., 2015). A total of 36 samples of rifabutin and des- rifabutin were available, and none of them BLQ.

607 Table 5.1. Patient demographic and study characteristics, as median (range) where applicable.

Study cohort	**<1-year-old n=3**	**1-to-3-year-old n=10**	**3-to-15-years-old** (Rawizza HE et al., 2021) **n=15**	**Validation data** (Moultrie *et al.*, 2015) **n=6**
ART duration (years)	ART-naïve	ART-naïve	3.8 (1.5, 8.9)	1 (0.5, 2.3)
Backbone ART	ABC+3TC	ABC+3TC	ABC+3TC	ABC/d4T+3TC
Age (months)	11 (8, 11)	18 (14, 28)	157 (123, 185)	25 (10, 41)
Weight (kg)	4.75 (4.50, 6.50)	7.33 (5.60, 11.0)	27.0 (20.0, 45.0)	10.6 (8.50, 12.2)
Height (cm)	75 (71, 78)	73 (70, 84)	138 (121, 164)	79 (74, 90)
ZWFA*	-4.95 (-5.15, -3.20)	-2.64 (-5.06, -1.39)	-3.25 (-4.38, -1.32)	-1.06 (-1.85, 0.951)
ZHFA*	0.884 (-1.52, 3.36)	-2.70 (-5.09, 0.650)	-2.03 (-3.61, -0.315)	-1.88 (-3.04, 1.89)
Serum creatinine (mg/dL)	0.25 (0.2, 0.46)	0.30 (0.20, 0.40)	0.4 (0.2, 0.6)	NA
Creatinine clearance‡ (mL/min/1.73 m^2)	124 (67.0, 161)	110 (74.3, 173)	145 (90, 289)	NA
CD4 count (cells/mm^3)	644 (465, 724)	1011 (271, 1708)	156 (24, 652)	1174 (982, 1695)
Absolute neutrophil count (cells/mm^3)	2235 (860, 3388)	436 (1697, 6787)	1480 (476, 8721)	3070 (1500, 2700)

D4T, stavudine; ABC, abacavir; 3TC, Lamivudine; NA, not available; ZWFA, weight-for-age z scores; ZHFA, height-for-age z scores

Participant demographics are at first pharmacokinetic sampling (week 2)

*The WHO and CDC tables were used for the calculation of z scores.

‡Calculated by modified Schwartz formula (Schwartz *et al.*, 2009):

$$0.413 \times \left(\frac{height(cm)}{serum\ creatinine(mg/dL)}\right)$$

Population pharmacokinetic model.

Structural model. The final joint model for rifabutin and des-rifabutin had two-compartment disposition models for both parent and metabolite with first-order elimination and absorption delay was best described by lag time (**Figure S. 5.4**Figure S. *5.4*. To account for differences in body weight, allometric scaling was incorporated *a priori* on all clearance and volume of distribution parameters, with normalization to the median weight of 10 kg.

The elimination of rifabutin and its metabolite des-rifabutin was best modelled with three distinct parameters: inhibitable CYP3A4 pathway (representing the elimination clearance of rifabutin by CYP3A4 that is inhibited by co-administration of LPV/r), clearance conversion (indicating the conversion of rifabutin to des-rifabutin by AADAC), and clearance metabolite (representing the elimination clearance of des-rifabutin). Although the two clearance pathways of rifabutin, by CYP3A4 and by AADAC, would normally not be separable, here we were able to do so due to the effect of LPV/r to inhibit the CYP3A4 pathway. Re-parametrizing the model by employing clearance conversion and a separate clearance for the parent that is considered as fully inhibited by LPV/r, led to a significantly enhanced model fit compared to estimating the fraction metabolized (FM) with only a single clearance parameter (ΔAIC = -36.6, df = 1). Consequently, we were able to estimate the volumes of distribution for the metabolite, which had initially been fixed to the volumes of distribution for the parent compound. This is all under the assumption that 100% of the rifabutin eliminated by the clearance conversion is transformed into des-rifabutin.

For a typical child weighing 10 kg not taking LPV/r, the estimated (95% confidence intervals) rifabutin inhibitable CYP3A4 pathway was 13.6 (9.22 – 19.1) L/h, clearance conversion was 16.2 (12.4, 21.1) L/h, and des-rifabutin clearance was 106 (80.8, 145) L/h.

Considering the complexity of the model, variability parameters were included parsimoniously, where most relevant and essential. Variability between subjects was accounted for by incorporating a common between-subject variability (BSV) random effect on the two clearance pathways of rifabutin (both rifabutin inhibitable CYP3A4 clearance and clearance conversion), and a separate BSV was included for des-rifabutin clearance. Between-occasion variability (BOV) was estimated for all absorption parameters. Parameter estimates of the final model, together with their precision, are presented in **Table 5.2.**

Covariate model. Co-treatment with LPV/r had a major impact on various pharmacokinetic parameters. Specifically, it increased rifabutin bioavailability by 2.58-fold (1.93, 3.46) (ΔOFV = - 45.7, 1 df , $p < .001$), it fully inhibited one of the clearance pathways of rifabutin which is mediated by the CYP3A4 pathway (ΔOFV = -40.6, 1 df , $p < .001$), and it reduced des-rifabutin clearance by 76.6% (74.4, 78.3), (ΔOFV = -78.6, 1 df , $p < .001$).

Additionally, we found that weight-for-age z score (ZWFA) had an impact on rifabutin bioavailability (ΔOFV = -27.1, 2 df , $p < .001$). It was observed that as ZWFA decreased below -3, corresponding to the WHO classification of severe malnutrition, there was an estimated decrease of 26.0% (17.9% – 33.7%) in bioavailability for each unit decrease in ZWFA ($p < 0.05$, df = 2). Finally, the younger cohort, aged ≤3 years, were estimated to have a 72.3% (48.5% – 85.7%) slower rate of absorption ($p < 0.05$, df = 1). Maturation was tested on all clearance parameters and did not show statistical significance (ΔOFV = -1.52, 2 df , $p > .05$). According to the parameter estimates, complete maturation was achieved at 8 months, which is the youngest age in the dataset. As a result, it was not incorporated into the model.

654 Table 5.2. Parameter estimates for rifabutin-des-rifabutin model.

Parameter	Typical Value (95% CI)[1]	RSE (%)	Parameter variability, % CV[2] (95% CI)[1]	RSE(%)	Shrinkage (%)
Rifabutin					
Clearance (Inhibitable CYP3A4 pathway) (L/h)[3]	13.6 (8.77, 18.8)	18.6	BSV: 20.7 (15.6 – 26.0)	26.7	14
Clearance conversion (AADAC pathway) (L/h)[3]	16.2 (12.8, 20.7)	12.7			
Central volume of distribution, $V_{C,P}$ (L)[3]	185 (135, 251)	16.3			
Peripheral volume of distribution, $V_{P,P}$ (L)[3]	232 (171, 313)	15.5			
Intercompartmental clearance, Q_P (L/h)3	25.1 (17.3, 33.1)	15.7			
Bioavailability, F	1 Fixed	-	BOV: 71.9 (59.5, 85.1)	15.4	3
Absorption rate constant, Ka (1/h)	1.27 (0.810, 2.14)	29.0	BOV: 118 (84.0, 175)	24.1	11
Absorption lag time, Lag (h)	0.544 (0.338,0.805)	21.9	BOV: 74.8 (44.4, 105)	32.6	42
Des-rifabutin					
Clearance metabolite (L/h)[3]	106 (82.1, 142)	14.2	BSV: 30.8 (23.2, 39.2)	26.0	8
Central volume of distribution, $V_{C,M}$ (L)[3]	43.0 (25.9, 64.4)	22.7			
Peripheral volume of distribution, $V_{P,M}$ (L)[3]	241 (169, 322)	16.2			
Intercompartmental clearance, Q_M (L/h)[3]	44.4 (31.5, 63.3)	18.7			
Covariates					
LPV/r effect on bioavailability (%)	+158 (+105, +239)	13.1			
LPV/r effect on rifabutin clearance (Inhibitable CYP3A4 pathway) (%)	-100 Fixed	-			
LPV/r effect on des-rifabutin clearance (%)	-76.6 (-79.8, -73.1)	7.76			
ZWFA effect (each point below -3) on bioavailability[4] (%)	-26.0 (-34.1, -18.1)	15.9			
Age effect (≤3 years old) on Ka (%)	-72.3 (-83.3, -57.1)	24.4			
Residual unexplained variability					
Rifabutin: proportional error (%)	18.8 (16.3, 21.7)	6.84			15.4
Rifabutin: additive error (µg/L)	10.1 (5.24, 15.9)	29.3			
Des-rifabutin: proportional error (%)	10.8 (8.41, 13.6)	12.3			15.4
Des-rifabutin: additive error (µg/L)	11.6 (9.75, 14.1)	9.62			
Correlation coefficient for measurement error (%)	28.2 (14.6, 42.1)	24.4			

[1]Confidence intervals were computed with sampling importance resampling (SIR) on the final model.

[2]Between-subject (BSV) and between-occasion variability (BOV) was obtained using $\sqrt{e^{(OM^2)}-1}$ and reported as approximate %CV.

[3]Allometric scaling with total body weight, values are reported for median weight of 10 kg.

[4]ZWFA effect on bioavailability per unit decrease in children with a ZWFA < -3.

655

Effect of LPV/r co-treatment on rifabutin and des-rifabutin exposures. When comparing model-derived individual exposures without and with the co-administration of LPV/r in the <3- year-old patients who received both treatments, the geometric mean ratio (GMR) (95% CI) of rifabutin AUC0-24 and Cmax with LPV/r co-treatment versus without were 1.25 (0.544 – 2.88) and 1.07 (0.464 – 2.46), respectively. For des-rifabutin, during LPV/r co-treatment, AUC0-24 increased by almost 5-fold, with GMR (95% CI) of 4.86 (2.11 – 11.2), while Cmax increased by over 3-fold, with GMR of 3.52 (1.53 – 8.10).

External validation. Validation of the base model with external data (from Moultrie et al. (Moultrie et al., 2015)), incorporating the effects of LPV/r, demonstrated the model's effectiveness in accurately predicting these data (**Figure S. 5.5**Figure **S**. *5.5*

Model diagnostics. The pcVPC for rifabutin and des-rifabutin, stratified by presence or absence of LPV/r co-treatment, shows that the 10th, 50th, and 90th percentiles of the data are consistent with the respective 95% confidence intervals from the model, indicating good fit (**Figure 5.1**).

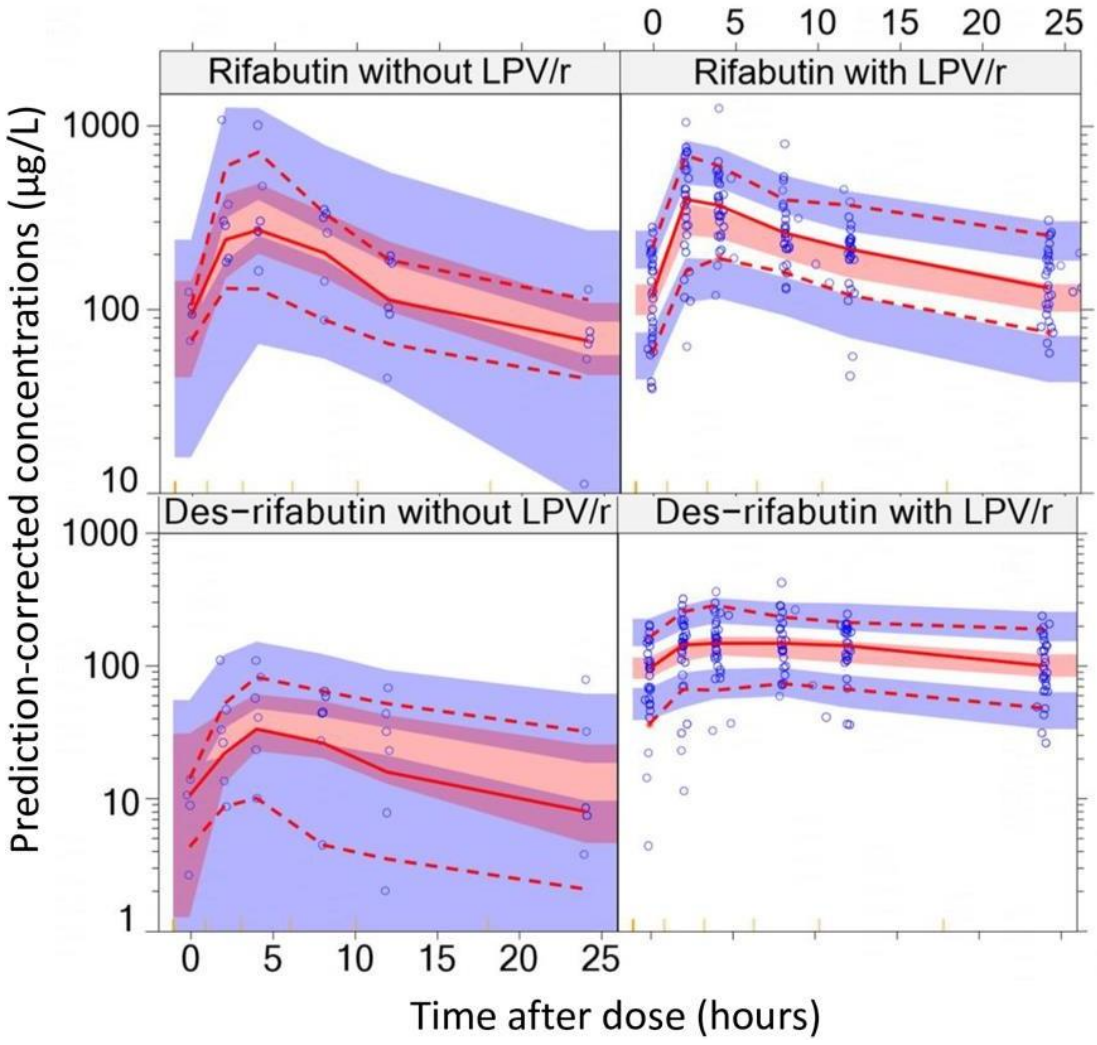

Figure 5.1. Prediction-corrected visual predictive check of the final rifabutin-des-rifabutin model. Blue circles represent observed plasma concentrations. The solid red line in the middle represents the median observed concentration, while the dashed red lines below and above represent the 10th and 90th percentiles of the observed concentrations, respectively. The shaded area around each line represents the 95% model-predicted confidence intervals for the same percentiles. The yellow ticks at the base of the plot show the bins.

Simulation Results.

Simulations with the doses used in the study showed that the rifabutin dose used during TB-only treatment resulted in higher median paediatric exposures compared to median adult exposures for both rifabutin (Tanuma et al., 2013; Naiker et al., 2014) and des-rifabutin (Lan et al., 2014; Naiker et al., 2014) in the weight range of 6-20 kg (**Figure 5.2** and **Figure S. 5.8**Figure S. *5.8*The highest exposure increase is in the 10-15 kg weight category, with a 30% increase for rifabutin and a 53% increase for des-rifabutin compared to the upper

limit of adult median exposures (5640 µg·h/L for rifabutin and 700 µg·h/L for des-rifabutin). During co-treatment with LPV/r, where the study dose was 2.5 mg/kg/day for the 1-3- and 3–15-year-old cohorts, median paediatric exposures aligned with median adult exposures for both rifabutin and des-rifabutin (Lan et al., 2014; Naiker et al., 2014). For the cohort using a dose of 5 mg/kg/day in the study, weight groups >7 kg exhibited higher median exposures, reaching up to 12% for rifabutin and 23% for des-rifabutin compared to the upper limit of median adult exposures during LPV/r co-treatment (7290 µg·h/L for rifabutin and 4130 µg·h/L for des-rifabutin) (see **Figure S. 5.8**Figure S. *5.8* Moreover, with the study doses, median C_{max} for both rifabutin and des-rifabutin remained below 900 µg/L (Pasipanodya and Gumbo, 2011; Wasmann *et al.*, 2021; Waalewijn, Almett, 2024) (see **Figure S. 5.6.** and **Figure S. 5.9**Figure S. *5.9*

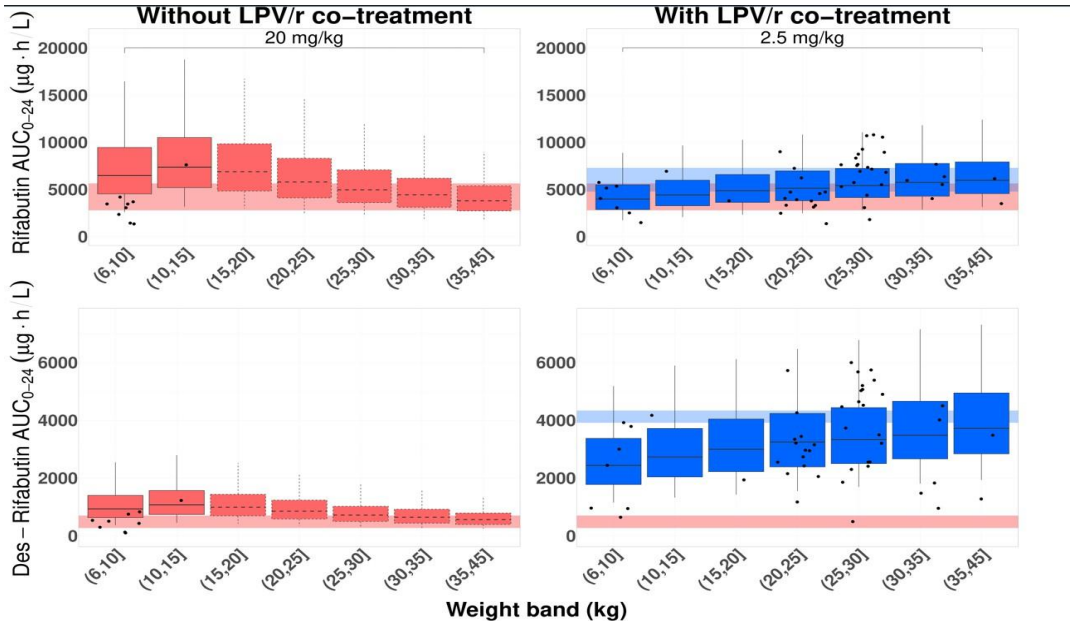

Figure 5.2. Simulated AUC_{0-24} for rifabutin and des-rifabutin with the doses used in the study. Boxplots with dashed edges show weights which were not observed in the study while the dots are model-derived AUCs for the study patients. Rifabutin dose without LPV/r co-treatment has been limited to 300 mg OD. Shaded areas indicate the median steady-state AUC0-24 reported in adults (grey for 300 mg OD rifabutin without lopinavir/ritonavir, blue for 150 mg OD with lopinavir/ritonavir). The blue shaded area for des- rifabutin is ±5% of reported AUC0-24 values in adults for visualization purposes. The boxes indicate the interquartile range, while the whiskers show the 5th and 95th percentiles.

To improve upon the study doses and achieve consistent exposures across the weight bands, rifabutin doses were optimized using harmonized weight-bands with and without LPV/r co-treatment, as shown in **Table 5.3.**

Table 5.3. Optimized rifabutin doses for harmonized weight bands.

	Rifabutin dose (mg)	
Harmonized weight bands (kg)	**Without LPV/r co-treatment**	**With LPV/r co-treatment**
≥6 to <10	115	25
≥10 to <15	160	35
≥15 to <20	200	45
≥20 to <25	250	55
≥25 to <30	300	65
≥30 to <35	300	70
≥35 to <45	300	85

With these doses, median rifabutin and des-rifabutin exposures are in line with those reported in adults both during standard TB treatment and during LPV/r co-treatment (**Figure 5.3**). Additionally, median peak concentrations remain below 900 µg/L across all weight bands and treatment groups (**Figure S. 5.7**Figure S. *5.7*

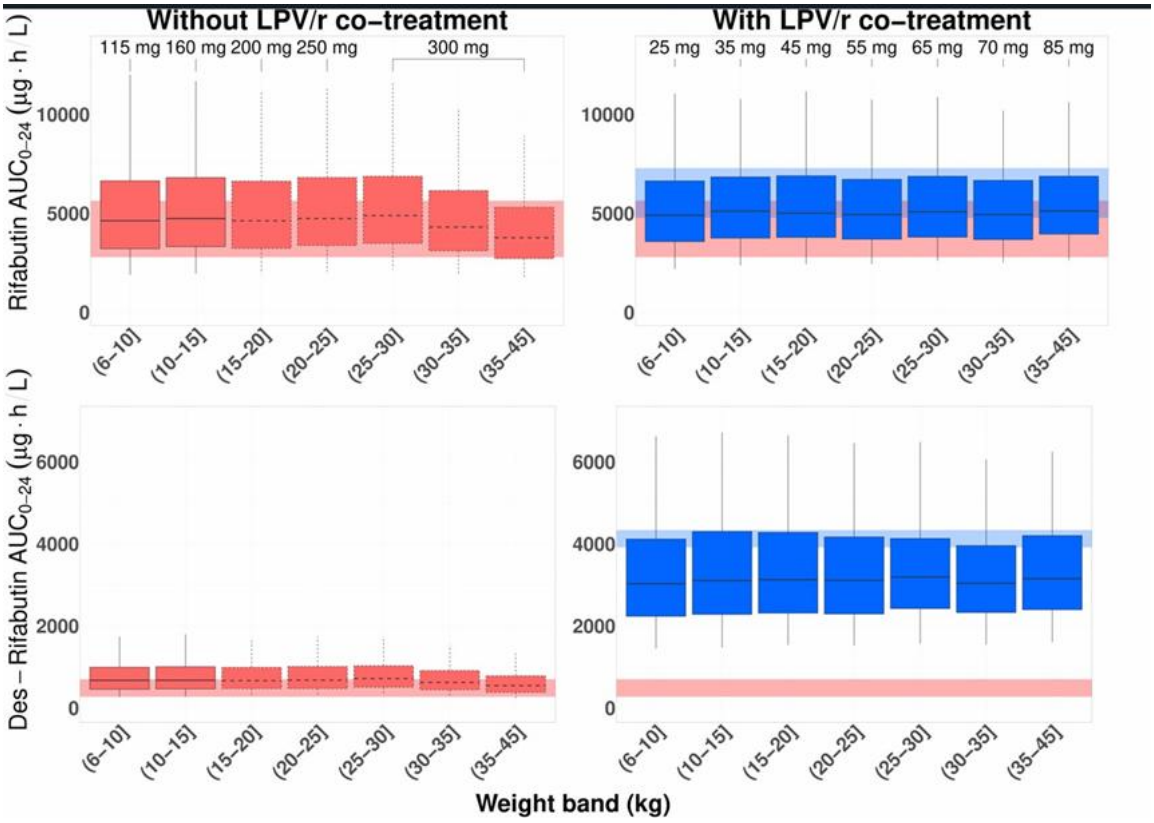

Figure 5.3. Simulated $AUC_{0\text{-}24}$ for rifabutin and des-rifabutin with suggested weight-band based doses. Left panels: without LPV/r co-treatment; Right panels: with LPV/r co-treatment. Shaded areas indicate the median steady-state AUC0-24 range in adults (grey for 300 mg OD without lopinavir/ritonavir, blue for 150 mg OD with lopinavir/ritonavir). Boxplots with dashed edges show weights which were not observed in the study. The blue shaded area for des-rifabutin is ±5% of reported AUC0-24 values in adults for visualization purposes. The boxes indicate the interquartile range, while the whiskers show the 5th and 95th percentiles.

5.5 Discussion

In this study, we used a model-based approach to characterize the population pharmacokinetics of rifabutin and des-rifabutin during co-treatment with LPV/r in children with TB and HIV. The co-administration of LPV/r significantly increases exposures of rifabutin and des-rifabutin by increasing the bioavailability and decreasing the clearance of both rifabutin and des-rifabutin. Furthermore, those severely underweight were associated with lower exposures due to a decreased bioavailability, and younger children were found to have slower absorption of rifabutin. In the context of LPV/r co-treatment, model-derived rifabutin and des-rifabutin exposures were higher compared to exposures without LPV/r co-

728 treatment, in line with previously reported exposures in adults (Lan et al., 2014; Naiker et al.,
729 2014). We performed Monte Carlo simulations to evaluate rifabutin and des-rifabutin
730 exposures with the mg/kg doses used in the studies. During LPV/r co-treatment, the rifabutin
731 dose of 2.5 mg/kg/day resulted in simulated exposures in line with those of adults, while the
732 dose of 5 mg/kg/day resulted in higher exposures than adults for children weighing > 7 kg.
733 During TB only treatment, at a rifabutin dose of 20 mg/kg/day up to 300 mg/day, simulated
734 exposures were higher than those reported in adults for weights 6-20 kg. We propose weight-
735 band based dosing, using harmonized weight bands, showing that with these doses, paediatric
736 exposures are consistent with those of adults across all weights and both treatment scenarios
737 (without and with LPV/r co-treatment).

738 Hennig et al. developed a two-compartment model for rifabutin and des-rifabutin based
739 mainly on data from adults, incorporating the impact of ritonavir-boosted protease inhibitor
740 (PI) interactions (Hennig et al., 2016). Our results align with their findings, indicating that co-
741 administration of LPV/r significantly decreases rifabutin clearance through non-des-rifabutin
742 routes by up to 100%, and reduces des-rifabutin clearance by up to 76%. Our inhibitable
743 rifabutin clearance extrapolated to a 70-kg adult of 58.5 L/h, corresponds closely to their
744 reported value of 58.8 L/h. However, our estimates of rifabutin clearance conversion and des-
745 rifabutin clearance are higher than their reported values. On the other hand, they estimated
746 higher steady-state volumes for both rifabutin and des-rifabutin, and while we found higher
747 bioavailability with LPV/r cotreatment, they reported lower bioavailability during co-
748 treatment with ritonavir-boosted PIs in TB/HIV patients. Their study consisted of data from
749 adults, including a mix of various PIs, not limited to lopinavir, which could contribute to
750 differences in the estimates.

High variability was observed in rifabutin bioavailability, which could be due to its complex pharmacokinetics. Rifabutin is partially metabolised by CYP3A4, present in both the gut and the liver (causing a significant first-pass effect), and partially by AADAC to des-rifabutin. Various factors such as enzyme maturation, age-related differences in CYP3A4 expression, and difference in absorption speed due to variable gastrointestinal motility between children could cause this (Batchelor and Marriott, 2015). Another element contributing to the high variability in bioavailability may stem from variability in adherence or medication intake, a notable concern in the administration of paediatric drugs (El-Rachidi, LaRochelle and Morgan, 2017). In the conducted studies, rifabutin was administered as a suspension compounded from capsules, and inadequate shaking prior to drug administration, leading to settling of the medication or the child partially swallowing the medication could cause lower drug concentrations. This could also potentially explain the low concentrations found after an unobserved dose compared to the concentrations after an observed dose. During modeling, we handled these low trough concentrations by the method of initialization described by Dansirikul et al. (Dansirikul, Silber and Karlsson, 2008), as detailed in the supplementary material.

Monte Carlo simulations were conducted to assess the doses utilized in the study, comparing the simulated exposures with literature findings in adults. Simulations showed that the study dose used during standard TB treatment (20 mg/kg/day) results in median rifabutin and des-rifabutin exposures exceeding those of adults in weights 6-20 kg, while the dose of 2.5 mg/kg/day used during LPV/r co-treatment was adequate, resulting in median exposures of both rifabutin and des-rifabutin which matched adult exposures. However, the dose of 5 mg/kg/day during LPV/r co-treatment resulted in higher exposure than those of adults in >7 kg weights. Median rifabutin Cmax remained below the toxicity threshold of 900 µg/L for both scenarios simulated, i.e., during TB treatment alone and with LPV/r co-treatment,

including in doses that resulted in increased exposures. We performed further simulations proposing rifabutin paediatric dosing by harmonized weight-bands to achieve median exposures that match those of adults consistently across the weights. Currently, there are no specific rifabutin formulations designed for paediatric use. The studies that informed this analysis utilized oral suspensions (20 mg/mL) compounded from Mycobutin® capsules. The limited availability of paediatric data may account for the absence of dedicated formulations. Using the available data from these paediatric studies, our study could provide potential step toward the development of rifabutin formulations tailored to the needs of paediatric patients.

Our study was limited by the absence of sufficient data for the cohort below 1-year-old. The study in this cohort was stopped after recruitment of three patients, the youngest of whom was 8 months old, since the formulation was no longer available. The impact of maturation on rifabutin and des-rifabutin clearances was deemed insignificant in our data, with complete maturation estimated at 8 months in the model. Additionally, when exploring maturation on all clearance parameters using the maturation function reported for midazolam, a CYP3A4 probe, it was observed that rifabutin and des-rifabutin clearances did not follow the same pattern (Anderson and Larsson, 2011). Thus, simulation results from this study are applicable to children above 8 months old.

Based on WHO 2021 guidelines, LPV/r-based ART is considered an alternative first-line regimen for children (at least 4 weeks old and under 10 years old) and is a preferred second-line regimen for all children and adolescents who fail non-PI based ART (World Health Organization, 2021). Rifabutin is recommended in the context of HIV co-treatment, highlighting the importance of optimizing its dose in paediatric use. We have established a population pharmacokinetic model for children undergoing LPV/r co-treatment, offering a tool for rifabutin dose optimization. We suggest weight-band dosing which aligns rifabutin

and des- rifabutin exposures across age groups and exposures in adults. Further investigations are warranted to explore the relationship between rifabutin and des-rifabutin exposures and potential adverse effects.

5.6 Supplementary Materials

Initialization

There were fifteen profiles in our data across different age cohorts and visits where the trough concentration (sample collected at pre-dose from unobserved dose) was unexpectedly low compared to the 24-hour concentration (**Figure S. 5.3**Figure S. *5.3*illustrates an example of such a profile). Rifabutin is expected to reach steady state within 10 days and in this study had been dosed for two weeks prior to sampling at each visit, therefore it would be expected that trough concentrations would be in line with the 24-hour concentrations. Model fit was inadequate for these trough concentrations, as observed by the visual predictive check, since model predictions were higher than the observations for those time points. These profiles were handled by initialization with the B2 method as suggested by Dansirikul et al. (Dansirikul, Silber and Karlsson, 2008), where the doses are discarded and the observed trough concentrations are used as a starting point (or the model is initialized to the first observation) with residual error to account for measurement error. Parameter estimates improved after initialization in terms of stability, and the additive error decreased (from 15.0 to 11.3 µg/L for rifabutin and from 13.5 to 10.7 µg/L for des-rifabutin after initialization). Moreover, the high variability which had been estimated for bioavailability and rifabutin inhibitable CYP3A4 clearance was reduced (between- occasion-variability (BOV) of bioavailability decreased from 103% to 66.7% after initialization and between-subject-variability (BSV) of rifabutin inhibitable CYP3A4 clearance decreased from 204% to 36.3%). Initialization improved the model fit, as observed by the pcVPC (**Figure 5.1**).

825 This confirms that the trough concentrations did not fit with the dosing information, possibly
826 due to a lack of adherence.

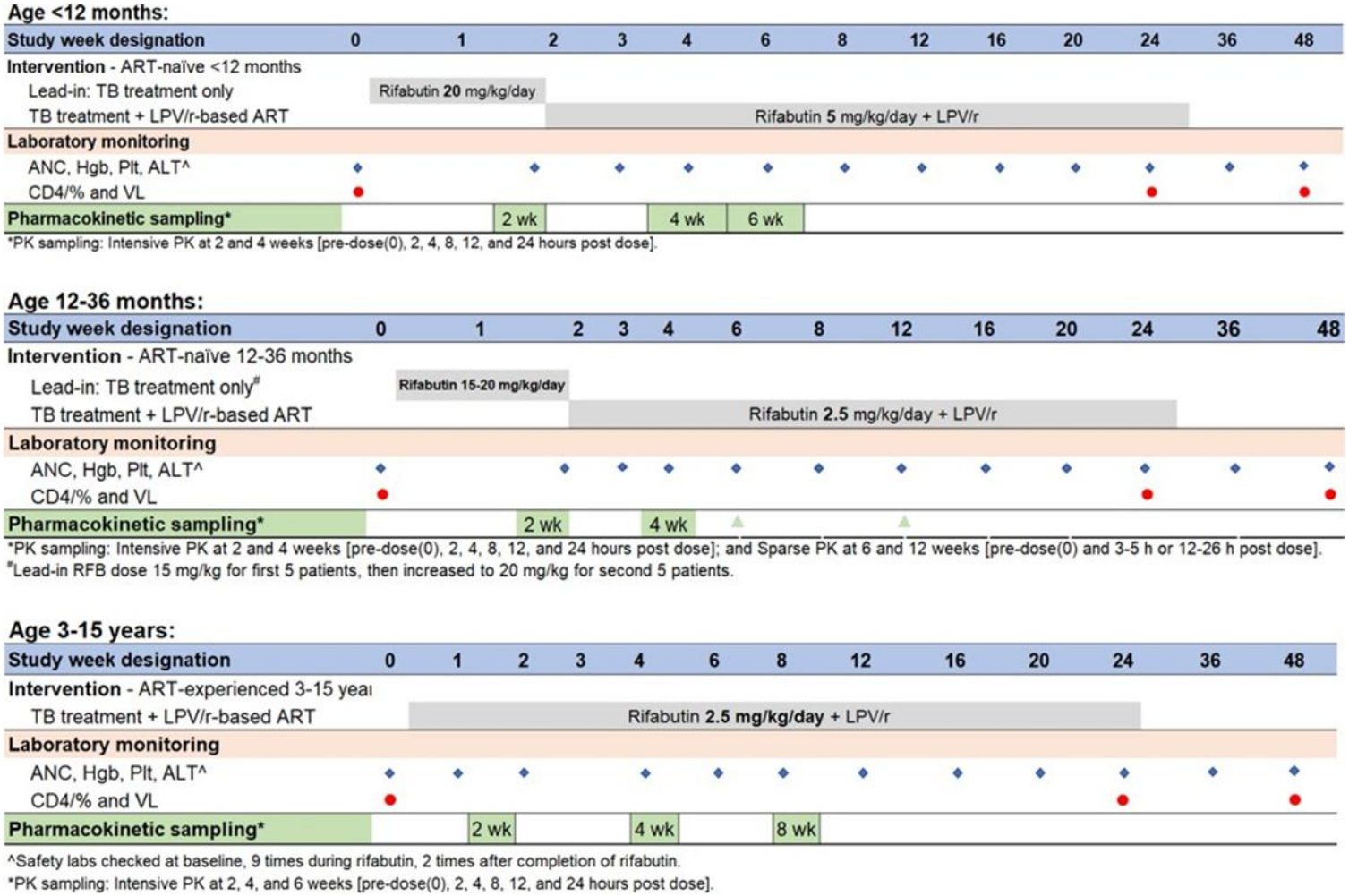

Figure S. 5.1. Study design for the three cohorts from which data were obtained for this analysis.

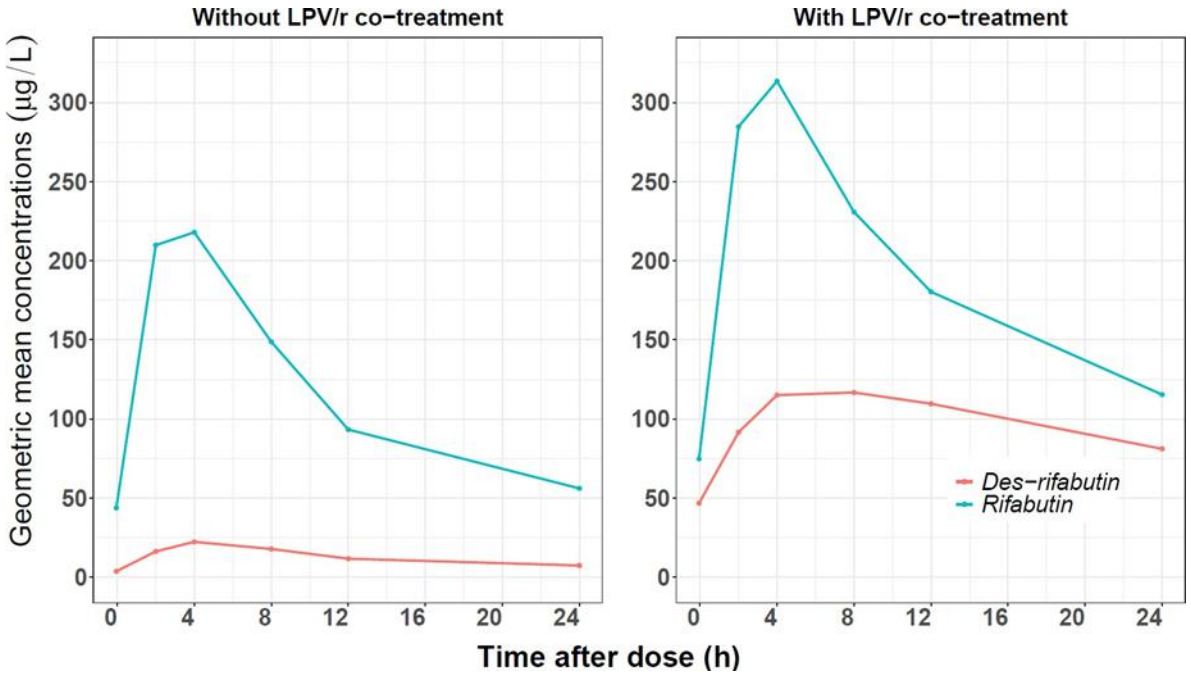

Figure S. 5.2. Summary (geometric mean) concentration-time profiles of rifabutin and des-rifabutin. The plots show summary (geometric mean) concentration-time profiles without and with lopinavir/ritonavir (LPV/r) co-treatment in the original data used for modeling. Without LPV/r co-treatment = data from <1-year-old and 1-to-3-year-old cohorts; With LPV/r co-treatment = data from <1-year-old, 1-to-3-year-old, and 3-to-15-year-old cohorts.

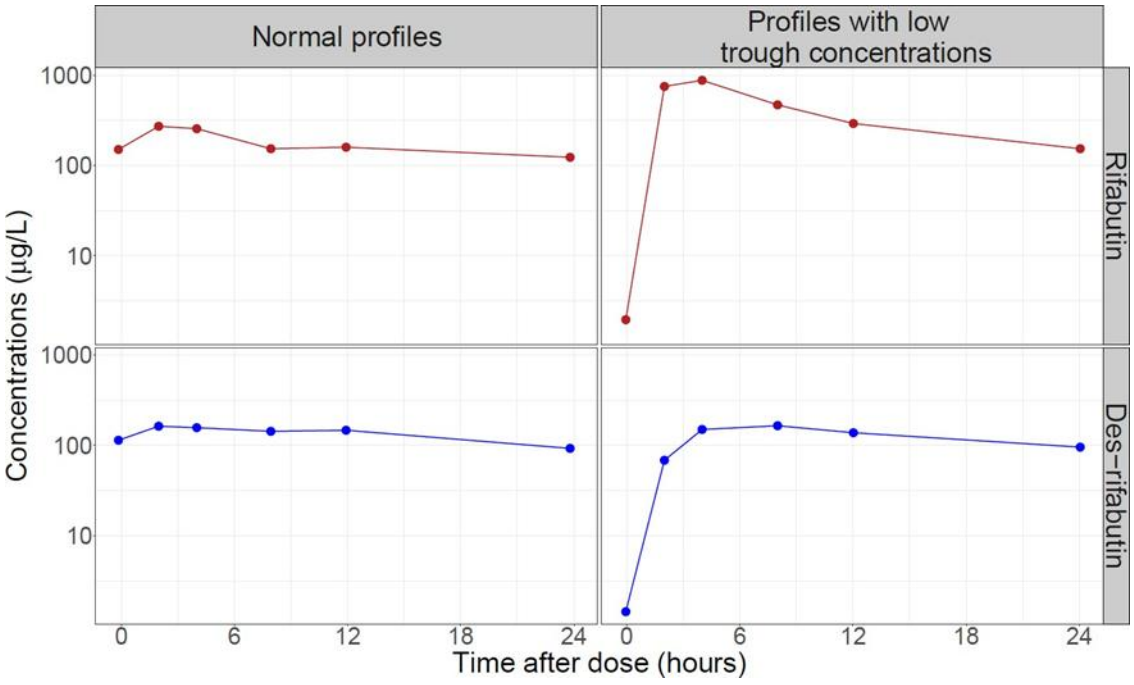

Figure S. 5.3. Raw data normal profiles (left panels) and profiles with low trough concentrations (right panels).

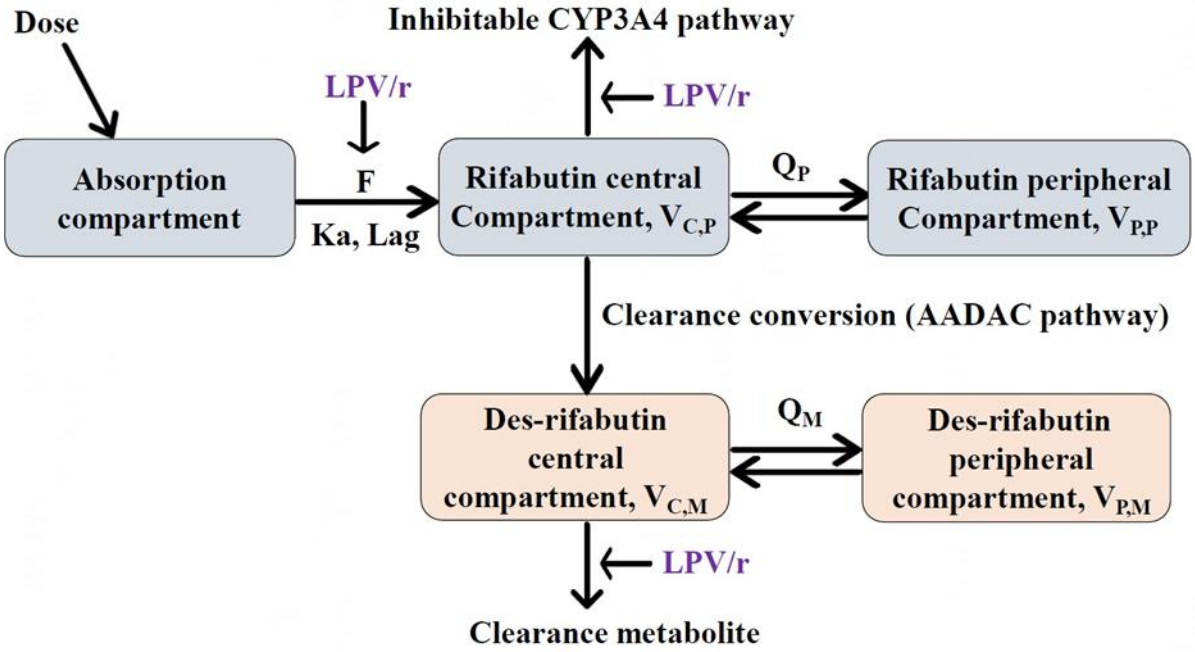

Figure S. 5.4. Model schematic for the final joint population pharmacokinetic model of rifabutin and des-rifabutin.

The model schematic shows the final rifabutin/des-rifabutin joint population pharmacokinetic model with lopinavir/ritonavir co-treatment. Bio, oral bioavailability; Ka, first-order absorption rate constant; Lag, absorption lag time; QP, parent intercompartmental clearance; QM, metabolite intercompartmental clearance; LPV/r, lopinavir/ritonavir; AADAC, arylacetamide deacetylase.

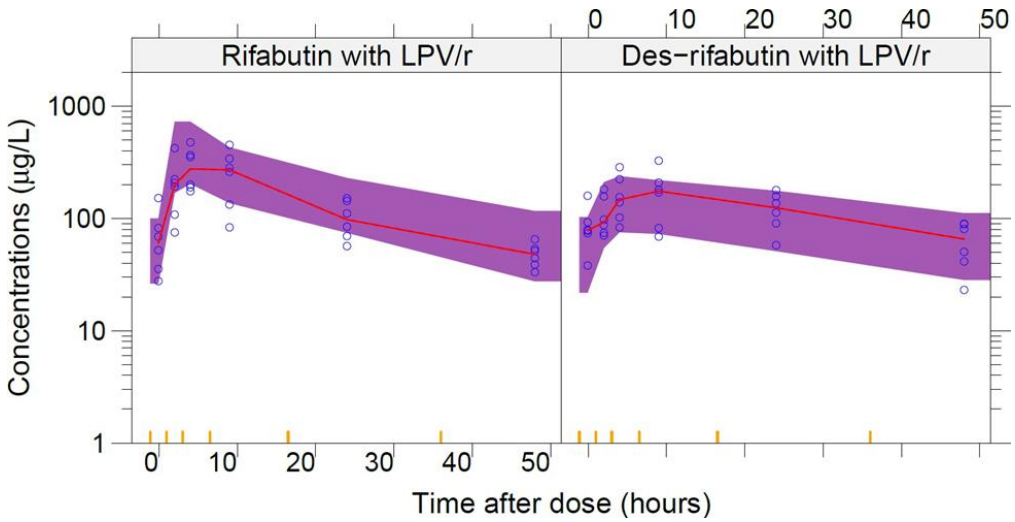

Figure S. 5.5. External model validation using data from six South African children by Moultrie et al.(Moultrie et al., 2015).

The solid line in the middle represents the median observed concentration while the shaded area around the line represents the 95% model-predicted confidence interval for the median. The yellow ticks at the base of the plot show the bins.

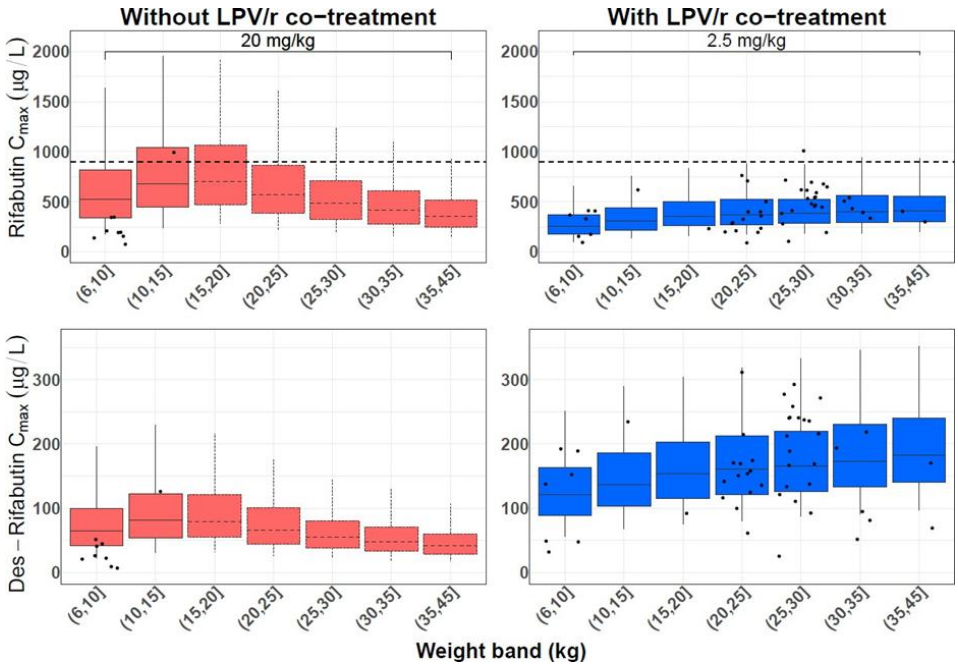

Figure S. 5.6. Simulated C_{max} values for rifabutin and des-rifabutin with the study doses. The black dashed line shows C_{max} value of 900 µg/L, which is a toxicity limit for rifabutin. Boxplots with dashed edges show weights which were not observed in the study while the dots are model-derived C_{max} values for the study patients. The boxes indicate the interquartile range, while the whiskers show the 5th and 95th percentiles.

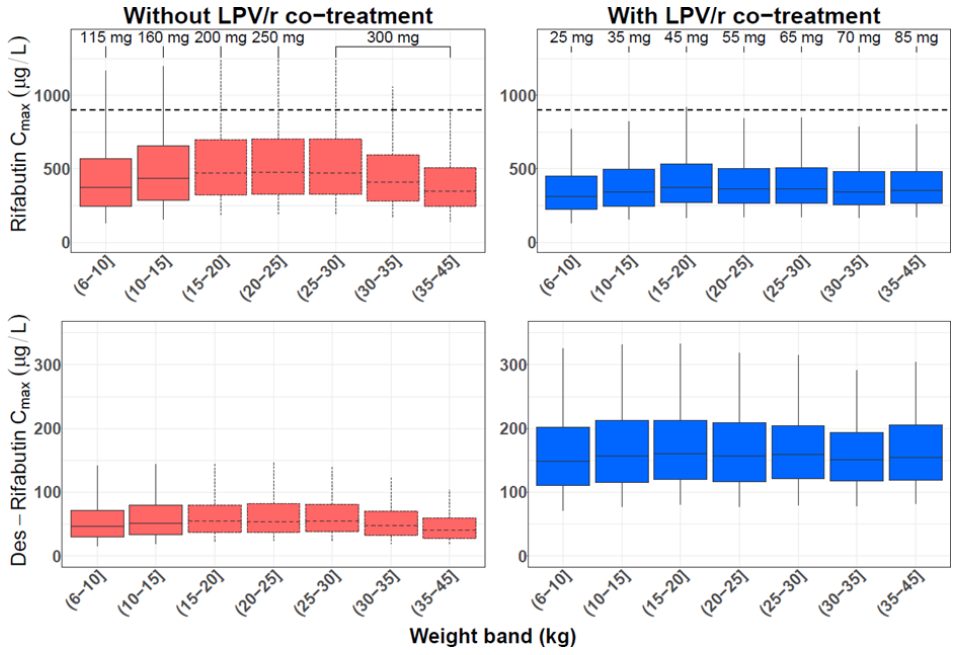

Figure S. 5.7. Simulated C_{max} values for rifabutin and des-rifabutin with suggested weight-band based doses. The black dashed line shows C_{max} value of 900 µg/L, which is a toxicity limit for rifabutin. Boxplots with dashed edges show weights which were not observed in the study. The boxes indicate the interquartile range, while the whiskers show the 5th and 95th percentiles.

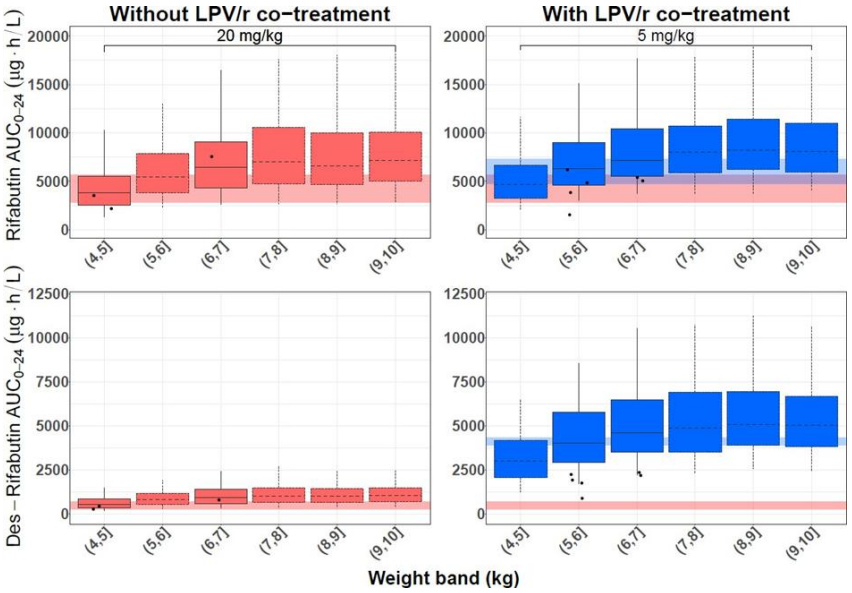

Figure S. 5.8. Simulated $AUC_{0\text{-}24}$ values for rifabutin and des-rifabutin with the doses used in the study for the <1-year-old cohort.

Shaded areas indicate the median steady-state $AUC_{0\text{-}24}$ range in adults (grey for 300 mg OD without lopinavir/ritonavir, blue for 150 mg OD with lopinavir/ritonavir). Boxplots with dashed edges show weights which were not observed in the study while the dots are model-derived AUCs for the study patients. The boxes indicate the interquartile range, while the whiskers show the 5th and 95th percentiles.

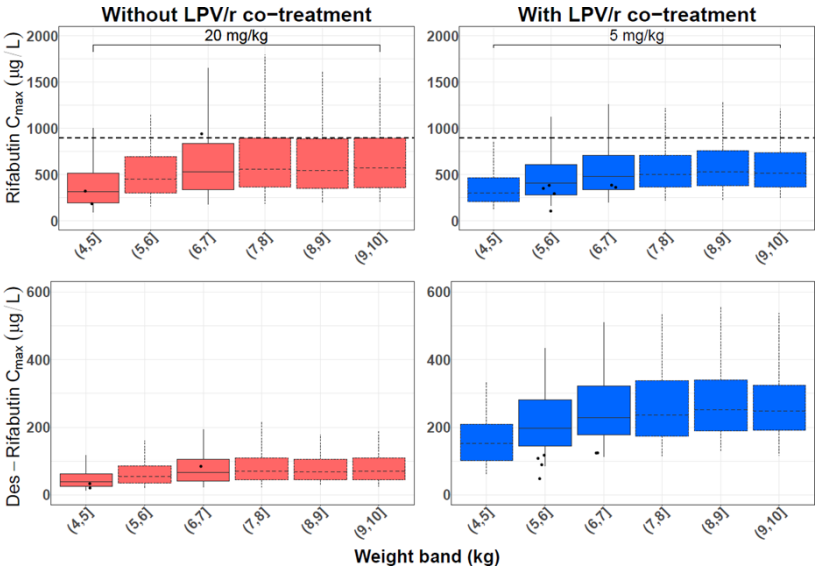

Figure S. 5.9. Simulated C_{max} values for rifabutin and des-rifabutin with the doses used in the study for the <1-year-old cohort.

The black dashed line shows C_{max} value of 900 µg/L, which is a toxicity limit for rifabutin. Boxplots with dashed edges show weights which were not observed in the study while the dots are model-derived AUCs for the study patients. The boxes indicate the interquartile range, while the whiskers show the 5th and 95th percentiles.

Chapter 6 Application of a population pharmacokinetic model as a tool for monitoring adherence in heart failure patients.

6.1 Abstract

Background: Medication adherence is crucial for heart failure patients, but data is limited, especially in Africa. Conventional methods assess adherence based on detectability of drug levels. Population pharmacokinetic modeling can improve adherence monitoring by predicting expected concentrations for specific populations. We developed a population pharmacokinetic model of enalaprilat in a small cohort of African heart failure patients to propose individualized reference concentrations for adherence monitoring.

Methods: Data were pooled from six South African patients with heart failure receiving 5 mg or 10 mg enalapril twice daily, and from 24 healthy volunteers who received a single 20 mg dose of enalapril as part of a bioequivalence study. The combined dataset was analysed using nonlinear mixed-effects modeling. Monte Carlo simulations predicted concentrations under perfect adherence for various weights and doses. The 5th percentile of predicted concentrations, 12 hours after dose and extending to the lower limit of quantification (LLOQ; 0.2 µg/L), are reported.

Results: A two-compartment model with first-order elimination, absorption using transit compartments, and weight-based allometric scaling was developed. Enalaprilat bioavailability was 49% higher in the heart failure patients. Reference tables are provided. For example, for a 90 kg patient on 20 mg enalapril BID, the 5th percentile of predicted concentrations 12 h after dose is 21.2 µg/L with assumption of adherence rejected if concentrations fall below 21.2 µg/L. It takes 7 days to reach concentrations below LLOQ for this patient, and if so, one can assume that the patient did not take their medication for at least 7 days.

Conclusions: We propose model-derived reference concentrations, individually tailored based on dosage and body weight, to monitor enalapril adherence in heart failure patients. Given the constraints of available data in our study, the model needs to be externally validated in a more extensive cohort of heart failure patients, with a broader range of covariates. The reference concentrations represent an improved method for adherence monitoring.

6.2 Introduction

Heart failure is a significant cause of morbidity and mortality, estimated to have affected around 64 million people globally in 2020 (Groenewegen et al., 2020). In Low- and Middle-Income Countries, including African countries, the burden of cardiovascular diseases (CVD) such as heart failure has been rising disproportionately.(Estel and Conti, 2016; Sliwa, 2016) An increasing exposure to CVD risk factors such as poor diet and smoking, as well as a shift from infectious to chronic disease in these regions due to lifestyle changes, are among factors contributing to this trend.(Yusuf et al., 2001) An important factor further exacerbating the impact of heart failure is the prevalence of poor medication adherence,(Ruf et al., 2010; Hood et al., 2018) which for chronic diseases has been reported to be approximately 24.8% (DiMatteo, 2004). According to systematic reviews, adherence to heart failure medication has been reported to be variable, ranging from 10% to 99%.(van der Wal and Jaarsma, 2008; Oosterom-Calo et al., 2013; Shah et al., 2015) In African chronic heart failure patients, there is little knowledge about medication adherence.(Verena et al., 2010) It is therefore critical to fill this knowledge gap to better understand the contribution of poor adherence in a disease that has an ever-increasing impact in the region.

Methods of evaluating medication adherence such as pill count and patient self-reporting are limited by bias and poor sensitivity. Biochemical screening to classify patients as non-adherent when the drug concentration is less than the lower limit of quantification (LLOQ) is

limited by a risk of misclassifying patients since it depends on the sensitivity of the assay. Moreover, more erratic or irregular adherence behaviour over a number of days may not be detected (Cramer, 1990; Stirratt et al., 2015; Groenland et al., 2021) Using LLOQ for all patients may also be crude as it does not account for interindividual pharmacokinetic differences and dose regimens, so it is only likely to detect extreme levels of non-adherence. An objective method is to use a model-based tool for monitoring adherence, where observed concentrations can be compared with individualized concentration ranges derived from the model, accounting for the prescribed dosage and patient characteristics (Mwita et al., 2023). In this study, we apply population pharmacokinetic modeling to highlight an improved adherence monitoring method in heart failure patients taking the angiotensin converting enzyme (ACE) inhibitor enalapril.

ACE inhibitors are first-line therapy and an important component of heart failure treatment regimen (McMurray et al., 2012; Sun et al., 2016; Yancy et al., 2017). Most ACE inhibitors, including enalapril, are ester prodrugs requiring hepatic biotransformation to active metabolites (Zaman, Oparil and Calhoun, 2002; Ferrari, 2008). Enalapril is hydrolyzed post-absorption by de-esterification in the liver by carboxylesterase 1 (CES1) to the only and active metabolite enalaprilat, which mediates its ACE-inhibitory effect (Zaman, Oparil and Calhoun, 2002; Wang et al., 2016). There is considerable genetic variation in CES1 expression and activity, which might lead to interindividual variability in the pharmacokinetics of enalapril (Hockings, Ajayi and Reid, 1986; Wang *et al.*, 2016; Her *et al.*, 2021). Enalaprilat steady state is achieved within 30 to 60 hours, and it is detectable in serum for up to 96 hours post-dose (Till et al., 1984; Tabacova and Kimmel, 2001). Enalaprilat is mainly renally excreted, and in patients with renal impairment, serum concentrations could increase not only due to a reduction in clearance, but also due to increased bioconversion since clearance of the prodrug enalapril is also reduced. A significant correlation of overall

enalaprilat plasma exposure and creatinine clearance has been reported for creatinine clearances below 60 mL/min (Lowenthal et al., 1985; Kelly et al., 1986).

Population pharmacokinetic models for enalaprilat are limited in literature, especially in heart failure patients. In this study, we developed a population pharmacokinetic model for enalaprilat using available data from African heart failure patients, as well as data from healthy participants, with the aim of applying the model to derive individualized concentrations to improve adherence monitoring.

6.3 Materials and methods

Patients and study procedures

Pharmacokinetic data for enalaprilat was obtained from a study conducted in the cardiology clinic at Groote Schuur Hospital in Cape Town, South Africa, which included patients followed up with a diagnosis of heart failure, ≥18 years of age, and were clinically stable (New York Heart Association Functional Class (NYHA) II-III) on background therapy with enalapril maleate tablet at 5 or 10 mg twice daily. Exclusion criteria included renal failure (on dialysis or creatinine > 220 µmol/L), nephrotic syndrome, hepatic failure or other causes of hypoalbuminemia, anaemia (Hemoglobin < 8 g/dL), pregnant or within 3 months post-partum. Enalaprilat plasma samples were obtained pre-dose and at 1.5, 3, 5, 8, and 12 h post-dose, and quantified using an LC-MS/MS assay at the division of clinical pharmacology, University of Cape Town. Concentrations were validated over a range of 0.2 to 200 µg/L, using a published analytical method (Joubert et al., 2022).

To strengthen model development, additional enalaprilat data was included from a crossover bioequivalence study in healthy volunteers by Cipla, India. The study compared two formulations of 20 mg enalapril maleate tablet administered as a single dose and separated by washout period of 7 days to separate dosing between the two formulations. Healthy

volunteers aged 18-55 years and within 15% of ideal body weight in relation to height were eligible for inclusion. Exclusion criteria were any clinically significant deviations from normal clinical results and laboratory test findings, history of allergic responses to ACE inhibitors, and repeated use of any drugs which could affect absorption or influence hepatic biotransformation up to 4 weeks prior to the start of the study. Participants fasted 10 h prior to the dose and food was given 4 h post-dose. Enalaprilat plasma samples were collected at 0, 0.5, 1, 1.5, 2, 2.33, 2.66, 3, 3.33, 3.66, 4, 5, 6, 8, 12, 16, 24, 36, 48, and 72 h post-dose on two occasions, and were quantified by a Liquid Chromatography with tandem mass spectrometry (LC-MS/MS) assay at Medlar Laboratories, validated as per FDA criteria over concentration ranges of 1 to 200 µg/L. Enalaprilat intra-day and inter-day accuracy was within 15% while intra-day and inter-day precision was below 15% for enalaprilat.

The study in the heart failure participants was approved by the University of Cape Town Faculty of Health Science Research Ethics Committee (HREC/REF:480/2018), while the study in healthy volunteers was approved by the Independent Ethics Committee, Cipla, India. Both studies were conducted according to the declaration of Helsinki and in compliance with ICMR guidelines for Biomedical Research on Human Subjects and the ICH GCP guidelines. Written informed consent was obtained from all participants.

Population pharmacokinetic modeling

Concentration-time data were analysed using nonlinear mixed-effects modeling with the software NONMEM v7.5.0 and the first-order conditional estimation method with interaction. Pirana v2.9.8, Perl-speaks-NONMEM v4.9.0, and R v3.6.1 were used for postprocessing and visualization of output (Keizer, Karlsson and Hooker, 2013). An enalaprilat population pharmacokinetic model was developed using the healthy volunteer data from Cipla, and the developed model was then adjusted to include the heart failure

participants. Various structural models were tested: one-, two- and three- compartment disposition, first-order elimination and absorption, with or without lag time or transit absorption model (Savic et al., 2007). Between-subject variance (BSV) and between-occasion variance (BOV) random effects were assumed to follow a log-normal distribution.

A combined additive and proportional error model was used to describe the unexplained residual variability (RUV). Concentrations below the lower limit of quantification (BLQ) were censored and handled with an approach similar to the M6 method by Beal (Beal, 2001), i.e., LLOQ/2 was imputed for all BLQ values and the additive error was increased by adding LLOQ/2 to mitigate the effect of the imputation for the last BLQ in absorption and the first BLQ in elimination. Trailing BLQ values were excluded from the model fit but included in diagnostic plots. Concentrations were deemed implausible and excluded from the analysis when the absolute value of their conditional weighted residuals (|CWRES|) was above 5 (i.e., the likelihood of the value to be arising from the expected statistical distribution is 1 in 16667).

Model selection was guided by the likelihood ratio test where the objective function value (OFV) is assumed to be $\chi 2$ distributed and for two nested models, a ΔOFV of at least 3.84 represents a better fit with $p < .05$ for one added degree of freedom (df). Successful minimization, inspection of diagnostic plots (goodness-of-fit plots and visual predictive checks (VPCs)), and physiological plausibility were also considered in choosing the best model.

Allometric scaling was added *a priori* to all disposition parameters to account for the effect of body size. Body size descriptors including total body weight, fat-free mass (FFM), and body fat were tested with allometric exponents fixed to 0.75 and 1 for clearances and volumes of distribution, respectively, before selecting the descriptor that provided the best fit

(Janmahasatian et al., 2005; Anderson and Holford, 2009). Covariates tested were creatinine clearance on clearance (estimated by Cockroft-Gault formula) (Cockcroft and Gault, 1976), and formulation on all absorption parameters in the initial model which included healthy participants, and upon adding the data from heart failure patients, creatinine clearance was re-tested and study effect was evaluated on bioavailability as well as disposition parameters. The Cockcroft–Gault equation was selected to calculate creatinine clearance, as it is preferred in adult population pharmacokinetic modeling due to its calculation of absolute clearance (mL/min), which is directly related to renal drug elimination. This is in line with US FDA guidance (FDA, 2020). In contrast, eGFR equations such as CKD-EPI and MDRD are normalized to 1.73 m^2 body surface area, which can misrepresent renal clearance in individuals with extreme body sizes. Additionally, CKD-EPI is primarily used for chronic kidney disease staging and not drug disposition, while MDRD is less frequently applied due to reduced accuracy at higher GFR levels (Levey et al, 2011). Covariate were tested one at a time and retained if the OFV decreased by at least 3.84 ($p < .05$, 1df) in forward addition and increased by more than 6.63 ($p < .01$, 1df) in backward elimination. A non-parametric bootstrap (1000 samples) was run on the final model with stratification by study to obtain 95% confidence intervals (CIs) for the parameter estimates to evaluate accuracy and model robustness.

Monte Carlo simulations

Monte Carlo simulations were performed to predict steady-state trough concentrations in heart failure patients every 12 hours since the last dose until BLQ. The simulated concentrations were obtained considering between-subject/ between-occasion variability as well as the residual error, to account for error in observed concentrations. The simulations were performed for three standard enalapril dose groups: 5, 10, and 20 mg twice daily with a weight range from 35 to 145 kg (in 5 kg steps) simulated per dose group. Five thousand

simulations were performed for each dose and weight combination. The 5th percentile of the simulated trough concentrations in each dose and weight group were chosen as reference values for evaluating adherence.

6.4 Results

Patient and study characteristics

The study in the heart failure patients included six participants (50% female) with stable heart failure with median (range) age of 42 (30 – 49) years, weight of 94 (75 – 125) kg, and creatinine clearance of 121 (80.0 – 155) mL/min. One patient was classified as NYHA Functional Class I, another Class III while four patients were Class II. Thirty-three enalaprilat concentrations were included in the analysis, none were BLQ, and no outliers were identified.

The study in the healthy volunteers included twenty-four participants (all male) with median (range) age of 24 (19 – 33) years, weight of 63 (54 – 73) kg, and creatinine clearance of 102 (82 – 133) mL/min. Enalaprilat concentrations were available in 935 samples. Concentrations from seven samples (0.7%) were identified as outliers and were excluded from the analysis. Of the included 928 samples, ~ 12% were BLQ (24 of these were at pre-dose as expected, 17 immediately post-dose, and 68 in the terminal phase). Baseline characteristics of participants in both studies are shown in **Table 6.1**.

Table 6.1 Baseline characteristics for healthy and heart failure participants

Characteristic Median (range)	**Healthy participants (n = 24)**	**Heart failure participants (n = 6)**
Age (years)	24 (19 - 33)	42 (30 - 49)
Height (cm)	169 (162 - 179)	161 (149 - 186)
Weight (kg)	62.5 (54.0 - 73.0)	93.7 (74.7 – 125)
FFM (kg)[1]	51.0 (45.7 – 57.9)	54.9 (40.8 - 74.0)
Creatinine clearance (ml/min)[2]	102 (82.3 – 133)	121 (80.0 – 155)
BMI (kg/m^2)	21.9 (18.6 – 25.5)	35.5 (21.6 – 45.5)

Sex Males – n (%) Females – n (%)	24 (100%)	3 (50%) 3 (50%)
[1]Fat-free mass (FFM) calculated by Janmahasatian *et al.*(Janmahasatian *et al.*, 2005) [2]Calculated using Cockroft-Gault formula (Cockcroft and Gault, 1976)		

1082

1083 **Population pharmacokinetic model**

1084 Enalaprilat pharmacokinetics was best characterized by a two-compartment disposition
1085 model (ΔOFV = -98.8, df = 2, $p < .001$ compared with one-compartment) with first-order
1086 elimination and absorption with transit compartments (Supplemental material - **Figure S.**
1087 **6.1**). Allometric scaling was added *a priori* on apparent clearance and volume of distribution
1088 in all the compartments, with total body weight providing a better fit than FFM. Between-
1089 subject variability (BSV) was included on clearance, and to account for within-subject
1090 variability on different occasions, between-occasion variability (BOV) was included on all
1091 absorption parameters. Testing formulation as a covariate on absorption parameters
1092 (absorption rate constant, mean transit time, and bioavailability) within the Cipla
1093 bioequivalence study did not result in a significant difference, confirming bioequivalence of
1094 the two formulations. Including BSV in addition to BOV on bioavailability improved the
1095 model significantly (ΔOFV = -32.5), which could be due to inter-individual differences in
1096 metabolism determining the conversion of the prodrug. Typical (95% CI) clearance of 14.0
1097 (12.0 − 16.3) L/h, central volume of distribution of 99.3 (73.0 − 125) L, and peripheral
1098 volume of distribution of 128 (36.3 – 321) L were estimated for a typical 70 kg individual.
1099 Adding study effect on bioavailability showed that the heart failure participants have 49%
1100 (13% - 88%) higher bioavailability. Including creatinine clearance as a covariate on clearance
1101 did not improve the model.

1102 Parameter estimates, and precisions for the enalaprilat model are given in the supplementary

materials, **Table S. 6.1.** The VPCs, **Figure 6.1**, show that the 5th, 50th, and 95th percentiles of the data are within the 95% confidence intervals of the model predictions for the respective percentiles. This shows that the model adequately described the observed data.

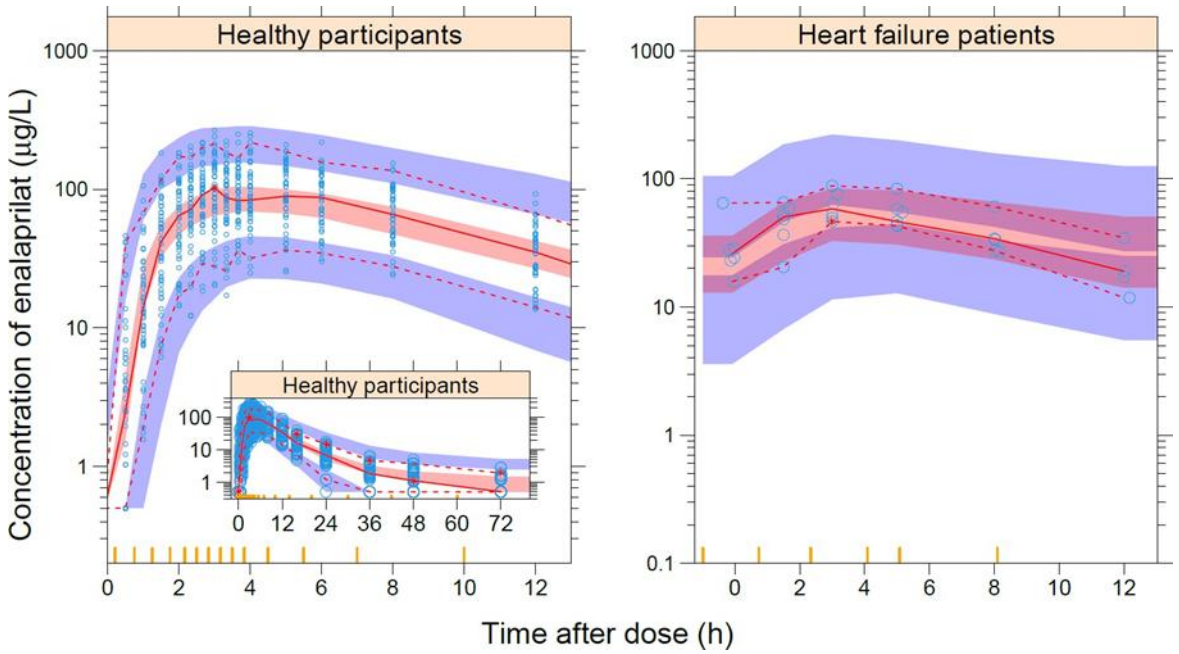

Figure 6.1. Visual Predictive Check of the final model for enalaprilat.
Blue circles represent observed plasma concentrations. The solid line in the middle represents the median observed concentration, while the dashed lines below and above represent the 5th and 95th percentiles of the observed concentrations, respectively. The shaded area around each line represents the 95% model-predicted confidence intervals for the same percentiles. The yellow ticks at the base of the plot show the bins.

Simulations

Using the final model, steady-state trough concentrations in heart failure patients 12 hours after the last dose and until BLQ were obtained through Monte Carlo simulations per dose and weight group. The 5th percentiles of these concentrations, per dose and weight group, as well as time for concentrations to reach BLQ, are reported as personalized reference concentrations for evaluating adherence (**Table 6.2** and **Table S. 6.3.** The results can be interpreted as follows: If a patient has taken the drug as prescribed, there is less than 5% probability that concentrations below the reference concentrations would be observed.

Table 6.2. Threshold concentrations (5th percentile) and time it takes for the concentrations to reach below the limit of quantification of assay. The results of these simulations are applicable for plasma concentrations

Weight (kg)	5th percentile of predicted concentrations at 12 h[1] (µg/L)	Time to below the LLOQ[2] (days)
5 mg twice daily		
40	7.35	3.5
60	6.60	3.5
80	5.09	3
90	4.85	3
100	4.72	2.5
120	4.08	2
140	3.75	2
10 mg twice daily		
40	16.9	5.5
60	12.9	5
80	10.9	5
90	10.2	5
100	9.51	4.5
120	8.37	4.5
140	8.03	4
20 mg twice daily		
40	32.6	7
60	25.1	7
80	22.4	7
90	21.2	7
100	18.4	7
120	17.0	6.5
140	16.3	6.5

[1]Predicted concentrations are at time=12 h (last dose was given at time = 0)
[2]Lower limit of quantification (LLOQ) = 0.2 µg/L

Weight bands of 20 kg
≤ 40 kg = results for 40 kg
41 kg – 60 kg = results for 60 kg
61 kg – 80 kg = results for 80 kg
81 kg – 100 kg = results for 100 kg
101 kg – 120 kg = results for 120 kg
121 kg – 140 kg = results for 140 kg

For example, for a 90 kg patient taking enalapril 20 mg twice daily dose, as given in **Table 6.2**, **Table S. 6.2.** and **Figure 6.2**, the 5th percentile of predicted steady-state trough concentrations 12 h after the last dose 279 is 21.2 µg/L, and BLQ concentrations were

observed at 168 h (7 days). For this weight and dose group, the below interpretations can be used to gauge adherence:

a. If observed concentrations are > 21.2 µg/L, then the concentrations are within the range of model-predicted concentrations, and the assumption of adherence is valid.

b. If observed concentrations are < 21.2 µg/L, then the assumption of adherence to a dose within the last 12 hours is rejected ($p < .05$).

c. If observed concentrations are at BLQ (LLOQ = 0.2 µg/L for the study in heart failure patients), consistent with the model-prediction that for this weight and dose group BLQ concentrations are observed on day 7, the assumption of adherence to a dose within the last 7 days is rejected ($p < .05$).

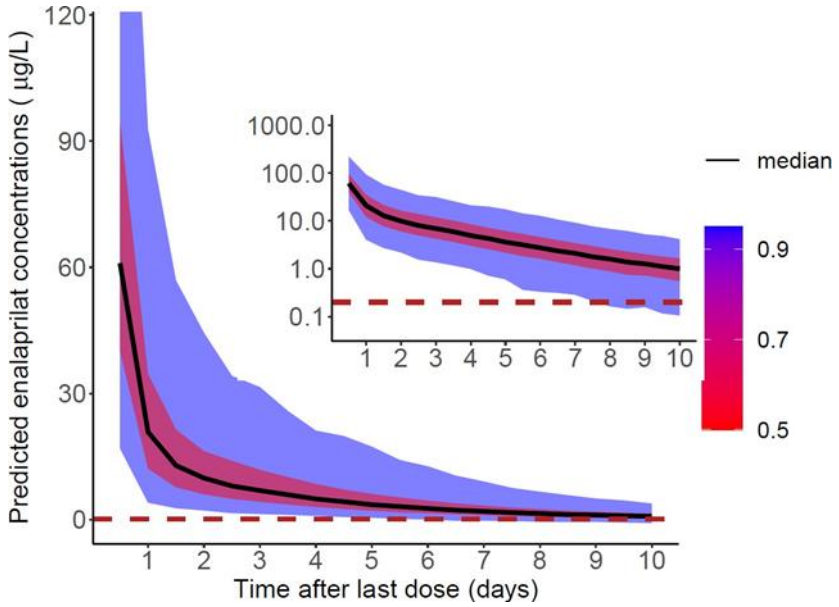

Figure 6.2. Probability distribution plot for a 90 kg patient on 20 mg enalapril twice daily. The horizontal red dashed line indicates the lower limit of quantification (LLOQ) of enalaprilat, i.e., 0.2 µg/L. The lower blue shaded area shows the 5th percentile of the probability distribution. The last dose was given at time = 0, assuming full adherence beforehand, and model-predictions observed thereafter. The plot has been capped to 120 µg/L to enable better visualization of the lower concentrations.

6.5 Discussion

In this study, we demonstrate the utility of population pharmacokinetic modeling to establish

reference concentrations for adherence monitoring. Although it is important to understand the contribution of poor adherence to suboptimal treatment outcomes in chronic diseases, there is limited knowledge regarding medication adherence among chronic heart failure patients, particularly in Africa. A model-based tool can provide an objective means of adherence monitoring. We report the 5th percentile of steady-state trough concentrations 12 hours after dose as individualized reference values which can be used to flag non-adherent patients.

Failure to detect drug concentrations, a traditional method of adherence assessment, is reliant on the sensitivity or specificity of the analytical method, and only extremes of non-adherence are detected. Through modeling, variability in trough concentrations among patients, which could be due to differences in dosing regimen or in patient demographics such as weight are accounted for, so that personalized reference concentrations can be derived. Unlike traditional methods, which provide a snapshot of adherence at one point in time, we report enalaprilat reference concentrations until BLQ, which can inform on number of missed doses, i.e., erratic pill taking behavior. For drugs with a long terminal half-life such as enalaprilat, which is detectable in plasma for up to 96 h, adherence behavior can be assessed, and very low concentrations could be used to evaluate when patients took their last dose. Medication adherence monitoring could be confounded by the “white coat” effect, which is where adherence increases around the clinic visit. However, Monte Carlo simulations after single dose enalapril using our model have demonstrated that this “white coat” effect can be circumvented. Specifically, if a patient takes their medication the day before the scheduled adherence monitoring, the 5th percentiles of single-dose trough enalaprilat concentrations are predicted to below enough compared to our steady-state trough concentrations to flag non-adherence.

The trough concentration (12 hours after dose) is a prudent cut-off value to report adherence, accounting for patients with the lowest concentrations due to variability in pharmacokinetic parameters. In this case, certain factors need to be considered when applying the reference concentrations for adherence monitoring: (i) it is possible to mislabel patients with low clearance as adherent or to mislabel patients with reduced bioavailability as non-adherent, (ii) 5% of patients might be mislabeled as non-adherent due to random chance, (iii) the proposed reference concentrations are based on simulations performed at 12 hours after the last dose, and are most precise for TDM sampling performed at 12 hour intervals after the last assumed dose.

We developed a two-compartment model for enalaprilat, which adequately described the data. The appearance of enalaprilat in plasma was described with a series of transit compartments followed by first-order absorption; this reflects the absorption of the prodrug enalapril, as well as its conversion to the active metabolite, enalaprilat. Our model is in line with the two-compartment model developed by Faisal et al (Faisal et al., 2019), and the rate constant of absorption estimated from our model, 0.601 h^{-1}, agrees with the rate of metabolite (enalaprilat) formation they report of 0.688 h^{-1}. Moreover, our estimated elimination rate constant of 0.141 h-1 is in agreement with the value they report of 0.175 h^{-1}, as well as with previous non-compartmental analysis report of 0.140 h^{-1} by Weisser et al, both in healthy volunteers (Weisser et al., 1991). For a 70 kg individual, our typical estimate for apparent clearance of 14 L/h is lower than the median apparent clearance by Lees et al in young and elderly healthy participants, but within the range they report for the individual participants, median (range), 15.5 (7.32– 32.2) L/h, while our apparent steady-state volume of distribution of 227 L is higher than theirs 133 (47.7 – 172) L (Lees and Reid, 1987). However, their model was one compartment, fitted with nonlinear least-squares regression, which could account for the difference in volume of distribution.

Disposition parameters were allometrically scaled using total body weight and, although renally cleared, creatinine clearance was not a significant covariate on enalaprilat clearance. A significant correlation of overall enalaprilat plasma exposure and creatinine clearance has been reported for creatinine clearances below 60 mL/min (Lowenthal et al., 1985; Kelly et al., 1986), and all our 348 participants had values above 80 mL/min. Bioavailability was estimated to be 49% higher in the heart failure patients relative to the healthy participants. This could be related to lower bioconversion of enalapril to enalaprilat in the healthy participants, since CES1 is known to be polymorphic, and genetic variation has been attributed to be a major contributor to the interindividual variability in CES1 activity (Wang et al., 2017; Her et al., 2021). Although higher serum concentrations of enalaprilat in heart failure patients compared to healthy has been previously reported (Schwartz et al., 1985; Dickstein et al., 1987), this had not been attributed to bioavailability, and larger studies in cardiac patients are needed to further investigate this.

Our data was limited in the number of heart failure patients available, and all of the participants had normal renal function. Given these limitations, it is important to externally validate the model before applying the reference concentrations for adherence monitoring within a patient population exhibiting a wider range of renal function. However, we have demonstrated an objective and quantitative method for adherence monitoring, and though our reference concentrations are preliminary, they represent an improved method compared to conventional adherence assessment methods.

6.6 Conclusion

Medication adherence is key to ensuring optimal treatment outcomes, especially for patients on chronic treatment, such as for cardiovascular disorders. Through this analysis, reference concentrations are proposed to evaluate adherence to enalapril in cardiac patients for a range

of weights and doses. These reference concentrations are useful to identify probable poor adherence and erratic pill taking behavior.

Acknowledgements: I would like to acknowledge and thank my co-authors: Andre Joubert,[1] Phumla Sinxadi,[1] Karen Sliwa,[2] Gary Maartens,[1] Lubbe Wiesner,[1] Paolo Denti,[1] and Roeland E.Wasmann[1] from the [1]Division of Clinical Pharmacology, Department of Medicine, University of Cape Town, Cape Town, South Africa and [2]Hatter Cardiovascular Research Institute, University of Cape Town, Cape Town, South Africa. I would also like to thank Professor Marc Blockman from the Division of Clinical Pharmacology, University of Cape Town, and Dr Nic de Jongh from Cipla, South Africa, for providing the data for this project and for helping with all queries regarding the data.

6.7 Supplementary material

Table S. 6.1. Parameter estimates of model for enalaprilat for healthy subjects and heart failure patients.

Parameter description	**Unit**	**Typical value (95% CI)[1]**	**Shrinkage (%)**
Absorption rate constant	1/h	0.601 (0.458 − 0.717)	
Relative bioavailability (healthy participants)	-	1 FIXED	
Absorption mean transit time	h	0.745 (0.562 − 0.944)	
Number of transit compartments	-	4.36 (2.96 − 6.57)	
Clearance[2]	L/h	14.0 (12.0 − 16.3)	
Central volume of distribution[2]	L	99.3 (73.0 − 125)	
Intercompartmental clearance[2]	L/h	2.22 (1.57 − 3.3)	
Peripheral volume of distribution[2]	L	128 (36.3 − 321)	
Bioavailability of heart failure patients relative to healthy participants[3]	-	+49.0% (+13.0% − +88.0%)	
Between-subject variability, %CV[4]			
Clearance	%	25.3 (16.9 − 32.3)	8.4
Bioavailability	%	46.4 (28.7 − 56.1)	5.7
Between-occasion variability, %CV[4]			
Bioavailability	%	18.4 (12.7 − 22.7)	31.6
Absorption rate constant	%	49.7 (35.2 − 54.4)	27.1
Absorption mean transit time	%	73.8 (46.9 − 86.0)	7.0
Residual unexplained variability			
Proportional error	%	22.1 (19.3 − 24.1)	11.6
Additive error: Cipla	µg/L	0.836 (0.602 – 1.43)	
Additive error: Pilot	µg/L	0.676 (0.442 – 1.27)	

[1]95% confidence intervals (CI) were obtained by bootstrap (n=1000, 78% successful)
[2]Allometric scaling was used for clearance and volume of distribution (by weight); the typical values reported are for typical weight of 70 kg
[3]The effect of study bioavailability was investigated. The value is reported as a fraction.
[4]Between-subject and between-occasion variability are reported as approximate %CV using the formula $\sqrt{\omega^2}$
Eta and epsilon shrinkage of between-subject and -occasion variabilities are below 20%

Table S. 6.2. Fifth percentile of predicted concentrations from the enalaprilat model for weight of 90 kg and dose of 20 mg twice daily.

Time (h)	Fifth percentile of predicted concentrations (µg/L)
12	21.2[ǂ]
24	5.75
36	3.65
48	2.90
60	2.27
72	1.98
84	1.61
96	1.45
108	1.01
120	0.768
132	0.458
144	0.333
156	0.150
168	0.0363

[ǂ]If measured concentrations for a 90 kg patient dosed 20 mg twice daily are below 21.2 µg/L, there is less than 5% probability that the patient was adherent within the last 12 hours (or it is likely that the patient has missed at least one dose)
LLOQ = 0.2 µg/L

Table S. 6.3. Threshold concentrations (fifth percentile) and time it takes for the concentrations to reach below the limit of quantification of assay. The results of these simulations are applicable for plasma concentrations.

5 mg twice daily		
Weight (kg)	**Fifth percentile of predicted concentrations at 12 h[1] (µg/L)**	**Time to below the LLOQ[2] (days)**
35	**8.19**	**3.5**
40	**7.35**	**3.5**
45	**7.56**	**3.5**
50	**6.92**	**3.5**
55	**6.49**	**3.5**
60	**6.60**	**3.5**
65	**5.75**	**3.5**
70	**5.66**	**3**
75	**5.66**	**3**
80	**5.09**	**3**
85	**5.17**	**3**
90	**4.85**	**3**
95	**4.74**	**2.5**
100	**4.72**	**2.5**
105	**4.35**	**2.5**
110	**4.22**	**2.5**
115	**4.16**	**2**
120	**4.08**	**2**
125	**4.05**	**2**
130	**3.80**	**2**
135	**4.12**	**2**
140	**3.75**	**2**
145	**3.52**	**1.5**
10 mg twice daily		
35	**16.5**	**5.5**
40	**16.9**	**5.5**
45	**14.5**	**5.5**
50	**14.8**	**5.5**
55	**13.4**	**5.5**
60	**12.9**	**5**
65	**12.1**	**5**
70	**10.7**	**5**
75	**10.6**	**5**
80	**10.9**	**5**
85	**10.1**	**5**
90	**10.2**	**5**
95	**9.01**	**5**
100	**9.51**	**4.5**
105	**9.24**	**4.5**
110	**8.81**	**4.5**
115	**8.49**	**4.5**
120	**8.37**	**4.5**
125	**8.45**	**4.5**
130	**7.74**	**4**
135	**7.93**	**4**
140	**8.03**	**4**
145	**7.40**	**4**
20 mg twice daily		
35	**31.9**	**7.5**
40	**32.6**	**7**
45	**29.4**	**7.5**
50	**27.4**	**7**
55	**26.9**	**7**
60	**25.1**	**7**
65	**25.2**	**7**
70	**21.9**	**7**
75	**22.5**	**7**
80	**22.4**	**7**
85	**19.8**	**7**
90	**21.2**	**7**
95	**19.1**	**7**
100	**18.4**	**7**
105	**17.8**	**6.5**
110	**18.2**	**7**
115	**18.0**	**7**
120	**17.0**	**7**
125	**16.4**	**7**
130	**16.2**	**6.5**
135	**15.2**	**6.5**
140	**16.3**	**6.5**
145	**16.0**	**6.5**

[1]Predicted concentrations are at time=12 h (last dose was given at time = 0)
[2]Lower limit of quantification (LLOQ) = 0.2 µg/L Weight bands of 5 kg
≤ 35 kg = results for 35 kg
> 35 kg – 40 kg = results for 40 kg
> 40 kg – 45 kg = results for 45 kg etc

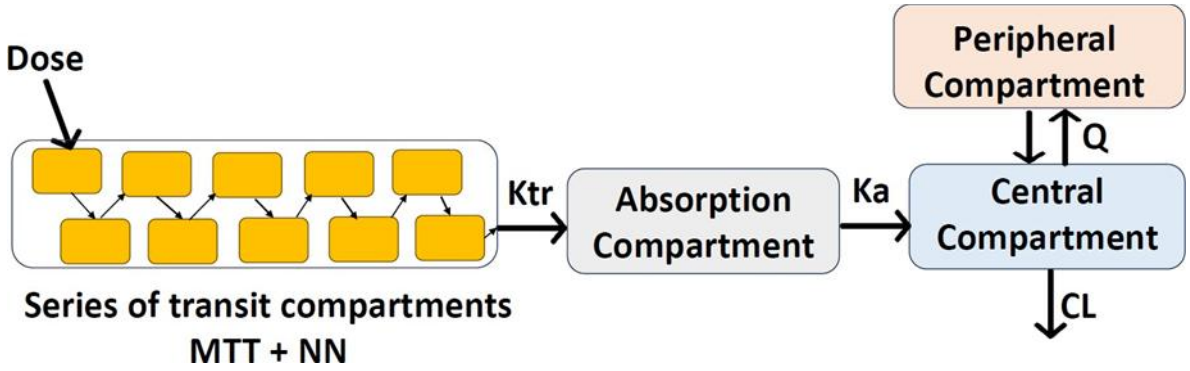

Figure S. 6.1. Structural model for the final enalaprilat model using data from healthy participants and cardiovascular patients.

Chapter 7 Population pharmacokinetics of esomeprazole in patients with preterm preeclampsia

7.1 What is already known about this subject

- Preclinical in vitro and in vivo studies showed that esomeprazole has efficacy to treat preeclampsia, but this was not confirmed in a phase II clinical trial in women with preterm preeclampsia treated with 40-mg once daily esomeprazole.
- Esomeprazole pharmacokinetics is complex. It is metabolized by CYP2C19, which is polymorphic, and by CYP3A4. With repeated dosing, it inhibits its own metabolism via CYP2C19, resulting in higher bioavailability and lower clearance.
- The pharmacokinetics of esomeprazole could be altered during pregnancy since CYP3A4 is expected to be induced and CYP2C19 is expected to be inhibited.
- Safety data from a phase II clinical trial which investigated esomeprazole for treatment of preterm preeclampsia, was reassuring, confirming that esomeprazole can be safely used during pregnancy.

What this study adds:

- We developed a population pharmacokinetic model of esomeprazole using pharmacokinetic data from pregnant women with preterm preeclampsia and non-pregnant controls.
- Our model shows that pregnant women have lower clearance after single dose compared to non-pregnant. This lower clearance could be due to inhibition of CYP2C19.

7.2 Abstract

Esomeprazole is a proton pump inhibitor being investigated for treatment of preeclampsia. Esomeprazole pharmacokinetics during pregnancy are unknown. We used data from 10 pregnant participants with preterm preeclampsia, and 49 non-pregnant participants to develop a population pharmacokinetic model of esomeprazole. A two-compartment model described the data well. In pregnant participants after single dose, clearance was 42.2% (14.9% - 61.6%) lower compared to non-pregnant, most likely due to inhibition of CYP2C19. In non-pregnant participants after repeated dosing, clearance was 54.9% (48.2% – 63.5%) lower in extensive metabolizers and bioavailability was 33% (10.0% – 52.0%) higher compared to single dosing, which could be due to autoinhibition of CYP2C19. During pregnancy, the CYP2C19 autoinhibition effect with repeated dosing is expected to lead to much lower increase in exposure compared to non-pregnant individuals, since CYP2C19 is already inhibited due to pregnancy.

7.3 Introduction

Esomeprazole is a proton pump inhibitor which is used for gastric acid-related disorders in all age groups, including in pregnancy (Katz, Gerson and Vela, 2013). Its pharmacokinetics are complex. After a single dose, two-thirds of esomeprazole is metabolized by cytochrome P450 (CYP) 2C19 to 5-hydroxy- and 5-O-desmethyl esomeprazole and one-third by CYP3A4 to esomeprazole sulphone (Andersson, Hassan-Alin, et al., 2001). CYP2C19 is a polymorphic enzyme, and, after a single dose esomeprazole exposure is at least three times higher in poor metabolizers compared to extensive metabolizers (Klotz, 2006; Dean, 2019). With repeated dosing, esomeprazole and esomeprazole sulphone inhibit CYP2C19, thus increasing exposure due to a lower clearance and higher bioavailability (caused by decreased first-pass effect) (Andersson, Röhss, et al., 2001). This autoinhibition effect might be more apparent for extensive metabolizers than for poor metabolizers (Andersson, Hassan-Alin, et al., 2001).

Esomeprazole pharmacokinetics are unknown during pregnancy but could be altered due to metabolic changes. During pregnancy, CYP2C19 is inhibited, which is expected to reduce esomeprazole clearance; however, this might only be of relevance for extensive metabolizers. Moreover, CYP3A4 is induced during pregnancy, which could result in a larger proportion of the drug being metabolized by CYP3A4. Since CYP3A4 is present in the intestines as well as the liver, this could increase the first-pass effect, decreasing bioavailability and increasing clearance (Anderson, 2005).

Preeclampsia is a major complication of pregnancy, a multi-system disorder where placental dysfunction results in maternal hypertension and multi-system organ injury (Chappell et al., 2021). An estimated 60 000 maternal and 500 000 fetal deaths annually, of which more than 95% are in low-and-middle-income countries, are due to preeclampsia (Duley, 2009; Machano and Joho, 2020). There is an urgent need to find treatment for preterm preeclampsia

which slows disease progression and prevents preterm delivery so that neonatal outcomes can be improved (Tong et al., 2020). Esomeprazole has been identified as potential therapeutic for preeclampsia (De Silva et al., 2019).

Preclinical studies showed that esomeprazole lowers placental production of anti-angiogenic factors thought to play an important role in the pathogenesis of preeclampsia and improves endothelial dysfunction (Onda et al., 2017). Given these findings, a clinical trial - the PIE trial - investigated the efficacy of a daily 40 mg oral esomeprazole dose in women with preterm preeclampsia (Cluver et al., 2018). The trial did not find a significant difference in clinical outcomes or circulating concentrations of anti-angiogenic factors among participants taking esomeprazole compared to those taking placebo. It was postulated that higher doses might be necessary for treating preeclampsia since concentrations in the pregnant participants were lower than concentrations which showed efficacy in the preclinical study (Cluver et al., 2018). The PIE trial generated pharmacokinetic data of oral esomeprazole in pregnant participants with preeclampsia, a population in whom esomeprazole pharmacokinetics has not been previously described.

Pharmacokinetic data from the pregnant population is scarce since pregnant women are usually excluded from clinical trials due to safety and ethical concerns. Population pharmacokinetic modeling is an innovative tool that can be used to make the best use of this existing sparse data from a pregnant population to inform future trials. Therefore, the aim of this work is to describe the population pharmacokinetics of oral esomeprazole during pregnancy using data from pregnant women with pre-eclampsia and healthy, non-pregnant participants.

7.4 Methods

Studies. Pharmacokinetic data were pooled from three studies where oral 40 mg esomeprazole was given. From PIE, Day 1 concentrations were available from pregnant participants treated with esomeprazole capsules (Nexium brand) (Cluver et al., 2018). Day 1 and Day 5 concentrations obtained from healthy, non-pregnant participants were included from two studies: those from Hunfeld et al. were treated with Nexium Multiple-Unit Pellet System tablets (MUPS) while those from Helgadóttir et al. were treated with generic Actavis tablets (Hunfeld et al., 2010; Helgadóttir et al., 2021). Mealtimes differed between the studies: 2 hours post-dose for PIE and Helgadóttir et al. and 5 minutes post-dose for Hunfeld et al. CYP2C19 genotype information was available for the study by Hunfeld et al, as detailed in the Supporting Information (Hunfeld et al., 2010).

Esomeprazole concentrations were quantified using validated liquid chromatography-tandem mass spectrometry (LC-MS/MS), the details of which are included in the original publications. The lower limit of quantifications (LLOQ) in mg/L were 0.001, 0.0260, and 0.00503, PIE, Hunfeld et al. and Helgadóttir et al., respectively (Hunfeld et al., 2010; Cluver et al., 2018; Helgadóttir et al., 2021).

Pharmacokinetic analysis. Population pharmacokinetic analysis was performed using non-linear mixed-effects software NONMEM (v7.4.3, Icon®), PsN v4.9.0, Pirana v2.9.8, and R v3.6.1 for data processing (Keizer, Karlsson and Hooker, 2013). The first-order conditional estimation method with interaction was used for model runs. Concentrations below the limit of quantification were handled similarly to the M6 method by Beal, with additive error inflated by LLOQ/2 (Beal, 2001).

A mixture model was used to assign genotype status for participants where genetic information was not available, with extensive and intermediate metabolizers grouped together

(Keizer et al., 2012). We used proportions fixed to 95% and 5%, for extensive and poor metabolisers, respectively, based on the literature (Strom et al., 2012). The clearance and bioavailability after a single dose in non-pregnant participants were used as a reference to report the percentage change in pregnancy or repeated dosing. The pregnancy and the repeated-dosing effects were then tested as a categorical covariate on clearance and bioavailability for each CYP2C19 genotype subgroup. Study effects were also tested as covariates on all absorption parameters. A non-parametric bootstrap (n=500) was run on the final model to obtain 95% confidence intervals (CIs) for the parameter estimates. More details of the methods used have been included in the Supporting Information.

Nomenclature of Targets and Ligands. Key protein targets and ligands in this article are hyperlinked to corresponding entries in http://www.guidetopharmacology.org, and are permanently archived in the Concise Guide to Pharmacology 2019/20 (Alexander et al., 2021).

Principal investigator statement. This work did not include interventions or administering substances to human participants and did not have a principal investigator. The principal investigators for the three studies from which the data were pooled are included as co-authors.

7.5 Results

Fifty-nine participants were included from three studies: 10 pregnant women with preterm preeclampsia from the PIE trial and 49 non-pregnant participants (55% female), 30 from Helgadóttir et al. and 19 from Hunfeld et al (Hunfeld et al., 2010; Cluver et al., 2018; Helgadóttir et al., 2021). Median (range) age was 30 (21 – 43) years for pregnant and 24 (18 – 46) years for the non-pregnant participants while weight was 99 (56 – 126) kg for pregnant

and 74 (54 – 107) kg for the non-pregnant participants. Participant characteristics are summarised in **Table 7.1**. A total of 1064 concentrations were obtained, of which 68 (6%) were below the limit of quantification (BLQ). Ten (1%) samples from PIE were identified as outliers through goodness-of-fit and individual plots and were removed from the analysis.

Table 7.1. Summary of study and participant characteristics, as median (range) when applicable.

	PIE (Cluver *et al.*, 2018) **(n = 10)**	**Helgadóttir *et al.*** (Helgadóttir *et al.*, 2021) **(n = 30)**	**Hunfeld *et al.*** (Hunfeld *et al.*, 2010) **(n = 19)**
Formulation	Nexium capsules	Actavis tablets	MUPS tablets
Mealtimes	2 h post-dose	2 h post-dose	5 min post-dose
Sampling times (h post-dose)	0.25, 0.5, 0.75, 1, 1.5, 2, 4, 8, 10, and 24	Pre-dose, 0.5, 1, 1.5, 2, 2.5, 3, 3.5, 4, 5, 6, 7, and 8	0.083, 1, 2, 3, 4, 5, 6, 7, and 8
Visit for sampling	Day one	Day one and day five	Day five
Number of samples	85	821	158
Excluded samples	10	0	0
LLOQ (mg/L)	0.001	0.00503	0.0260
Male, n (%) **Female, n (%)**	0 10 (100%)	15 (50%) 15 (50%)	7 (37%) 12 (63%)
Age (years)	30 (21−43)	24 (18−46)	21 (18−27)
Weight (kg)	99 (56−126)	76 (62−107)	69 (54−89)
CYP2C19 Genotype	NA	NA	9 EM 9 IM1 PM
Abbreviations: LLOQ = lower limit of quantification, homEM = homozygous extensive metabolizers, IM = intermediate metabolizers, PM = poor metabolizers			

Esomeprazole pharmacokinetics was best characterized by a two-compartment disposition model (ΔOFV=-225, $p < 0.0001$ compared with one-compartment) with first-order elimination and absorption with transit compartments. Allometric scaling with body weight improved the model fit (ΔOFV=-14.4). Final parameter estimates and precision are presented in **Table 7.2**. For a typical 70-kg individual, clearance in extensive metabolisers was more than three times faster than in slow metabolisers, 24.3 (20.5 – 29.3) versus 7.87 (6.04 – 9.75) L/h.

Table 7.2. Parameter estimates for the final esomeprazole model.

Parameter	Typical value (95% CI)[a]	RSE (%)	Parameter variability, %CV[c]	RSE (%)	Shrinkage, %
Clearance extensive metabolizers (L/h)[b]	24.3 (20.5, 29.3)	7.5	BSV: 23.1 (15.2, 32.9)	34.3	13.3
Clearance poor metabolizers (L/h)[b]	7.87 (6.04, 9.75)	13.6	BSV: 23.1 (15.2, 32.9)		
Central volume of distribution (L)[b]	14.4 (8.70, 20.3)	14.1			
Intercompartmental clearance (L/h)[b]	6.47 (2.80, 11.3)	42.9			
Peripheral volume of distribution (L)[b]	7.71 (5.78, 10.5)	23.8			
Relative bioavailability ()	1 Fixed		BOV: 23.1 (15.2, 29.9)	29.4	22.5
Absorption rate constant (1/h)	4.80 (2.89, 6.39)	41.8	BOV: 485 (211, 916)	45.9	33.7
Mean transit time (h)	1.75 (1.54, 1.94)	7.8	BOV: 38.8 (29.1, 48.5)	23.6	20.0
Number of transit compartments	10 Fixed[d]				
Covariates[e]					
Change in clearance on day five for non-pregnant extensive metabolizers (%)*	-54.9 (-63.5, -48.2)	5			
Change in bioavailability on day five for non-pregnant (%)*	+33.0 (10.0, 52.0)	11.3			
Change in clearance on day one for pregnant (%)*	-42.2 (-61.6, -14.9)	12.4			
Change in mean transit time for PIE (%)*	-71.9 (-79.3, -58.2)	19.2			
Change in mean transit time for Hunfeld *et al.* (%)*	-43.1 (-68.7, -30.0)	19.8			
Residual unexplained variability					
Proportional error (%)	36.7 (32.7, 40.5)	3.2			11.8
Additive error (mg/L)	20% of LLOQ[f]	74.9			

Condition number = 331.86

[a]95% confidence intervals obtained by non-parametric bootstrap (n=500, of which 59.2% were successful)

[b]Allometric scaling with total body weight for a reference individual of 70 kg

[c]Between-subject (BSV) and between-occasion variability (BOV) were obtained using the formula $sqrt(\exp(OM^2) - 1)$ and reported as approximate %CV

[d]The number of transit compartments was fixed to 10 to make parameter estimates more stable

[e]Study effect was tested on parameters with day one data from healthy, non-pregnant participants as reference group

*Reference group is day one non-pregnant (non-pregnant group after single dose)

[f]Lower limit of quantification (LLOQ) (mg/L) was study-specific: 0.001 for PIE, 0.0260 for Hunfeld *et al.*, and 0.00503 for Helgadóttir *et al.*

In pregnant women, clearance was 42.2% (14.9% − 61.6%) slower compared to non-pregnant participants after a single dose (ΔOFV=-8.57, $p < 0.005$). Bioavailability was not found to be significantly different in pregnant women. In non-pregnant participants, clearance was 54.9% (48.2% – 63.5%) slower in extensive metabolizers on Day 5 compared to Day 1 (ΔOFV=-142, $p < 0.0001$), and this effect could not be estimated for poor metabolizers. Bioavailability was 33.0% (10.0%-52.0%) higher on Day 5 (ΔOFV=-14.4, $p < 0.0001$), and this effect could not be isolated by genotype.

We found a fast absorption with large between-occasion variability of 485% (211% – 916%). Absorption was slowest for participants in the study by Helgadóttir et al., with a mean transit time (MTT) of 1.74 h, compared to those in PIE and the study by Hunfeld et al. (0.491 h and 0.988 h, respectively). The visual predictive check (**Figure 7.1**) shows acceptable agreement between the model and the data.

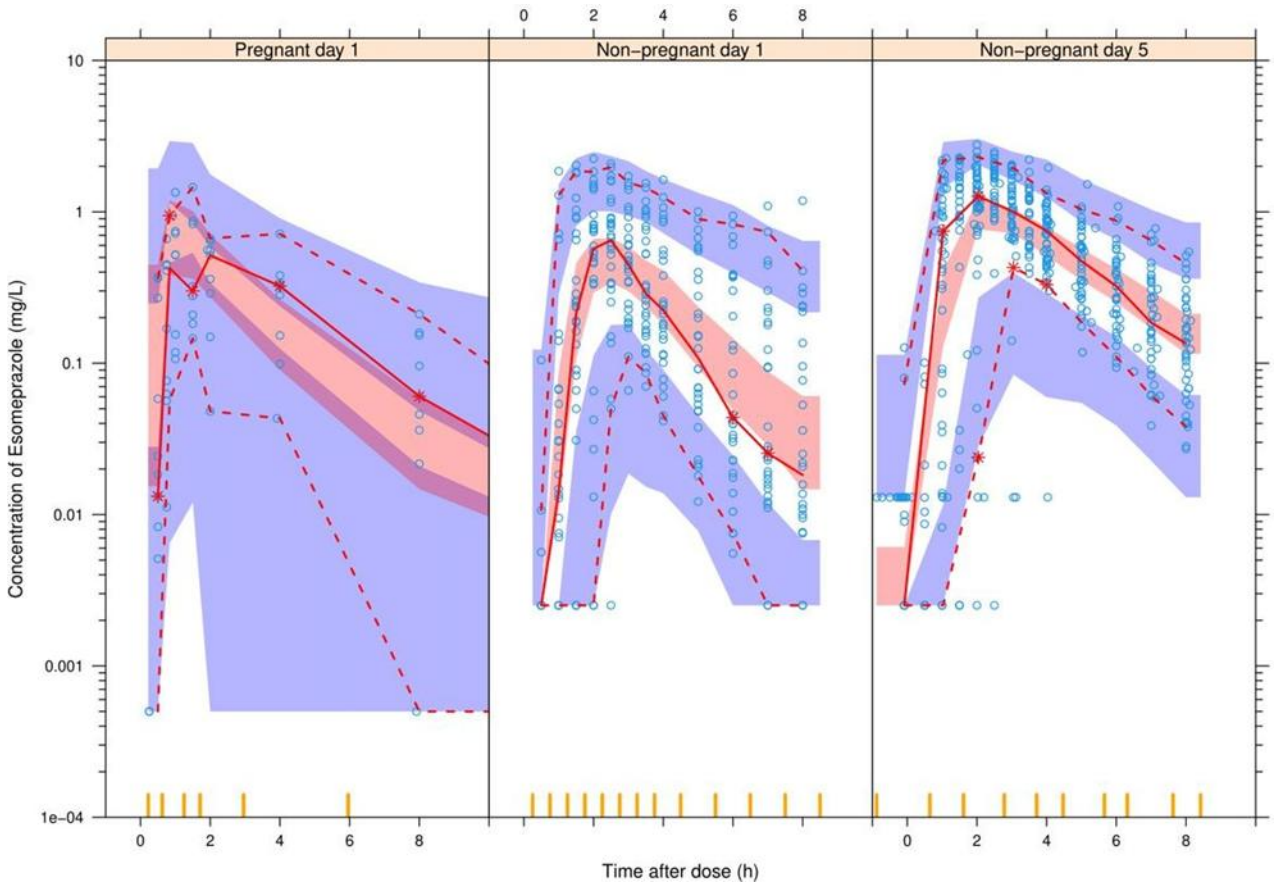

Figure 7.1. Visual predictive check of the final esomeprazole model.
Blue circles represent observed plasma concentrations. The solid line in the middle represents the median observed concentration, while the dashed line below and above represents the 5th and 95th percentiles of the observed concentrations, respectively. The shaded area around each line represents the 95% model predicted confidence intervals for the same percentiles.

7.6 Discussion

We developed a population pharmacokinetic model to describe the pharmacokinetics of esomeprazole in pregnant women with preeclampsia. To our knowledge, this is the first population pharmacokinetic model describing esomeprazole pharmacokinetics during pregnancy. We found that clearance was 42.2% (14.9% – 61.6%) lower in pregnant women with preterm preeclampsia after a single dose of esomeprazole compared to non-pregnant participants. In non-pregnant participants, clearance was 54.9% (48.2% – 63.5%) lower in extensive metabolizers and bioavailability was 33% (10.0% – 52.0%) higher after repeated dosing compared with single dose.

Increases in concentration of hormones such as oestrogen and progesterone during pregnancy could inhibit CYP2C19 and induce CYP3A4 (Andersson et al., 1990; Anderson, 2005; Jeong, 2010). We modelled these effects as categorical covariates while they might be gradual (Jeong, 2010; Poweleit et al., 2022), since we only had data from the third trimester. The lower clearance in the pregnant participants is likely to be due to this inhibition of CYP2C19. Since CYP3A4 is abundantly present in the gut as well as the liver, one would expect a lower bioavailability and higher clearance. We did not find this effect in our model.

The lower clearance in extensive metabolizers in non-pregnant participants with repeated esomeprazole dosing is likely to be due to auto-inhibition of CYP2C19 while the higher bioavailability could be because of a decreased first-pass effect associated with CYP2C19 auto-inhibition (Andersson, Hassan-Alin, et al., 2001; Andersson, Röhss, et al., 2001). Moreover, it has previously been reported for omeprazole that a decrease in intragastric acidity with repeated doses could lower its degradation in the stomach, improving its absorption (Andersson et al., 1990). Hence, with repeated administration of esomeprazole, there could be improved bioavailability due to increase in pH and lower degradation in the

stomach. Esomeprazole disposition has mostly been described in literature with one-compartment kinetics for oral data and two-compartment kinetics for IV data (Liu et al., 2016; Nagase et al., 2020). Two-compartment disposition showed better fit in our model, similar to a model by Standing et al (Joseph F Standing, Marie Sandstrom, Tommy Andersson, Kerstin Rohss, 2009). We estimated a typical clearance which was more than three times higher in extensive metabolizers compared to poor metabolizers. This finding is consistent with previous reports that poor metabolizers have up to three times higher exposure than extensive metabolizers (Klotz, 2006; Dean, 2019). Our estimate of clearance in poor metabolizers agrees with models by Nagase et al. (Nagase et al., 2020) and Standing et al. (Joseph F Standing, Marie Sandstrom, Tommy Andersson, Kerstin Rohss, 2009). The typical central apparent volume of distribution of 14.9 L in our study is similar to that found in healthy participants (~16 L) (Shin and Kim, 2013; Nagase et al., 2020). High variability in speed of absorption was observed in our model, likely due to differences in gastric acidity between-individuals and occasions (Nagase et al., 2020).

Our study shows that esomeprazole clearance is lower during pregnancy which is probably due to CYP2C19 inhibition. This has several implications: first, although there is not conclusive evidence, we speculate that metabolism during pregnancy may be more dependent on CYP3A4. The pregnancy effect of CYP3A4 induction might have been eclipsed by CYP2C19 inhibition resulting in an overall clearance inhibition effect, since esomeprazole has less CYP3A4 affinity and the extent of CYP3A4 induction is unknown (Andersson, Hassan-Alin, et al., 2001). This might mean there is less need for CYP2C19 genotyping during pregnancy, which has previously been suggested for proton pump inhibitors due to genotype-dependent variations in exposure and therapeutic/adverse outcomes (El Rouby, Lima and Johnson, 2018). This might also mean fewer drug-drug interactions that involve CYP2C19. Second, the nonlinearity in esomeprazole pharmacokinetics with repeated dosing

and with dose increases would be expected to be less in pregnancy. Specifically, the increase in exposure with repeated dosing, which is due to CYP2C19 autoinhibition, is not expected to be as high as in non-pregnant individuals. Esomeprazole exposure increases more than dose-dependently with dose increases above 20 mg, due to saturation of CYP2C19-based clearance and first pass effect (Hassan-Alin et al., 2000; Andersson, Röhss, et al., 2001). This nonlinear increase in exposure might not be as high during pregnancy since metabolism might be CYP3A4-dependent, which is generally considered linear (Hassan-Alin et al., 2000; Andersson, Röhss, et al., 2001; Nagase et al., 2020).

It was a limitation in our study that we couldn't isolate the actual effect of pregnancy and repeated dosing because there were other factors that were different between the studies, such as mealtimes and formulation, which could affect the absorption of esomeprazole. However, we believe that with the available data, our model can adequately describe changes during pregnancy and repeated dosing. Only single dose data were available for pregnant participants, so the effect of repeated dosing during pregnancy could not be investigated. Nevertheless, esomeprazole metabolism might be less dependent on CYP2C19 during pregnancy, and we expect pregnant participants to have similar exposure after repeated doses as after a single dose. CYP2C19 genotype was only known for Hunfeld et al., with only one poor metabolizer in the data, and the effect on poor metabolizers could not be identified. However, we used a mixture model to assign genotype status to the other datasets and were able to identify the effect on extensive metabolizers.

We used the first oral esomeprazole data from pregnant participants generated by the PIE trial to describe esomeprazole pharmacokinetics in pregnancy. PIE had found similar esomeprazole exposure in pregnant women to non-pregnant individuals. In our model, we identified a lower clearance in pregnant women, but no significant change in bioavailability.

More data with CYP2C19 genotyping and at steady state from pregnant participants and healthy, non-pregnant controls are needed to further investigate this. PIE reported no clinical benefit of esomeprazole for preeclampsia. Preclinical studies are needed to identify the pharmacodynamic target for preeclampsia and how esomeprazole acts on this target. Further clinical trials are also needed to investigate whether the preclinical efficacy target can be met with higher esomeprazole doses at steady state and our model can help to inform the design of these studies as well as to establish the pharmacokinetic metric that relates with pharmacodynamic markers for preeclampsia.

Acknowledgements: I would like to acknowledge Professors Stephen Tong and Susan Walker from the department of Obstetrics and Gynaecology, University of Melbourne in Australia who are authors of the pre-clinical work that led to the PIE clinical study.

7.7 Supplementary material

Studies. The Preeclampsia Intervention with Esomeprazole (PIE) study was approved by the South African Medicines Control Council and had Health Research Ethics Committee (HREC) approval. The study participants had provided written informed consent (Cluver et al., 2018). The study by Hunfeld et al. was approved by the institutional review board of the Haga Teaching Hospital and all subjects gave written informed consent (Hunfeld et al., 2010). The study by Helgadóttir et al. was approved by the National Bioethics Committee of Iceland and informed consent was obtained from all individual participants (Helgadóttir et al., 2021). CYP2C19 genotype information was available for the study by Hunfeld et al. Nine individuals were either homozygous for the wildtype or had one gain of function allele (*1/*1 or *1/*17) and were classified as extensive metabolisers, nine individuals had one loss of function allele (*1/*2 or *2/*17) and were classified as intermediate metabolisers, and one

individual was homozygous for the loss of function allele (*2/*2) and was classified as poor metaboliser (Strom et al., 2012; El Rouby, Lima and Johnson, 2018).

Pharmacokinetic analysis. Population pharmacokinetic analysis was performed using non-linear mixed-effects software NONMEM (v7.4.3, Icon®), PsN v4.9.0, Pirana v2.9.8, and R v3.6.1 for data processing (Keizer, Karlsson and Hooker, 2013). The first-order conditional estimation method with interaction was used for model runs. Various structural models were tested including one- and two- compartment disposition, first-order elimination and absorption, with or without absorption lag time and transit compartments (Savic et al., 2007).

Between-subject and -occasion random effects were assumed to be log-normally distributed, and a combined error model with an additive and proportional component was used to describe residual variability. Values below the lower limit of quantification (below the LLOQ or BLQ) were imputed to LLOQ/2 and their additive error was inflated by LLOQ/2. The last BLQ value in a series during the absorption phase and the first BLQ value in the drug disappearance phase were retained in the model fit, all other BLQ values were excluded from the model fit but retained for model diagnostics. Concentrations were deemed implausible and excluded from the analysis when the absolute value of their conditional weighted residuals (|CWRES|) was above 5 ($p < 0.00006$).

Model selection was based on decreases in the objective function value (OFV), which were assumed to be chi-squared distributed (a drop of > 3.84 for 1 degree of freedom (df) has $p < 0.05$). Additionally, we inspected goodness-of-fit plots and visual predictive checks (VPCs) and evaluated the biological plausibility of the parameter estimates obtained.

Allometric scaling was used to account for the effect of body size on disposition parameters and total body weight and fat-free mass were tested as descriptors of body size (Janmahasatian et al., 2005). After the inclusion of allometry, other covariates were included

using a supervised stepwise approach with forward inclusion ($p < 0.05$) and backward elimination ($p < 0.01$).

A mixture model was used to assign genotype status to participants who did not have genotype information. We assumed two groups, extensive and poor metabolisers, and used proportions fixed to 95% and 5%, respectively, based on literature (Strom et al., 2012). Although we tried three genotype groups (extensive, intermediate, and poor), the model could not estimate this, probably because the data was not rich enough. Similarly, during our model building, testing two phenotype groups, with the intermediate metabolizers (or hetEM) grouped together with the poor metabolizers did not yield significant results. Additionally, in the Hunfeld et al. study, no statistically significant differences in AUC were reported between the extensive (homozygous extensive) and intermediate (heterozygous extensive) metabolisers after single dose and after repeated dose of esomeprazole (Hunfeld et al., 2010). Therefore, we proceeded with grouping the heterozygous extensive metabolisers together with the homozygous extensive metabolisers in our mixture model.

To investigate changes in clearance and bioavailability that may occur due to pregnancy and during repeated dosing, the model was organised using as reference the single-dose data from non-pregnant individuals. The pregnancy and the repeated-dosing effects were then tested as a categorical covariate on clearance and bioavailability for each CYP2C19 genotype subgroup – i.e., for both CYP2C19 poor and CYP2C19 extensive metabolizer subgroups (with the extensive and intermediate subgroups grouped together).

Study effect was tested as covariate on all absorption parameters, taking into consideration the various differences between the studies that could affect absorption, such as formulation type, mealtimes, single versus repeated esomeprazole dosing, and pregnant versus non-pregnant.

A non-parametric bootstrap (n=500) was run on the final model to obtain 95% confidence intervals (CIs) for the parameter estimates.

Chapter 8 Discussion

8.1 Overall summary

The overall aim of the analyses conducted in this thesis was to develop mathematical models that characterize PK changes in specific understudied populations and utilize them to improve treatment.

In **Chapter 4**, I developed a cefazolin model for children undergoing on-pump cardiac surgery, incorporating the cardiopulmonary bypass pump (CPB). I identified renal function (eGFR) as a significant covariate on clearance and included allometric scaling by weight *a priori* for disposition parameters. Including the CPB device as an additional compartment in the model accounts for changes in the volume of distribution caused by the CPB priming fluids, but I did not observe an effect of the CPB device on clearance. In the context of surgical prophylaxis in children, my investigation revealed that administering cefazolin as a continuous infusion with a priming dose into the CPB, as opposed to an intermittent mg/kg regimen, leads to 100% target attainment during surgery and recovery in the ICU. This approach provides stable profiles and has the potential to counteract any drug loss in the CPB. I proposed a user-friendly dose calculating tool to individualize doses for the continuous infusion regimen, considering weight and estimated glomerular filtration rate (eGFR).

In **Chapter 5**, I developed a model for rifabutin and its metabolite, 25-O-desacetyl rifabutin (Des-rifabutin), in children receiving treatment for both TB and HIV. Rifabutin is cleared by Arylacetamide deacetylase (AADAC) to Des-rifabutin and by CYP3A4 to other metabolites, while Des-rifabutin is further cleared by CYP3A4. My findings revealed that LPV/r inhibits the CYP3A4 pathway of both rifabutin and Des-rifabutin. Through inhibition of gut and liver CYP3A4, rifabutin bioavailability is increased, and rifabutin clearance by the CYP3A4 pathway is inhibited. This results in more conversion to Des-rifabutin through the AADAC pathway and also

slower clearance of Des-rifabutin. Bioavailability was also reduced in children with severe malnutrition. My simulations indicated elevated rifabutin and Des-rifabutin exposures compared to those reported in adults when utilizing a 20 mg/kg/day (up to 300 mg/day) dose for TB treatment, and increased exposures during TB/HIV treatment in children under one year old receiving 5 mg/kg/day. I propose implementing weight-banded rifabutin dosing for TB treatment and TB-HIV co-treatment to ensure consistent exposure levels across various weight groups, aligning with exposure levels observed in adults.

In **Chapter 6**, I pooled data from a limited number of African cardiac patients with data from healthy participants to develop a model for enalaprilat. Using this model, I generated reference ranges for concentrations to assess treatment adherence, considering PK changes influenced by individual dose and weight. This approach can also be employed to identify the duration of non-adherence.

In **Chapter 7**, I pooled data from a limited number of pregnant women with preterm preeclampsia with data from healthy participants to develop an esomeprazole pharmacokinetic model. My findings indicate that pregnancy, CYP2C19 phenotype, and repeated dosing influence esomeprazole PK. Pregnant patients exhibited a 42.2% (95% CI: -14.9%, -61.6%) reduction in clearance after a single dose compared to non-pregnant healthy participants. In non-pregnant healthy participants receiving repeated dosing, there was an increase in bioavailability by 33% (95% CI: 10.0%, 52.0%), along with reduced clearance in CYP2C19 extensive metabolizers by 54.9% (95% CI: 48.2%, 63.5%) compared to single dose PK.

8.2 General considerations and Lessons learnt

8.2.1 Reflections on the analyses performed in this thesis

8.2.1.1 Utility of Population pharmacokinetic modeling

The introduction of pharmacometrics has addressed the limitations of traditional individual PK analysis, as discussed in the thesis introduction. Population pharmacokinetic (PopPK) modeling offers benefits by incorporating underlying physiological mechanisms or other extrinsic factors that may influence PK. In **Chapter 4**, integrating the extracorporeal cardiopulmonary bypass (CPB) device into the cefazolin model allowed me to predict changes in cefazolin PK when the CPB device was connected and primed with an extra dose of cefazolin. This involved anticipating a decrease in cefazolin concentration due to an increase in the volume of distribution resulting from the priming fluids of the CPB. In **Chapter 5**, simultaneous modeling of rifabutin and its metabolite, des-rifabutin, facilitated feedback from the metabolite data to inform parameter estimation of the parent and accurate characterization of their joint interactions with LPV/r. Additionally, it enabled the prediction of metabolite exposures, as both parent and metabolite exposures could be associated with adverse effects. Understanding the PK of both the parent and metabolite was essential for optimizing the dose.

Another benefit of PopPK modeling is the integration of data from single or multiple studies with variations in dosing regimens, sampling times, incomplete or sparse individual sampling, studies with unbalanced arms, and data collected at both single doses and steady state and from adult and children, or from individuals with different age, genetic makeup, etc. These factors can be built into the model or tested to enable a cohesive analysis. In **Chapter 4**, the cefazolin data exhibited diversity, with surgical durations ranging from 0.567 to 5.63 hours, variable number of doses corresponding to short or long surgeries, and differences in dosing practices (with only six out of twenty-two patients receiving an additional dose in the

CPB device). **Chapter 5** involved pooling data from three age cohorts of children with varying participant sizes and arm imbalances; the younger cohorts (<1-year-old and 1-3-year-old) had a control arm with rifabutin-only and visits with rifabutin-LPV/r co-treatment, while the oldest cohort (3-15-year-old) lacked a control arm. In **Chapter 6**, the limited participant size in the study in African patients (only six for enalaprilat) prompted the pooling of patient data (which was collected at steady state) with healthy participants (collected after a single enalapril dose). In **Chapter 7**, the esomeprazole data from pregnant patients exhibited variation in individual PK profiles and was only after the first dose, prompting pooling with healthy participant data collected after the first dose as well as at steady state.

When modeling pooled pharmacometric data, there is a potential risk that variability parameters may become biased when one dataset is substantially smaller or sparser than the other(s), particularly if random effects are estimated jointly across all individuals. In such scenarios, the estimated variability may be disproportionately influenced by the larger dataset. This can result in either an overestimation of variability in the smaller dataset, particularly if systematic differences between datasets are not accounted for, or an underestimation, due to the limited informativeness of the smaller dataset. In **Chapter 6**, I developed a population pharmacokinetic model using pooled data from two studies: one involving six heart failure patients and another with twenty-four healthy participants who were richly sampled. To account for structural differences between the populations, I tested and included heart failure status as a covariate on bioavailability, which was statistically significant. I modelled the residual variability, including BSV and BOV, as random effects common to all individuals in the pooled dataset. To assess whether the estimated variability parameters were sufficiently robust to support simulations, I performed a stratified bootstrap, preserving the group structure of the original data. The bootstrap results indicated that the estimates of OMEGA, i.e., the variance of the random effects, had reasonably narrow 95%

confidence intervals, with approximately symmetric normal distributions and centered away from zero. These findings suggest that the variability parameters were well estimated and thus provide sufficient confidence in the model's suitability for simulation-based prediction of concentration percentiles.

Another application of pharmacometrics is the handling of missing data, as exemplified in **Chapter 7**, where to address the absence of CYP2C19 phenotype information, a mixture model was used, and individual phenotype status was determined based on the observed individual data, thus informing the model on the probability of polymorphisms within populations.

More importantly, model-informed precision dosing (MIPD) can be applied to customize doses for populations with altered PK. This is an improvement over traditional therapeutic drug monitoring (TDM). TDM involves assessing the need for dose adjustment post-treatment, based on whether measured drug concentrations fall within a predefined therapeutic range, and adjusting the dose using drug nomograms (often with one or two covariates) or an educated guess. The TDM approach has several drawbacks. Steady-state sampling is required, posing challenges for drugs with nonlinear PK or long half-lives, as dose adjustment might not occur early enough. Multiple samplings may be necessary to quantify the area under the curve (AUC) rather than a trough concentration (C_{min}) since despite similar trough concentrations, PK profiles may vary for different dose and dosing intervals, leading to conflicting results with respect to the therapeutic range. Additionally, samples must be collected within a specific timeframe for accurate interpretation. In contrast, MIPD utilizes multiple covariates influencing PK and considers the extent of inter/intra-individual variability in a population to determine an optimal initial dose. Further dose customization can be performed using even a single measured sample from a patient, which

need not be at steady state or time-restricted, to derive individual PK parameters through Bayesian estimation using previous PopPK models as priors combined with patient concentrations and performing simulations that maximize target attainment (Wicha *et al.*, 2021). In **Chapters 4 and 5**, after evaluating standard or study doses through simulations, I proposed alternative dosing regimens for optimal outcomes, which can be further validated through clinical trials. In **Chapter 6**, I demonstrate that population PK modeling can enhance adherence monitoring by enabling simulations that provide model-derived reference concentrations. Unlike traditional methods that rely solely on detecting drug presence in biological matrices, this approach accounts for interindividual pharmacokinetic variability and can help infer the duration and extent of non-adherence.

Efficacy and toxicity targets for dose optimization

A challenge in dose optimization is identifying targets for efficacy and toxicity. In some cases, such as antimicrobial therapy, PK can be correlated with effect or pharmacodynamics (PD) without necessitating PD modeling, using the minimum inhibitory concentration (MIC), the lowest concentration of the antibiotic required to prevent growth of the pathogen in vitro (Standing, 2017). PK/PD efficacy metrics for antibiotics depend on the type of antimicrobial activity – for time-dependent activity, such as the beta-lactams, percentage of time free drug concentrations are above MIC (fT>MIC), and for concentration-dependent activity, such as the rifamycins, fCmax/MIC, are used while fAUC/MIC can be used for both. However, MIC assay results have been shown to vary between laboratories due to differences in assay conditions and biological variations between strains of the same pathogen (Mouton et al., 2018). Pooled MIC distributions from international studies, along with antibiotic-pathogen breakpoints, are published by various bodies such as CLSI, EUCAST, CDER, and FDA, although these also provide conflicting results at times due to methods used to get MIC reports (Labreche, Graber and Nguyen, 2015), and undergo updates based on clinical data –

for instance, the susceptibility breakpoint for meropenem was revised to ≤1 μg/mL from ≤4 μg/mL based on poor outcomes in patients with enterobacteria at MICs of 2-4 (Patel et al., 2023). Clinical breakpoints are MIC values used to determine in vivo efficacy and based on clinical studies; they compare outcomes to separate a pathogen's strains that have a high likelihood of treatment success from those strains where treatment is likely to fail. Determining clinical breakpoints is often challenging due to various factors such as economic constraints, underlying patient conditions which could complicate the isolation of antibiotic efficacy, and variations in pathogen strain susceptibility based on the in situ localization within the body. Epidemiological cutoff (ECOFF) values break the MIC distribution of a large collection of a pathogen's clinical isolates to wild type versus resistant. Though this might not necessarily predict in vivo efficacy, it can be used when an antibiotic is known to be generally effective for the pathogen (Turnidge and Paterson, 2007; Lockhart, Ghannoum and Alexander, 2017).

As demonstrated in **Chapter 4**, antibiotic dose can be optimized using model-informed precision dosing (MIPD). Here, an alternative dose is determined based on population parameters, informed by individual covariates, and a target concentration. Subsequently, this dose is assessed via Monte Carlo simulations, evaluating attainment of the PK/PD efficacy metric for the majority of the target population across the MIC distribution of the pathogen. The challenge lies in determining the target concentration. Critically ill patients have pathophysiologic alterations not only limited to PK (Rodríguez-López *et al.*, 2022) and there is often a lack of clinical outcome data in these patients with the specific pathogen, which makes it difficult to identify MIC breakpoint or threshold values. Moreover, for deep tissue infections, higher tissue penetration would result in greater fT>MIC and fAUC/MIC even at higher MIC values (Labreche, Graber and Nguyen, 2015). For surgical prophylaxis, plasma antibiotic concentrations at wound closures predict the risk of surgical site infections. For

example, for cefazolin, despite the PK/PD efficacy metric of fT>MIC, higher target concentrations have been recommended during complex and prolonged cardiac surgeries in critically ill patients for effective prophylaxis (Zelenitsky *et al.*, 2018). Thus, PK/PD efficacy metrics need to be evaluated against clinical data specific to the condition and immune system functionality (Wicha *et al.*, 2021).

Another approach to antibiotic dose optimization is aligning steady-state exposures, which serve as a measure of long-term efficacy, with those observed in a well-studied population. Paediatric dosing has often been extrapolated from adults based on exposure matching, as shown in **Chapter 5**. This is feasible when expecting a similar clinical response but facing uncertainty regarding the appropriate dosage or plasma exposure in the new population (FDA, 2003).

In vitro efficacy targets

Preclinical studies aim to provide evidence of efficacy and insights into a human starting dose where serious adverse effects are avoided. However, ~ 40% to 50% of failures in drug development have been linked to lack of clinical efficacy. A potential reason for this is the challenge in accurately mimicking human pathophysiology (Sun *et al.*, 2022). The use of *in vitro* target concentrations to determine starting doses which can be taken forward in drug development is not always optimal, as exemplified by the Preeclampsia Intervention with Esomeprazole (PIE) trial, in **Chapter 4**. The PIE trial found no significant difference between esomeprazole and placebo arms in improving maternal and foetal outcomes in preterm preeclampsia (Cluver *et al.*, 2018). This is despite preclinical *in vitro*, *ex vivo*, and *in vivo* experiments which had shown esomeprazole reduces preeclampsia biomarkers and lowers blood pressure (Onda *et al.*, 2017). Phase II trials for drug repurposing, exemplified by trials like the PIE trial, offer efficiency in drug development in terms of cost and timelines

compared to *de novo* drug discovery. Nevertheless, challenges may arise as these trials are frequently initiated based on observed signals and unclear target identification. As shown in previous work, directly attempting to attain similar concentrations in pregnant women to those reported to be effective in preclinical studies would require large doses for which safety data are unavailable and dosing guidelines for esomeprazole's established indication of gastric hyperacidity does not support (Gebreyesus, 2020). This indicates that prior to committing time and resources to Phase II clinical trials for drug repurposing, modeling and simulation should be employed to assess *in vitro* potency data (such as EC50) against documented clinically attainable exposures at the approved dosage (such as Cave,ss, Cmax,ss). Upon observing promising translatability of results, potential changes in pharmacokinetics within the target population can be incorporated and simulated. Furthermore, PK/PD modeling can characterize the relationship between human-equivalent dosage and response, such as the reduction in biomarkers in the context of preeclampsia, along with potential adverse effects. This aids in forecasting safe initial doses for Phase I trials, considering that the dose for the new indication may differ from approved doses for established indications (Dodds *et al.*, 2021).

Toxicity targets

Depending on the mechanism of toxicity, parameters such as AUC, C_{min}, or C_{max} could correlate with toxicity, with a threshold value predicting toxicity. When derived from a single dose PK study (same dose level), these parameters are strongly correlated and the real PK/PD relationship is generally inextricable based solely on the data. In general, acute, and concentration-dependent toxicity is usually correlated with C_{max} while long term toxicity correlates best with AUC. C_{min} might be used as a surrogate for AUC when multiple sampling might not be feasible, however its correlation with AUC might vary among individuals or with different dosing intervals. In some cases, the mechanism underlying toxicity is unclear

and the exposure-adverse effect profile might not be characterized, but dose optimization can be refined by including information regarding adverse effects from routine clinical practice. This is not ideal but can serve as a starting point for dose optimization. In **Chapter 4**, individual patient case reports indicated seizures at high cefazolin C_{min} while the toxicity threshold was unclear. This prompted me to use the lowest concentration at which seizures had been reported in adults as a toxicity target for children. In other cases, reports of adverse effects from PK trials could lead to establishment of a therapeutic range. For instance, TDM is recommended for rifabutin since C_{max} values > 1µg/L are associated with adverse effects, while AUC is associated with efficacy (Alsultan and Peloquin, 2014). Model-informed dose optimization, as shown in **Chapter 5**, can predict optimal exposures within the therapeutic range.

8.2.1.2 Methodological considerations

One of the challenges encountered during my analyses was missingness of pertinent information. Missingness is classified as missing completely at random (MCAR – not dependent on observed data), missing at random (MAR – dependent on observed data and can be explained by the data), or missing not at random (MNAR – dependent on unobserved data). When there is high missingness, i.e. >15% of individuals in the data have missing information, the method of handling is important. Excluding individuals with missing information could lead to loss of valuable data and introduce bias to parameter estimates, not to mention that it would be impossible if all individuals in the data are missing the information. Single imputation involves replacing the missing value with the typical population vale (e.g., median), but this might underestimate covariate-parameter correlations. For MAR, it is possible to model the missingness based on another observed covariate in the model - e.g., modeling missing weight based on observed sex and age across individuals. Another way to handle missingness is by using mixture models (Keizer *et al.*, 2012). In

Chapter 4, flow rates of the CPB device were not available in the dataset, while in **Chapter 7**, CYP2C19 phenotype status was missing in two of the three pooled datasets. Regarding missing flow rates for the CPB device, I conducted a sensitivity analysis with three imputations. Upon finding no significant difference between the objective function values (OFVs) of the three models, I selected the imputation that aligned with physiological expectations. Concerning missing phenotype information, I employed a mixture model where individual phenotype status assignment was based on the probability distribution of phenotypes for the demographic in the dataset, which remained fixed in the model. For individuals with phenotype information, I also compared the model's phenotype assignment compatibility with the observed phenotype status. In **Chapter 7**, baseline pre-pregnancy weight or early pregnancy records were not available in my dataset, which included a pooled population of pregnant and non-pregnant participants. For pregnant individuals, current body weight may overestimate metabolically active body size, as weight gain during pregnancy includes non-metabolic tissues such as the placenta, fetus, and amniotic fluid. Additionally, pregnancy introduces time-varying physiological changes—such as alterations in enzyme activity—that are not reliably proportional to weight gain. While pre-pregnancy weight would have been the preferred basis for allometric scaling, I applied allometric scaling using the available current body weight at the time of PK sampling. I judged that estimating pre-pregnancy weight from gestational age–based weight gain norms would introduce greater uncertainty, given the limitations of the dataset. To mitigate the risk of misattributing clearance changes to body weight alone, I also included pregnancy status as a separate covariate on clearance in the model.

Another challenge, observed in **Chapter 5**, was high variability in the pre-dose samples C_{trough} among individuals in the dataset. The pre-dose sample is from an unobserved dose, often self-administered by the patient at home, and generally, it is treated as a separate

occasion from the PK Day samples, with between-occasion variability (BOV) included on absorption parameters. This BOV would have the same variability distribution (omega), but different random effects between the occasion of the unobserved and observed doses. High variability in the pre-dose sample could be due to inaccurate recording of dosing times, since for patients on chronic medication, usually nominal dosing times are used in the dataset for doses other than the PK Day dose. It could also be due to non-adherence or inappropriate medication intake, a case usually observed in paediatric patients. This would lead to inflated BOV and high residual unexplained variability in the model, as well as interfering with parameter estimation. In the rifabutin-des-rifabutin joint model, there was model instability, high BOV in absorption parameters and model misfit in the absorption phase. There are various ways to handle high variability in pre-dose samples, such as estimating extra variability as a factor on the random variability of the unobserved doses, estimating a separate distribution (omega) for absorption parameters for the unobserved and observed doses, or initialization (Dansirikul, Silber and Karlsson, 2008). In **Chapter 5**, I used initialization, which involved identifying profiles that had pre-dose samples at steady state which were conspicuously incongruent with the trough samples for the observed doses and adjusting the dataset so that dosing history was discarded for those profiles, and the initial concentrations in the disposition compartments were set to the pre-dose sample concentrations. At first, I began by initializing all profiles in the dataset, rather than just those with incongruent pre-dose samples as mentioned above. However, this approach led to loss of valuable information, and the estimates for the peripheral compartments became implausible, unstable, and unreliable. Subsequently, I focused on identifying profiles with incongruent steady-state pre-dose samples compared to the trough samples for the observed doses, which resolved these issues. Compared to the other methods, I observed that initialization stabilized the model, improved model fit, and reduced the BOVs on absorption parameters. Thus, this is

a useful approach when dealing with unexplained variability in pre-dose samples as observed in my data and for complex models, such as my parent-metabolite model in **Chapter 5**.

Another consideration in the methodology of PK modeling is handling BLQ concentrations. M3/M4 have been suggested to have lower bias for handling BLQ concentrations, especially when the dataset contains more BLQ concentrations. These methods censor BLQ data and estimate the likelihood of the data being BLQ. Throughout my analyses, I have used a modified version of the M6 method – specifically, I imputed LLOQ/2 to BLQ values which are last in absorption and the first in elimination in the PK profile, which are most informative, discarding trailing BLQ values. Imputing LLOQ/2 is more conservative than imputing with LLOQ or 0, as it is unlikely to introduce strong upward or downward bias to PK parameters. Since these BLQ concentrations have been imputed and thus more uncertain, I increased additive error for these imputed concentrations by LLOQ/2. To ensure that during simulations concentrations can be simulated with plausible precision, I increased the additive error estimate by 20% of the LLOQ since the error for the concentration range that can be reliably quantified during bioanalytical assay cannot be guaranteed to be less than 20%. There are several reasons why I chose to use this modified M6 method over M3/M4 methods. M3/M4 require estimation methods like LAPLACE or SAEM in NONMEM, which especially with small datasets, can become numerically unstable, have slow convergence, long run times, leading to more complexity while M6 is more stable for parameter estimation and less computationally intensive. Moreover, I have treated simulated BLQ values as being lower than the LLOQ (post hoc LLOQ censoring), without interpreting them directly. For example, in **Chapter 6**, only 9% of non-pre-dose concentrations were BLQ and I simulated trough concentrations after missed doses, and simulated all concentrations, detecting when concentrations reached BLQ (i.e., after how many missed doses). In doing so, I did not interpret BLQ simulated values directly but only treated them as below the LLOQ – my only

aim was to see after how many days LOOQ concentration was attained. This means my main simulation goal was above the LLOQ range with the only aim of seeing how many days it took to reach the LLOQ value. Thus, my method of handling BLQ was adequate in that it was not simple imputation, but considered precision of my simulation result in trough concentrations (Wijk *et al.*, 2025).

Involvement of pharmacometricians in studies

One of the experiences gained during the analyses in this thesis is the importance of involving pharmacometricians early in PK studies. The sample size for all analyses conducted in this thesis was limited. In certain cases, this was due to challenges in recruitment and a shortage of medicines, but there is a general misconception that pharmacometrics can always yield results regardless of the data quality. In reality, the quality of the developed model is linked to the quality of the data. Often, pharmacometricians receive data after a study is completed and are involved at the data analysis stage. They then face technical difficulties during model development due to poor data quality such as missing data, data collection errors, participant non-compliance, or laboratory-related errors. Through early involvement, pharmacometricians can assist with identifying the feasibility of conducting a clinical trial and with study design. For instance, before Phase II trials are initiated based on preclinical investigations, the feasibility of attaining effective concentrations in humans at approved doses could be investigated by pharmacometricians early on. In study design, pharmacometricians can inform on sample size, optimal sampling windows for efficient data collection, duration of sampling in line with expected PK characteristics, and type of data to be collected (for e.g., sampling matrix, quantification of unbound concentrations, covariates which might influence PK and enrich the analysis). Often, simple changes in the design that do not increase invasiveness of the sampling or cost, can greatly enhance the quality of the information collected. For instance, it was observed in

the PIE trial (**Chapter 7**) that PK sampling was performed in the pregnant women after single dose with only pre-dose samples collected on day 5, while esomeprazole PK is known to be altered with repeated dosing, thus sampling both after single and multiple dosing would have been beneficial. Moreover, considering that esomeprazole has a short half-life of 1 to 1.5 hours, taking the pre-dose sample on day 5, and even the 24-hour sample after single dose would not have been necessary. For drugs that are metabolized by polymorphic enzymes, phenotype information can enrich the analysis, such as in the case of esomeprazole in **Chapter 7**. Where alterations in protein binding could affect the PK, unbound concentrations should be quantified, as in the case of cefazolin in critically ill patients in **Chapter 4**. Before a study starts, pharmacometricians can train research teams on accurate collection of data critical to an analysis, such as dosing and sampling times, and through interim analysis, can audit the collected data to identify issues so that these can be addressed before a study is completed. Participant non-compliance or drug administration errors can be identified through an early interim analysis, especially in paediatrics, as observed with rifabutin in **Chapter 5**.

8.2.2 Clinical trials and study design in understudied populations

Clinical trials in pregnant women

The exclusion of pregnant women in Phase I and II clinical trials, as mandated by the FDA in 1977, was due to birth defects observed with thalidomide, a morning sickness drug, and vaginal adenocarcinoma observed in women who had been exposed in utero to diethylstilbesterol, a medication previously prescribed to prevent pregnancy complications. The potential foetal risks then led to the research community's reluctance to include women of childbearing potential in clinical trials up to Phase IV. After the FDA's advocation for women's participation in clinical trials in the 1990s, this then led to women's inclusion under adequate contraception, which still left pregnant women excluded. However, pregnant

women use medications, either for new or chronic indications, while changes during pregnancy could alter exposure and hence effective or safe dose. There is no mandate during drug approval requiring trials in pregnant or lactating women, which leads to a lack of incentive for sponsors to conduct these trials. Thus, most medication use is 'off-label', with pregnancy-related outcomes gathered through post-marketing surveillance, which then informs the need for trials in this population, but this delay in labelling might be detrimental, as shown by the delay in identifying the lower exposure to cobicistat-boosted antiretrovirals during pregnancy (Sheffield et al., 2014; Colbers et al., 2019). While the potential risks of trials in pregnant or lactating women must never be taken lightly, pregnant, or lactating women have a right to receive timely, effective, and safe treatment, which necessitates clinical research.

Extrapolating dose from nonpregnant participants to pregnant or lactating patients is inadequate in the face of the myriad of physiologic alterations. The FDA published guidance for clinical trials in pregnancy in 2004, indicating that PK and PD data needs to be obtained in this population to inform dosing for drugs expected to be prescribed for pregnant women, if the drug is expected to be used during pregnancy, and even if use might be rare but the potential risks of use with uninformed doses could be great (e.g., drugs with narrow therapeutic index). According to the guidance, in vitro, ex vivo and pregnant animal preclinical studies needs to demonstrate no greater than minimal risk to the foetus and clinical trials in nonpregnant women needs to have been conducted (FDA, 2004). However, this is a guidance document, and there should be incentives and mandates by regulatory bodies for clinical studies in pregnant women premarketing or through submission of an investigation plan at drug approval to ensure studies are conducted within a short time frame post-marketing. As the PHASES working group has outlined, preclinical developmental and reproductive toxicology studies need to be conducted for all drugs during early drug

development (Lyerly et al., 2021). Preclinical studies include assessment of placental transfer in vitro through placental cell and tissue cultures and ex vivo through human placental perfusion models, as well as pregnant animal foetal toxicity investigations. Once these preclinical studies indicate minimal foetal risk and clinical studies in non-pregnant participants, including women, have been conducted to exclude further safety concerns and confirm efficacy, clinical studies in pregnant women can be conducted (Sheffield et al., 2014). When it comes to clinical trials, for new indications with a drug already in market, opportunistic Phase II trials can be conducted in pregnant or lactating women who are receiving treatment in clinical practice. If a drug is not commonly used in clinical care or to assess dose for different indications than marketing labels, a dedicated trial would be needed once the drug is deemed to be of minimal risk to the foetus. High disease prevalent regions or countries should be identified to enable adequate recruitment. Modeling and simulation can be used to characterize dose-exposure-response profiles and inform dose selection for such trials through integrating data from preclinical studies and clinical studies in nonpregnant women along with anticipated PK changes during pregnancy. Safety should be assessed during PK trials in pregnancy, and pregnancy outcomes should be monitored closely and made available in pregnancy registry databases to inform clinicians. For PK assessments, intensive sampling during dosing and postpartum and random sampling for long half-life drugs would be beneficial. For drugs with short-term dosing, participants at different trimesters and at post-partum can be compared, and although this could require a larger sample size to adequately capture interindividual variability related to gestational age-related changes, it limits exposures of the trial drug during pregnancy. For drugs with chronic dosing, the same participant can be assessed during pregnancy and post-partum. If a drug is expected to be present during delivery, cord blood, maternal blood, and neonatal blood samples should be taken to characterize placental transfer of a drug to the foetus as well as neonate drug

elimination. In case of postpartum, breast milk can also be analysed to evaluate transfer to the infant (Sheffield et al., 2014; Colbers et al., 2019).

Clinical trials in children

Before the 1990s, only ~20% of FDA approved drugs were labelled for paediatric use, leading to off-label prescriptions for children. This was often based on clinician experience, where the adult dosage and administration form were modified, such as using a fraction of crushed adult tablets, mainly based on a child's weight. However, this trial-and-error method can result in negative consequences, as demonstrated by mortality of newborns treated with chloramphenicol for penicillin-resistant infections (U.S. Food & Drug Administration, 2016). This occurred despite the drug having a similar indication in adults, highlighting the issue of immature metabolism in infants. Considered a vulnerable population, ethical reasons were cited for lack of dedicated paediatric research, although lower financial returns and challenges in conducting studies in this population also likely played a role. Since then, regulatory agencies have made efforts to incentivize paediatric studies by pharmaceutical companies in the form of extension of market exclusivity for six months. The FDA's Paediatric Research Equity Act (PREA) of 2003 has required that paediatric studies be conducted for medicinal products expected to be used in children, with the use of appropriate formulations per age group. The European Medicines Agency (EMA) has made a stronger stance in 2008, mandating the integration of a Paediatric Investigation Plan (PIP) after Phase I studies in adults for all new marketing authorization submissions (Zisowsky, Krause and Dingemanse, 2010).

A 2017 EMA report has indicated the resulting positive impact, with 260 new medicines for paediatric use approved since the mandate (European Commission, 2017). However, more work is needed to ensure completion of paediatric research as an integral part of drug development. Conducting clinical trials in children is challenging. Developmental and

physiological variations across various age groups necessitates sub-categorization of the paediatric population, but it is often difficult to recruit enough participants per category to represent the whole population. A possible approach for this is conducting multicentre trials, although these could be difficult to manage, with a risk of random or site-related errors that could interfere with outcomes of the analysis. Bayesian study design, in which sample size for paediatric trials can be informed through prior information regarding treatment effect from adult studies, is useful for paediatric trials, where possible. Even with small sample sizes, Bayesian analyses can provide more precise estimates of treatment effects by integrating prior information with the observed data. Adaptive design could be used in cases where the effect size is unclear, through enabling modification of sample size based on interim analysis results (Baiardi et al., 2011). Another challenge is that traditional placebo-controlled trials could raise ethical concerns in paediatrics. Randomized placebo-phase designs could be useful to address this, where participants start with placebo, followed by a switch to treatment arm and are followed until they respond or the end of the study. Each participant acts as their own control, and the period from study enrolment to switch to treatment arm is randomized, which limits the period on placebo for each participant (Feldman et al., 2003). Randomized withdrawal designs could also be useful, in which all trial participants receive the treatment drug for a period of time, enabling all participants opportunity to experience potential benefits from the treatment. Non-responders then stop the trial, while responders are randomized to placebo and treatment arms, minimizing the time that individual participants are on placebo (Baiardi et al., 2011).

Blood sampling is challenging due to the distress in paediatric patients, which could lead to parents' reluctance to participate and higher withdrawal rates from trials. Modeling and simulation can be used to reduce the need for frequent blood draws, through sparse sampling at different time windows (Autmizguine et al., 2014). PopPK, using data from other

populations, can be used to simulate profiles and optimize sampling time points, enabling informative sparse samples (De Cock et al., 2011). Blood volume allowed for collection in paediatric trials is limited, so that no more than 1% of total blood volume is collected at one time and not exceeding 3% of total blood volume over 4 weeks. To reduce sample volume, especially in children <2 years old, dried blood spot (DBS) sampling could be adopted, which quantify drug concentrations in whole blood and require minimal volume 5-30 μL, compared to 1-2 mL with conventional plasma sampling (Autmizguine et al., 2014). Moreover, DBS samples do not require freezing, due to better drug stability, which could also be suitable for resource-limited settings. Its minimal invasiveness, i.e., capillary blood sampling through finger or heel prick, makes it also more attractive for children through less discomfort. DBS is not without drawbacks, such as inability to conduct multiple tests due to low sample volume and interindividual variation in haematocrit, which can affect the plasma volume in a DBS sample, interfering with accuracy and precision. However, the technique is undergoing continuous development and is promising for young children (Wicha et al., 2021).

Clinical trials in resource-limited settings

Historically, developing countries have been underrepresented in global clinical trials due to limited research capacity and lower commercial viability. This is despite a disproportionate disease burden with poor outcomes - for instance, ~ 50% of the global disease burden is in sub-Saharan Africa, with more deaths in vulnerable populations such as children below 15 years old. Leading causes of disease include infectious diseases like TB, HIV, malaria, and respiratory infections, as well as neglected diseases such as sleeping sickness and leishmaniasis. There has also been a rising incidence of chronic conditions like diabetes and cardiovascular diseases (Toto et al., 2020). Biological and non-biological variations necessitate careful consideration of the treatment context, and extrapolating treatments from

Western settings is not always applicable. Limited access to healthcare and lower health literacy means that populations in these settings may not be aware of their health status, making clinical research an opportunity to provide clinical care. However, conducting clinical trials in these settings is challenging due to factors such as inadequate healthcare infrastructure, poor transportation, a shortage of trained research personnel and laboratories, and socio-cultural attitudes towards clinical research.

Pilot studies having similar study parameters as planned trials could provide insight into real-life challenges. Obtaining regulatory approval in developing countries tends to be a time-consuming process, and the trial needs to include a dedicated staff who is experienced with regulatory and ethics approvals in the country so that approvals are obtained timeously (Toto et al., 2020). Moreover, potential protocol amendments should be anticipated, and timelines planned to meet study deadlines. Multisite studies could help with recruitment rates, and strategies should be put in place in case of slower enrolments, such as expanding to outreach sites. During planning of the trial, factors such as locations of laboratories at or near the study site, potential backup labs, and suppliers of lab materials should be identified. Trials should be initiated with an awareness of the social, cultural, and religious attitudes towards research practices such as blood draws, and staff and participants should be educated to address this. Research related theoretical and specific hands-on training should be provided to local study staff, by collaborations with experienced local research teams if available.

8.3 Future work

The population PK models developed in **Chapters 4** and **5** help identify potential drug under- or overexposure and inform preliminary dosing strategies in paediatric populations with limited clinical data. Unlike empirical dosing (e.g., rifabutin scaled from adults in Chapter 5), these models support individualized or weight-banded dosing. However, the

recommendations are not definitive and should be used in research or monitored clinical settings—particularly where no guidelines exist, such as paediatric rifabutin dosing with lopinavir/ritonavir. In these cases, therapeutic drug monitoring (TDM) is essential to ensure adequate exposure. Due to small sample sizes and limited external validation, the models' generalizability and ability to detect covariates are constrained. The simulated thresholds from **Chapter 6**, however, are clinically applicable and can help distinguish PK variability from poor adherence, guiding dose adjustments and supporting adherence counseling. This can improve care efficiency by targeting patients who need closer monitoring. **Chapter 7** fills a gap in the literature by characterizing esomeprazole PK in pregnancy and provides a foundation for future simulation and pharmacodynamic work linking exposure to preeclampsia biomarkers. Overall, these models highlight data limitations, inform future studies, and should be refined as new data emerge.

Dose optimization of cefazolin in South African children undergoing cardiac surgery with cardiopulmonary bypass

The use of a continuous infusion cefazolin regimen for surgical prophylaxis has been demonstrated in adult studies, but not in paediatric populations. I recommend conducting a study to validate my proposed individualized dosing algorithm for continuous infusion with CPB doses, comparing this regimen to the current standard practice at a hospital. Additionally, the feasibility of implementing the dosing app at the hospital should be assessed. As previously mentioned, I encountered several challenges during this analysis, which should be considered in the study design for future research. First, it is crucial to include a larger paediatric population with a wide range of weight and renal function to ensure statistical significance during covariate testing. Given the recruitment challenges in paediatric studies and the fact that paediatric cardiac surgeries with CPB are not always routine, a multi-site study could be a viable approach.

Second, relevant data collection is essential, including parameters related to the CPB device (such as individual priming fluid volume and CPB flow rate), repeated renal function measures (at baseline, during, and after surgery) to assess CPB's effect on clearance, unbound cefazolin concentrations (as cefazolin is highly albumin-bound, and free concentration is the target, especially since albumin levels may fluctuate in critically ill children), cefazolin concentrations in the device after detachment to evaluate adsorption (since cefazolin can bind to the tube used in CPB systems, based on the length and type of tubing used (Jeffrey J Cies et al., 2019)), and monitoring for any adverse effects and infection occurrences up to 30 days post-surgery.

Another challenge was determining the appropriate efficacy and toxicity targets for dose optimization. In my analysis, I selected the target concentration based on the MIC of Staphylococcus aureus; however, dose optimization could be further refined by considering additional bacteria responsible for surgical site infections and using hospital-specific MIC values. Furthermore, multi-country observational studies in paediatrics are necessary to generate public reports on cefazolin concentrations associated with infection and seizure risks.

Population pharmacokinetics of rifabutin among co-infected children on lopinavir/ritonavir-based antiretroviral therapy

In this analysis, I developed a joint rifabutin/des-rifabutin pharmacokinetic model in children, determined the effect of lopinavir/ritonavir co-treatment on their pharmacokinetics, and performed dose optimization, recommending weight-based dosing regimen using harmonized weight bands. Clinical studies need to be conducted to validate this recommendation (implementing the suggested weight-banded doses) and after validation, child-friendly formulations, such as liquid formulations or dispersible tablets, need to be developed to improve adherence.

Some of the challenges I encountered during model development can be used to provide insights into study design for future studies. A challenge in my analysis was the limited number of participants in certain age groups, only three in the <1-year-old group, the youngest at 8 months old, and although there was a cohort of 3-15-year-olds, data was available only for 10–15-year-old ages. This was due to both limitations in formulation availability and recruitment challenges. I recommend conducting multi-site, multi-country studies to recruit larger sample sizes across different weight bands to capture a wide range of covariates, such as comorbidities and other co-medications, and ensure inclusion of larger sample size of younger age groups, particularly <3 years-old, to capture early developmental changes and enzyme maturation. These studies should be conducted in collaboration with a pharmaceutical company to supply rifabutin formulations to develop age-appropriate formulations and ensure that adequate resources are allocated for paediatric-specific research. It is useful, furthermore, to have a balanced study design, specifically to have matched data after TB-only treatment as well as during co-treatment with lopinavir/ritonavir for all weight bands to compare rifabutin/des-rifabutin levels without and with lopinavir/ritonavir co-treatment. During my analysis, I observed literature inconsistency in that although there are

reports that exposures below 4500 µg·h/L are associated with acquired rifamycin resistance, there are literature reports of adult exposures lower than this, with no reports of treatment failure. Thus, future clinical studies should also assess clinical outcomes and the potential for rifabutin drug resistance during treatment of paediatric tuberculosis and HIV co-infections. The association between rifabutin/des-rifabutin exposure and the risk of adverse effects also needs to be determined so that this can be used to refine dose optimization.

Application of a population pharmacokinetic model as a tool for monitoring adherence in heart failure patients

In this analysis, I demonstrate the application of population PK modeling as an objective and quantitative tool for monitoring adherence. This approach predicts individualized concentrations (by patient covariates and dosing regimens), using these predicted values as references to compare with real-world concentrations and assess adherence. This tool is useful for drugs with long half-lives, as it can not only detect the likelihood of a missed dose but also estimate the number of missed doses by tracking concentrations until they fall to BLQ following missed doses at each expected dosing interval.

In a clinical setting, this tool can be used as follows. A patient on chronic enalapril treatment goes to the clinic for a follow up. A single blood sample is collected, ideally the trough level before the next dose (12 h after the previous dose). Based on the patient's weight and dose, the pre-simulated table which shows the 5^{th} percentile of expected trough concentrations under full adherence is consulted. If the patient's enalaprilat concentration is at or higher than the reference range, the patient was likely adherent. If the concentration is below the 5^{th} percentile, the assumption of adherence is rejected. If non-adherence is likely based on this assessment, the clinician should initiate counseling, possibly adjust dose or switch therapy if there is a clinical reason for non-adherence (such as side effects) or introduce interventions to

improve adherence depending on the patient's circumstance. The simulated concentration thresholds have already been used to compare with clinical observations (Mwita *et al.*, 2023).

I used enalapril data from a study involving African heart failure patients, a demographic where adherence data is limited, and where it is crucial to rule out adherence as a factor contributing to suboptimal treatment outcomes. Unfortunately, the study had a small sample size, but I also demonstrate how historical data, such as bioequivalence data, can be leveraged to strengthen modeling. To validate the enalaprilat model for adherence monitoring in African heart failure patients, I recommend conducting a clinical study within this demographic to generate richer data (including intensive sampling and a larger number of participants). In my analysis, I was unable to identify the effect of renal function on enalaprilat clearance, despite the drug being renally cleared, as all participants had normal renal function. Thus, the study should include a diverse range of participants, capturing key covariates like body weight and renal function, to adequately assess their impact. Including a randomized control group of healthy participants would also be valuable for identifying PK differences between healthy individuals and cardiac patients, which I observed in my analysis but need to confirm in a larger population.

Population pharmacokinetics of esomeprazole in patients with preterm preeclampsia

Characterizing esomeprazole PK is no small feat due to multiple factors. First, it is metabolized mainly by CYP2C19 and also by CYP3A4, which are subject to inhibition and induction. Second, repeated dosing can lead to autoinhibition of CYP2C19, potentially reducing clearance and increasing bioavailability. Furthermore, the increase in gastric pH with repeated dosing may enhance esomeprazole bioavailability. Third, CYP2C19 is polymorphic, meaning extensive metabolizers exhibit higher clearance after a single dose and repeated dosing could increase exposure due to CYP2C19 autoinhibition whereas poor

metabolizers' exposure is unlikely to be affected by repeated dosing. Finally, dose non-linearity has been observed at doses higher than 20 mg, likely due to CYP2C19 saturation. To accurately characterize esomeprazole pharmacokinetics during pregnancy, these factors must be taken into account.

In my analysis, I hypothesized changes in esomeprazole pharmacokinetics with repeated dosing and higher doses during pregnancy, but these need further validation. Therefore, I recommend that future studies in pregnant women collect data on concentrations after both single and multiple doses(on day one and day five) and include dose non-linearity studies. This would help support my hypothesis that exposure changes during pregnancy are likely dose independent due to a shift in metabolism to CYP3A4, potentially caused by pregnancy-related CYP2C19 inhibition. Additionally, while I speculated that CYP2C19 genotyping might be unnecessary in pregnancy, given the expectation that CYP3A4 is the primary metabolizing enzyme and there may be less variation in exposure between poor and extensive metabolizers, this still needs confirmation, and genotype data should be collected. Since esomeprazole is highly albumin-bound in non-pregnant individuals (97%) but albumin levels are lower during preeclampsia, collecting unbound concentrations could provide a more accurate pharmacokinetic profile.

Moreover, I recommend conducting studies throughout each trimester of pregnancy, with repeated dosing of esomeprazole, as well as postpartum, to better capture the gradual changes in CYP3A4 induction and CYP2C19 inhibition. Using pregnant women as their own control postpartum is useful, as a challenge in my analysis was that comparator data for non-pregnant participants were drawn from other studies with varying designs, including differences in demographics, mealtimes, and esomeprazole formulations.

In terms of evaluating esomeprazole as a treatment for preeclampsia, larger clinical studies are needed to establish the relationship between esomeprazole concentrations and preeclampsia-associated biomarkers across trimesters. Identifying the pharmacokinetic metric that correlates with biomarker reduction could help define the appropriate dosing regimen for preeclampsia patients. Additionally, clinical data on the maximum tolerable esomeprazole dose during pregnancy is essential to evaluate efficacy at doses higher than 40 mg.

8.4 Conclusions

Clinical research involving populations such as pregnant women, children, and individuals from resource-limited settings is often limited, with many studies conducted post-marketing. This delay results in late product labelling, posing risks to safety and restricting access to timely and effective treatments. Additionally, data from these studies are typically sparse, with small sample sizes and limited sampling. In this thesis, I have demonstrated that pharmacometrics can be leveraged to work with such limited data by integrating information from studies conducted in other populations to improve model development. However, more clinical research in these specific populations is crucial to draw robust conclusions. Regulatory bodies need to establish frameworks that facilitate research in these groups and create ethical guidelines to ensure safety while promoting inclusion. Including these populations in clinical trials alongside others can help avoid the challenges I encountered in integrating data from different studies with varying designs. To improve clinical research, strategies such as conducting multi-centre trials to enhance recruitment and increase result generalizability, using longitudinal studies to capture changes over time (e.g., during pregnancy, post-partum, and in children during development), and offering flexibility in trial schedules are essential. Engaging local stakeholders and institutions to ensure cultural sensitivity, encouraging participation, and building capacity in resource-limited settings is also important. Collaboration with pharmaceutical companies to ensure the accessibility,

appropriateness, and affordability of formulations for these populations, as well as utilizing pharmacometric modeling to optimize dosing regimens and sampling times, are key to advancing clinical research in these underrepresented groups.

References

Abegaz, T.M. *et al.* (2017) 'Nonadherence to antihypertensive drugs a systematic review and meta-analysis', *Medicine*, 96(4). Available at: https://doi.org/10.1097/MD.0000000000005641.

Adembri, C. *et al.* (2010) 'Cefazolin bolus and continuous administration for elective cardiac surgery: Improved pharmacokinetic and pharmacodynamic parameters', *Journal of Thoracic and Cardiovascular Surgery*, 140(2), pp. 471–475. Available at: https://doi.org/10.1016/j.jtcvs.2010.03.038.

Alexander, S.P.H. *et al.* (2021) 'THE CONCISE GUIDE TO PHARMACOLOGY 2021/22: Enzymes', *British Journal of Pharmacology*, 178(S1), pp. S313–S411. Available at: https://doi.org/10.1111/bph.15542.

Alli, A. *et al.* (2023) 'Peri-operative pharmacokinetics of cefazolin prophylaxis during valve replacement surgery', *PLoS ONE*, 18(9 September), pp. 1–14. Available at: https://doi.org/10.1371/journal.pone.0291425.

Alsultan, A. and Peloquin, C.A. (2014) 'Therapeutic drug monitoring in the treatment of tuberculosis: An update', *Drugs*, 74(8), pp. 839–854. Available at: https://doi.org/10.1007/s40265-014-0222-8.

Anderson, B.J. and Holford, N.H.G. (2008) 'Mechanism-Based Concepts of Size and Maturity in Pharmacokinetics'. Available at: https://doi.org/10.1146/annurev.pharmtox.48.113006.094708.

Anderson, B.J. and Holford, N.H.G. (2009) 'Mechanistic basis of using body size and maturation to predict clearance in humans', *Drug Metabolism and Pharmacokinetics*, pp. 25–36. Available at: https://doi.org/10.2133/dmpk.24.25.

Anderson, B.J. and Larsson, P. (2011) 'A maturation model for midazolam clearance', *Paediatric Anaesthesia*, 21(3), pp. 302–308. Available at: https://doi.org/10.1111/j.1460-9592.2010.03364.x.

Anderson, G.D. (2005) 'Pregnancy-induced changes in pharmacokinetics: A mechanistic-based approach', *Clinical Pharmacokinetics*, 44(10), pp. 989–1008. Available at: https://doi.org/10.2165/00003088-200544100-00001.

Andersson, T. *et al.* (1990) 'Pharmacokinetics and bioavailability of omeprazole after single and repeated oral administration in healthy subjects.', *British Journal of Clinical Pharmacology*, 29(5), pp. 557–563. Available at: https://doi.org/10.1111/j.1365-2125.1990.tb03679.x.

Andersson, T., Hassan-Alin, M., *et al.* (2001) 'Pharmacokinetic studies with esomeprazole, the (S)-isomer of omeprazole', *Clinical Pharmacokinetics*, 40(6), pp. 411–426. Available at: https://doi.org/10.2165/00003088-200140060-00003.

Andersson, T., Röhss, K., *et al.* (2001) 'Pharmacokinetics and pharmacodynamics of esomeprazole, the S-isomer of omeprazole', *Alimentary Pharmacology and Therapeutics*, 15(10), pp. 1563–1569. Available at: https://doi.org/10.1046/j.1365-2036.2001.01087.x.

Asada, M. *et al.* (2018) 'Effects of cardiopulmonary bypass on the disposition of cefazolin in patients undergoing cardiothoracic surgery', (April), pp. 1–8. Available at: https://doi.org/10.1002/prp2.440.

Autmizguine, J. *et al.* (2014) 'Pharmacokinetic Studies in Infants Using Minimal-Risk Study Designs', *Current Clinical Pharmacology*, 9(4), pp. 350–358. Available at: https://doi.org/10.2174/1574884709666140520153308.

Baiardi, P. *et al.* (2011) 'Innovative study design for paediatric clinical trials', *European Journal of Clinical Pharmacology*, 67(SUPPL. 1), pp. 109–115. Available at: https://doi.org/10.1007/s00228-011-0990-y.

Ban, K.A. *et al.* (2017) 'American College of Surgeons and Surgical Infection Society: Surgical Site Infection Guidelines, 2016 Update', *Journal of the American College of Surgeons*, 224(1), pp. 59–74. Available at: https://doi.org/10.1016/j.jamcollsurg.2016.10.029.

Batchelor, H.K. and Marriott, J.F. (2015) 'Paediatric pharmacokinetics: Key considerations', *British Journal of Clinical Pharmacology*, 79(3), pp. 395–404. Available at: https://doi.org/10.1111/bcp.12267.

Bath, S. *et al.* (2016) 'Impact of standardization of antimicrobial prophylaxis duration in paediatric cardiac surgery', *Journal of Thoracic and Cardiovascular Surgery*, 152(4), pp. 1115–1120. Available at: https://doi.org/10.1016/j.jtcvs.2016.04.091.

Bauer, R.J. (2019) 'NONMEM Tutorial Part II: Estimation Methods and Advanced Examples', *CPT: Pharmacometrics and Systems Pharmacology*, 8(8), pp. 538–556. Available at: https://doi.org/10.1002/psp4.12422.

Beal, S.L. (2001) 'Ways to fit a PK model with some data below the quantification limit - reference for BLQ handling', *Journal of Pharmacokinetics and Pharmacodynamics*, 28(5), pp. 481–504. Available at: https://doi.org/10.1023/A:1012299115260.

Beal, S.L. and Sheiner, L.B. (2008) *NONMEM Users Guide-Part II Users Supplemental Guide April 1988.*

Bechtel, T. P., Slaughter, R.L. and Moore, T.D. (1980) 'Seizures associated with high cerebrospinal fluid concentrations of cefazolin', *American Journal of Hospital Pharmacy*, 37(2), pp. 271–273. Available at: https://doi.org/10.1093/ajhp/37.2.271.

Bergstrand, M. *et al.* (2011) 'Prediction-corrected visual predictive checks for diagnosing nonlinear mixed-effects models',

AAPS Journal, 13(2), pp. 143–151. Available at: https://doi.org/10.1208/s12248-011-9255-z.

Blaschke, T.F. *et al.* (2006) 'The clinical pharmacokinetics of rifabutin', *Clinical Pharmacokinetics*, 45(4), pp. 325–350. Available at: https://doi.org/10.2165/00003088-200645040-00001.

Borchardt, R.A. and Tzizik, D. (2018) 'Update on surgical site infections: The new CDC guidelines', *Journal of the American Academy of Physician Assistants*, 31(4), pp. 52–54. Available at: https://doi.org/10.1097/01.JAA.0000531052.82007.42.

Boulanger, C., Hollender, E., Farrell, K., Stambaugh, J.J., Maasen, D., Ashkin, D., Symes, S., Espinoza, Luis A., *et al.* (2009) 'Pharmacokinetic Evaluation of Rifabutin in Combination with Lopinavir-Ritonavir in Patients with HIV Infection and Active Tuberculosis', *Clinical Infectious Diseases*, 0486(9), pp. 1305–1311. Available at: https://doi.org/10.1086/606056.

Bozkurt, B. *et al.* (2021) 'Universal definition and classification of heart failure: a report of the Heart Failure Society of America, Heart Failure Association of the European Society of Cardiology, Japanese Heart Failure Society and Writing Committee of the Universal Definition o', *European Journal of Heart Failure*, 23(3), pp. 352–380. Available at: https://doi.org/10.1002/ejhf.2115.

Bratzler, D.W. *et al.* (2013) 'Clinical practice guidelines for antimicrobial prophylaxis in surgery', 70, pp. 195–283. Available at: https://doi.org/10.2146/ajhp120568.

C. S. Mott Children's Hospital University of Michigan Medical Center (1998) *Protocols and guidelines for paediatric perfusion*. Available at: https://www.rch.org.au/uploadedfiles/main/content/cardiac_surg/cs_mott_hospital_cpb_protocol.pdf (Accessed: 15 November 2022).

Caffarelli, A.D. *et al.* (2006) 'Plasma cefazolin levels during cardiovascular surgery: Effects of cardiopulmonary bypass and profound hypothermic circulatory arrest', *The Journal of Thoracic and Cardiovascular Surgery*, 131(6), pp. 1338–1343. Available at: https://doi.org/10.1016/j.jtcvs.2005.11.047.

Calic, D. *et al.* (2018) 'Evaluation of cefazolin antimicrobial prophylaxis during cardiac surgery with cardiopulmonary bypass', (May 2014), pp. 768–771. Available at: https://doi.org/10.1093/jac/dkx439.

Calitz, C. *et al.* (2014) 'Impact of traditional African medicine on drug metabolism and transport', *Expert Opinion on Drug Metabolism and Toxicology*, 10(7), pp. 991–1003. Available at: https://doi.org/10.1517/17425255.2014.920321.

Carnethon, M.R. *et al.* (2017) *Cardiovascular Health in African Americans: A Scientific Statement From the American Heart Association*, *Circulation*. Available at: https://doi.org/10.1161/CIR.0000000000000534.

Cattaneo, D. and Gervasoni, C. (2023) 'Dolutegravir dosing with rifampicin', *The Lancet HIV*, 10(10), pp. e635–e636. Available at: https://doi.org/10.1016/S2352-3018(23)00229-1.

Chappell, L.C. *et al.* (2021) 'Pre-eclampsia', *The Lancet*, 398(10297), pp. 341–354. Available at: https://doi.org/10.1016/S0140-6736(20)32335-7.

Chung, E.K. *et al.* (2023) 'Population Pharmacokinetics and Pharmacodynamics of Cefazolin Using Total and Unbound Serum Concentrations in Patients with High Body Weight', *International Journal of Antimicrobial Agents*, p. 106751. Available at: https://doi.org/10.1016/j.ijantimicag.2023.106751.

Cies, Jeffrey J. *et al.* (2019) 'Pharmacokinetics of cefazolin delivery via the cardiopulmonary bypass circuit priming solution in infants and children.', *The Journal of antimicrobial chemotherapy*, 74(5), pp. 1342–1347. Available at: https://doi.org/10.1093/jac/dky574.

Clinton Health Acess Initiative (CHAI) (2023) *HIV Market Report*. Available at: https://www.clintonhealthaccess.org/report/2023-hiv-market-report-the-state-of-hiv-market-in-low-and-middle-income-countries/.

Cluver, C.A. *et al.* (2018) 'Esomeprazole to treat women with preterm preeclampsia: a randomized placebo controlled trial', *American Journal of Obstetrics and Gynecology*, 219(4), pp. 388.e1-388.e17. Available at: https://doi.org/10.1016/j.ajog.2018.07.019.

De Cock, P.A.J.G. *et al.* (2017) 'Population pharmacokinetics of cefazolin before, during and after cardiopulmonary bypass to optimize dosing regimens for children undergoing cardiac surgery', *Journal of Antimicrobial Chemotherapy*, 72(3), pp. 791–800. Available at: https://doi.org/10.1093/jac/dkw496.

De Cock, R.F.W. *et al.* (2011) 'The role of population PK-PD modeling in paediatric clinical research', *European Journal of Clinical Pharmacology*, 67(SUPPL. 1). Available at: https://doi.org/10.1007/s00228-009-0782-9.

Cockcroft, D.W. and Gault, M.H. (1976) 'Prediction of creatinine clearance from serum creatinine', *Nephron*, 16(1), pp. 31–41. Available at: https://doi.org/10.1159/000180580.

Colbers, A. *et al.* (2019) 'Importance of Prospective Studies in Pregnant and Breastfeeding Women Living with Human Immunodeficiency Virus', *Clinical Infectious Diseases*, 69(7), pp. 1254–1258. Available at: https://doi.org/10.1093/cid/ciz121.

Costantine, M.M. (2014) 'Physiologic and pharmacokinetic changes in pregnancy', *Frontiers in Pharmacology*, 5 APR(April), pp. 1–5. Available at: https://doi.org/10.3389/fphar.2014.00065.

Crabol, Y. *et al.* (2016) 'Rifabutin: Where do we stand in 2016?', *Journal of Antimicrobial Chemotherapy*, 71(7), pp. 1759– 1771. Available at: https://doi.org/10.1093/jac/dkw024.

Cramer, J.A. (1990) 'Compliance Declines Between Clinic Visits', *Archives of Internal Medicine*, 150(7), p. 1509. Available at: https://doi.org/10.1001/archinte.1990.00390190143023.

Dansirikul, C., Silber, H.E. and Karlsson, M.O. (2008) 'Approaches to handling pharmacodynamic baseline responses', *Journal of Pharmacokinetics and Pharmacodynamics*, 35(3), pp. 269–283. Available at: https://doi.org/10.1007/s10928-008- 9088-2.

Dean, L. (2019) 'Esomeprazole Therapy and CYP2C19 Genotype Drug class : Proton Pump Inhibitors', (Md), pp. 1–7. Available at: https://www.ncbi.nlm.nih.gov/books/.

Decloedt, E.H. *et al.* (2011) 'Pharmacokinetics of lopinavir in HIV-infected adults receiving rifampin with adjusted doses of lopinavir-ritonavir tablets', *Antimicrobial Agents and Chemotherapy*, 55(7), pp. 3195–3200. Available at: https://doi.org/10.1128/AAC.01598-10.

Denti, P. *et al.* (2022) 'One dose does not fit all: revising the WHO paediatric dosing tool to include the non-linear effect of body size and maturation', *The Lancet. Child & adolescent health*, 6(1), pp. 9–10. Available at: https://doi.org/10.1016/S2352-4642(21)00302-3.

Denti, P. (2024). Handling within-subject/between-occasion variability in longitudinal data: Common challenges and Practical Solutions. Presented at the PAGE meeting, PAGE [2024], Abstract 11282. Retrieved from https://www.page-meeting.org/default.asp?abstract=11282.

Department of Health and Human Services. (2022) *Panel on Antiretroviral Guidelines for Adults and Adolescents. Guidelines for the Use of Antiretroviral Agents in Adults and Adolescents with HIV.* Available at: https://clinicalinfo.hiv.gov/en/guidelines/hiv-clinical-guidelines-adult-and-adolescent-arv/drug-interactions-protease- inhibitors (Accessed: 29 September 2023).

Department of Health and Human Services (2023) *Panel on Opportunistic Infections in Children with and Exposed to HIV. Guidelines for the Prevention and Treatment of Opportunistic Infections in Children with and Exposed to HIV.* Available at: https://clinicalinfo.hiv.gov/en/guidelines/hiv-clinical-guidelines-paediatric-opportunistic-infections/whats-new- guidelines. (Accessed: 9 March 2023).

Dhont, E. *et al.* (2020) 'Augmented renal clearance in paediatric intensive care: are we undertreating our sickest patients?', *Paediatric Nephrology*, 35(1), pp. 25–39. Available at: https://doi.org/10.1007/s00467-018-4120-2.

Dickstein, K. *et al.* (1987) 'The pharmacokinetics of enalapril in hospitalized patients with congestive heart failure.', *British Journal of Clinical Pharmacology*, 23(4), pp. 403–410. Available at: https://doi.org/10.1111/j.1365- 2125.1987.tb03069.x.

DiMatteo, M.R. (2004) 'Variations in patients' adherence to medical recommendations: A quantitative review of 50 years of research', *Medical Care*, 42(3), pp. 200–209. Available at: https://doi.org/10.1097/01.mlr.0000114908.90348.f9.

Dodds, M. *et al.* (2021) 'Model-informed drug repurposing: A pharmacometric approach to novel pathogen preparedness, response and retrospection', *British Journal of Clinical Pharmacology*, 87(9), pp. 3388–3397. Available at: https://doi.org/10.1111/bcp.14760.

Dokainish, H. *et al.* (2017) 'Global mortality variations in patients with heart failure: results from the International Congestive Heart Failure (INTER-CHF) prospective cohort study', *The Lancet Global Health*, 5(7), pp. e665–e672. Available at: https://doi.org/10.1016/S2214-109X(17)30196-1.

Dosne, A.G., Bergstrand, M. and Karlsson, M.O. (2017) 'An automated sampling importance resampling procedure for estimating parameter uncertainty', *Journal of Pharmacokinetics and Pharmacodynamics*, 44(6), pp. 509–520. Available at: https://doi.org/10.1007/s10928-017-9542-0.

Duley, L. (2009) 'The Global Impact of Pre-eclampsia and Eclampsia', *Seminars in Perinatology*, 33(3), pp. 130–137. Available at: https://doi.org/10.1053/j.semperi.2009.02.010.

Eke, A.C. *et al.* (2023) 'Physiologic Changes During Pregnancy and Impact on Small-Molecule Drugs, Biologic (Monoclonal Antibody) Disposition, and Response', *The Journal of Clinical Pharmacology*, 63(S1). Available at: https://doi.org/10.1002/jcph.2227.

El-Rachidi, S., LaRochelle, J.M. and Morgan, J.A. (2017) 'Pharmacists and paediatric medication adherence: Bridging the gap', *Hospital Pharmacy*, 52(2), pp. 124–131. Available at: https://doi.org/10.1310/hpj5202-124.

Engelman, R. *et al.* (2007) 'The Society of Thoracic Surgeons Practice Guideline Series: Antibiotic Prophylaxis in Cardiac Surgery, Part II: Antibiotic Choice**For the full text of the STS Guideline on Antibiotic Prophylaxis

in Cardiac Surgery, as well as other titles in the STS Prac', *Annals of Thoracic Surgery*, 83(4), pp. 1569–1576. Available at: https://doi.org/10.1016/j.athoracsur.2006.09.046.

Estel, C. and Conti, C.R. (2016) 'Global Burden of Cardiovascular Disease', *Cardiovascular Innovations and Applications*, 1(4), pp. 369–377. Available at: https://doi.org/10.15212/cvia.2016.0029.

Ette, E.I. and Williams, P.J. (2007) *Pharmacometrics: The Science of Quantitative Pharmacology*. Available at: https://www.ptonline.com/articles/how-to-get-better-mfi-results.

European Commission (2017) 'State of Paediatric Medicines in the EU: 10 years of the EU Paediatric Regulation', *DG Health and Consumers*, pp. 1–17.

Faisal, M. *et al.* (2019) 'Simultaneous semi-mechanistic population pharmacokinetic modeling analysis of enalapril and enalaprilat serum and urine concentrations from child appropriate orodispersible minitablets', *Frontiers in Paediatrics*, 7(JULY), pp. 1–11. Available at: https://doi.org/10.3389/fped.2019.00281.

FDA (2003) 'Guidance for Industry: Exposure-Response Relationships - Study Design, Data Analysis and Regulatory Applications', *FDA Guidance*, (April), pp. 1–25.

FDA (2004) 'Guidance for Industry - Pharmacokinetics in Pregnancy - Study Design, Data Analysis, and Impact on Dosing and Labeling', *FDA Guidance* [Preprint], (October).

FDA (2018) *Guidance for Industry: Bioanalytical method validation*. Available at: https://doi.org/10.1201/9780203026427-15.

US Food and Drug Administration. (2020). Pharmacokinetics in patients with impaired renal function—study design, data analysis, and impact on dosing. Washington, DC: US Food and Drug Administration.

Feghali et al. (2018) 'Pharmacokinetics of drugs in pregnancy', *Physiology & behavior*, 176(1), pp. 139–148. Available at: https://doi.org/10.1053/j.semperi.2015.08.003.Pharmacokinetics.

Feldman, B. *et al.* (2003) 'The randomized placebo-phase design for clinical trials', *Physical Therapy in Sport*, 4(3), pp. 129–136. Available at: https://doi.org/10.1016/S1466-853X(03)00073-7.

Ferrari, R. (2008) 'Treatment with angiotensin-converting enzyme inhibitors: Insight into perindopril cardiovascular protection', *European Heart Journal, Supplement*, 10(G), pp. 13–20. Available at: https://doi.org/10.1093/eurheartj/sun025.

Food & Drug Administration (2020) *2015-2019 Drug Trials Snapshots Summary Report: Five-year summary and Analysis of Clinical Trial Participation and Demographics*, *Industry and Environment*. Available at: https://www.fda.gov/media/143592/download (Accessed: 16 November 2023).

Food and Drug Administration (2020) '(FDA) Enhancing the Diversity of Clinical Trial Populations — Eligibility Criteria, Enrollment Practices, and Trial Designs Guidance for Industry', (November), p. November.

Gallagher, D. *et al.* (2020) 'Body Composition Measurements from Birth through 5 Years: Challenges, Gaps, and Existing & Emerging Technologies—A National Institutes of Health workshop', *Obesity Reviews*, 21(8). Available at: https://doi.org/10.1111/obr.13033.

Gebreyesus, M.S. (2020) *Population pharmacokinetic modeling for dose optimization of esomeprazole to treat early-onset preeclampsia.*, *University of Cape Town*. Available at: http://hdl.handle.net/11427/34033.

Groenewegen, A. *et al.* (2020) 'Epidemiology of heart failure Measuring an epidemic', pp. 7–9. Available at: https://doi.org/10.1002/ejhf.1858.

Groenland, E.H. *et al.* (2021) 'Plasma Trough Concentrations of Antihypertensive Drugs for the Assessment of Treatment Adherence: A Meta-Analysis', *Hypertension*, 77(1), pp. 85–93. Available at: https://doi.org/10.1161/HYPERTENSIONAHA.120.16061.

Gtif, I. *et al.* (2021) 'Heart failure disease: An African perspective', *Archives of Cardiovascular Diseases*, 114(10), pp. 680–690. Available at: https://doi.org/10.1016/j.acvd.2021.07.001.

Gumbo, T. *et al.* (2015) 'Correlations between the hollow fiber model of tuberculosis and therapeutic events in tuberculosis patients: Learn and confirm', *Clinical Infectious Diseases*, 61(Suppl 1), pp. S18–S24. Available at: https://doi.org/10.1093/cid/civ426.

Hafner, R. *et al.* (1998) 'Tolerance and pharmacokinetic interactions of rifabutin and clarithromycin in human immunodeficiency virus-infected volunteers', *Antimicrobial Agents and Chemotherapy*, 42(3), pp. 631–639. Available at: https://doi.org/10.1128/aac.42.3.631.

Haslam, J.L. *et al.* (1999) 'Stability of rifabutin in two extemporaneously compounded oral liquids', *American Journal of Health-System Pharmacy*, 56(4), pp. 333–336. Available at: https://doi.org/10.1093/ajhp/56.4.333.

Hassan-Alin, M. *et al.* (2000) 'Pharmacokinetics of esomeprazole after oral and intravenous administration of single and repeated doses to healthy subjects', *European Journal of Clinical Pharmacology*, 56(9–10), pp. 665–670. Available at: https://doi.org/10.1007/s002280000206.

Hawkshead, J. and Krousel-Wood, M.A. (2007) 'Techniques for measuring medication adherence in hypertensive patients in outpatient settings: Advantages and limitations', *Disease Management and Health Outcomes*, 15(2), pp. 109–118. Available at: https://doi.org/10.2165/00115677-200715020-00006.

Helgadóttir, H. *et al.* (2021) 'Pharmacokinetics of single and repeated oral doses of esomeprazole and gastrin elevation in healthy males and females', *Scandinavian Journal of Gastroenterology*, 56(2), pp. 128–136. Available at: https://doi.org/10.1080/00365521.2020.1859610.

Hennig, S. *et al.* (2016) 'Population pharmacokinetic drug-drug interaction pooled analysis of existing data for rifabutin and HIV PIs', *Journal of Antimicrobial Chemotherapy*, 71(5), pp. 1330–1340. Available at: https://doi.org/10.1093/jac/dkv470.

Her, L.H. *et al.* (2021) 'Effect of CES1 genetic variation on enalapril steady-state pharmacokinetics and pharmacodynamics in healthy subjects', *British Journal of Clinical Pharmacology*, 87(12), pp. 4691–4700. Available at: https://doi.org/10.1111/bcp.14888.

Hockings, N., Ajayi, A. and Reid, J. (1986) 'Age and the pharmacokinetics of angiotensin converting enzyme inhibitors enalapril and enalaprilat.', *British Journal of Clinical Pharmacology*, 21(4), pp. 341–348. Available at: https://doi.org/10.1111/j.1365-2125.1986.tb05205.x.

Holford, N., Heo, Y. and Anderson, B. (2013) 'A Pharmacokinetic Standard for Babies and Adults', 102(9), pp. 2941– 2952. Available at: https://doi.org/10.1002/jps.

Holford, N.H.G. and Anderson, B.J. (2017) 'Allometric size: The scientific theory and extension to normal fat mass', *European Journal of Pharmaceutical Sciences*, 109(November), pp. S59–S64. Available at: https://doi.org/10.1016/j.ejps.2017.05.056.

Hood, S.R. *et al.* (2018) 'Association Between Medication Adherence and the Outcomes of Heart Failure', *Pharmacotherapy: The Journal of Human Pharmacology and Drug Therapy* [Preprint]. Available at: https://doi.org/10.1002/phar.2107.

Hunfeld, N.G. *et al.* (2010) 'A comparison of the acid-inhibitory effects of esomeprazole and pantoprazole in relation to pharmacokinetics and CYP2C19 polymorphism', *Alimentary Pharmacology and Therapeutics*, 31(1), pp. 150–159. Available at: https://doi.org/10.1111/j.1365-2036.2009.04150.x.

Illamola, C.S.M. *et al.* (2016) 'Evaluating renal function and age as predictors of amikacin clearance in neonates : model- based analysis and optimal dosing strategies', pp. 793–805. Available at: https://doi.org/10.1111/bcp.13016.

Ingrande, J. *et al.* (2019) 'Pharmacokinetics of Cefazolin and Vancomycin in Infants Undergoing Open-Heart Surgery With Cardiopulmonary Bypass.', *Anaesthesia and analgesia*, 128(5), pp. 935–943. Available at: https://doi.org/10.1213/ANE.0000000000003876.

Izquierdo-Blasco, J. *et al.* (2015) 'Impact of the implementation of an interdisciplinary infection control program to prevent surgical wound infection in paediatric heart surgery', *European Journal of Paediatrics*, 174(7), pp. 957–963. Available at: https://doi.org/10.1007/s00431-015-2493-9.

Janmahasatian, S. *et al.* (2005) 'Quantification of Lean Bodyweight', *Clinical Pharmacokinetics*, 44(10), pp. 1051–1065. Available at: https://doi.org/10.2165/00003088-200544100-00004.

Jaworski, R. *et al.* (2019) 'Antibiotic Prophylaxis in Paediatric Cardiac Surgery: Where Are We and Where Do We Go? A Systematic Review', *Surgical Infections*, 20(4), pp. 253–260. Available at: https://doi.org/10.1089/sur.2018.272.

Jeong, H. (2010) 'Altered drug metabolism during pregnancy: Hormonal regulation of drug-metabolizing enzymes', *Expert Opinion on Drug Metabolism and Toxicology*, 6(6), pp. 689–699. Available at: https://doi.org/10.1517/17425251003677755.

Johnson, T. N., & Ke, A. B. (2021). Physiologically Based Pharmacokinetic Modeling and Allometric Scaling in Paediatric Drug Development: Where Do We Draw the Line? Journal of clinical pharmacology, 61 Suppl 1, S83–S93. https://doi.org/10.1002/jcph.1834

Jongmans, C. *et al.* (2022) 'An Overview of the Protein Binding of Cephalosporins in Human Body Fluids: A Systematic Review', *Frontiers in Pharmacology*, 13(June). Available at: https://doi.org/10.3389/fphar.2022.900551.

Joseph F Standing, Marie Sandstrom, Tommy Andersson, Kerstin Rohss, M.O.K. (2009) *Population Pharmacokinetic Modeling of Esomeprazole Nonlinearity - PAGE 18 (2009) Abstract 1577 [www.page-meeting.org/?abstract=1577]*, *Population Approach Group Europe*.

Joubert, Andre *et al.* (2022) 'Simultaneous Determination of Carvedilol, Enalaprilat, and Perindoprilat in Human Plasma Using LC–MS/MS and Its Application to a Pharmacokinetic Pilot Study', *Chromatographia*, 85(5), pp. 455–468. Available at: https://doi.org/10.1007/s10337-022-04154-y.

Karlsson, M.O. and Sheiner, L.B. (1993) 'The importance of modeling interoccasion variability in population pharmacokinetic analyses', *Journal of Pharmacokinetics and Biopharmaceutics*, 21(6), pp. 735–750. Available at: https://doi.org/10.1007/BF01113502.

Katz, P.O., Gerson, L.B. and Vela, M.F. (2013) 'Guidelines for the diagnosis and management of gastroesophageal reflux disease', *American Journal of Gastroenterology*, 108(3), pp. 308–328. Available at: https://doi.org/10.1038/ajg.2012.444.

Ke, A.B. *et al.* (2014) 'Pharmacometrics in pregnancy: An unmet need', *Annual Review of Pharmacology and Toxicology*, 54, pp. 53–69. Available at: https://doi.org/10.1146/annurev-pharmtox-011613-140009.

Kearns, G.L. *et al.* (2003) 'Developmental Pharmacology — Drug Disposition, Action, and Therapy in Infants and Children', *New England Journal of Medicine*. Edited by A.J.J. Wood, 349(12), pp. 1157–1167. Available at: https://doi.org/10.1056/nejmra035092.

Keizer, R.J. *et al.* (2012) 'Performance of methods for handling missing categorical covariate data in population pharmacokinetic analyses', *AAPS Journal*, 14(3), pp. 601–611. Available at: https://doi.org/10.1208/s12248-012-9373-2.

Keizer, R.J., Karlsson, M.O. and Hooker, A. (2013) 'Modeling and simulation workbench for NONMEM: Tutorial on Pirana, PsN, and Xpose', *CPT: Pharmacometrics and Systems Pharmacology*, 2(6), pp. 1–9. Available at: https://doi.org/10.1038/psp.2013.24.

Kelly, J. *et al.* (1986) 'Pharmacokinetics of enalapril in normal subjects and patients with renal impairment.', *British Journal of Clinical Pharmacology*, 21(1), pp. 63–69. Available at: https://doi.org/10.1111/j.1365-2125.1986.tb02823.x.

Khachi, H. *et al.* (2009) 'Pharmacokinetic interactions between rifabutin and lopinavir/ritonavir in HIV-infected patients with mycobacterial co-infection', *Journal of Antimicrobial Chemotherapy*, 64(4), pp. 871–873. Available at: https://doi.org/10.1093/jac/dkp263.

Khan, B. *et al.* (2022) 'Preeclampsia Incidence and Its Maternal and Neonatal Outcomes With Associated Risk Factors', *Cureus*, 14(11). Available at: https://doi.org/10.7759/cureus.31143.

Klotz, U. (2006) 'Clinical impact of CYP2C19 polymorphism on the action of proton pump inhibitors: a review of a special problem', *Int. Journal of Clinical Pharmacology and Therapeutics*, 44(07), pp. 297–302. Available at: https://doi.org/10.5414/CPP44297.

Labreche, M.J., Graber, C.J. and Nguyen, H.M. (2015) 'Recent updates on the role of pharmacokinetics-pharmacodynamics in antimicrobial susceptibility testing as applied to clinical practice', *Clinical Infectious Diseases*, 61(9), pp. 1446–1452. Available at: https://doi.org/10.1093/cid/civ498.

Lan, N.T.N. *et al.* (2014) 'Randomised pharmacokinetic trial of rifabutin with lopinavir/ritonavir- antiretroviral therapy in patients with HIV-associated tuberculosis in Vietnam', *PLoS ONE*, 9(1). Available at: https://doi.org/10.1371/journal.pone.0084866.

Lanckohr, C. *et al.* (2016) 'Pharmacokinetic characteristics and microbiologic appropriateness of cefazolin for perioperative antibiotic prophylaxis in elective cardiac surgery', *Journal of Thoracic and Cardiovascular Surgery*, 152(2), pp. 603–610. Available at: https://doi.org/10.1016/j.jtcvs.2016.04.024.

Lanoiselée, J. *et al.* (2021) 'Population pharmacokinetic model of cefazolin in total hip arthroplasty', *Scientific Reports*, 11(1), pp. 1–11. Available at: https://doi.org/10.1038/s41598-021-99162-7.

Lavielle, M. and Aarons, L. (2016) 'What do we mean by identifiability in mixed effects models?', *Journal of Pharmacokinetics and Pharmacodynamics*, 43(1), pp. 111–122. Available at: https://doi.org/10.1007/s10928-015-9459-4.

Lees, K.R. and Reid, J.L. (1987) 'Age and the pharmacokinetics and pharmacodynamics of chronic enalapril treatment', *Clinical Pharmacology and Therapeutics*, 41(6), pp. 597–602. Available at: https://doi.org/10.1038/clpt.1987.81.

Levey, A. S., Stevens, L. A., Schmid, C. H., Zhang, Y. L., Castro, A. F., 3rd, Feldman, H. I., Kusek, J. W., Eggers, P., Van Lente, F., Greene, T., Coresh, J., & CKD-EPI (Chronic Kidney Disease Epidemiology Collaboration) (2009). A new equation to estimate glomerular filtration rate. Annals of internal medicine, 150(9), 604–612. https://doi.org/10.7326/0003-4819-150-9-200905050-00006

Lindbom, L., Pihlgren, P., & Jonsson, N. (2005). PsN-Toolkit—a collection of computer intensive statistical methods for non-linear mixed effect modeling using NONMEM. Computer methods and programs in biomedicine, 79(3), 241-257.

Liu, D. *et al.* (2016) 'Pharmacokinetic and Pharmacodynamic Modeling Analysis of Intravenous Esomeprazole in Healthy Volunteers', *Journal of Clinical Pharmacology*, pp. 816–826. Available at: https://doi.org/10.1002/jcph.733.

Lockhart, S.R., Ghannoum, M.A. and Alexander, B.D. (2017) 'Establishment and use of epidemiological cutoff values for molds and yeasts by use of the clinical and laboratory standards institute M57 standard', *Journal of Clinical Microbiology*, 55(5), pp. 1262–1268. Available at: https://doi.org/10.1128/JCM.02416-16.

Lowenthal, D.T. *et al.* (1985) 'The effect of renal function on enalapril kinetics', *Clinical Pharmacology and Therapeutics*, 38(6), pp. 661–666. Available at: https://doi.org/10.1038/clpt.1985.242.

Lyerly, A.D. *et al.* (2021) 'Ending the evidence gap for pregnancy, HIV and co-infections: ethics guidance from the PHASES project', *Journal of the International AIDS Society*, 24(12). Available at: https://doi.org/10.1002/jia2.25846.

Machano, M.M. and Joho, A.A. (2020) 'Prevalence and risk factors associated with severe pre-eclampsia among postpartum women in Zanzibar: A cross-sectional study', *BMC Public Health*, 20(1), pp. 1–10. Available at: https://doi.org/10.1186/s12889-020-09384-z.

Marín, R. *et al.* (2020) 'Oxidative stress and mitochondrial dysfunction in early-onset and late-onset preeclampsia', *Biochimica et Biophysica Acta - Molecular Basis of Disease*, 1866(12), p. 165961. Available at: https://doi.org/10.1016/j.bbadis.2020.165961.

Matteelli, A. *et al.* (2012) 'Lopinavir pharmacokinetic profiles in HIV-infected patients during rifabutin-based anti- mycobacterial therapy', *Journal of Antimicrobial Chemotherapy*, 67(10), pp. 2470–2473. Available at: https://doi.org/10.1093/jac/dks218.

McMurray, J.J.V. *et al.* (2012) 'ESC Guidelines for the diagnosis and treatment of acute and chronic heart failure 2012: The Task Force for the Diagnosis and Treatment of Acute and Chronic Heart Failure 2012 of the European Society of Cardiology. Developed in collaboration with the Heart', *European heart journal*, 33(14), pp. 1787–1847. Available at: https://doi.org/10.1093/eurheartj/ehs104.

Milad A. Alshaya, *et al.* (2021) 'Surgical site infections following paediatric cardiac surgery in a tertiary care hospital: Rate and risk factors', *Journal of the Saudi Heart Association*, 33(1). Available at: https://doi.org/10.37616/2212-5043.1234.

Morad Asaad, A. and Ahmad Badr, S. (2016) 'Surgical Site Infections in Developing Countries: Current Burden and Future Challenges', *Clinical Microbiology: Open Access*, 05(06), pp. 8–9. Available at: https://doi.org/10.4172/2327- 5073.1000e136.

Mould, D. and Upton, R. (2012) 'Basic Concepts in Population Modeling, Simulation, and Model-Based Drug Development', *CPT: Pharmacometrics & Systems Pharmacology*, 1(9), p. 6. Available at: https://doi.org/10.1038/psp.2012.4.

Mould, D. and Upton, R. (2013) 'Basic Concepts in Population Modeling, Simulation, and Model-Based Drug Development—Part 2: Introduction to Pharmacokinetic Modeling Methods', *CPT: Pharmacometrics & Systems Pharmacology*, 2(4), pp. 1–14. Available at: https://doi.org/10.1038/psp.2013.14.

Moultrie, H. *et al.* (2015) 'Pharmacokinetics and safety of rifabutin in young hiv-infected children receiving rifabutin and lopinavir/ritonavir', *Journal of Antimicrobial Chemotherapy*, 70(2), pp. 543–549. Available at: https://doi.org/10.1093/jac/dku382.

Mouton, J. W., Brown, D. F., Apfalter, P., Cantón, R., Giske, C. G., Ivanova, M., MacGowan, A. P., Rodloff, A., Soussy, C. J., Steinbakk, M., & Kahlmeter, G. (2012). The role of pharmacokinetics/pharmacodynamics in setting clinical MIC breakpoints: the EUCAST approach. Clinical microbiology and infection : the official publication of the European Society of Clinical Microbiology and Infectious Diseases, 18(3), E37–E45. https://doi.org/10.1111/j.1469-0691.2011.03752.x

Mouton, J.W. *et al.* (2018) 'Variation of MIC measurements: The contribution of strain and laboratory variability to measurement precision', *Journal of Antimicrobial Chemotherapy*, 73(9), pp. 2374–2379. Available at: https://doi.org/10.1093/jac/dky232.

Mwita, J.C. *et al.* (2023) 'Objectively measured medication adherence using assays for carvedilol and enalaprilat in patients with heart failure in Mozambique and Nigeria', *International Journal of Cardiology Cardiovascular Risk and Prevention*, 19(July), p. 200213. Available at: https://doi.org/10.1016/j.ijcrp.2023.200213.

Nagase, M. *et al.* (2020) 'Population pharmacokinetic analysis of esomeprazole in Japanese subjects with various CYP2C19 phenotypes', *Journal of Clinical Pharmacy and Therapeutics*, 45(5), pp. 1030–1038. Available at: https://doi.org/10.1111/jcpt.13129.

Naiker, S. *et al.* (2014) 'Randomized pharmacokinetic evaluation of different rifabutin doses in African HIV-infected tuberculosis patients on lopinavir/ritonavir-based antiretroviral therapy', *BMC Pharmacology and Toxicology*, 15(1), pp. 1–11. Available at: https://doi.org/10.1186/2050-6511-15-61.

Nakajima, A. *et al.* (2011) 'Human arylacetamide deacetylase is responsible for deacetylation of rifamycins: Rifampicin, rifabutin, and rifapentine', *Biochemical Pharmacology*, 82(11), pp. 1747–1756. Available at: https://doi.org/10.1016/j.bcp.2011.08.003.

National Collaborating Centre for Women's and Children's Health (UK). Surgical Site Infection: Prevention and Treatment of Surgical Site Infection. London: RCOG Press; 2008 Oct. (NICE Clinical Guidelines, No. 74.) 5, P. phase. A. 2022/11/15. 'Available from: https://www.ncbi.nlm.nih.gov/books/NBK53719/'.

Nepogodiev, D. *et al.* (2019) 'Global burden of postoperative death', *The Lancet*, 393(10170), p. 401. Available at: https://doi.org/10.1016/S0140-6736(18)33139-8.

O'Hara, K. *et al.* (2015) 'Pharmacokinetics in neonatal prescribing: Evidence base, paradigms and the future', *British Journal of Clinical Pharmacology*, 80(6), pp. 1281–1288. Available at: https://doi.org/10.1111/bcp.12741.

Olafuyi, O. *et al.* (2021) 'Inter-ethnic differences in pharmacokinetics—is there more that unites than divides?', *Pharmacology Research and Perspectives*, 9(6), pp. 1–24. Available at: https://doi.org/10.1002/prp2.890.

Onda, K. *et al.* (2017) 'Proton pump inhibitors decrease soluble fms-like tyrosine kinase-1 and soluble endoglin secretion, decrease hypertension, and rescue endothelial dysfunction', *Hypertension*, 69(3), pp. 457–468. Available at: https://doi.org/10.1161/HYPERTENSIONAHA.116.08408.

Oosterom-Calo, R. *et al.* (2013) 'Determinants of adherence to heart failure medication: A systematic literature review', *Heart Failure Reviews*, 18(4), pp. 409–427. Available at: https://doi.org/10.1007/s10741-012-9321-3.

Overton, E., Tobes, D. and Lee, A. (2022) 'Preeclampsia diagnosis and management', *Best Practice and Research: Clinical Anaesthesiology*, 36(1), pp. 107–121. Available at: https://doi.org/10.1016/j.bpa.2022.02.003.

Owen, J.S. and Fiedler-kelly, J. (2014) *Introduction to Population Pharmacokinetic/Pharmacodynamic analysis with nonlinear mixed effects models.*

Paruk, F. *et al.* (2017) 'Dosing antibiotic prophylaxis during cardiopulmonary bypass—a higher level of complexity? A structured review', *International Journal of Antimicrobial Agents*, 49(4), pp. 395–402. Available at: https://doi.org/10.1016/j.ijantimicag.2016.12.014.

Pasipanodya, J. and Gumbo, T. (2011) 'An oracle: Antituberculosis pharmacokinetics-pharmacodynamics, clinical correlation, and clinical trial simulations to predict the future', *Antimicrobial Agents and Chemotherapy*, 55(1), pp. 24–34. Available at: https://doi.org/10.1128/AAC.00749-10.

Patel, J.B. *et al.* (2023) 'Updating breakpoints in the United States: a summary from the ASM Clinical Microbiology Open 2022', *Journal of Clinical Microbiology*, 61(10), pp. 1–18. Available at: https://doi.org/10.1128/jcm.01154-22.

Peloquin, C. (2023) 'The Role of Therapeutic Drug Monitoring in Children', *Gastroenterology Clinics of North America*, 52(3), pp. 549–563. Available at: https://doi.org/10.1016/j.gtc.2023.05.002.

Poweleit, E.A. *et al.* (2022) 'Selective Serotonin Reuptake Inhibitor Pharmacokinetics During Pregnancy : Clinical and Research Implications', 13(February), pp. 1–8. Available at: https://doi.org/10.3389/fphar.2022.833217.

Rangel, S.J. *et al.* (2011) 'Recent trends in the use of antibiotic prophylaxis in paediatric surgery', *Journal of Paediatric Surgery*, 46(2), pp. 366–371. Available at: https://doi.org/10.1016/j.jpedsurg.2010.11.016.

Rawizza, H.E. *et al.* (2019) 'Safety and efficacy of rifabutin among HIV/TB-coinfected children on lopinavir/ritonavir- based ART', *Journal of Antimicrobial Chemotherapy*, 74(9), pp. 2707–2715. Available at: https://doi.org/10.1093/jac/dkz219.

Rawizza HE, *et al.* (2021) ‘Rifabutin pharmacokinetics and safety among TB/HIV-coinfected children receiving lopinavir/ritonavir-containing second-line ART.’, *J Antimicrob Chemother.*, 76(3), pp. 710–717. Available at: https://doi.org/10.1093/jac/dkaa512.

Reller, L.B. *et al.* (1973) ‘Evaluation of cefazolin, a new cephalosporin antibiotic.’, *Antimicrobial agents and chemotherapy*, 3(4), pp. 488–497. Available at: https://doi.org/10.1128/AAC.3.4.488.

Ricci, Z. *et al.* (2020) ‘Population Pharmacokinetics of Cefoxitin Administered for Paediatric Cardiac Surgery Prophylaxis’, *Paediatric Infectious Disease Journal*, 39(7), pp. 609–614. Available at: https://doi.org/10.1097/INF.0000000000002635.

Riegel, B. and Knafl, G.J. (2013) ‘Electronically monitored medication adherence predicts hospitalization in heart failure patients’, *Patient Preference and Adherence*, 8, pp. 1–13. Available at: https://doi.org/10.2147/PPA.S54520.

Roberts, J.A. *et al.* (2008) ‘Antibiotic resistance—What’s dosing got to do with it?’, 36(8), pp. 2433–2440. Available at: https://doi.org/10.1097/CCM.0b013e318180fe62.

Rodríguez-López, J.M. *et al.* (2022) ‘Inflammatory Response, Immunosuppression and Arginase Activity after Cardiac Surgery Using Cardiopulmonary Bypass’, *Journal of Clinical Medicine*, 11(14). Available at: https://doi.org/10.3390/jcm11144187.

El Rouby, N., Lima, J.J. and Johnson, J.A. (2018) ‘Proton pump inhibitors: from CYP2C19 pharmacogenetics to precision medicine’, *Expert Opinion on Drug Metabolism and Toxicology*, 14(4), pp. 447–460. Available at: https://doi.org/10.1080/17425255.2018.1461835.

Ruf, V. *et al.* (2010) ‘Medication adherence, self-care behaviour and knowledge on heart failure in urban South Africa: the Heart of Soweto study.’, *Cardiovascular journal of Africa*, 21(2), pp. 86–92.

van Saet, A. and Tibboel, D. (2023) ‘The influence of cardiopulmonary bypass on paediatric pharmacokinetics’, *Expert Opinion on Drug Metabolism and Toxicology*, 19(6), pp. 333–344. Available at: https://doi.org/10.1080/17425255.2023.2227556.

Salvador, E. *et al.* (2021) ‘Population pharmacokinetics of cefazolin in critically ill children infected with methicillin- sensitive Staphylococcus aureus’, *Clinical Microbiology and Infection*, 27(3), pp. 413–419. Available at: https://doi.org/10.1016/j.cmi.2020.04.022.

Sarkar, M. and and Prabhu, V. (2019) ‘Basics of cardiopulmonary bypass’, *Indian Journal of Anaesthesia*, 49(4), pp. 257–262. Available at: https://doi.org/10.4103/ija.IJA.

Savic, Radojka M *et al.* (2007) ‘Implementation of a transit compartment model for describing drug absorption in pharmacokinetic studies’, *J Pharmacokinet Pharmacodyn*, 34, pp. 711–726. Available at: https://doi.org/10.1007/s10928- 007-9066-0.

Schwartz, G.J. *et al.* (2009) ‘New equations to estimate GFR in children with CKD’, *Journal of the American Society of Nephrology*, 20(3), pp. 629–637. Available at: https://doi.org/10.1681/ASN.2008030287.

Schwartz, J.B. *et al.* (1985) ‘Pharmacokinetics and Pharmacodynamics of Enalapril in Patients with Congestive Heart Failure and Patients with Hypertension’, *Journal of Cardiovascular Pharmacology*, 7(4), pp. 767–776. Available at: https://doi.org/10.1097/00005344-198507000-00023.

Shah, D. *et al.* (2015) ‘Improving medication adherence of patients with chronic heart failure: challenges and solutions’, *Research Reports in Clinical Cardiology*, p. 87. Available at: https://doi.org/10.2147/RRCC.S50658.

Sharma, A. and Palaniappan, L. (2021) ‘Improving diversity in medical research’, *Nature Reviews Disease Primers*, 7(1), pp. 1–2. Available at: https://doi.org/10.1038/s41572-021-00316-8.

Sheffield, J.S. *et al.* (2014) ‘Designing drug trials: Considerations for pregnant women’, *Clinical Infectious Diseases*, 59(2), pp. S437–S444. Available at: https://doi.org/10.1093/cid/ciu709.

Shin, J.M. and Kim, N. (2013) 'Pharmacokinetics and pharmacodynamics of the proton pump inhibitors', *Journal of Neurogastroenterology and Motility*, 19(1), pp. 25–35. Available at: https://doi.org/10.5056/jnm.2013.19.1.25.

De Silva, M. *et al.* (2019) 'A Systematic Review of Proton Pump Inhibitors for the Prevention and Treatment of Preeclampsia and Gestational Hypertension', *Open Journal of Obstetrics and Gynecology*, 09(01), pp. 21–28. Available at: https://doi.org/10.4236/ojog.2019.91003.

Sliwa, K. (2016) 'The heart of Africa: succeeding against the odds', *The Lancet*, 388(10063), pp. e28–e36. Available at: https://doi.org/10.1016/S0140-6736(16)31660-9.

Standing, J.F. (2017) 'Understanding and applying pharmacometric modeling and simulation in clinical practice and research', *British Journal of Clinical Pharmacology*, 83(2), pp. 247–254. Available at: https://doi.org/10.1111/bcp.13119.

Stiles, M.L., Tu, Y.H. and Allen, L. V. (1989) 'Stability of cefazolin sodium, cefoxitin sodium, ceftazidime, and penicillin G sodium in portable pump reservoirs', *American Journal of Hospital Pharmacy*, 46(7), pp. 1408–1412. Available at: https://doi.org/10.1093/ajhp/46.7.1408.

Stirratt, M.J. *et al.* (2015) 'Self-report measures of medication adherence behavior: recommendations on optimal use', *Translational Behavioral Medicine*, 5(4), pp. 470–482. Available at: https://doi.org/10.1007/s13142-015-0315-2.

Strom, C.M. *et al.* (2012) 'Testing for variants in CYP2C19: population frequencies and testing experience in a clinical laboratory', *Genetics in Medicine*, 14(1), pp. 95–100. Available at: https://doi.org/10.1038/gim.0b013e3182329870.

Sun, D. *et al.* (2022) 'Why 90% of clinical drug development fails and how to improve it?', *Acta Pharmaceutica Sinica B*, 12(7), pp. 3049–3062. Available at: https://doi.org/10.1016/j.apsb.2022.02.002.

Sun, H. *et al.* (2018) 'Extrapolation of Efficacy in Paediatric Drug Development and Evidence-based Medicine: Progress and Lessons Learned', *Therapeutic Innovation and Regulatory Science*, 52(2), pp. 199–205. Available at: https://doi.org/10.1177/2168479017725558.

Sun, W. *et al.* (2016) 'Comparison of the Efficacy and Safety of Different ACE Inhibitors in Patients with Chronic Heart Failure', *Medicine (United States)*, 95(6), pp. 1–8. Available at: https://doi.org/10.1097/MD.0000000000002554.

Svensson, E. *et al.* (2012) 'Integration of data from multiple sources for simultaneous modeling analysis: Experience from nevirapine population pharmac okinetics', *British Journal of Clinical Pharmacology*, 74(3), pp. 465–476. Available at: https://doi.org/10.1111/j.1365-2125.2012.04205.x.

Tabacova, S.A. and Kimmel, C.A. (2001) 'Enalapril: Pharmacokinetic/dynamic inferences for comparative developmental toxicity', *Reproductive Toxicology*, 15(5), pp. 467–478. Available at: https://doi.org/10.1016/S0890-6238(01)00161-7.

Tanuma, J. *et al.* (2013) 'Pharmacokinetics of Rifabutin in Japanese HIV-Infected Patients with or without Antiretroviral Therapy', 8(8), pp. 1–6. Available at: https://doi.org/10.1371/journal.pone.0070611.

'"The European Committee on Antimicrobial Susceptibility Testing. Breakpoint tables for interpretation of MICs and zone diameters, version 12.0, 2022".http://www.eucast.org/clinical_breakpoints/.'

Thomson, A.H. and Elliott, H.L. (2011) 'Designing simple PK-PD studies in children', *Paediatric Anaesthesia*, 21(3), pp. 190–196. Available at: https://doi.org/10.1111/j.1460-9592.2010.03436.x.

Thummel, K.E. and Lin, Y.S. (2014) 'Sources of Interindividual Variability BT - Enzyme Kinetics in Drug Metabolism: Fundamentals and Applications', in S. Nagar, U.A. Argikar, and D.J. Tweedie (eds). Totowa, NJ, NJ: Humana Press, pp. 363–415. Available at: https://doi.org/10.1007/978-1-62703-758-7_17.

Till, A.E. *et al.* (1984) 'Pharmacokinetics of repeated single oral doses of enalapril maleate (mk-421) in normal volunteers', *Biopharmaceutics & Drug Disposition*, 5(3), pp. 273–280. Available at: https://doi.org/10.1002/bdd.2510050309.

Tjoa, M.L. *et al.* (2011) 'Angiogenic factors and preeclampsia', *Placental Bed Disorders: Basic Science and its Translation to Obstetrics*, 31(1), pp. 229–242. Available at: https://doi.org/10.1017/CBO9780511750847.022.

Tong, S. *et al.* (2020) 'Pravastatin, proton-pump inhibitors, metformin, micronutrients, and biologics: new horizons for the prevention or treatment of preeclampsia', *American Journal of Obstetrics and Gynecology* [Preprint]. Available at: https://doi.org/10.1016/j.ajog.2020.09.014.

Tortoriello, T.A. *et al.* (2003) 'Mediastinitis after Paediatric Cardiac Surgery: A 15-Year Experience at a Single Institution', *Annals of Thoracic Surgery*, 76(5), pp. 1655–1660. Available at: https://doi.org/10.1016/S0003-4975(03)01025-7.

Toto, N. *et al.* (2020) 'Conducting clinical trials in sub-Saharan Africa: Challenges and lessons learned from the Malawi Cryptosporidium study', *Trials*, 21(1), pp. 1–8. Available at: https://doi.org/10.1186/s13063-020-04620-8.

Trang, M., Dudley, M.N. and Bhavnani, S.M. (2017) 'Use of Monte Carlo simulation and considerations for PK-PD targets to support antibacterial dose selection', *Current Opinion in Pharmacology*, 36, pp. 107–113. Available at: https://doi.org/10.1016/j.coph.2017.09.009.

Trent Magruder, J. *et al.* (2015) 'Continuous Intraoperative Cefazolin Infusion May Reduce Surgical Site Infections during Cardiac Surgical Procedures: A Propensity-Matched Analysis', *Journal of Cardiothoracic and Vascular Anaesthesia*, 29(6), pp. 1582–1587. Available at: https://doi.org/10.1053/j.jvca.2015.03.026.

Turnidge, J. and Paterson, D.L. (2007) 'Setting and revising antibacterial susceptibility breakpoints', *Clinical Microbiology Reviews*, 20(3), pp. 391–408. Available at: https://doi.org/10.1128/CMR.00047-06.

U.S. Food & Drug Administration (2016) *Drug research and children.*, *FDA*. Available at: https://www.fda.gov/drugs/information-consumers-and-patients-drugs/drug-research-and-children.

Verena, R. *et al.* (2010) 'Medication adherence, self-care behaviour and knowledge on heart failure in urban South Africa: The heart of Soweto study', *Cardiovascular Journal of Africa*, 21(2), pp. 86–92.

Vonasek, B.J. *et al.* (2022) 'Tuberculosis in Children Living With HIV: Ongoing Progress and Challenges', *Journal of the Paediatric Infectious Diseases Society*, 11(Suppl 3), pp. S72–S78. Available at: https://doi.org/10.1093/jpids/piac060.

Waalewijn, Almett, W. et al (2024) 'Simplifying Dosing by Harmonizing Weight-Band-Based Dosing Across Therapeutic Areas in Children', in *Pharmacokinetics, Dosing, and Safety of Antiretrovirals for Infants, Children, and Adolescents*. Denver, USA: Conference of Retrovirusses and Oppertunistic Infections.

van der Wal, M.H.L. and Jaarsma, T. (2008) 'Adherence in heart failure in the elderly: Problem and possible solutions', *International Journal of Cardiology*, 125(2), pp. 203–208. Available at: https://doi.org/10.1016/j.ijcard.2007.10.011.

Waltrip, T. (2006) 'A pilot study to determine the feasibility of continuous cefazolin infusion', *International Journal of Gynecology and Obstetrics*, 95(SUPPL. 1), pp. 5–9. Available at: https://doi.org/10.1016/S0020-7292(06)60027-1.

Wang, P.F., Neiner, A. and Kharasch, E.D. (2019) 'Efavirenz metabolism: Influence of polymorphic CYP2B6 variants and stereochemistry', *Drug Metabolism and Disposition*, 47(10), pp. 1195–1205. Available at: https://doi.org/10.1124/dmd.119.086348.

Wang, X. *et al.* (2016) 'CES1 genetic variation affects the activation of angiotensin-converting enzyme inhibitors', *Pharmacogenomics Journal*, 16(3), pp. 220–230. Available at: https://doi.org/10.1038/tpj.2015.42.

Wang, X. *et al.* (2017) 'A Comprehensive Functional Assessment of Carboxylesterase 1 Nonsynonymous Polymorphisms s', (November), pp. 1149–1155.

Wasmann, R.E. *et al.* (2021a) 'Constructing a representative in-silico population for paediatric simulations: Application to HIV-positive African children', *British Journal of Clinical Pharmacology*, 87(7), pp. 2847–2854. Available at: https://doi.org/10.1111/bcp.14694.

Weiner, M., Benator, D., Burman, W., *et al.* (2005) 'Association between acquired rifamycin resistance and the pharmacokinetics of rifabutin and isoniazid among patients with HIV and tuberculosis', *Clinical Infectious Diseases*, 40(10), pp. 1481–1491. Available at: https://doi.org/10.1086/429321.

Weiner, M., Benator, D., Peloquin, C.A., *et al.* (2005) 'Evaluation of the drug interaction between rifabutin and efavirenz in patients with HIV infection and tuberculosis', *Clinical Infectious Diseases*, 41(9), pp. 1343–1349. Available at: https://doi.org/10.1086/496980.

Weisser, K. *et al.* (1991) 'Pharmacokinetics and converting enzyme inhibition after morning and evening administration of oral enalapril to healthy subjects', *European Journal of Clinical Pharmacology*, 40(1), pp. 95–99. Available at: https://doi.org/10.1007/BF00315146.

Wesley, M.C. *et al.* (2015) 'Pharmacokinetics of tranexamic acid in neonates, infants, and children undergoing cardiac surgery with cardiopulmonary bypass', *Anesthesiology*, 122(4), pp. 746–758. Available at: https://doi.org/10.1097/ALN.0000000000000570.

WHO (2023) *Fact Sheet Tuberculosis*. Available at: https://www.who.int/news-room/fact-sheets/detail/tuberculosis.

WHO: *Consolidated Guidelines on the Use of Antiretroviral Drugs for Treating and Preventing HIV Infection: Recommendations for a Public Health Approach, Second edition. Geneva, Switzerland. 2016.* Available at: https://www.who.int/publications/i/item/9789241549684. (Accessed: 3 October 2023).

Wicha, S.G. *et al.* (2021) 'From Therapeutic Drug Monitoring to Model-Informed Precision Dosing for Antibiotics', *Clinical Pharmacology & Therapeutics*, 109(4), pp. 928–941. Available at: https://doi.org/10.1002/cpt.2202.

Wijk M, Wasmann RE, Jacobson KR, Svensson EM, Denti P. A Pragmatic Approach to Handling Censored Data Below the Lower Limit of Quantification in Pharmacokinetic Modeling. CPT Pharmacometrics Syst Pharmacol. 2025;14(6):1042-1049. doi:10.1002/psp4.70015

World Health Organization. and Geneva: World Health Organization. License: CC BY-NC-SA 3.0 IGO. (2022) *Global tuberculosis report.*

World Health Organization (2018) *WHO recommendations: drug treatment for severe hypertension in pregnancy*, *Geneva*. Available at: https://apps.who.int/iris/handle/10665/277234.

World Health Organization (2021) *Consolidated guidelines on HIV prevention, testing, treatment, sevice delivery and monitoring: recommendations for a public health approach.* Available at: https://www.who.int/publications/i/item/9789240031593.

Yan, T. *et al.* (2023) 'Burden, Trends, and Inequalities of Heart Failure Globally, 1990 to 2019: A Secondary Analysis Based on the Global Burden of Disease 2019 Study', *Journal of the American Heart Association*, 12(6). Available at: https://doi.org/10.1161/JAHA.122.027852.

Yancy, C.W. *et al.* (2017) '2017 ACC/AHA/HFSA Focused Update of the 2013 ACCF/AHA Guideline for the Management of Heart Failure: A Report of the American College of Cardiology/American Heart Association Task Force on Clinical Practice Guidelines and the Heart Failure Society of Amer', *Circulation*, 136(6). Available at: https://doi.org/10.1161/CIR.0000000000000509.

Yusuf, S. *et al.* (2001) 'Clinical Cardiology : New Frontiers Global Burden of Cardiovascular Diseases', (C), pp. 2746– 2753. Available at: https://doi.org/10.1161/hc4601.099487.

Zaman, M.A., Oparil, S. and Calhoun, D.A. (2002) 'Drugs targeting the renin-angiotensin-aldosterone system', *Nature Reviews Drug Discovery*, 1(8), pp. 621–636. Available at: https://doi.org/10.1038/nrd873.

Zeilmaker-Roest, G.A. *et al.* (2020) 'Recovery of cefazolin and clindamycin in in vitro paediatric CPB systems', *Artificial Organs*, 44(4), pp. 394–401. Available at: https://doi.org/10.1111/aor.13595.

Zelenitsky, S.A. *et al.* (2018) 'Antimicrobial Prophylaxis for Patients Undergoing Cardiac Surgery: Intraoperative Cefazolin Concentrations and Sternal Wound Infections', *Antimicrobial Agents and Chemotherapy*, 62(11), pp. 1–5. Available at: https://doi.org/10.1128/AAC.01360-18.

Zisowsky, J., Krause, A. and Dingemanse, J. (2010) 'Drug development for paediatric populations: Regulatory aspects', *Pharmaceutics*, 2(4), pp. 364–388. Available at: https://doi.org/10.3390/pharmaceutics2040364.

Appendix

UNIVERSITY OF CAPE TOWN
Faculty of Health Sciences
Human Research Ethics Committee

Room 45 E-52-E-Floor- Old Main Building
Groote Schuur Hospital
Observatory 7925
Telephone [021] 406 6492
Email: hrec-submissions@uct.ac.za
Website: www.health.uct.ac.za/home/human-research-ethics

07 December 2022

HREC REF: 798/2022

Dr P Denti
Division of Pharmacology
K-45 OMB
Email: Paoli.denti@uct.ac.za
Student: smrman003@myuct.ac.za

Dear Prof Denti

PROJECT TITLE: POPULATION PHARMACOKINETIC/PHARMACODYNAMIC MODELLING IN NEGLECTED POPULATION-
(PHD CANDIDATE-MRS MANNA GEBREYESUS)

Thank you for submitting your study to the Faculty of Health Sciences Human Research Ethics Committee (HREC) for review.

It is a pleasure to inform you that the HREC has **formally approved** the above-mentioned study.

Approval is granted for one year until the 7th December 2023.

You are required to submit a progress report form, using the standardised Annual Report Form (FHS016) or (FHS017) if the study continues beyond the approval period. Please submit a Standard Closure form if the study is completed within the approval period.
(Forms can be found on our website: www.health.uct.ac.za/fhs/research/humanethics/forms)

The HREC acknowledge that the student: Mrs M Gebreyesus will also be involved in this study.

Please quote HREC REF 798/2022 in all your correspondence.

Please note that the ongoing ethical conduct of the study remains the responsibility of the principal investigator.

Please note that for all studies approved by the HREC, the principal investigator **must** obtain appropriate institutional approval, where necessary, before the research may occur.

Yours sincerely

PROFESSOR M BLOCKMAN
CHAIRPERSON, FACULTY OF HEALTH SCIENCES HUMAN RESEARCH ETHICS COMMITTEE

Federal Wide Assurance Number: FWA00001637. Institutional Review Board (IRB) number: IRB00001938 NHREC-registration number: REC-210208-007
This serves to confirm that the University of Cape Town Human Research Ethics Committee complies to the Ethics Standards for Clinical Research with a new drug in patients, based on the Medical Research Council (MRC-SA), Food and Drug Administration (FDA-USA), International Council for Harmonisation of

Technical Requirements for Pharmaceuticals for Human Use: Good Clinical Practice (ICH GCP), South African Good Clinical Practice Guidelines (DoH 2020), based on the Association of the British Pharmaceutical Industry Guidelines (ABPI), and Declaration of Helsinki (2013) guidelines. The Human Research Ethics Committee granting this approval is in compliance with the ICH Harmonised Tripartite Guidelines E6: Note for Guidance on Good Clinical Practice (CPMP/ICH/135/95) and FDA Code Federal Regulation Part 50, 56 and 312.

UNIVERSITY OF CAPE TOWN
IYUNIVESITHI YASEKAPA • UNIVERSITEIT VAN KAAPSTAD

FACULTY OF HEALTH SCIENCES
Human Research Ethics Committee

Form FHS006: Protocol Amendment

HREC office use only (FWA00001637; IRB00001938)		
☑ Approved	☑ Type of review: Expedited	☐ Full committee
This serves as notification that all changes and documentation described below are approved.		
Signature HREC Chairperson / Designee		Date 18/10/2023

Note: All **Major** amendments must include a **Cover Letter** and a local **PI Synopsis** justifying the changes for the amendment. Please note that incomplete amendment submissions will not be reviewed.

Please email this form and supporting documents (if applicable) in a combined pdf-file to HREC enquiries@uct.ac.za with subject line: FHS006 + (HREC Reference number).

HUMAN RESEARCH ETHICS COMMITTEE
16 OCT 2023
HEALTH SCIENCES FACULTY
UNIVERSITY OF CAPE TOWN

The latest forms are found on our website.

http://www.health.uct.ac.za/fhs/research/humanethics/forms

Please also clarify your plan for research-related activities during COVID-19 lockdown.

Comments from the HREC to the Principal Investigator:
Subject to all the DTAs. Thankyou
Note: The approval of this protocol amendment does not grant annual approval. Please complete the FHS016 / FHS017 form for annual approval at least one month before study expiration.

Principal Investigator to complete the following:

1. Protocol information

Date (when submitting this form)	2023-10-16
HREC REF Number	798/2022
Protocol Title	Application of pharmacometrics to characterize drug pharmacokinetics and optimize treatment in neglected populations
Protocol Number (if applicable)	NA
Principal Investigator	Prof. Paolo Denti
Department / Office Internal Mail Address	Division of Clinical Pharmacology K-45 OMB Email of PI: paolo.denti@uct.ac.za Student: smrman003@myuct.ac.za

1.1 Is this a major or a minor amendment? (see FHS006hlp) Major (tick box) Minor (tick box)	☐ Major	☑ Minor
1.2 Does this protocol receive US Federal funding?	☐ Yes	☑ No
1.3 If the amendment is a major amendment and receives US Federal Funding, does the amendment require full committee approval? **Note:** Any protocol amendments for **Full Committee Review** MUST be submitted on the monthly HREC submission dates. (Please email an electronic copy to hrec-enquiries@uct.ac.za)	☐ Yes	☑ No
1.4 Did the initial study require UCT No-Fault Insurance	☐ Yes	☑ No

2. List of Proposed Amendments with Revised Version Numbers and Dates

Please itemise on the page below, all amendments with revised version numbers and dates, which need approval.
This page will be detached, signed, and returned to the PI as notification of approval. Please add extra pages if necessary.

The amendments include data from 2 additional projects whose ethical approval is attached in the appendix. The objectives of these projects are:

1. Population pharmacokinetics of esomeprazole in patients with preterm preeclampsia – to characterize the pharmacokinetics of esomeprazole in pregnant women with preeclampsia combined with data from healthy, non-pregnant participants.

2. Population pharmacokinetic modelling of enalaprilat to predict adherence in heart failure patients – to perform pharmacokinetic modelling of enalaprilat using data from heart failure patients, combined with data from healthy participants, and use the model to derive concentrations that can be used to predict adherence to enalapril.

The amendment also includes removal of 1 project which had been included in the previous protocol, the title of which is below, since data collection for this project is still ongoing and completion would be beyond the timelines for my PhD:

Optimizing treatment of community acquired pneumonia for pediatric patients in a Sub-Sahara African setting.

3. Protocol status (tick ✓)

☐	Open to enrolment
☐	No participants have been enrolled
	Closed to enrolment (tick ✓)
☐	Research-related activities are ongoing
☐	Research-related activities are complete, long-term follow-up only
☑	Research-related activities are complete, data analysis only

4. Proposed changes will affect: (tick ✓ all the categories that apply)

Protocol	
☑	Study objectives, design (including investigator's brochure, clinical activities, study length)
☐	Study instruments, questionnaires, interview schedules
☐	Sample size
☐	Recruitment methods
☐	Eligibility criteria (inclusion and exclusion criteria)
☐	Drug/device (composition, amount, schedule, route of administration, combination with other drugs/devices, safety information)
☐	Data collection/ analysis
☐	Principal Investigator. (Please attach revised conflict of interest and PI declaration statements. Refer: sections 7 and 8.4 in the New Protocol Application Form FHS013)
☐	Consent form and information sheet
☐	Recruitment materials (e.g. advertisements)
☐	Administrative (e.g. change in sponsor's name, change in contact information)
☐	Other. Please specify:

**Note: Amendment changes involving study length, sample size, additional sites and eligibility criteria (i.e. inclusion of minors and /or pregnant woman) need to be declared to the Insurance office. Please liaise via fhs.sponsorship@uct.ac.za regarding the required documentation and information to be submitted to obtain an updated UCT No-fault Insurance Certificate- it should be included herewith*

4.1 In your opinion, will there be any **increase** in risk, discomfort or inconvenience to participants?	☐ Yes	☑ No
If yes, please provide a detailed justification/explanation:		

4.2 What follow-up action do you propose for participants who are already enrolled in the study?	
☐	Inform current participants as soon as possible
☐	Re-consent current participants with revised consent/assent forms (append)
☑	No action required
☐	Other. Please describe:

5. Detailed description of the change(s)

Please attach, for each amendment, a summary of all changes which clearly indicates:

i. Old wording (e.g. ~~strikethrough~~ text, CHANGED FROM and CHANGED TO)

ii. New wording (e.g. *italicized*, **bold**, tracked)

iii. Detailed rationale/ justification/ explanation for each change

6. Ethics Review for Amendment Levy – cost including vat

Amendment Review Costs including VAT

Please tick amount to be billed:

Submission Type	***Description***	***New fee (Vat Incl.)***	***tick ✓***
Research funded solely from UCT departmental/ divisional/group budget	Major/ Minor Amendments	**R0,00**	☐
Non-sponsored student research for degree purposes at UCT/Other Universities & Colleges	Major/ Minor Amendments	**R0,00**	☑
Protocol amendment - Major (FHS006 Form)	Clinical Trial & International Grant Funded Research - Any changes to the protocol that requires Full Committee review	**R8 000.00**	☐
Protocol amendment - Major (FHS006 Form)	Clinical Trial & International Grant Funded Research - Any change to the protocol that requires Expedited review that does not require Full Committee Review	**R5 000,00**	☐
Protocol amendment - Minor (FHS006 Form)	Clinical Trial & International Grant Funded Research - Minor amendments, administrative changes that do not affect study design e.g. changes to informed consent form, changes in study staff, etc.	**R2 250,00**	☐
Protocol amendment - Major (FHS006 Form)	National grant funded research - Any change to the protocol that requires Full Committee review	**R7 000,00**	☐
Protocol amendment - Major (FHS006 Form)	National grant funded research - Any change to the protocol that requires Expedited review that does not require Full Committee review	**R2 500,00**	☐
Protocol amendment - Minor (FHS006 Form)	National grant funded research - Minor amendments, administrative changes that do not affect study design e.g. changes to informed consent form, changes in study staff, etc.	**R1 000,00**	☐

NB: Protocols funded by UCT (e.g. departmental funding / student research) and by certain grant funding organizations (e.g. MRC, NRF, CANSA,) are exempt from these charges.

Please provide details for Invoicing, either complete section 1 or 2 :

1. Invoice billing – Directly to Sponsor

Sponsor's name	
Billing Address of Sponsor:	
Vat Number:	
Contact person:	
Telephone number:	

Email Address:	
2. Internal Journal Billing:	
Fund Number:	
Cost Centre Number:	
Account Holder Name:	
Division of Account Holder:	

7. Amendment Submission checklist (tick ✓)

7.1 Please tick that all the documents are attached before submitting to the HREC. NB: Incomplete submissions will not be processed	
☑	Latest FHS006 form completed with all sections completed as per our website
☑	Cover Letter
☑	PI Justification/ Summary for the reasons for the amendment
☑	Protocol - Track changes & Clean Copy (where necessary)
☐	Informed Consent Forms (ICF), if applicable (Any changes made to ICF tracked & clean copy)
☑	Any other additional documentation in support of amendment
☐	Updated no fault insurance certificate (if applicable)

Please email this form and supporting documents (if applicable) in a combined pdf-file to hrec-enquiries@uct.ac.za with subject line: FHS006 + (HREC Reference number). The latest forms are found on our website.

8. Signature

My signature certifies that I will maintain the anonymity and/ or confidentiality of information collected in this research. If at any time I want to share or re-use the information for purposes other than those disclosed in the original approval, I will seek further approval from the HREC.			
Signature of PI		Date	16-10-2023

2874
2875

FHS017: Annual Progress Report / Renewal

Record Reviews/Audits/Collection of Biological Specimens/Repositories/Databases/Registries

HREC office use only (FWA00001637; IRB00001938)			
This serves as notification of annual approval, including any documentation described below.			
☐ Approved	Annual progress report	Approved until/next renewal date	30.12.2025
☐ Not approved	See attached comments		
Signature Chairperson of the HREC/ Designee		Date Signed	17/12/24

Note: Please note that incomplete submissions will not be reviewed.
Our website address: **https://health.uct.ac.za/home/human-research-ethics**

HUMAN RESEARCH ETHICS COMMITTEE
17 DEC 2024
HEALTH SCIENCES FACULTY
UNIVERSITY OF CAPE TOWN

Please email this form and supporting documents (if applicable) in a combined pdf-file to hrec-enquiries@uct.ac.za.

Principal Investigator to complete the following:

1. Protocol information

Date (when submitting this form)	13-Dec-2024		
HREC REF Number	798/2022	Current Ethics Approval was granted until	30-Nov-2024
Protocol title	Population Pharmacokinetic/Pharmacodynamic Modelling In A Neglected Population - PhD Candidate-Mrs Manna Gebreyesus		
Principal Investigator	Professor Paolo Denti		
Department and email address	Division of Clinical Pharmacology, K45, Old Main Building, Groote Schuur Hospital		
1.1 Does this protocol receive US Federal funding?		☐ Yes	✓ No

2. Protocol status (tick ✓)

✓	Research-related activities are ongoing
☐	Data collection is complete, data analysis only
☐	Publication or thesis submitted and final completion?
Please indicate (in the block below) the titles and HREC reference numbers of any projects currently making use of the Database/registry/repository.	
Ongoing PhD student research.	

3. Protocol summary

Total number of records or specimens collected, reviewed or stored since the original approval		N/A
Total number of records or specimens collected, reviewed or stored since last progress report		N/A
Have any research-related outputs (e.g. publications, abstracts, conference presentations) resulted from this research? If yes, please list and attach with this report.	✓ Yes	☐ No
Please complete the Closure form (FHS019) if the study is completed within the approval period		

4. Signature

Signature of PI		Date	13 Dec 2024

2878
2879

HREC office use only (FWA00001637; IRB00001938)			
This serves as acknowledgement of a protocol deviation as described below.			
Chairperson of the HREC signature/ Designee		Date	17/12/24

Note: Please note that incomplete submissions will not be reviewed.
Please email this form and supporting documents (if applicable) in a combined pdf-file to hrec-enquiries@uct.ac.za. Our website address: https://health.uct.ac.za/home/human-research-ethics

Principal Investigator to complete the following:

1. Protocol information

Date (when submitting this form)	13 December 2024
HREC REF Number	798/2022
Project Title	Population Pharmacokinetic/Pharmacodynamic Modelling In A Neglected Population - PhD Candidate-Mrs Manna Gebreyesus
Protocol number (if applicable)	
Principal Investigator	Professor Paolo Denti
Department and Email address	Division of Clinical Pharmacology, K45, Old Main Building, Groote Schuur Hospital

2. Protocol deviation description

Please describe the deviation below, including the reason why the deviation has occurred.
There was a delay in the ethics renewal due to an increased workload and compiling the supporting documentation.

3. Follow-up actions

3.1 Please describe any follow-up action(s) taken or planned as a result of this deviation e.g. DSMB reporting, report to sponsor, informing participants.
No impact. No patient samples have been used or received.
3.2 Please describe what action(s) have or will be taken to prevent similar deviations in future.
A new tracking system has been implemented and this will ensure timely submissions in the future.

2880
2881

Form FHS011: Study deviation

4. Principal Investigator's acknowledgement of responsibility

The required signature indicates the PI has reviewed the deviation, taken appropriate follow-up action and implemented or plans to implement preventative steps where possible.		
Signature of PI	Date	13 Dec 2024

2882